The Effects of Intake Charge Stratification on HCCI Combustion

by

Robert J. Iverson

A thesis submitted in partial fulfillment
of the requirements for the degree of

Master of Science
(Mechanical Engineering)

at the

University of Wisconsin – Madison
2004

Approved: _____

David E. Foster

Professor – Mechanical Engineering
University of Wisconsin – Madison

Date: _____

Abstract

A laboratory was constructed to investigate what effects could be generated in an HCCI engine by altering the properties of the engine's intake charge. The principle changes investigated were altering the spatial distribution of the fuel in the intake and adding thermal gradients to the charge. The primary goal of the work was to develop a method to separate the effects of the spatial stratification of the charge from the effects of the thermal gradients in the charge and to study both independently.

The laboratory included faculties for measuring the exhaust emissions, recording cylinder pressure, and monitoring and controlling the many engine inlet and outlet parameters. Auto-ignition state was achieved by externally adding thermal energy to the intake charge utilizing heaters wrapped around the intake piping, this allowed us to generate an intake charge with a very uniform temperature distribution unlike an engine that uses exhaust rebreathing or recompression strategies. Intake temperatures in excess of 350 °C were achievable in this laboratory.

Two fueling systems were developed for this work. One was located over two meters away from the inlet to enable thorough mixing and a homogeneous mixture. The other utilized the traditional fueling port to introduce a concentrated shot of fuel and keep it separated from the air as long as possible in order to minimize mixing. In order to separate the thermal and the spatial effects the fuel was heated up to the same temperature as the bulk of the inlet air. The goal was to ensure that the charge in the cylinder started the compression process with a known and controlled temperature. The level of stratification was controlled by manipulating the timing of the injection of the fuel.

The results of these experiments validated the experimental setup and confirmed that consistent and repeatable results could be obtained. A series of experiments performed with spatial stratification of the fuel, as well as thermal stratification in the charge, showed that increasing thermal stratification shifted the window of acceptable intake temperatures, over which combustion could be achieved, to higher temperatures. The engine also emitted higher levels of NO_x and CO as the stratification increased, but all other indicators were constant when reviewed as a function of the combustion efficiency. In this setup the premixed fueling system had the lowest window of intake air temperatures and generated the lowest pollutant emissions.

A set of experiments conducted with only stratification of the fuel showed that the engine operated over the same set of intake air temperatures for both fueling methods and for all injection timings investigated. In these experiments the engine still emitted higher amounts of NO_x and CO compared to the premixed system, but these emissions were lower in this setup than they were in the setup that also introduced thermal stratification. The spatial stratification did not alter the engine's behavior, in terms of cylinder pressure. Over a range of speeds, air/fuel ratios, and fueling rates the effects of fuel stratification, generated in the intake system, only caused slight increases in the emissions of NO_x and CO. While empirical evidence leads to the conclusion that stratification of the fuel does exist inside the cylinder, the results do not provide any evidence as to what level of stratification is actually generated. However, an optically accessible engine has been constructed and installed in the laboratory and will be used, in the near future, to quantify the level of stratification generated.

Acknowledgements

I would like to acknowledge the help and assistance of Dr. David Foster and Dr. Jaal Ghandhi for their technical advice, analytical opinions, and encouragement. Without their help I would not have been at the Engine Research Center nor would this work have been half the success it is.

The financial contributions of General Motors were invaluable for this research. Besides paying my salary the financial contributions of GM also paid for almost all of the research equipment used in this research. GM also graciously donated all of the engine components as well as the emissions benches that were installed in the laboratory.

The contributions from Jim Eng at General Motors Research were also very important. Jim's opinions, advice, and assistance were invaluable throughout the course of the research.

I also must thank Craig Marriott at General Motors Powertrain for his technical advice and help in repairing and replacing engine components. Craig was able to drop whatever he was working on to get me replacement parts and without that help this project would have taken significantly longer.

There are a number of people at the Engine Research Center that worked on portions of this project. Special note must be given to Ralph Braun, Glen Bower, Anton Koslovsky, Eric Fox and Chris Mullhul who all helped in machining and installing components and many other aspects of the laboratory setup. I must also thank Ralph and Anton for always being willing to talk about a problem and for explaining how a part could or could not be machined. Also the work of Lonny Peet on the data analysis software and Igor programming was invaluable for streamlining the data analysis process.

My coworkers on this project were Rinaldo Augusta and Randy Herold. Both supplied help in every aspect of the project from laboratory setup to data analysis. Their conversation and advice also helped clear up many of the problems in the experiment that would have left me tied up in knots had I been left to figure them out alone.

I must also thank every person who has shared this office with me: Terry Dembroski, Nathan Forster, Randy Herold, Matt Borden, and Jon Filipa. They have all listened to my problems and offered useful advice on solving them.

Finally I need to thank my parents for their tolerance in my pursuit of a Master's Degree. They have provided countless amounts of encouragement over the course of the project.

Table of Contents

List of Figures

List of Tables

Nomenclature

HCCI	Homogeneous Charge Compression Ignition
EPA	Environmental Protection Agency
cc	Cubic centimeter
JSFR	Jet-Stirred Flow Reactor
s	Seconds
min	Minutes
PRF	Primary Reference Fuel blend (n-heptane and isooctane mixture)
TDC	Top Dead Center
dBTDC	Degrees Before Top Dead Center
dATDC	Degrees After Top Dead Center
IMEP	Indicated Mean Effective Pressure
COV	Coefficient of Variation
LPP	Location of Peak Pressure
NO_x	Nitrogen Oxide compound of any composition
HC	Any partially reacted Hydrocarbon compound
CO	Carbon Monoxide
CO_2	Carbon Dioxide
O_2	Oxygen Molecule
N_2	Nitrogen Molecule
SOI	Start Of Injection
EOI	End Of Injection
NTC	Negative Temperature Coefficient
LTR	Low Temperature Reactions
HTR	High Temperature Reactions
SI	Spark Ignition engine

Chapter 1 - Introduction

Section 1.1 Power System Pollutants

Considerable scientific research has demonstrated that certain emissions from combustion based power generating systems can have significant effects on the Earth's atmosphere, as well as the plants and animals in the environment. Various pollutants have different effects. Carbon monoxide (CO) reduces the oxygen carrying capacity of the blood stream and can be deadly if inhaled in large enough quantities. Oxides of nitrogen (NO_x) are lung irritants, have been identified as a key participant in the formation of photochemical smog and acid rain, and have also been linked to the destruction of the stratospheric ozone layer. Hydrocarbon (HC) and particulate emissions are also lung irritants and have been linked to certain cancers in some studies. Emissions of sulfur dioxide are another pollutant emission that has been identified as a key participant in the formation of acid rain. [1]

Starting with the 1990 amendments to the Clean Air Act, the United Stated Environmental Protection Agency (EPA) has embarked upon a path designed to bring about drastic reductions in pollutant emissions from combustion based systems. This move is not limited to just the United States. Regulatory bodies around the world are tightening pollutant emission standards. One justification for the tightening of emissions regulations is shown in Figure 1-1. [2] The figure shows estimated NO_x emissions, in Tons, in the United States through the year 2030 with and without the EPA's upcoming Tier 2 emissions standards. The estimates were performed with two different models, and the results from both models

are shown on this figure, the solid lines denote the original analysis performed by the EPA and the dashed line are the results of an analysis performed with an updated model also developed by the EPA.

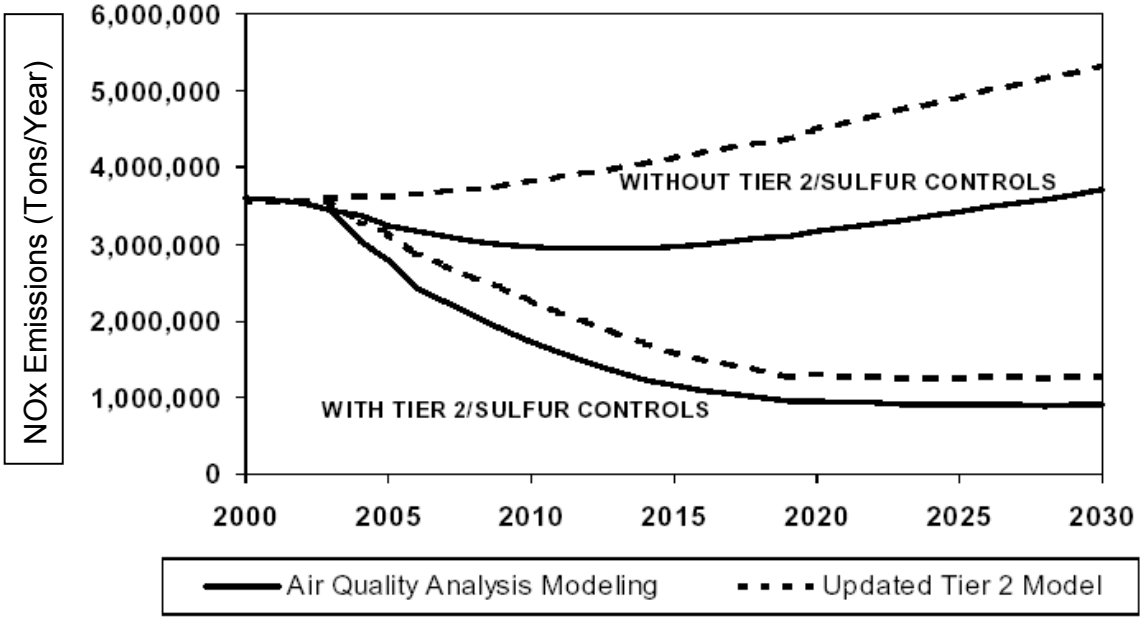

Figure 1-1 EPA estimation of NO_x emissions, in tons, through 2030 [2]

Looking at the predictions shown in Figure 1-1, it can be seen that it is projected that NO_x emissions would increase considerably by 2030 if the Tier 1 standard of 0.6 grams/mile was maintained. Assuming implementation of the Tier 2 standard of 0.07 grams/mile, the EPA estimates that the emissions of NO_x in 2030 will be on the order of 1 million tons - a reduction of about 60% from the 2000 emissions levels of 3.5 million tons. The significance of the predicted reduction of NO_x emissions were justification for the establishment of the Tier 2 standard that will take full effect in the US in the year 2007.

Oxides of Nitrogen are not the only pollutant produced in power generating systems to be regulated by the EPA. The governing body also regulates carbon monoxide emissions, unburned hydrocarbon emissions, and the content of sulfur in the fuel. For each of these various other emissions there are graphs very similar to that shown in Figure 1-1 predicting that, without stricter regulations, each of these emissions will increase each year, as the number of automobiles on the road increases.

These upcoming government regulations have led almost everyone who manufactures a combustion based system to put considerable effort into understanding and controlling the generation of pollutants, or at the very least to remove them from the system's exhaust stream. A major problem with controlling the emissions of an internal combustion engine lies in the very small quantities of pollutants that each individual engine generates. In fact, most pollutant emissions are measured in ranges on the order of parts per million. However, when one takes into account the number of vehicles on the road and the amount of use they receive, the total amount of emissions generated each year is rather large.

Control of the formation of pollutants inside the engine is often difficult, or impossible, to implement. Because of this difficulty, most efforts in pollution control have focused on removing the pollutants from the exhaust stream. However, as the government regulations tighten, it has become more and more essential to look for methods of preventing or at least reducing, the formation of pollutants inside the cylinder.

One technique of reducing emissions generated inside the cylinder, that is currently receiving considerable interest and investigation, is Homogeneous Charge Compression Ignition (HCCI) combustion. HCCI combustion is a combination of the spark ignition (SI) and diesel (CI) combustion techniques. The goal, when implementing HCCI combustion, is

to take the best attributes of both the SI and diesel combustion methods and combine them together to form an efficient and low polluting engine. In order to get a good feeling for HCCI combustion it is first necessary to develop a basic understanding of the SI and diesel combustion techniques.

Section 1.2 Spark Ignition Combustion

In the spark ignition engine, the fuel and air are mixed together in the intake system prior to entering the engine. The mixture is then brought into the engine, compressed, and at some point during the compression an electrical discharge is used to generate a spark inside the cylinder, which causes ignition of the fuel near the source of the spark. A flame then begins to radialy propagate away from the ignition source through the cylinder until it has consumed all of the fuel or is quenched by the cold wall or lack of fuel.

Because the air and fuel are mixed before entering the engine, the only way to control the power output of the engine is to control the mass flow of the mixture into the engine. Mass flow control is accomplished by throttling the gasses as they travel through the intake system. Throttling causes low pressures in the cylinder at the start of the cycle, this leads to lower peak cylinder pressures. Throttling also diverts work, which could be applied to the flywheel, to pumping the gasses into and out of the cylinder, which reduces the thermal efficiency of the engine.

The spark ignition engine is limited in that the air/fuel ratio needs to be fairly close to stoichiometric. Flame development near the spark and propagation of the flame through the cylinder becomes difficult if the mixture is too lean or too rich. However, when the engine is

running at stoichiometric air/fuel ratios the flame temperatures are the highest and thus a lot of NO_x is generated in the cylinder.

The fact that the fuel and air are mixed prior to entering the engine is another drawback to the spark ignition engine. There is the potential for a significant portion of the fuel to become lodged in the crevice volumes of the combustion chamber. Heat transfer to the cylinder walls quenches the flame before it can enter the crevice volumes, leaving significant portions of the fuel unburned. The unburned fuel will exit the engine as hydrocarbon fragments, a regulated pollutant, and also represent lost work capacity and lower thermal efficiencies.

Another problem in the spark ignition engine is the need to avoid knocking. If the fuel reaches a certain temperature and pressure before it is ignited by the flame it will auto-ignite. If auto-ignition occurs, the cylinder pressure can rise dramatically, which creates a supersonic pressure wave that travels back and forth through the chamber. These pressure rises and oscillations generate a characteristic pinging noise and, if left unchecked, can lead to thermal and mechanical damage to the engine's components. To prevent auto-ignition of the fuel, the engine's compression ratio is kept fairly low, which lowers peak cylinder pressures and avoids the potential for auto-ignition. This, however, also lowers the thermal efficiency of the engine. Modern engine control systems can also utilize a knock sensor and retard the spark timing when knock is detected, thus reducing the peak cylinder pressure. However, this solution will also reduce the engine's efficiency very much like lowering the compression ratio. [3]

Section 1.3 Diesel Combustion

In a diesel engine, the air is brought into the cylinder without any fuel mixed with it. The air is then compressed, which increases its temperature. The fuel is injected into the cylinder at some point near the top of the piston travel, where the temperature of the gas is very high. As the fuel is injected, it begins to evaporate and mix with the air. The portion of the fuel that evaporated will begin to burn in what is termed a premixed burn, however, a significant portion of the fuel does not mix with the air before combustion is initiated. Oxygen begins to diffuse through the premixed fuel, towards the portions of the fuel that did not mix with air prior to the onset of combustion. When enough oxygen has reached to fuel to bring the air/fuel ratio to stoichiometric the fuel begins to burn, in what is termed a diffusion burn. As the diffusion brings the air/fuel ratio close to stoichiometric the fuel begins to oxidize. This oxidation continues as the piston travels downwards until expansion effects and heat transfer causes the gasses in the cylinder to cool to a point where they are no longer hot enough to perpetuate the reactions. Because the diesel engine does not need to support propagation of a flame as the fuel burns the engine can be run unthrottled, which eliminates the pumping losses that occur in the spark ignition engine. The power output of the engine is controlled by varying the amount of fuel injected into the cylinder.

The drawbacks of the diesel engine stem from the mixing of the fuel and air. The fuel burns in the regions of the cylinder where the air/fuel ratio is near the stoichiometric level, even though the global air/fuel ratio is often very fuel lean. This means that the local temperatures in the area of the combustion zones are very close to the adiabatic flame temperatures, which, for most fuels is large enough to generate significant amounts of NO_x. The high temperatures also cause the fuel to bond to itself, forming benzene rings which

most of the fuel that doesn't participate in the premixed burn will form soot particles. The soot oxidizes from the outside of the particle inwards as the air diffuses through the burning gasses towards the particle. Soot oxidation is often stopped in the middle of the expansion stroke by the rapidly falling cylinder temperatures, before the particle is completely oxidized, and is the reason for the high amounts of soot particles that are emitted from the diesel engine.

The best way to reduce the amount of soot generated in a diesel engine is to increase the amount of mixing of the fuel with the air. This, however, increases the amount of fuel burning stoichiometrically and causes the amount of NO_x generated to increase. For similar reasons any steps taken to reduce NO_x generation leads to an increase in soot and hydrocarbon emissions. A major challenge to diesel engine designers today is the simultaneous reduction of both NO_x and soot particles emitted from the engine. [3]

Section 1.4 HCCI Combustion

HCCI combustion is a combination of the SI and diesel combustion that blends the best characteristics of both types of combustion, achieving low emissions and high efficiency. In HCCI combustion, the air/fuel mixture is prepared early in the cycle. This can be done either in the intake system prior to the gasses entering the cylinder, or the fuel can be directly injected into the cylinder early in the compression stroke. The homogeneous mixture of fuel and air is then compressed until auto-ignition occurs. HCCI combustion occurs relatively quickly, typically between ten and twenty crank angles, and comes very close to the ideal Otto cycle of constant volume combustion, helping to yield a more efficient engine.

In the HCCI combustion process, most of the fuel reaches the point of auto-ignition at about the same time. The mixture will usually ignite in many locations simultaneously; this is the cause of the short duration of the combustion event. [4, 5] HCCI combustion can occur with very lean air/fuel ratios since chemical kinetics controls the combustion instead of flame propagation. The heat and pressure rise generated at each local ignition area will help to compress and heat the fuel that didn't initially auto-ignite. This process is thought to act sort of like flame propagation in an SI engine, but only in a limited sense since the mixture is typically too lean for the flame to directly ignite the fuel. [6, 7] The possibility of running the engine on ultra lean air/fuel ratios results in lower peak cylinder temperatures since a significant portion of the cylinder gasses do not participate in the combustion process. The lower cylinder temperatures lead to little or no NO_x production, researchers reported NO_x concentrations as low as 5 parts per million. [8] Also, because the fuel is premixed with the air, the tendency for soot formation is negligible, this has resulted in some speculation that HCCI combustion could be used to help diesel engines meet upcoming exhaust pollutant emission regulations.

There are, of course, a few drawbacks to HCCI combustion that have challenged researchers and prevented wide scale implementation of HCCI in the transportation sector. HCCI combustion is controlled solely by chemical kinetics; this means, that for most engines, once the intake valve has closed there is no longer any way to control the combustion process. The fuel will only burn when the mixture reaches auto-ignition conditions. Often the mixture reaches the auto-ignition criteria at a point that is not the optimum point in the cycle. Incorrect phasing of the combustion leads to lost power and inefficiency.

There are certain operating regimes in HCCI combustion where the pressure can rise too rapidly, very much like knock in an SI engine. Practical experience in this laboratory has shown that there are knocking like operating conditions where there is the potential for thermal and mechanical damage to the engine. This rapid pressure rise causes an irritating pinging noise that increases in intensity as the magnitude of the pressure oscillations increase. In order to slow down the combustion event and reduce the pressure oscillations, a large amount of non-reacting thermal mass, or diluents, must be added to the air/fuel mixture. [5, 8, 9]

Another drawback to HCCI combustion is that a large amount of initial energy must be applied to the fresh charge in order for auto-ignition to occur, especially if the engine has a low compression ratio or if the fuel has a high octane number. [5, 9] The lower density of a preheated air/fuel mixture coupled to the need for a large amount of dilution limits the maximum amount of fuel that can be inducted into the cylinder. This places a fairly low limit on the amount of power that can be generated by an HCCI engine. The maximum power output from an HCCI engine is considerably lower than what is achievable in a diesel or spark ignition engine. The nature of the chemical kinetics control limits the speeds over which an HCCI engine can operates since the chemical reactions take a certain amount of time to occur in. [5] If the engine speed is too high, the compression and expansion strokes will occur in less time than is required for the combustion to initiate and complete.

Despite these problems with HCCI combustion, the low NO_x and soot emissions offer enough promise to warrant investigations into the concerns listed above. Besides research into the practical aspects of applying HCCI, studies are also being conducted to detail the fundamental mechanisms and principles behind the combustion phenomenon.

Section 1.5 Focus

This thesis details efforts to establish an experimental test cell to investigate HCCI combustion. One focus of the research is the effects of inhomogeneity of the air/fuel mixture on HCCI combustion. The work concentrated on installing a single cylinder all metal engine for the purpose of conducting HCCI research. Development of systems to deliver the fuel in a well mixed and stratified conditions were also undertaken.

The initial experiments conducted in the laboratory were designed to evaluate the operation of the engine and the testing methodology being used in the lab. The goal of the experiments was to establish and explore a defined set of baseline operating points for the engine to which future experiments can then be compared. The baseline conditions were able to establish the repeatability of a condition throughout a single day and over the course of several different days. Work was also conducted to identify the range over which reliable and consistent results could be obtained. The major focus of the baseline experiments was to evaluate how the performance of an HCCI engine changed as a function intake air temperature for various speed and fueling conditions.

Through the course of the establishment of the baseline data an unacceptable variability in the day-to-day repeatability of the engines performance was detected. It was noticed that the engine showed an extreme sensitivity to the way the air and fuel mixture was treated in the intake system prior to entering the engine. This sensitivity and its causes were explored. Finally, an exploration into the effects of non-uniformity in the air/fuel mixture on HCCI combustion was conducted.

This thesis will present an overview of the important aspects of auto-ignition chemistry, review past and present investigations relating to HCCI combustion, discuss the setup of the laboratory, and present data collected on fuel stratification. The thesis then concludes with some suggestions for future work to be performed in this laboratory.

Chapter 2 - Background and Discussion

The number of HCCI combustion research projects has grown considerably over the last decade, and this research has broadened the knowledge base relating to lean homogeneous auto-ignition. This chapter will review topics important to understanding HCCI combustion. First, some of the relevant terminology and chemical reactions important to auto-ignition are reviewed, and then results of some past research into HCCI will be discussed.

Section 2.1 Fuel Chemistry

2.1.1 Molecule naming conventions

Fuels composed of open chains are identified by the number of carbon atoms in longest chain and the maximum number of carbon to carbon bonds in the molecule. The prefix of the molecule name will be determined by the maximum number of carbon atoms in a chain. Table 2-1 lists the standard prefixes for various lengths of molecule chains. [10]

The second portion of a molecule's name is based upon the maximum number of bonds shared by any two carbon atoms in the molecule. A fuel composed only of single carbon-carbon bonds is termed an alkane or paraffin, and the name will end with the letter combination "ane". A molecule that has a double bond between two carbon atoms is termed an alkene or olefin, and its name will end with the letters "ene". A fuel molecule that

contains a triple bond between two carbon atoms is termed an alkyne or acetylene, and its name will end with the letters “yne”. [10]

# Carbons	Prefix	# Carbons	Prefix	# Carbons	Prefix
1	meth	5	pent	9	non
2	eth	6	hex	10	dec
3	prop	7	hep	11	undec
4	but	8	oct	12	dodec

Table 2-1 Prefixes for the naming conventions of hydrocarbon molecules of various lengths [10]

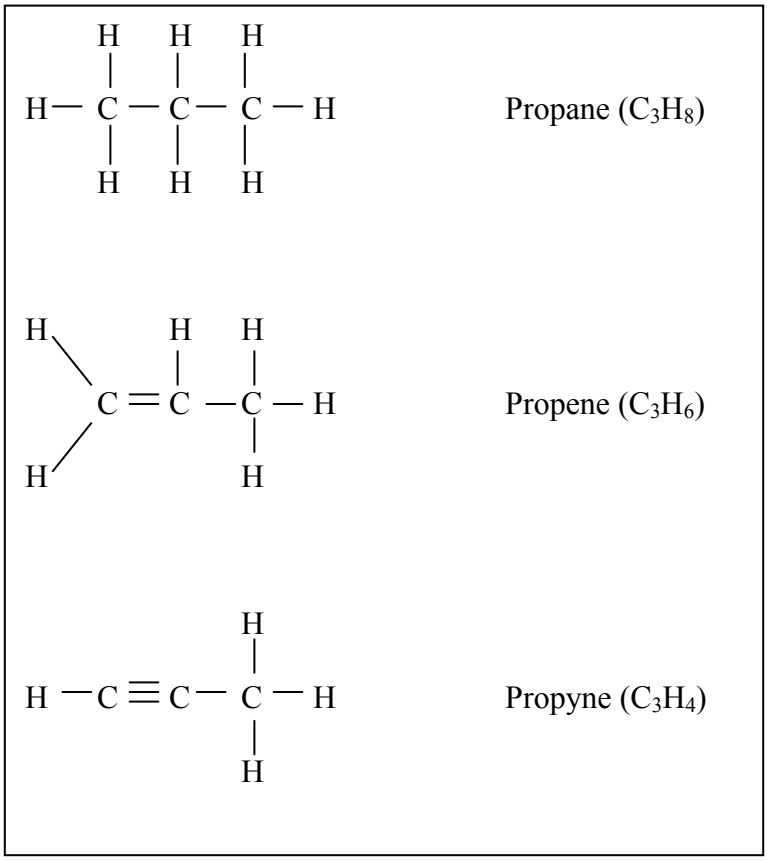

Figure 2-1 Examples of fuel types, bonds, and naming [10]

Molecules where the carbon atoms are bonded in a ring structure are termed cyclanes or aromatics. Cyclanes is the term given to any molecule that forms a ring while aromatics are strictly molecules based upon the C_6H_6 benzene ring. Finally, alcohols are molecules that have an OH group attached that replaces a hydrogen atom. Figure 2-1 shows variations of a molecule with three carbon atoms and shows the name of each of these molecules. [10, 11]

The propane molecule shown in Figure 2-1 is termed a "normal" molecule. The term "normal" means that there are only single bonds between all of the carbons and there are no side branches on the chain; note that the propene and propyne molecules are not normal molecules. It is not necessary for all of the carbon atoms to be in a straight chain. Often the molecule is very complex with several branches. Figure 2-2 shows the structure of the isooctane molecule, which is a very important fuel in engine research. [10]

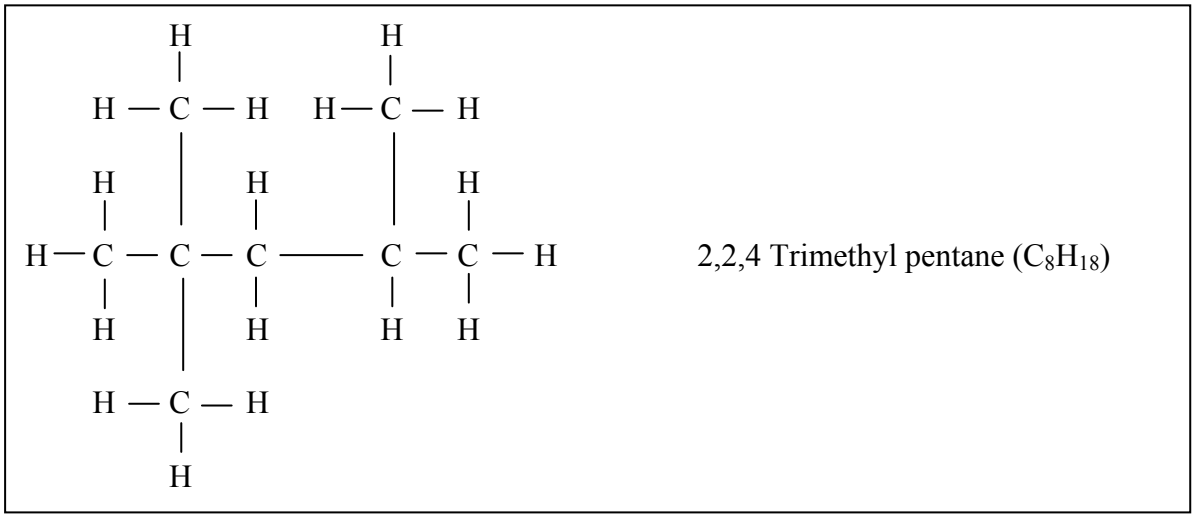

Figure 2-2 Isooctane molecule [10]

The isooctane molecule can be used to illustrate several other important points about molecule naming conventions. First, note that while the molecule has eight carbon atoms in it, the longest chain of carbon atoms in the molecule is five, and there are no double or triple

bonds, so this is why it is named as a pentane molecule. Second, attached to the pentane chain are three CH_3 (methyl) groups, which is where the "trimethyl" part of the name comes from. Thirdly, the 2, 2, 4 denotes where the methyl groups are attached to the pentane molecule. If one looked at the molecule from the right hand side instead of the left then it could be labeled 2, 4, 4, but convention is to keep the numbers as small as possible, which is why the 2, 2, 4 numbering is used. [11]

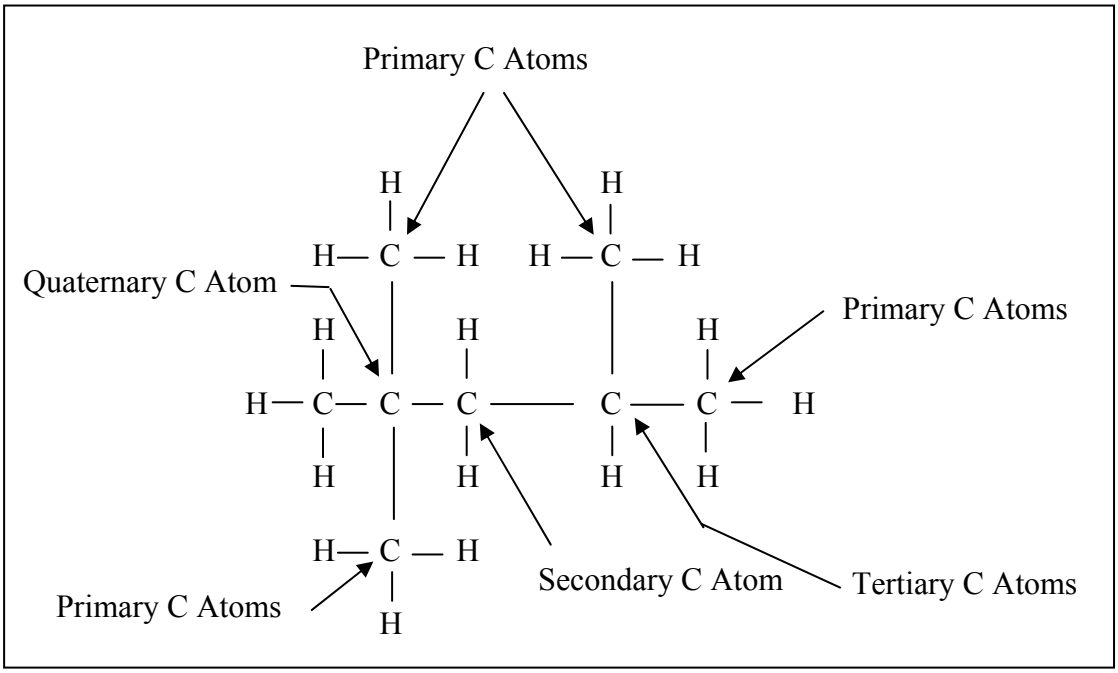

Figure 2-3 Carbon atom types and labels [12]

Another point about terminology and fuel chemistry is shown in Figure 2-3, which details the different carbon atom location types in the isooctane molecule. The atoms labeled primary atoms are those that are bonded only to one other carbon atom and these carbon atoms tend to hold their hydrogen atoms more tightly than do atoms in other locations. The atoms labeled secondary atoms are bonded to two other carbon atoms. The energy needed to

remove a hydrogen atom from a secondary atom is less than from the primary atoms but is more so than from a tertiary atom. The tertiary atoms are those bonded to three different carbon atoms. A hydrogen atom can be removed from these locations relatively easily. A carbon atom that is bonded to four other carbon atoms is termed quaternary. [13, 14]

Section 2.2 Chemical Kinetics

The auto-ignition behavior of a mixture depends primarily upon the fuel type of which the mixture is composed. [15] Fuels such as normal heptane, which is a straight chained molecule tend to isomerize at low intake air temperatures, and therefore auto-ignite fairly easily. A fuel such as isooctane, which is a complexly branched molecule that holds its atoms tightly, will not break down as easily and thus resists auto-ignition. [15] A fuel that is composed primarily of simple loosely bonded molecules will be easier to ignite in an HCCI engine while complex, branched fuels will be more difficult to ignite. The less easily ignited fuels also tend to exhibit little or no cool flame or negative temperature coefficient behavior, just rapid consumption of the fuel and release of energy.

There are several different types of reactions which are important to the combustion process. A reaction that generates one or more radical species from an unreacted species is termed an initiation reaction. A reaction that generates the same number of radical species as it consumes is called chain propagating. A reaction that generates more radical species than it consumes it is referred to as chain branching. Finally, a reaction that consumes more radicals than it generates is called chain terminating. The chain branching reactions are the

most important in terms of bringing about a chemical reaction in a timely manner, because they offer the potential for exponential growth in the radical pool and for quick consumption of the fuel. [16]

The sequence of reactions through which a reacting mixture proceeds, and the relative importance of each reaction, constantly changes throughout the combustion process. This is a result of changes in fuel composition and concentration as the reactions proceed. Changes in the mixture's pressure and temperature also change the reaction pathways. This is especially true in reciprocating engines where the temperature and pressure are always changing. [17]

In general, the reactions a mixture goes through can be split into two groups. The first group is the low temperature reactions that mostly occur before the mixture has reached 1000 K. [17] In the low temperature reactions a series of complex chain branching reactions occur that cause the fuel molecules to react with oxygen and other radicals, generating fuel radical species. The second reaction group is the high temperature reactions, which are composed of the reactions that occur at temperatures greater than 1000 K. In the high temperature reactions the carbon-carbon bonds in the fuel and radicals begin to break down and oxidation to CO and H_2O quickly occurs along with most of the heat release. [5] The following sections will discuss both of these regimes in more detail.

2.2.1 Low Temperature Reactions

Low temperature reactions are slow reactions and primarily act as precursors leading to the main high temperature reactions. Low temperature reactions are characterized by the

interaction of a fuel molecule with oxygen molecules. [17] In auto-ignition the primary function of the low temperature reactions is to generate a radical pool and raise the mixture's temperature to allow for the high temperature kinetics. Depending upon the operating parameters of the engine, the low temperature reactions can consume up to 10% of the fuel in the cylinder.

The radicals formed in low temperature reactions will eventually begin to attack the fuel and break it down. A very important chain branching reaction sequence is listed in the following reactions. [14, 16, 17]

$$H + O_2 + M \rightarrow HO_2 + M \quad (2.1)$$

$$RH + HO_2 \rightarrow R + H_2O_2 \quad (2.2)$$

$$H_2O_2 + M \rightarrow OH + OH + M \quad (2.3)$$

The H_2O_2 molecule generated in Reaction (2.2) is formed throughout the low temperature reactions, and it remains fairly inactive until the temperature increases above 1000 K, at which point it breaks down into two OH molecules almost as soon as it is formed. The OH radical formed in Reaction (2.3) is particularly good at breaking down the fuel. Once OH is formed in significant quantities, it begins to abstract hydrogen atoms from the fuel molecules forming water and releasing heat. The reactions quickly begin to accelerate and move into the high temperature regimes described in the next section. [14-17]

The predominant reactions and mechanisms that occur during the low temperature reactions are detailed in Figure 2-4. [17] The mechanisms show how the reactions are initiated, where the chain branching reactions are developed, and how the reactions move into the high temperature chemistry.

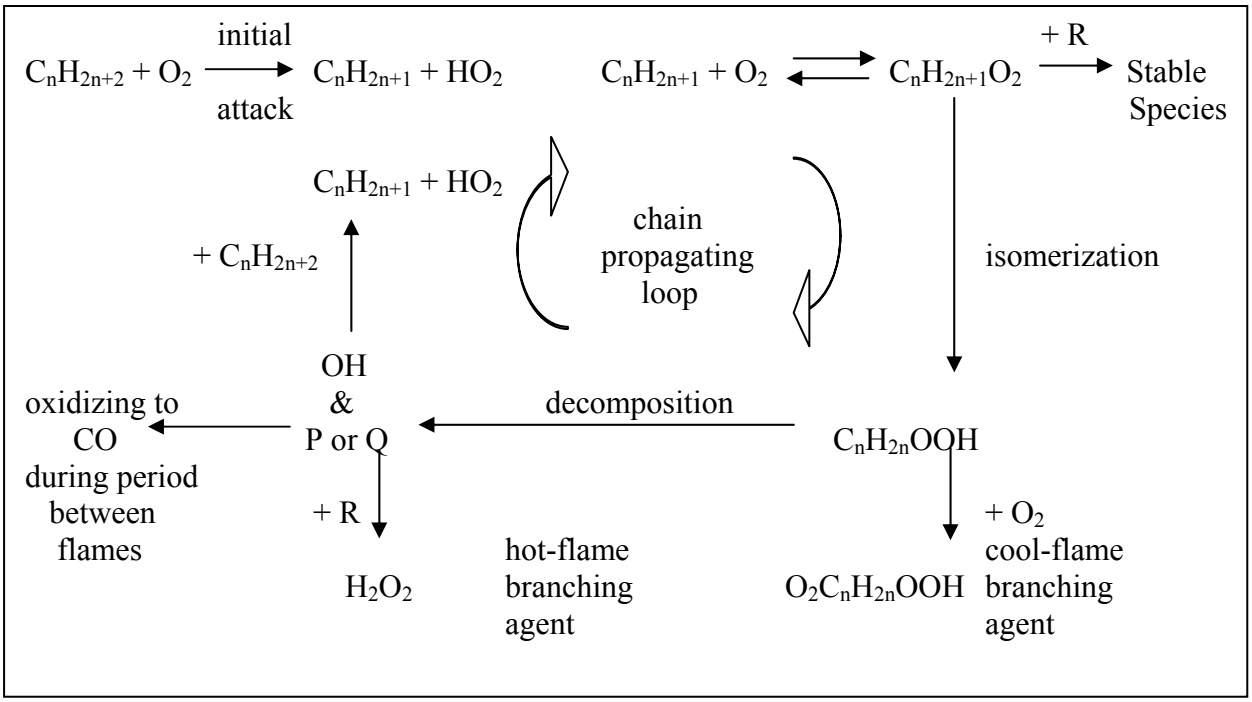

Figure 2-4 Predominant low temperature reaction scheme [17]

Initiation

The first step in consuming the fuel is to generate a radical pool. A typical initiation step is shown in Reaction (2.4). The interaction of a fuel molecule with an oxygen molecule will generate a free alkyl radical and an HO_2 radical. As was shown in Reaction (2.2) the HO_2 radical is an important intermediary on the path to forming OH and initializing the high temperature reactions.

$$\text{Fuel} + O_2 \rightarrow R + HO_2 \qquad (2.4)$$

The hydrogen removed from the fuel will typically be one that is bonded to a tertiary carbon atom because it takes the least amount of energy for a collision to remove atoms at these locations. If there is no tertiary carbon atom, then the oxygen will attack a secondary atom, but these bonds take more energy to break and removing a hydrogen atom from here

will slow down the reaction rate. The reactions will be slower still if the abstraction process is limited to primary carbon atoms.

Alkyl Radical Reactions

There are two primary reaction pathways for the alkyl radical once it has been generated. The first pathway is for the radical to attack a fuel molecule. This would generate an alkyl radical and a small combustion product. The reaction shown in Reaction (2.5) details this pathway. R_1 could be any of the following species: OH, H, O, CH_3, HO_2, CH_3O, O_2, C_2H_5, C_2H_3, CH_3O_2, et cetera. [14, 17]

$$\text{Fuel} + R_1 \rightarrow R_2 + \text{Product} \tag{2.5}$$

The other pathway for the alkyl radical is for it to bond with an oxygen atom as shown in Reaction (2.6). The RO_2 species has an equilibrium constant that is very temperature dependant: for low temperatures the reaction will tend towards forming the RO_2 radical, and as the temperature increases, it trends towards $R + O_2$. It is this temperature sensitivity of the RO_2 equilibrium that causes the NTC behavior of most fuels. [14, 17]

$$R + O_2 \rightarrow RO_2 \tag{2.6}$$

RO_2 Consumption

The RO_2 molecule has three major reaction pathways it could traverse after it has formed. The route that the RO_2 molecule takes is very important in determining much of the auto-ignition characteristics of the mixture. The first pathway for RO_2 to follow involves the chain branching sequence detailed in Reactions (2.7) and (2.8). The species, labeled as R_2H, from which the R_1O_2 molecule abstracts the hydrogen atom, could be any species with a hydrogen atom, but is often a fuel molecule or another alkyl radical. The RO molecule

formed in Reaction (2.8) will go through further reactions to form other radical species and to regenerate an alkyl radical. [14]

$$R_1O_2 + R_2H \rightarrow R_2 + R_1OOH \quad (2.7)$$

$$ROOH \rightarrow RO + OH \quad (2.8)$$

The second pathway for RO_2 is for it to simply decompose back into the original alkyl radical and the oxygen molecule. Decomposition of the RO_2 molecule begins to occur as the temperature increases above 800 K due to the extreme temperature sensitivity of the equilibrium constant for Reaction (2.6). Once the temperature is above 900 K the RO_2 decomposes almost as quickly as it forms which precludes the other pathways for RO_2 consumption. [14]

The third pathway for an RO_2 molecule is for it to extract a hydrogen atom from itself. This occurs when the bending and strain energy in the molecule act to move the O-O radical site near a hydrogen atom in the molecule. The amount of energy needed to perform this reaction is minimal when the molecules are composed of a chain of six or seven atoms. As with the hydrogen abstraction reactions that initiated the low temperature reactions, this abstraction also takes the least energy when the hydrogen atom removed from the main molecule chain is attached to a tertiary carbon atom. The general equation for this mechanism is shown in Reaction (2.9) and a specific example is shown in Reaction (2.10).

$$RO_2 \rightarrow QOOH \quad (2.9)$$

$$C_2H_5O_2 \rightarrow C_2H_4OOH \quad (2.10)$$

Once the QOOH radical has been formed it can degenerate in several ways. The molecule can either shed the entire OOH radical as shown in Reaction (2.11), or the O-O bond can break releasing an OH radical as shown in Reaction (2.12). The Q molecule

formed in Reaction (2.11), turns into a fairly stable olefin, while a QO molecule formed in Reaction (2.12) would turn into a cyclic ether.

$$QOOH \rightarrow Q + HO_2 \quad (2.11)$$

$$QOOH \rightarrow QO + OH \quad (2.12)$$

$$O_2 + QOOH \rightarrow O_2QOOH \quad (2.13)$$

Another possible reaction for QOOH is shown in Reaction (2.13), where an oxygen molecule attaches to the QOOH chain. If this occurs, then the radical would most likely isomerize into a ketohydroperoxide and an OH radical. The ketohydroperoxide is a relatively stable molecule until the temperature reaches 800 K, at which point it will decompose into at least two radicals. It is this reaction pathway that provides the best chain branching sequence in the low temperature regime prior to the sequence detailed in Reactions (2.1) through (2.3). Since sequence from Reactions (2.11) to (2.13) is the major source of chain branching once the RO_2 molecules begin to decompose the chain branching pathways will be cut off. This then causes the reaction rates to slow down which is the explanation for the NTC behavior in fuels that tend to form QOOH radicals. [16]

2.2.2 Some Species Generated During Low Temperature Reactions

The work by Ciajolo [18] can be used as a good reference for the species that are created due to low temperature reactions of n-heptane and isooctane. A 100 cc jet-stirred flow reactor (JSFR) was used to oxidize stoichiometric mixtures of n-heptane at pressures of two bar and residence times of 0.2 s, and isooctane at pressures of 7 bar and residence times of 0.4 s. The reactor's temperatures ranged from about 550 to 700 K for the n-heptane

fueling conditions and from about 600 to 700 K for the isooctane fueling conditions. Fuel conversion efficiencies as high as 60 % for the n-heptane fueling conditions and about 40% for the isooctane fueling conditions, were observed. For both fuels the conversion efficiency dropped off as the temperature increased, which was due to negative temperature coefficient activity. A GC Mass Spec was used to analyze the combustion products.

For the n-heptane a number of species were found in the intake mixture including but were not limited to formaldehyde, acetaldehyde, propionaldehyde, butyraldehyde, Cyclic ethers such as 2-methyl-5-ethyl-tetrahydrofuran, C_7 conjugates such as 1-heptene, and small amounts of 1-hexene, 1-pentene, 1-butene, and propene. Formation of aldehydes occurred at temperatures around 580 K, while temperatures above 600 K tended to yield more species such as C_7 conjugates and cyclic ethers.

For the isooctane species found in the mixture included 2-propanone and C_8 cyclic ethers, the most prominent of which was 2,2,4,4-tetramethyl-tetrahydrofuran [$C_8H_{16}O$]. Trace amounts of species such as 4,4-dimethyl-2-pentanone, 2,4 dimethyl-2-pentene, and 4,4-dimethyl-2-pentene were also found. For isooctane, the onset of cool flame activity and therefore start of oxidation was observed at temperatures near 600 K. The molecules that resulted from these low temperature reactions typically retained the structure of the isooctane molecule. These species are typically cyclic ethers and conjugate olefins such as $C_8H_{17}OO$. Of the resulting cyclic ethers, 2,2,4,4-tetramethyl-tetrahydrofuran is the most likely to be formed since its formation requires the lowest amount of strain energy. Small amounts of aldehydes were also detected at the onset of isooctane oxidation. At temperatures greater than 630 K, the yield of cyclic ethers and olefins decreased in favor of aldehydes and ketones like 2-propanone.

2.2.3 Cool Flames and Negative Temperature Coefficients

A typical characteristic of homogeneous lean burn combustion of many hydrocarbon fuels is termed Negative Temperature Coefficient (NTC) behavior. Figure 2-5 is a plot of heat release from an engine that has been operated on a fuel that exhibits NTC behavior.

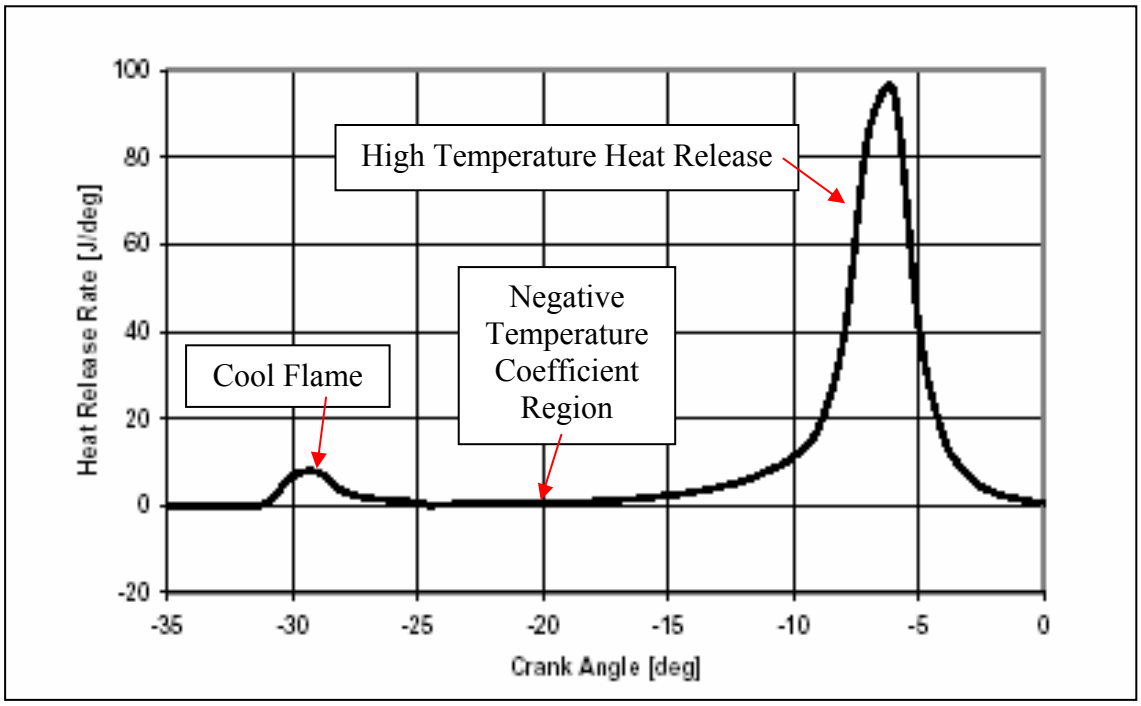

Figure 2-5 Heat release curve exhibiting two stage heat release [19]

The ignition of a fuel is a complex phenomenon, and the onset of auto-ignition is not an easily discernable event. Auto-ignition of a fuel is characterized by rapid increases in pressure and temperature in what is termed a thermal explosion. But prior to these rapid increases in temperature and pressure, the fuel is reacting and releasing energy. A simplified correlation for the onset of auto-ignition is the time where equation (2.1) is satisfied. In the equation, t_i is the time of ignition onset and τ is the ignition delay of the fuel. The ignition

delay is a property of the air/fuel mixture that varies with the temperature and pressure of the mixture. [3]

$$\int_{t=0}^{t_i} \frac{d\tau}{\tau} = 1 \qquad (2.1)$$

An example of how the ignition delay for a mixture changes during the compressions process can be seen in Figure 2-6. In the figure lines of constant ignition delay are plotted as a function of the mixtures temperature and pressure. The red line shown on the plot is a typical trace of the temperature and pressure state of the mixture in an engine. As the engine state moves to areas of smaller ignition delay, the integral in Equation (2.1) comes closer to being satisfied. Once the auto-ignition criterion, from Equation (2.1) has been satisfied, the ignition is said to have occurred.

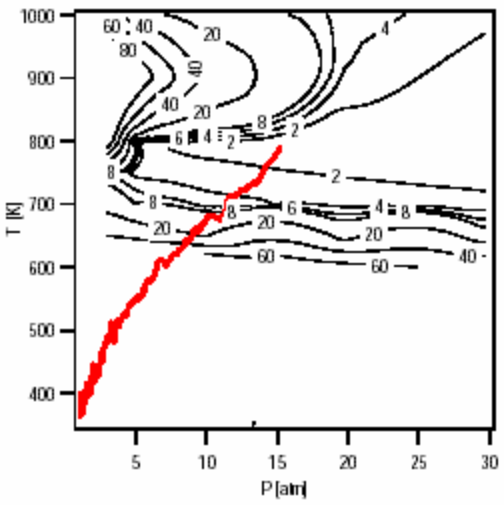

Figure 2-6 Ignition delay as a function of temperature and pressure [20]

Looking at the lines in Figure 2-6 it can be seen that there is a peninsula of lower ignition delay periods. If the engine state were to move out of the peninsula of lower ignition delay into the higher ignition delay area, the rate at which the integral in (2.1) builds toward

unity slows down, and the heat release slows down or even stops. This period of reduced heat release is what is termed the Negative Temperature Coefficient (NTC). Eventually the compression will heat the mixture sufficiently and move the mixture out of this region and into the ignition event. If the mixture temperature does begin to decrease prior to the conditions in (2.1) being satisfied, the auto-ignition is most likely not going to occur.

The small rise in the heat release rate is the result of "cool flame" chemistry, this is energy released by consumption of the fuel by low temperature reactions. The low temperature reactions occur primarily while the charge is below a temperature of approximately 750 K (these reactions will be discussed in further detail in Section 2.2.1 of this chapter). It is not necessary for there to be only one cool flame event. Literature has reported as many as five separate and distinct cool flame reactions, each accompanied by a regime of negative temperature coefficient behavior and finally the primary heat release. [21]

Depending on how fast the temperature increases, it is also possible for the low temperature reactions to transition into the high temperature reactions so quickly that the cool flame chemistry and negative temperature coefficient are undetectable. This is termed single stage combustion and is prevalent for tightly bonded complex fuels. [17] The reasons that negative temperature coefficient behavior appears for some fuels is detailed in the next section.

2.2.4 High Temperature Reactions

High temperature reactions are very dependant upon the cool flame reactions. The ignition delay between the cool flame and the hot flame, or the time spent in the NTC regime, depends upon the intensity of the cool flame. A small amount of cool flame activity leads to a long delay between the cool flame and the high temperature heat release, while large amounts of cool flame activity leads to a much shorter delay between the two reaction regimes. This indicates that the energy released in the early fuel consumption steps as well as the species generated at that time are very important to the high temperature reactions. [15, 17]

High temperature reactions are characterized by rapid decomposition of the carbon bonds in the fuel radical. A general reaction scheme for the high temperature reactions can be seen in the following reaction sequences. [17]

Initialization

$$C_nH_{2n+2} + OH \rightarrow C_nH_{2n+1} + H_2O \quad (2.2)$$

$$C_nH_{2n+2} + O \rightarrow C_nH_{2n+1} + OH \quad (2.3)$$

$$C_nH_{2n+2} + H \rightarrow C_nH_{2n+1} + H_2 \quad (2.4)$$

Thermal Decomposition

$$C_nH_{2n+1} \rightarrow C_aH_{2a} + C_bH_{2b+1} \quad (2.5)$$

$$C_nH_{2n+1} \rightarrow C_nH_{2n} + H \quad (2.6)$$

Chain Branching

$$H + O_2 \rightarrow OH + O \quad (2.7)$$

After the OH concentration has increased to sufficient levels, Reaction (2.7) dominates the chemistry. The formation of water from Reaction (2.2) helps to increase the temperature until the main ignition occurs. Once the temperature has passed 1100 K, the carbon bonds in the fuel radicals begin to thermally decompose, creating smaller alkene radicals, such as ethene, propene, and butene. These reactions are not chain branching but are important for the oxidation of the carbon atoms into CO.

$$CO + OH \rightarrow CO_2 + H \tag{2.8}$$

CO will oxidize to CO_2 through Reaction (2.8), where the primary portion of the energy release occurs. However, CO oxidation is a very slow process compared to the other reactions occurring simultaneously. As has been noted, OH is a very important radical and participates in many of the low and high temperature reactions throughout the combustion process. Reactions that occur at a faster rate than CO oxidation, such as those associated with the initiation steps and water formation, will compete with the CO oxidation reactions for the available OH radicals and will most often win such battles. This means that the oxidation of the CO and therefore the majority of the heat release will not occur until the end of the combustion process. [17]

As the piston begins to move downwards, the cylinder temperature begins to decrease, and it is possible for the reacting mixture to cool below the point where reaction (2.8) can occur. If this happens, a significant amount of CO will be expelled from the engine with the exhaust. Large amounts of CO exhausted from an engine, represents heat release that was not generated and lowers the efficiency of the combustion process.

Section 2.3 Pollutant Emissions Formation and Control

A particular environmental concern that has received considerable attention recently is the depletion of the ozone layer, a thin layer of O_3 molecules located in the upper portions of the atmosphere called the stratosphere. The mechanisms of ozone formation are shown in equations (2.9) through (2.12), where UV-B is radiation with wavelengths between 290 and 340 nm, and UV-C is radiation between 240 and 290 nm. Ultraviolet radiation in the UV-C range is known to destroy some proteins and nucleic acids (RNA and DNA), so the ozone layer is important because it absorbs radiation in the UV-C range, preventing this dangerous radiation from reaching the earth's surface.

$$O_2 \xrightarrow{UV-C} 2O \tag{2.9}$$

$$O + O_2 \rightarrow O_3 + Heat \tag{2.10}$$

$$O_3 \xrightarrow{UV-B\&UV-C} O_2 + O^* \tag{2.11}$$

$$O_3 + O \rightarrow 2O_2 \tag{2.12}$$

Studies show that chemicals such as chlorofluorocarbons (CFCs), which were widely used in industry as refrigerants, solvents, aerosol propellants, and Nitrogen oxide (NO), a common byproduct of combustion, can break up ozone. CFC's break up and release their chlorine atoms ($Cl^{\bullet}$) to attack Ozone, as shown in equations (2.13) and (2.14). The mechanisms through which NO breaks up ozone are shown in equations (2.15) and (2.16).

$$Cl^{\bullet} + O_3 \rightarrow ClO^{\bullet} + O_2 \tag{2.13}$$

$$ClO^{\bullet} + O \rightarrow Cl^{\bullet} + O_2 \tag{2.14}$$

$$NO^{\bullet} + O_3 \rightarrow NO_2^{\bullet} + O_2 \tag{2.15}$$

$$NO_2^{\bullet} + O \rightarrow NO^{\bullet} + O_2 \quad (2.16)$$

$$O_3 + O \rightarrow 2O_2 \quad (2.17)$$

The net result of these sequences, shown in reaction (2.17), is a destruction of an ozone molecule without any absorption of UV-C radiation. Also, the $Cl^{\cdot}$ and NO ions are both regenerated and are free to attack another ozone molecule. The NO and $Cl^{\cdot}$ each remain in the atmosphere for significant periods of time and will continue to break down ozone molecules. This mechanism does not only occur in the upper atmosphere either, ozone can be formed closer to the ground and it will, along with NO, form photochemical smog.

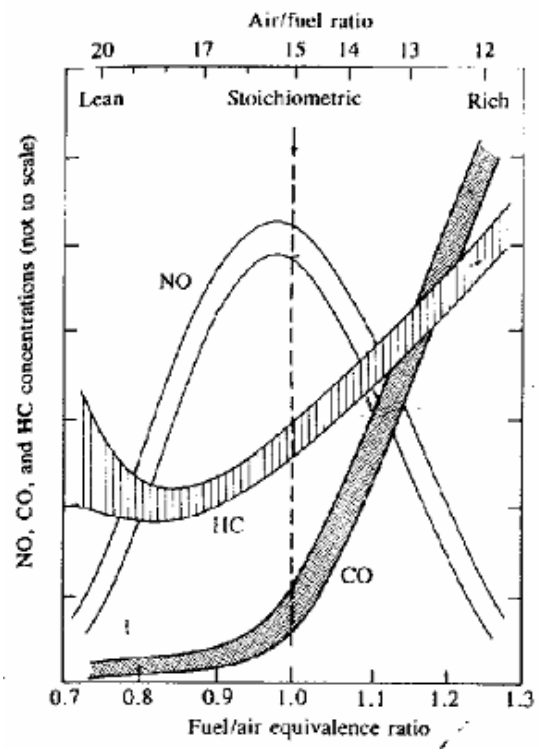

Figure 2-7 Variations of HC, CO, and NO emissions from a spark ignition engine as a function of fuel/air equivalence ratio [3]

Nitrogen Oxide (NO_x) formation is incredibly sensitive to temperature. As combustion temperature increase above 1800 K, the rate at which NO_x is generated increase exponentially. However, for combustion temperatures below 1800 K, little to no NO_x is generated. [10] Therefore, in order to keep NO_x emissions to a minimum, the combustion temperature can not rise above 1800 K. This can be achieved by running the engine in an ultra fuel lean or an ultra fuel rich mode. However, the lower combustion temperatures increase the likelihood of incomplete combustion resulting in increased unburned hydrocarbons and carbon monoxide emissions. The emission generation trends can be seen in Figure 2-7, which qualitatively shows the trends in pollutant generation for a typical spark ignition engine as a function of air/fuel ratio. [3] At fuel rich operating conditions there is not enough oxygen to burn all of the fuel and at fuel lean operating conditions the flame doesn't propagate through the entire cylinder.

The nature of the pollutant emissions also tends to make treating them in the exhaust stream difficult due to the need to perform different actions on the exhaust stream to remove each pollutant. NO_x is an oxygen rich species; so an O atom needs to be removed from the N atom. Carbon monoxide and unburned hydrocarbons are species that are not completely oxidized so it is desirable to add oxygen to these species. Three-way catalytic converters are used to treat all three of the major pollutants simultaneously. One problem with these systems is that they use expensive and rare precious metals in the converter. [10] Another problem is that their conversion efficiency drops off quite quickly if the exhaust composition is outside of a very narrow window corresponding to stoichiometric operation in a spark ignition engine. This problem means that complicated control systems have to be added to the engine to precisely control the air/fuel ratio and reduce emissions. Lastly the efficiency

of catalytic converts decreases over time, which eventually begins to negate the pollution reduction they provided. [3]

Section 2.4 Origins of HCCI

The phenomenon of homogeneous auto-ignition has been known in terms of knock almost since the inception of the internal combustion engine, in fact Niklaus Otto himself is said to have noted a strong noise from his engine as the combustion process destroyed the engine. [22] Most investigations into such auto-ignition trends were focused primarily on how to avoid it. It was not until late in the Twentieth Century that any investigations into the possibilities of using homogeneous auto-ignition to control emissions and raise engine efficiency were performed. In 1979 two papers were published by the Society of Automotive Engineers detailing sustained auto-ignition combustion phenomenon in two stroke engines, these papers are the starting point for most current HCCI research.

The first paper on homogeneous lean burning auto-ignition was written by Onishi et al. [23] In this work the authors were looking at the possibility of using lean air/fuel ratios to reduce the pollutant emissions of a two stroke engine. Exhaust gasses were used to dilute the fuel air mixture, this was done by designing a special scavenging port, in order to retain more exhaust gas in the cylinder than would be retained in a traditional two stroke engine. The results of this change opened up entire regimes of operation where the spark plug could be disabled without adversely affect the combustion, in fact in these regimes it was noted that the combustion was smoother and more consistent than in the regimes where the engine was ran solely on the spark plug. These observations showed that the fuel was auto-igniting in

the cylinder. Onishi et al called this auto-ignition combustion Active-Thermo Atmosphere Combustion or ATAC.

Using Schlieren photography it was shown that while running in ATAC mode the combustion occurred in several different and discernable regions of the cylinder, at nearly the same instant with no discernable flame front propagation. This is contrary to what occurs in a well running spark ignition engine where combustion is initiated only in the vicinity of the ignition source and moves in a deliberate path through the cylinder. The combustion showed less variation in peak pressure and less misfiring cycles when running in ATAC mode and as a result the hydrocarbon emissions were lower then when the engine was run in pure spark ignition mode.

In order to achieve ATAC the gas temperature inside the cylinder had to be raised above a threshold level in order to allow for auto-ignition to occur, this was accomplished by the development of the special scavenging port that allowed more of the hot exhaust residuals to be retained in the cylinder. It was also speculated that the exhaust residuals would be composed of one or more chemical species that would enhance the chemistry and allow an easier auto-ignition of the fuel, possibly by speeding up the initiation reactions. This last speculation has been debated in the literature ever since and over twenty years later has not been proved or disproved. [5, 23, 24]

The other important paper about auto-ignition in a two stroke engine was written by Noguchi et al. [4] In this research an opposed piston engine was operated in auto-ignition mode. The amount of exhaust retained inside the cylinder could be controlled by the location of the exhaust port in the crankcase, the opposed pistons were used in order to improve mixing of the fresh air and the exhaust residual which helped increase the charge temperature

allowing auto-ignition. The study included normal operation of the engine as well as optical work in order to study radical formation during the combustion process.

In addition to the trends that were noted by Onishi et al, Noguchi and coworkers noted that the auto-ignition event occurred at temperatures and pressures that were lower than is typically achieved in a diesel engine. They also noted that the engine achieved higher peak cylinder pressures and temperatures in auto-ignition mode then were achieved in spark ignition mode, also that the combustion duration was significantly shorter than what was observed spark ignition operation.

Photographs of the combustion showed that ignition occurred in two preferential areas, one location was near the exhaust valve where the gas temperatures were higher and the other was near the intake valve where more fresh air and fuel was located. The combustion then would spread in all directions through the cylinder from these two ignition locations. In spark ignition mode combustion was only noted in the area of the spark and then at the propagating flame front. The paper also describes a setup to detect the presence of several radicals in the cylinder; the species tracked were H, OH, HO_2, O, CHO, CH, and C_2. During the tracking of radical formation the species CHO, HO_2 and O were the first species to be noted in the cylinder. The next radicals detected in the combustion process included CH, C_2, and H. OH was the last species to be detected during the combustion development.

The first researchers to study extended auto-ignition operation in a four stroke engine were Najt and Foster. [5] This work used a Cooperative Fuels Research engine to study the performance of an engine operating solely in auto-ignition mode as changes were made to parameters such as compression ratio, speed, intake temperature, and EGR. In their engine,

Najt and Foster noted that the auto-ignition heat release was not like the violent energy release of knock in a spark ignition engine, which can destroy the engine. The HCCI auto-ignition was observed to be a smooth energy release that did not seem to endanger the engine.

The CFR engine did not retain a large fraction of the hot residual gasses like the two stroke engines used by Onishi and Noguchi, therefore the authors used intake air heating to bring the charge temperature up to the point where auto-ignition was possible. EGR could be added to the intake charge by connecting the exhaust pipes to the intake system which would mix the air, fuel, and EGR prior to entering the cylinder. Like the results from the two stroke engines, homogeneous auto-ignition in a four stroke engine displayed very low cyclic variability in peak pressure and IMEP. The research also showed that the ignition properties were very responsive to changes in intake temperature, with higher intake temperatures advancing ignition.

In 1989 Thring published a paper on HCCI research conducted in a Labeco Cooperative Lubricants Research engine. This engine was fueled by either gasoline or diesel fuel introduced in the intake port prior to entering the cylinder. Thring's research was the first to map out a set of operating regimes for an engine running in HCCI mode. It was Thring who first suggested a method for using this combustion technique in an automotive application. The suggestion was to use HCCI in conjunction with spark ignition where auto-ignition would be used at light load steady state operations when it is most efficient, and in spark ignition mode at high load and transient operating conditions where high power output is required.

In the last ten years the amount of research in the area of HCCI combustion has grown dramatically. Research areas have grown from proof of concept work to include aspects such as mapping and defining of operating windows, integration of HCCI with spark and diesel ignition modes, studies of different fuels and additives and their affects on the combustion process, as well as studies into how varying the level of homogeneity affects the combustion. In the following sections some of the primary traits of HCCI combustion will be discussed and then a detailed look will be taken at studies on the effects of homogeneity of the air/fuel mixture on the combustion.

Section 2.5 Types of HCCI Experiments

There are a wide variety of ways to achieve HCCI combustion and many of them have been tested in laboratory experiments. One of the big differences in the various types of experiments performed is the way in which the fuel is introduced into the cylinder. Fuel can be mixed with the air prior to entering the cylinder, either with a carburetor or a fuel injector located somewhere in the intake system, or the fuel can be injected directly into the cylinder. [25-28]

Along with the location of the fuel and air mixing the type of fuel used in HCCI experiments varies widely, engines have been run on standard gasoline, both direct and port injected, almost any combination of isooctane and n-heptane mixtures, diesel fuel both direct and port injected, methane, ethanol, and many other fuels. EGR can be retained in the cylinder to heat the incoming charge and reduce the amount of intake charge preheating necessary to achieve auto-ignition, all of the exhaust can be expelled from the cylinder and

EGR can be cooled and mixed with the intake air before it enters the cylinder, or the engine can be run without any exhaust residuals. Many different intake pressures have been used by running with the intake throttled, unthrottled, or boosted. [29]

Engineers and researchers have also experimented with a number of valve train systems to control the effective compression ratio as well as the residuals that are retained in the cylinder. On top of all of this, any number of parameters can be varied from fueling rate to the timing of the fuel injections, and in systems equipped with variable valve trains the timing of the valve events can also be changed. Studies have also shown that, for regions of less robust and stable combustion, the energy supplied by a spark discharge into the cylinder can aid the combustion development and stabilize the operation of the engine. [30]

The research detailed later in this thesis was conducted in a four stroke gasoline fueled engine with the fuel being introduced in the intake system prior to entering the cylinder. The engine also had a fixed valve train and compression ratio. The following discussion of the trends and tendencies of HCCI combustion will focus on those trends observed when engines have been run under conditions similar to those of the engine used for the research detailed later on in this paper.

Section 2.6 Characteristics of HCCI

HCCI is a combustion phenomenon that relies predominantly upon the chemical kinetics behavior of the fuel and air mixture, this is the first and foremost consideration when looking for a method of controlling the combustion. In HCCI there is no active method of controlling the initiation of the combustion, unlike in the spark ignition engine where the

timing of the spark discharge controls the timing of the heat release or in the diesel engine where the timing of the fuel injection controls the phasing of the heat release. In HCCI the combustion develops along the lines of the reaction scheme laid out previously, if there is not enough energy generated to trigger the high temperature reactions then the engine will run poorly with significant variation in cylinder pressure or it will not run at all.

The fact that the combustion depends upon the auto-ignition characteristics of the fuel means that any changes in the engine or air-fuel mixture that enable the mixture to auto-ignite more easily will enhance the reaction progress, and typically advance the combustion in the engine. Conversely anything that would tend to restrict the auto-ignition characteristics of the fuel-air mixture will likewise retard the combustion in the engine.

Computer simulations of HCCI have shown that the portions of the cylinder where the gasses are the hottest are where the ignition begins initially. As the gasses in the highest temperature portions of the cylinder react, their temperature and pressure rise will compress and heat other portions of the gas in the cylinder causing them to reach their auto-ignition point and react. [7, 31] This process continues until this compression heating effect fails to bring any pockets of cold gas up to their auto-ignition criteria or until all of the fuel has been burned.

When running an engine in HCCI mode the auto-ignition event will most often occur at a point in the cycle that is not the most desirable from the viewpoint of power output and thermal efficiency. Considerable effort has been put into researching methods to control the phasing of the auto-ignition event to the most desirable point in the cycle. The easiest and perhaps most direct way to change the ignition characteristics of the mixture is to change the intake temperature. An increase in charge temperature will enable the charge to reach the

point where the high temperature reactions occur at an earlier point in the compression process. Several studies on the HCCI process document the fact that the combustion is very sensitive to changes in intake temperature. [5, 7] The intake temperature is a suitable control device when the temperature does not change regularly, but current control devices do not allow for rapid changes in intake temperature, certainly not on a cycle-by-cycle basis. For applications where the engine's load and state are very transient, such as automotive applications, then intake temperature does not offer sufficiently fast response times for effective control of the combustion. In applications where the engine does not need to change states often or quickly thermal management may provide sufficient combustion control.

Another way of changing the combustion phasing is to change the intake pressure and/or the compression ratio. [32] As the mass in the cylinder is compressed into a smaller volume its temperature and pressure increases which induces the mixture to auto-ignite. The higher the pressure is at the start of the compression process the higher the pressure and temperature is at the end of the process. As with higher initial pressures, the higher the compression ratio, or the smaller clearance volume, the higher the final pressure and temperature will be which will in turn speed up the reactions and ignite the fuel earlier in the cycle. [33] In early HCCI studies lower compression ratios were employed due to the resulting lower reaction rates, in more recent studies higher compression ratios have been employed in order the reduced need for initial intake charge heating as well as to increase the thermal efficiency of the process. [5, 9, 32, 33]

In modern engines the compression ratio is fixed which would be a problem in duel mode engines, where a high compression ratio would be desirable for HCCI operation but

would generate disastrous knock in SI mode. Until variable valve or compression ratio systems become more viable, compression ratio is not likely to be a widely used control method in production HCCI engines. The use of a throttle and a supercharger could make controlling the intake pressure a viable technique to control the combustion phasing, but there will be efficiency and power losses as a result of employing such a method.

Changing the engine speed affects the combustion in several different ways. Increasing the speed will shorten the amount of time available for heat transfer from the cylinder gasses to the cold walls. Lower heat transfer rates will mean an increase in the gas temperature, which will lower the need for preheating of the intake. However, increasing the speed will also retard the ignition; this is because the chemical kinetics phenomenon involved in the HCCI process take a certain amount of time in milliseconds in which to occur. As the engine speed increases the amount of physical time, in milliseconds, for the reactions to occur is less. This smaller amount of time available for combustion will, in the extreme, preclude any reactions from reaching completing, or even occurring. [5] Ignition will not occur if the temperature of the gasses in the cylinder decreases too much before a sufficient number of radicals have been generated to enable high temperature reactions.

There are several facets of the HCCI process directly related to the mixture inside the cylinder that are very interesting to examine. First of all, because the process does not rely upon the propagation of a flame through the mixture to release the energy, the mixture can be run considerably leaner than a spark ignition engine. Running with leaner air/fuel ratios enables the engine to be run unthrottled. Operation without a throttle reduces the amount of work the engine has to do to expel exhaust from the cylinder and induct in the fresh mixture. As a direct result of running unthrottled more power per unit mass of fuel is available at the

flywheel of the engine, which directly leads to higher thermal efficiencies. Operation without a throttle also raises the initial charge pressure which as noted earlier makes for easier auto-ignition.

A second aspect of combustion related to the mixture goes hand in hand with the first point. Since the mixture is for the most part evenly distributed in the cylinder and is being heated evenly, most of the fuel in the cylinder reaches its auto-ignition point at the same time. This means that a large amount of heat is released into the cylinder within a very short time period. The nearly instantaneous release of fuel energy into the cylinder comes very near to the ideal cycle approximation of constant volume heat release which would be the most efficient that a cycle could be. [7] Though, just like knock in an SI engine, the high rate of energy release can also set up pressure oscillations that emit irritating noise and also pose a potential hazard to the engine's structure. [34, 35]

In order to slow down the reaction rate and lessen the threat to the engine structure it is necessary to run the engine with large amount of diluents in the cylinder, which is another reason to run unthrottled. The diluents can be either excess air or exhaust residuals. However, it is important that there be enough oxidizer in the cylinder for the reactions to go to completion, otherwise the unburned hydrocarbon and carbon monoxide emissions will be too large. Thring could not run his engine at fuel air equivalence Ratios lower than 0.4. [9]

A third aspect of HCCI combustion that is primarily tied to the fuel air mixture properties is the rather low limit on the maximum amount of fuel that can be reacted in the cylinder each cycle. The higher temperatures necessary for ignition to occur reduce the density of the intake air, which reduces the mass of air that can be brought into the cylinder each cycle. The mass of oxidizer in the cylinder of an HCCI engine is considerably lower

than for an identical SI or diesel engine at the same inlet conditions. The low mass of oxidizer limits the amount of fuel that can be inducted into the cylinder while maintaining a globally fuel lean mixture with sufficient dilution to maintain acceptable reaction rates. This limit on the mass of fuel equates to a limit on the maximum possible power out of the engine. This limit on the power output is a major challenge in HCCI combustion research, second only to development of a strategy to adequately control the combustion phasing. One way to overcome this challenge is by increasing the pressure of the intake air to counteract the affect that the high temperature has on the air's density. However, the peak pressures reached in the cylinder will also increase and there is a limit to the peak pressure that an engine will withstand. [36]

The use of internal gas residuals in the cylinder has a significant effect in HCCI combustion as well. The primary objective for using internal EGR is to raise the temperature of the resultant mixture inside the cylinder. The increased temperature in the cylinder means that fresh charge requires less external heating to achieve auto-ignition. The use of internal EGR is a very common way of preheating the mixture to achieve auto-ignition. [28, 37-41] Another benefit of exhaust residuals is that it absorbs some of the energy released during the combustion thus lowering the rate of pressure and temperature rise in the cylinder, this also keeps the NO_x emissions low. Over the years a debate has raged over whether the radicals and partially burned hydrocarbons generated during the combustion help to ignite the gasses during the next cycle, the literature on this topic is for the most part split with little convincing evidence either for or against this theory. However, HCCI seems to be much more sensitive to intake temperature than it is to the exhaust residual composition.

The principle reason for investigating HCCI combustion lies in the reduction of pollutant emissions emitted by an engine operating in this mode. HCCI engines produce little to no NO_x, and for most fuels and fueling rates used in HCCI engine's there is almost no soot emissions either. The reasons for this lie in the lean burn characteristics. Because the air/fuel ratio is very lean and there is a significant amount of diluents in the cylinder the peak temperature achieved during combustion is very low, especially when compared with a diesel of spark ignition engine. NO_x chemistry is very sensitive to the temperature which means that the low combustion temperatures of HCCI inhibit the formation of NO_x. The short burn duration, low cylinder temperature, and homogeneous mixing of the fuel and air also limits the amount of soot that can be formed. HCCI engines do not emit measurable amounts of soot or smoke.

From a pollutant emissions viewpoint a considerable drawback to HCCI is that significant amounts of CO and unburned hydrocarbons are typically emitted from the engine. This is a direct result of the low combustion temperatures that reduce the NO_x emissions. Recent analysis has shown that as the combustion temperatures drop the bulk gasses cool prior to reacting to completion, this yields significant amounts of CO and HC emissions, especially for light load and low intake temperature operating conditions. [26]

The amounts of CO and HC emissions can be reduced through higher intake heating or by lowering the amount of excess air and diluents in the cylinder thereby raising the peak combustion temperature, but conversely this would increase the NO_x emissions. These emissions could also be reduced by preventing the fuel from entering the crevice volumes and areas near the walls where the temperatures are not high enough to allow the fuel to oxide completely. Charge stratification is one method for achieving this goal and will be

discussed in the next section. An oxidation catalyst is also a possible way to remove the CO and HC emissions in a pure HCCI engine but it would not reduce NO_x emissions and therefore would not help a dual mode engine meet regulated emissions levels. A dual mode engine would still have to have an expensive 3-way catalyst which is more effective for removing CO and HC under lean operating conditions.

Despite the fact that HCCI engines can be run at incredibly high air/fuel ratios there is still a limit to how high the air/fuel ratio can be increased. If the amount of fuel is too low then there is not enough energy released nor enough power generation for the engine to overcome its internal friction losses, in such a case the engine would not continue to rotate. In many laboratories the engine speed is maintained constant by a dynamometer which can drive the engine as easily as it is able to absorb the power generated by the engine. This allows the examination of ultra high air/fuel ratios. Results show that even when the combustion is not generating enough power to perpetuate the engine motion HCCI combustion is still very stable with few variations and continues to follow the trends described above. As the air/fuel ratio is raised even more, the engine begins to misfire and the unburned hydrocarbon and CO emissions elevate rapidly. The tendency to misfire occurs because while the fuel molecules in the hottest portions of the cylinder still react, there is not enough heat release in these portions of the cylinder to help ignite the colder portions of the cylinder. The energy released by the fuel that does burn is not sufficient enough to compress and heat the rest of the fuel in the cylinder to the ignition point, the unburned fuel will likely participate only in the hydrogen abstraction reactions. The apparent randomness and variation in the combustion at these conditions is most likely due to cycle-to-cycle variations in the fueling rate as well as the temperature distribution inside the cylinder. The cycle-to-

cycle variations in the amount of internal residual also begin to impact the amount of trapped fuel, as well as the temperature distribution inside the cylinder.

Section 2.7 Air/Fuel Mixture Stratification

One of the principle assumptions of HCCI combustions is that the fuel and air are homogeneously, or uniformly, mixed throughout the entire cylinder. However, no engine actually operates under perfectly homogeneous conditions; even systems where great pains are taken to mix the fuel and air still tend to show significant spatial variations in the mixture. [42, 43] Variations in the intake charge mixedness will yield some regions in the cylinder that are richer, and some that are leaner, than the global air/fuel ratio. The effects of the evaporation of the fuel will then stratify the temperature distribution inside the cylinder.

The richer areas will tend to burn hotter and more completely than the leaner areas. It is possible that the hotter burning rich zones in the cylinder will generate more NO_x than the leaner zones. Several investigations have recently been undertaken to determine if charge stratification can be used to control the performance of an HCCI engine while still yielding the ultra low NO_x emissions that is characteristic of the HCCI process. The effects of temperature distribution are less easy to predict and have been studied less.

The most common way to investigate the effects of air/fuel stratification is to use a fuel injector mounted in the cylinder head to spray the fuel directly into the combustion chamber. Studies have shown that if the fuel injection is completed at or near bottom dead center then the fuel has plenty of time to mix with the air and the engine behaves the same as it would with a fuel injection system introducing fuel into the intake air system. [26, 27, 44]

For direct fuel injection, stratification of the fuel and air has been shown to improve HCCI combustion in certain operating regimes. The conditions where stratification has been shown to be beneficial are typically those of very low load near the lean limit of operation. The lean limit is the area where under premixed operation there isn't enough energy released to completely combust all of the fuel and large amounts of CO and unburned hydrocarbons are emitted from the engine.

The reason that stratification is beneficial at the low loads is thought to be due to the existence of rich regions in the cylinder, which will burn hotter. Higher combustion temperatures will cause the fuel that burns to do so to completion which releases more energy into the cylinder. The higher local energy release in the richer regions will increase the temperature of other regions of the cylinder, this should cause most of the fuel in the cylinder to more completely react when compared to fully mixed operation at the same global air/fuel ratio. Marriott and coworkers were able to use the timing of the injection of the fuel to at least partially control the onset of combustion demonstrating that air/fuel stratification, coupled with thermal stratification, may provide a way to control the HCCI process. [44]

On the other hand, stratification induced by direct injection has been shown to have few positive effects when the engine is running near to the rich limit. In fact stratification most often has detrimental effects at the rich limit. For the most part studies have shown an increase in CO and HC emissions at the rich limit, as well as a degradation of the combustion stability. [26, 27] The current theory as to why this occurs focuses on the fact that the fuel is directly injected into the cylinder. As the amount of the fuel injected increases the penetration length of the spray increases, which eventually leads to the fuel spray impinging

upon the wall of the cylinder. Any fuel that hits the cylinder wall will adhere there, and while some of the fuel will vaporize and burn most will stay on the wall. This leads to poorer operation of the engine and higher pollutant emissions output. The investigations into the effects of stratification generated by direct injection provide insight into the ways that air/fuel stratification changes the combustion process. Any stratification generated, in this type of system, is primarily a function of the time that it takes the fuel spray to breakup into droplets, vaporize, and then mix with the air as well as the swirling motion of the gasses in the cylinder.

In port injection systems stratification of the fuel and air is generated in several ways. First there is unmixedness from the spray breakup just like in the direct injection system. Also unmixedness can result from the flow of the fresh charge into the cylinder. The mixture entering the engine possesses velocities in many directions causing it to swirl through the cylinder. Depending on where and when the fuel is injected into the intake stream, as well as the injection duration, the fuel could enter the cylinder with the first air into the engine just after the valve opens, somewhere in the middle of the intake stroke, or with the last of the air to enter the engine. Depending on when the fuel enters the cylinder a layering effect could be generated that might trap the fuel in a layer of gasses in the cylinder, isolating it from other regions in the cylinder. After the fuel has entered the engine the gas motion will then determine the distribution of the fuel throughout the cylinder and also its temperature prior to combustion. All of these factors then go into determining how the combustion event will progress. There are very few papers studying how stratification generated with a port injection system actually affect the HCCI process but each one deserves some careful

consideration as the research presented in the rest of this paper was focused on this very issue.

The effects of the port fuel injection location, on the engine emissions and cylinder pressure, were researched by Girard et al. [42] The work consisted of using a specially developed probe to measure the radial distribution of the fuel in the intake pipe as well as inside the cylinder, the results of these distribution measurements were then correlated to the engine's performance. The fuel was injected into the intake in two locations, the first was 120 cm away from the inlet valves and the second was 40 cm away from the intake valves. It was expected that when the fuel was injected at 120 cm it would be better mixed than when it was injected 40 cm from the inlet.

The engine used in this work was a Caterpillar Model 3401 single cylinder research engine with a displacement of 2.44 liters and a compression ratio of 16.25. The engine had a symmetric shallow bowl piston geometry with a four valve cylinder head. The speed was maintained at 1800 RPM for all tests and the intake pressure was kept at 1.7 bar with a temperature of 420 K. There were two fuels used in these experiments. The first was propane and the second was methane. The use of a gaseous fuel is advantageous because it should remove any possible thermal effects that could be caused by fuel vaporization.

The primary goal of the experiment was to test the probe for measuring stratification and to quantify the level of uniformity for the two injection points. The detector consisted of a small diameter tube leading to an absorption cell through which a laser beam was passed, the beam then hit a collector on the other end of the absorption cell. The intensity of the laser beam incident on the collector is an inverse function of fuel concentration, as the concentration of the fuel increases less of the beam makes it through the absorption cell to

the collector. The probe's axial position in the intake runner or the cylinder was changed and a reading of the spatial variation of the fuel concentration was achieved.

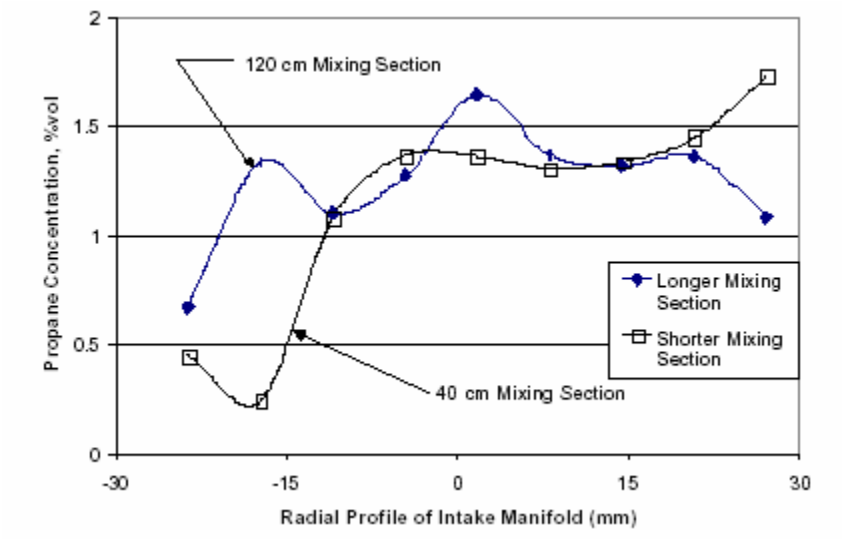

Figure 2-8 Radial profile of fuel concentration in the intake manifold [42]

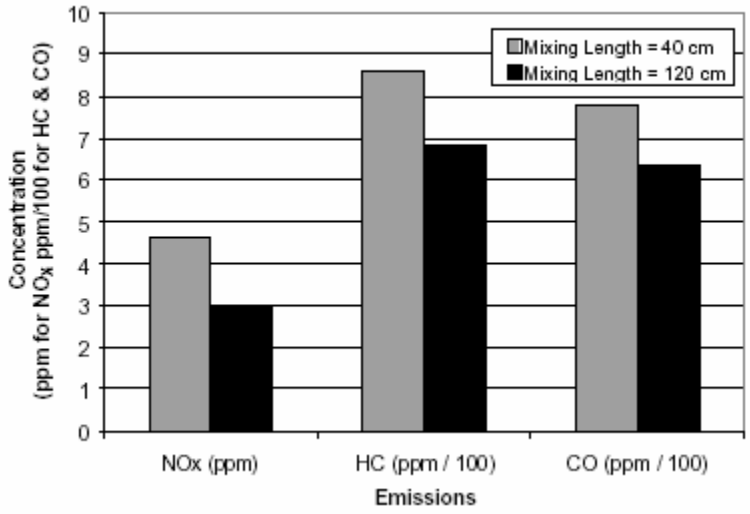

Figure 2-9 Emissions trends for engine run with two fuel introduction locations [42]

The sampling probe confirmed the expectation that unmixedness of the air and fuel entering the cylinder decreases with longer mixing distances and time. This trend can be seen in Figure 2-8 which shows the radial concentration of propane in the intake manifold

measured for both injection locations. Emissions trends were shown for operation of propane for both of the injection locations. The magnitude of the NO_x, HC, and CO emissions all increased when the fuel was more stratified, these trends are shown in Figure 2-9.

A pressure trace included in the results shows that the phasing and magnitude of the cylinder pressure did not change with the fuel injection location. The authors do, however, note a change in the IMEP value from 5.1 bar at the 120 cm injection point to 5.0 bar at 40 cm. Simulations were also conducted that indicated that changes in mixedness would not affect the combustion phasing or magnitude significantly. It is interesting to note that the authors saw a decrease in cycle-to-cycle variations in the peak pressure value as the level of mixing increased; this seems to imply that the mixedness may affect the variability of the combustion process.

The effect of spatial variations in the intake charge on HCCI combustion was also investigated by Richter et al. [43] Unlike the work performed by Girard et al, the two locations of the fuel injection were established so that one was at the head through a conventional port, and the other was upstream of a mixing tank located in the air stream. The mixing tank was used to stir the air and fuel in order to form a uniform mixture. This work utilized imaging by planer laser induced fluorescence (PLIF) to study the position of the fuel in the cylinder as well as the formation of OH during the combustion process.

The PLIF study was performed with acetone as the fuel dopent. Acetone was used as the dopent because it begins to vanish as the combustion begins which means that it can be used as a marker of the unburned areas in the cylinder. Imaging of the OH formation was done because the OH exists in the largest quantities during the high temperature reactions

and is the key to quickly breaking down the fuel, thus images of the location of OH can give key information about the flame development.

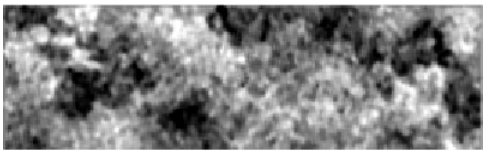

Figure 2-10 Image of fuel distribution for a port injection setup [43]

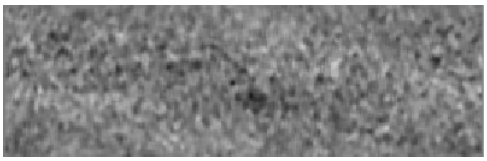

Figure 2-11 Image of fuel distribution for a mixing tank setup [43]

The engine used in this study was a Volvo TD-100, six-cylinder engine with all but one of the cylinders deactivated; the engine had also been modified to allow for optical access. The compression ratio for this experiment was 10 and the engine had a displacement of 1.6 liters, and a pancake combustion chamber. PLIF images were taken of the fuel in the cylinder with the engine running in each of the two mixing configurations and then were compared. The port injection fueling system showed greater spatial variations in the cylinder as would be expected; images of the fuel distribution for the port injection setup as well as for the mixing tank setup are shown in Figure 2-10 and Figure 2-11 respectively.

Interestingly the images of the combustion formation showed no trends relative to the level of mixedness. The images of the OH formation throughout the cylinder show that the combustion initiation has a large spatial variation for both fuel preparation methods, i.e. the location of the start of combustion showed no dependence on the level of mixing of the air and fuel. This implies that the fuel homogeneity is not responsible for the start of combustion and will not affect the combustion phasing significantly. Examples of these spatial variations can be seen in Figure 2-12.

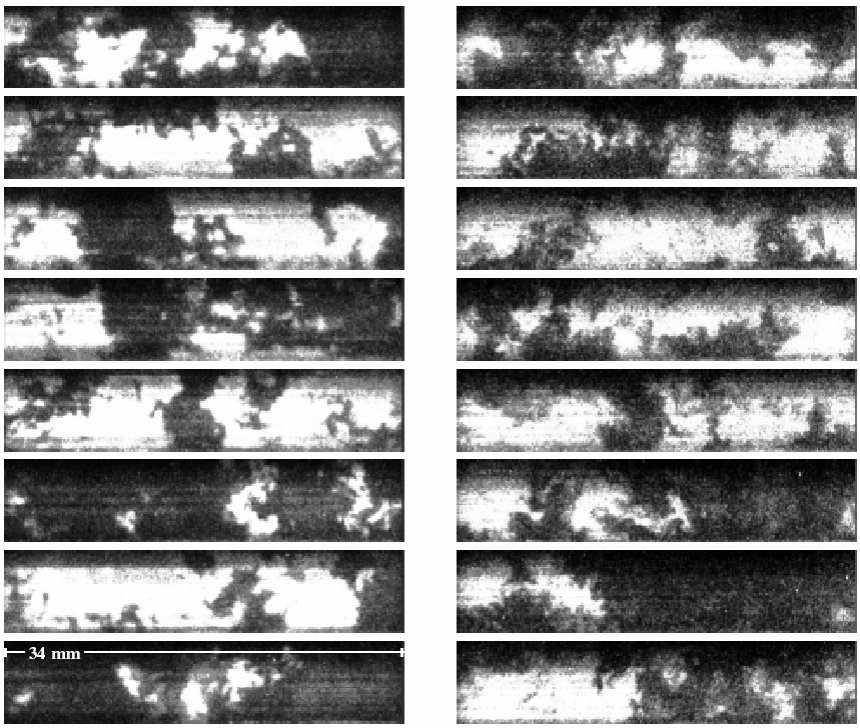

Figure 2-12 Photographs of OH distribution during HCCI combustion. The left hand photographs are different cycles for the standard port injection case. The right hand photographs are different cycles for the mixing tank case. [43]

Chapter 3 - Experimental Setup

The experimental work conducted in this laboratory will be done so on two venues, one being standard engine tests to study combustion phenomenon, the other being optical visualization work conducted in a specially constructed see-through engine. The test cell has been constructed to accommodate two engines and much of the experimental setup detailed in this section applies to both engines. However, no work with the optical engine is to be presented here, so future researchers will detail the setup and operation of the optical engine. This section will focus solely on the standard engine and data collection systems setup.

Section 3.1 Mechanical Systems

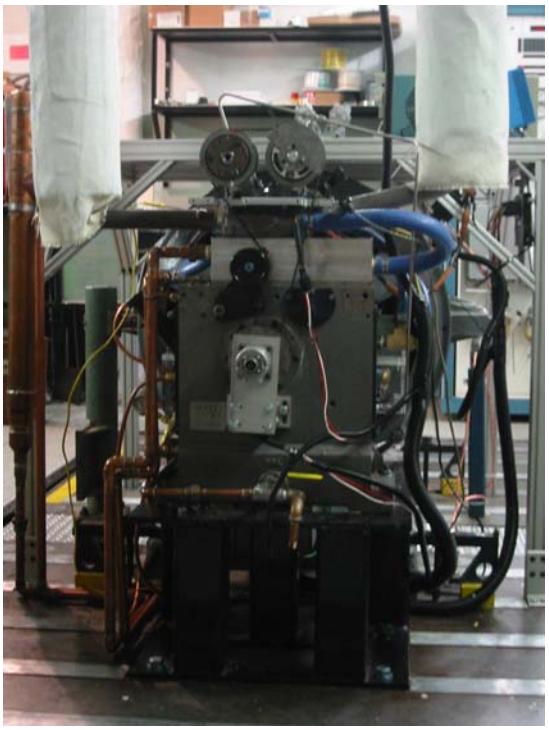

Figure 3-1 Standard engine

3.1.1 Engine

The engine used in these experiments is a single cylinder four-stroke engine built on a Ricardo Hydra block with a cylinder liner adaptor bolted onto the block; the head mounts to the bore adapter. The cylinder head used in this experiment was originally designed for a spark ignited, port fuel injected engine. The cylinder head was provided by General Motors Research and was originally used in the development of the General Motors L850 engine. The head has four valves actuated by a belt driven dual overhead cam system.

Several cams with various geometries and lifts were provided by General Motors but for the work presented here only the baseline production cams were used, the baseline cam profile is shown in Figure 3-2. For archival purposes the other cam profiles can be found in **Error! Reference source not found.** of the appendix. Different valve timings can be investigated by changing the phasing between the cam and the belt driven pulley, but care must be taken to avoid valve and piston interference. For this work only a single set of valve timings was investigated. The properties of the engine are listed in Table 3-1.

Compression Ratio	10.95
Bore	86 mm (3.39 in.)
Stroke	94.6 mm (3.72 in)
Displacement	550 cm^3 (33.58 in^3)
Clearance Volume	50.18 cm^3 (3.06 in^3)
Connecting Rod Length	152.5 mm (6.00 in)
Top Land Height	3.6 mm (0.142 in)
Intake Valve Diameter	30.0 mm (1.184 in)
Exhaust Valve Diameter	35.1 mm (1.382 in)
Exhaust Valve Open	131 dATDC (589 dBTDC)
Intake Valve Open	350 dATDC (370 dBTDC)
Exhaust Valve Close	375dATDC (345 dBTDC)
Intake Valve Close	595 dATDC (125 dBTDC)

Table 3-1 Standard engine geometry

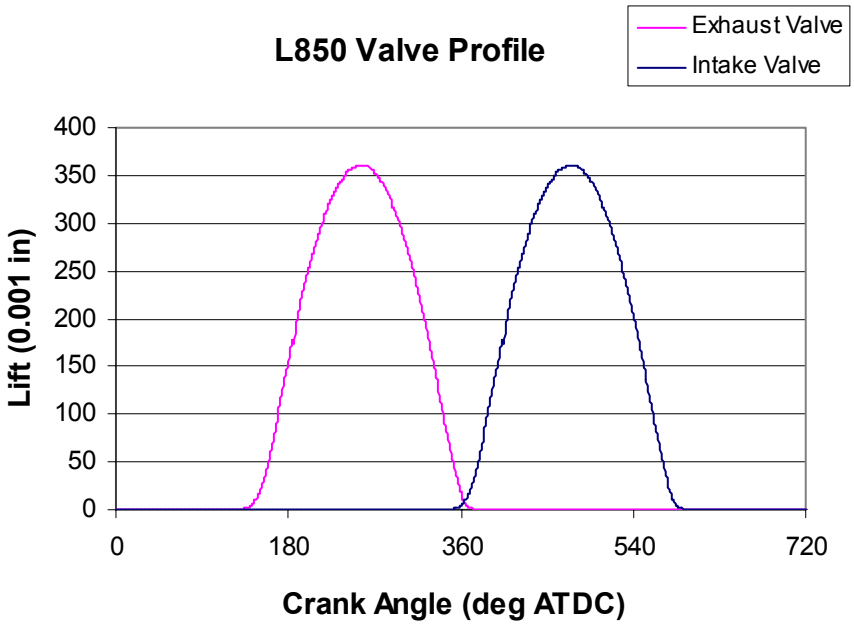

Figure 3-2 Valve profile

3.1.2 Dynamometer and Engine Coupling

The dynamometer used for load control is a General Electric DC double-ended dynamometer capable of absorbing 74.5 kW (100 HP). The dynamometer is rated for a maximum speed of 4000 RPM. Control of the motor is performed with a Dyne Systems Co. DYN-LOC IV digital control system. More information about the DYN-LOC IV system can be found in reference [45]. An Omega LC101-2K strain gauge load cell, which can absorb up to 8900 N (2000 lbs) of force, is attached to the motor to measure torque generated by the engine. Due to the large size of the dynamometer, and the windage losses associated with a motor so large, all brake specific calculations are close to zero and will therefore be omitted from the results presented in this thesis. The engine and dynamometer speed is controlled using a remote controller unit located in the test cell.

The dynamometer is capable of running both clockwise and counter clockwise. The direction of the dynamometer rotation is selected with a DIP switch setting in the controller power box located in room B129 of the ERB building. The engine valve train cannot be driven in the counterclockwise direction without damaging the cams. It is essential to always make sure that the correct dynamometer direction has been selected before starting the dynamometer. To prevent damage to the engine valve trains there is only one engine connected to the dynamometer at any time.

The engines are coupled to the dynamometer with a Falk Wrapflex™ coupling system, the basic components of this system can be seen in Figure 3-3. The coupling is a flexible hard rubber element that joins two metal hubs; one hub is taper fit and keyed to the dynamometer shaft while the other hub is attached to the flywheel of the engine. Removing the engine coupler consists simply of loosening the cover over the rubber element and pulling the coupler element away from the metal hubs. This design is very compact and allows for a minimal distance between the engine and dynamometer, which allowed two engines to be placed in the test cell. Also with this coupler design disconnecting the engine from the dynamometer and switching between the two engines can be performed very quickly.

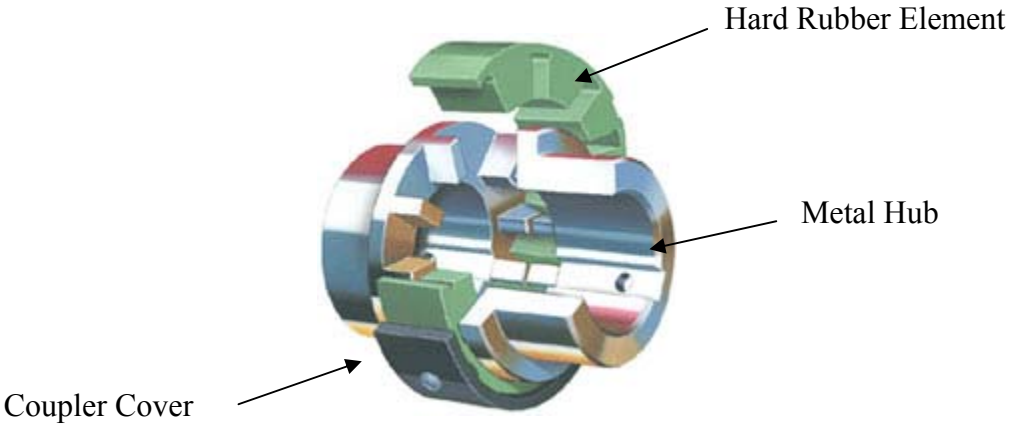

Figure 3-3 Wrapflex™ coupling system

3.1.3 Coolant

The engine cooling system is a closed loop system consisting of a pump, a heat exchanger, a water reservoir, an immersion heating element, the engine, and an overflow reservoir. Cooling water is circulated around the cylinder head and then around the cylinder liner, the flow then travels into a reservoir and is finally supplied to the pump. Flow from the pump goes through a heating element and then back to the engine. The complete system is shown schematically in Figure 3-4.

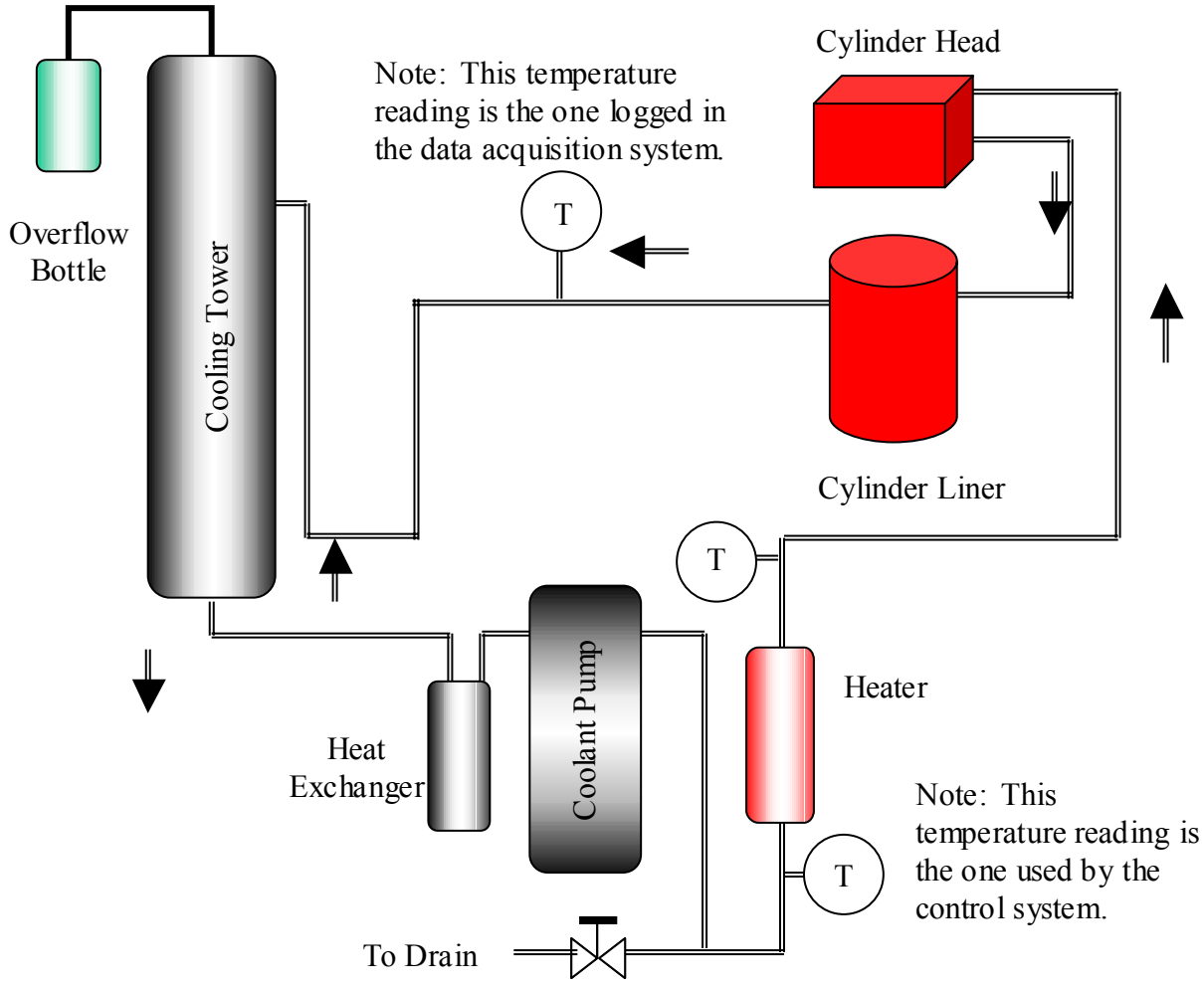

Figure 3-4 Engine coolant system

The working fluid of the system is a mixture of 50 % distilled water and 50% ethylene glycol antifreeze. The operating temperature of the engine coolant is controlled to 95 ºC (203 ºF). In order to decrease the warm-up time of the engine, prior to operation of the engine the working fluid is circulated through the engine with the immersion heater turned on. Preheating the coolant warms up the engine components before engine operation begins and allows the experiment to quickly reach steady state.

Once the coolant has achieved the operating temperature, a shell in tube heat exchanger cooled with city water is used to maintain this temperature. The city water is pulsed through the heat exchanger using a solenoid valve controlled by an Omega i-series dual output temperature controller. This unit controls both of the solid-state relays that send power to both the immersion heater and the solenoid valve, thus the one unit can be used to control both the heating and cooling of the water and ethylene glycol mixture.

Good control of the coolant temperature was achieved by monitoring the temperature at the pump. This thermocouple location allowed good temperature control but, is too far from the engine to be used as an accurate monitor of coolant temperature entering the engine. A thermocouple located at the outlet of the engine was recorded by the data acquisition system in order to keep track of the performance of the engine. Once the engine had reached steady state, the coolant temperature was always within a range of temperatures from 93 to 95 ºC (199 - 203 ºF).

The pressure in the system is regulated using a standard automotive radiator cap that has been soldered onto the top of the coolant reservoir. When the pressure in the system rises above 70 kPa gauge (10 PSIG) a relief valve opens and some of the coolant moves into an overfill bottle. When the pressure drops the subsequent vacuum in the reservoir draws the

coolant from the overfill bottle back into the cooling tower. All of the lines to and from the pump are ¾" OD copper tubing. The lines into and out of the engine are 5/8" ID high temperature silicone hose, which was used because it is flexible. The cooling tower is constructed of 2" low carbon steel pipe, steel was used for the cooling tower because suitable fittings could be found for steel construction but not for copper.

3.1.4 Lubrication

The standard engine lubrication system consists of a pump, a filter, a relief valve, a heat exchanger, a block mounted heater, and the engine. The gear pump pressurizes the oil and moves it into a heat exchanger. After the heat exchanger the oil is filtered and an adjustable pressure relief valve maintains the system pressure by relieving excess oil into a sump in the block. After the relief valve the oil is sent into an oil gallery in the block. The Ricardo Hydra block has an internal oil gallery that supplies oil to passages drilled in the block for lubricating the crankshaft as well as the connecting rod bearings. The oil lines to the cam shafts in the cylinder head also are supplied by this same oil gallery. The bearings and the cam shafts all drain back into the oil sump in the bottom of the block. The oil drains from the sump back to the inlet of the gear pump. This sequence is shown schematically in Figure 3-5. The oil supply lines are constructed from 3/8" stainless steel tubing in order to withstand the high pressures. The return lines are constructed of ¾" copper tubing to facilitate drainage back to the pump; smaller tubing sizes do not allow for sufficient flow back to the pump and result in cavitation.

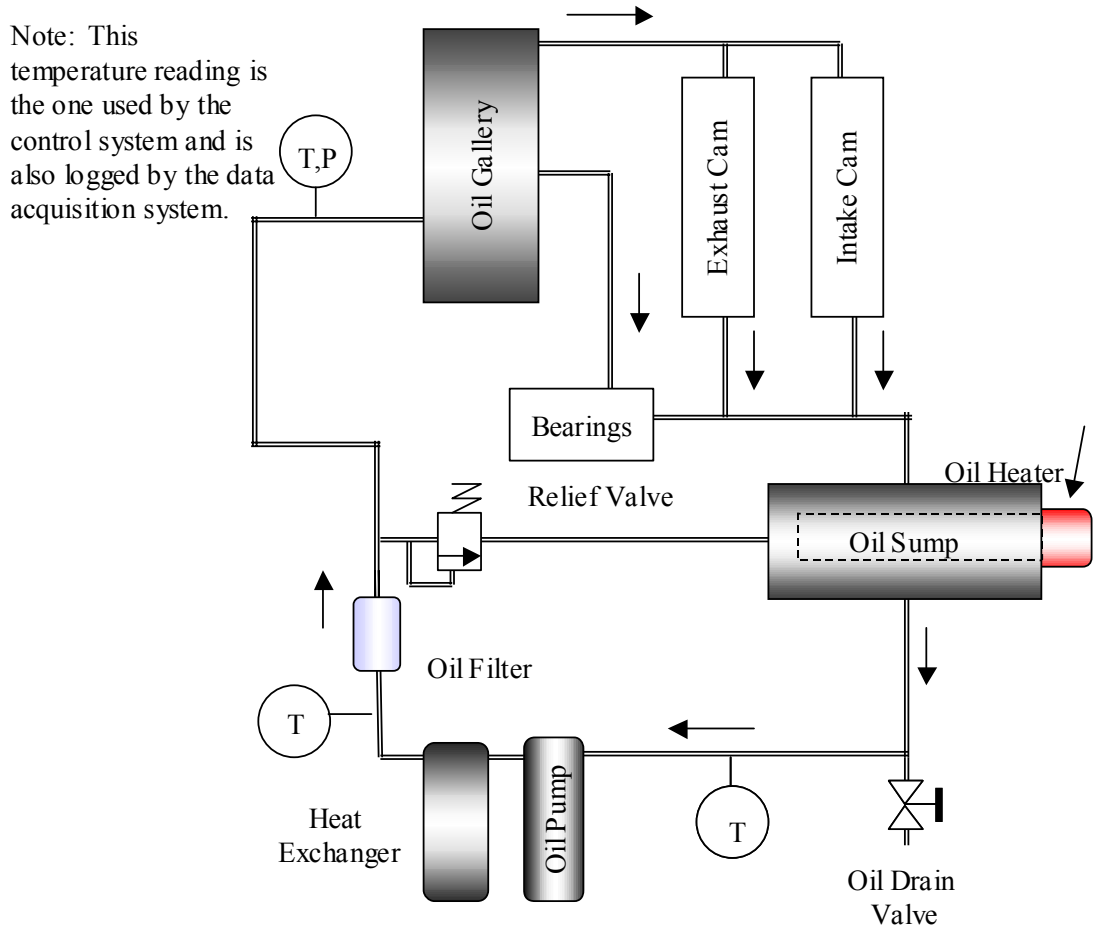

Figure 3-5 Engine lubrication system

The fluid used in the engine is a standard 15W-40 engine oil which can be purchased at any automotive parts store. The filter used on the engine is NAPA part number 21515. A 110 V 1000 W oil compatible immersion heater is installed in the sump and is used to warm the oil to the operating temperature. In order to control the oil temperature a shell and tube heat exchanger is installed in the supply line. The heat exchanger is cooled with city water pulsed on and off with a solenoid valve. An OMEGA dual output i-series controller is used to control both of the solid state relays sending power to the heater and the solenoid valve controlling the city water flow. The operating temperature of the oil is 90 ºC. Once the oil

temperature and the engine have reached steady state the oil temperature was in a range from 87 to 90 ºC (176 to 194 ºF).

The pressure in the system is controlled by an adjustable relief valve that relieves oil into the sump when the pressure increases above 310 kPa gauge (40 PSIG). The oil pump also has an integral relief valve incorporated as a fail safe, the cracking pressure of this valve is adjustable but need to be set so that it does not actuate for more than 10 seconds, otherwise damage to the pump may result. The maximum outlet pressure that the pump can generate without sustaining damage is 690 kPa gauge (100 PSIG). The pressure in the supply system is measured with an Omega PX212 pressure transducer, this value is used as a safety check, an Omega i-series controller constantly monitors this value and will cut the power to the fuel pumps, as well as the electronic engine control system, if the oil pressure drops below 210 kPa gauge (30 PSIG).

Mounted to the oil sump is a sight glass that allows for checking the oil level. If the oil level drops far enough to expose the immersion heater then damage can occur to the heater so it is important to maintain a certain amount of oil in the system. Currently there is no indication of any oil consumption or leaks but this may change with time and engine wear. The oil level gauge can only be read when the oil sump is not under vacuum. To check the oil level the oil filler cap needs to be removed. This causes the crankcase pressure to be atmospheric and the oil will fill the sight glass indicating the oil level in the sump. There is a line on the glass indicating the minimum amount of oil that should be maintained in the system. There is also a line indicating the maximum amount of oil that can be in the system without the crankshaft moving through the oil and aerating it.

Section 3.2 Air and Fuel Delivery Systems

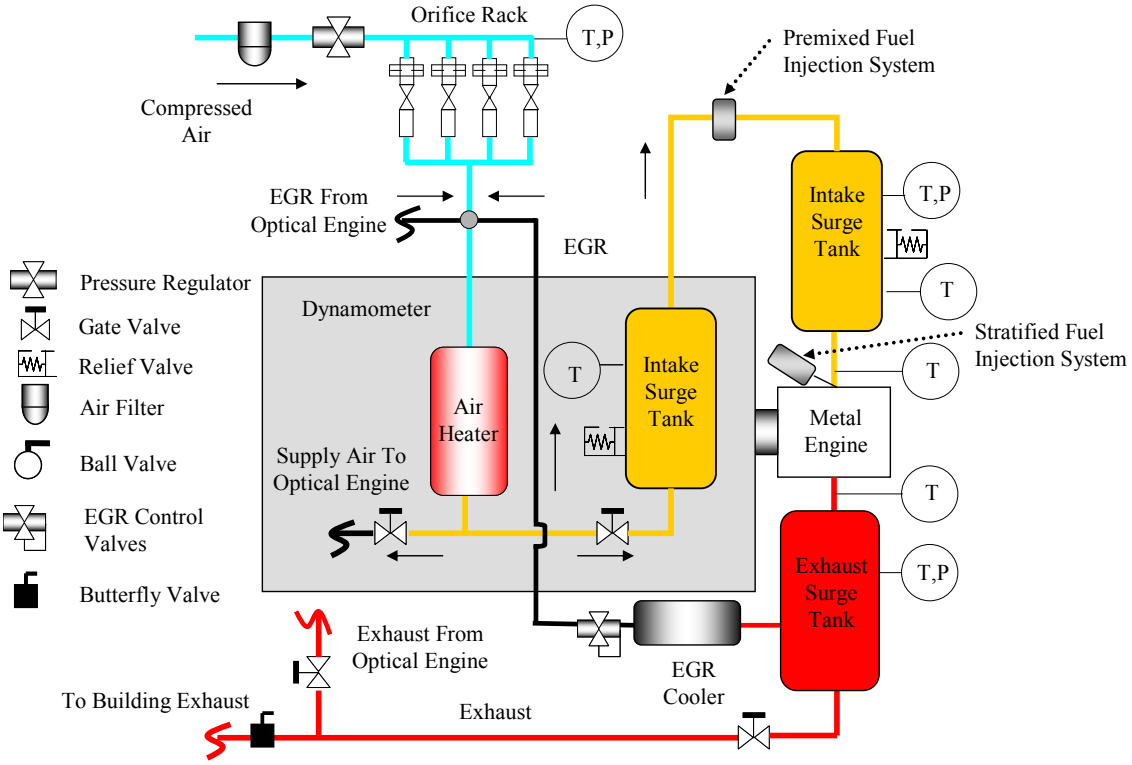

Figure 3-6 Metal engine air flow schematic

The intake and exhaust air systems were designed with several important aspects in mind. First of all in order to accommodate two engines air, fuel, and exhaust had to be routed to both engines with the flow to either engine being shut off when it was not in operation. Secondly in order to achieve HCCI combustion without the use of exhaust rebreathing strategies the intake air had to be heated to high temperatures. Therefore the pipes and joints had to be able to withstand high temperatures. Accommodations also had to be made to heat the pipes and air up to the desired temperatures. The exhaust system would naturally be at high temperatures and so those pipes also had to withstand heating as well as any corrosive gasses from the engine. Finally care had to be taken to prevent leaks into or

out of either system, if a leak develops then the measurements taken in the experiment are distorted and there is also a potential safety hazard from any exhaust leaks.

3.2.1 Intake Air

The fresh air supplied to the engine originates from compressed air supplied to the laboratory by an external compressor. The air is filtered prior to entering the intake system and the flow rate is regulated through the use of a pressure regulator and a calibrated orifice system. The air is mixed with cold EGR from the engine and then heated with an inline heater. The stream then moves into a surge tank where it mixes. After leaving the surge tank there is a fuel injector that is used to introduce fuel into the system. The mixture then flows into another surge tank where it again mixes before moving into the intake runner and the engine.

The compressed air is supplied at a pressure of approximately 585 kPa gauge (85 PSIG). The temperature of the compressed air is room temperature approximately 21 ºC (70 ºF) and the dew point temperature of the stream is 5 ºC (40 ºF). The airflow to the engine is metered through one of four calibrated critical flow orifices; the orifice is selectable based upon the amount of airflow needed by the engine for a specific test. The mass flow through the orifice is calculated from a calibration curves for the orifices. These calibrations can be seen in Figure 3-7.

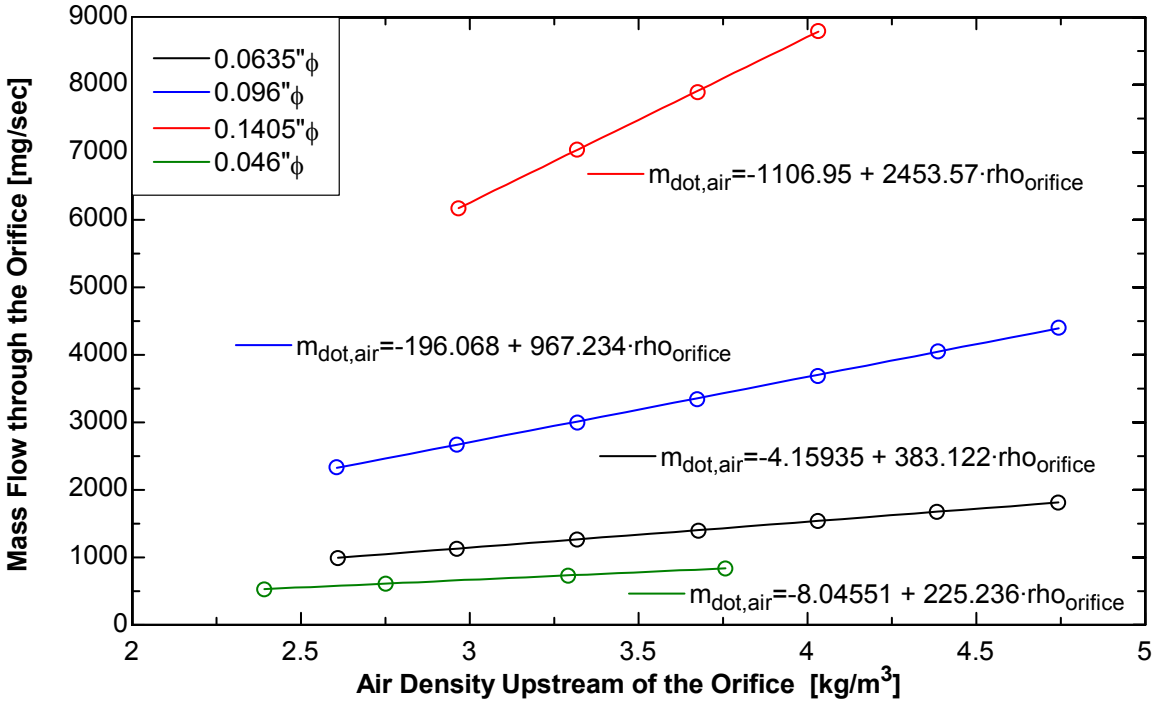

Figure 3-7 Critical flow orifice calibrations

The air pressure upstream of the orifice is monitored and controlled by a Newport Micromega CN77000 controller which receives a signal from an Omega PX212 pressure transducer. The controller uses a PID routine to output a 4 to 20 mA control signal to a Parker Pneumatics VIP-F pneumatic control board. The control board outputs a pneumatic pressure signal, proportional to the input current, to a pneumatically controlled pressure regulator which controls the air pressure and density at the orifice inlet. When operating at steady state the orifice upstream pressure is in a range of plus or minus 1 kPa (0.15 PSI) of the set point pressure.

Measurements of the upstream pressure and temperature for calculating the amount of flow through the orifices are obtained from a Dresser DXD model combination pressure transducer and thermocouple. This unit has a pressure range of 0- 690 kPa absolute (0-100

PSIA) and a quoted measurement accuracy of 0.02%. The Dresser transducer has higher accuracy, than the PX212 pressure transducers, and also has no tendency to drift.

Prior to the inline heater the intake system is constructed of 1" OD copper tubing. The temperatures of these gasses are at room temperature so there is no need for any other type of material. Also correctly soldered and rigidly mounted copper tubing has a lower tendency to leak. After the intake heaters low carbon steel pipe was used. Copper could not be used, after the heater, because the high intake temperatures would melt the solder out of the joints in a copper tubing system. In order to take care of any alignment and vibration issues several stainless steel flexible hoses were installed in the system as well.

The two surge tanks installed in the intake system are 37.9 Liter (10 gal) steel tanks, which is approximately 65 cylinder volumes per surge tanks. The tanks provide two useful functions, the first is that the tanks provide is to damp out pressure pulses generated during the intake stroke. The other is mixing of the gasses before entering the engine, while the mixing is not very large or effective it is one more area where the gasses mix prior to entering the engine, which helps keep the spatial gradients of the mixture components, entering the engine, to a minimum.

As is shown in Figure 3-6 the premixed fuel is added to the air stream in the pipe between the two surge tanks, this is a distance of over 1.5 meters from the inlet of the engine. The remote distance of the fuel injection allows for thorough mixing of the fuel and air but also provides a large volume of premixed fuel and air that is often at elevated temperatures. In order to ensure laboratory safety a Kemp model FA70-G flame arrestor is installed in the intake system to prevent flame propagation past the first surge tank. This is the closest to the engine that the arrestor could be placed. Also a two inch diameter 340 kPa (50 PSI) pop off

safety valve has been installed in each of the intake surge tanks and vented to the building's engine exhaust system. These valves relieve any building pressure that would be associated with ignition of the fuel in the intake. The surge tank, closest to the engine, also has a 690 kPa (100 PSI) relief valve installed as a backup for the 340 kPa valve.

3.2.2 Intake Air Heating

The intake air is heated in two ways, first it is passed over an inline heater for an initial temperature rise and then it is heated up to the desired operating temperature by the intake air pipes that are heated by external band heaters. A diagram of the intake air heating system is shown in Figure 3-8. The inline air heater is a 3000 W 240 V Chromolox GCHI model heater. The heater is controlled in an on-off manner with an Omega i-series dual output controller. The controller pulses a 110 V signal to a mercury displacement relay that controls the flow of the 240 V electricity to the heater. The primary function of this heater is to help keep the temperature of the air uniform through the intake system. Due to a lack of available control units this heater is controlled by the same controller that manipulates the intake air temperature in the intake runner. This controller receives a temperature signal from a thermocouple in the intake runner which is noted as T_{in} in Figure 3-8. Because the thermocouple reading being used to control the inline heater is very far away from the heater, it is important to keep a close watch on the gas temperatures in the first surge tank (T_{g3}) to make sure that the air entering the first surge tank isn't being heated too high.

To speed up the time it takes for the air temperature entering the engine to reach the desired temperature the air is heated by several heater strips wrapped around the intake pipes

and surge tanks. There are three types of heater strips installed in the system, the first type is a 63.5 mm X 3.05 m (2.5 in X 10 ft) 2351 W 240 V heater strip, the second type is a .25.4 mm X 2.44 m (1 in X 8 ft) 1256 W 240 V heater strip, the third and final type of heater is a 2.44 m long 400 W 110 V rope heater.

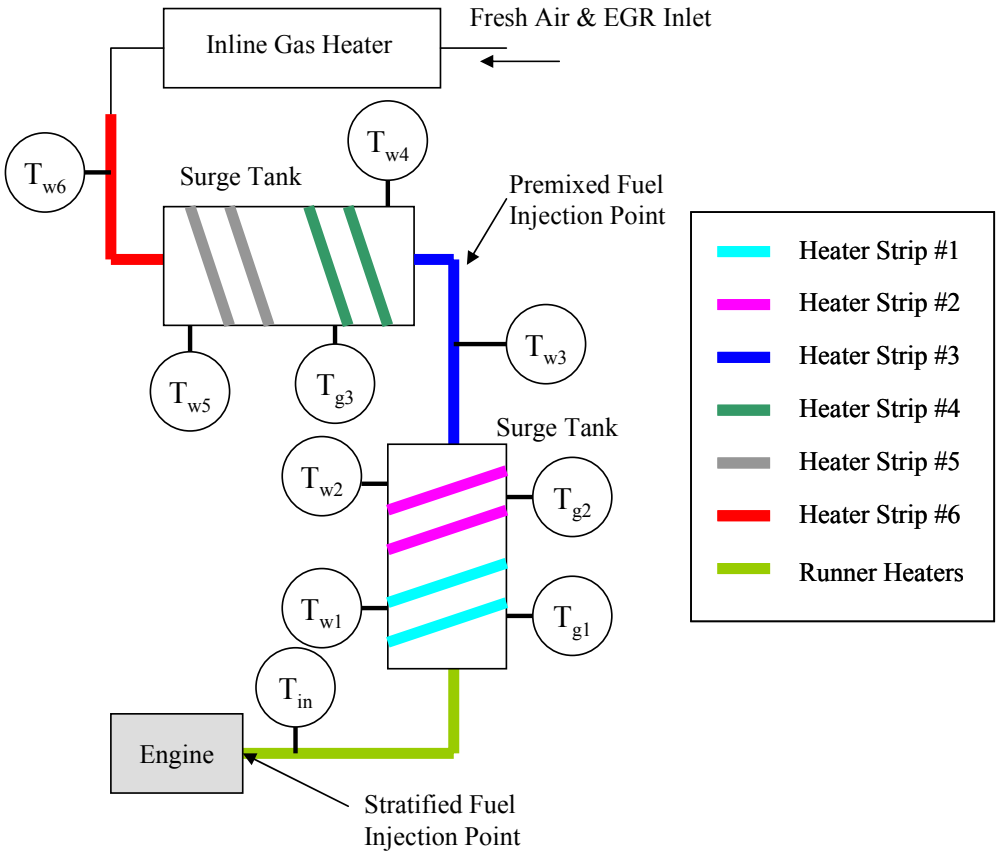

Figure 3-8 Intake air heater layout

In total there are six heater strips wrapped around the intake system components and two rope heaters wrapped around the runner. Figure 3-8 shows the locations of each of the different heaters in the intake system. Also Table 3-2 details what type of heater is used at each location. The 25.4 mm X 2.44 m heaters were purchased to replace some of the 63.5 mm X 3.05 m that had been damaged due to excessive heating during the initial setup of the

system. Omega does not keep the higher wattage heaters in stock and the turnaround time was deemed to excessive to wait for exact replacements so the closest available heater strips were purchased and installed.

Heater Designation	Width	Length	Wattage
1	25.4 mm (1 in)	2.44 m (8 ft)	1256
2	63.5 mm (2.5 in)	3.05 m (10 ft)	2351
3	63.5 mm (2.5 in)	3.05 m (10 ft)	2351
4	63.5 mm (2.5 in)	3.05 m (10 ft)	2351
5	63.5 mm (2.5 in)	3.05 m (10 ft)	2351
6	25.4 mm (1 in)	2.44 m (8 ft)	1256
Runner	-	2.44 m (8 ft)	400

Table 3-2 Inlet heater strip properties

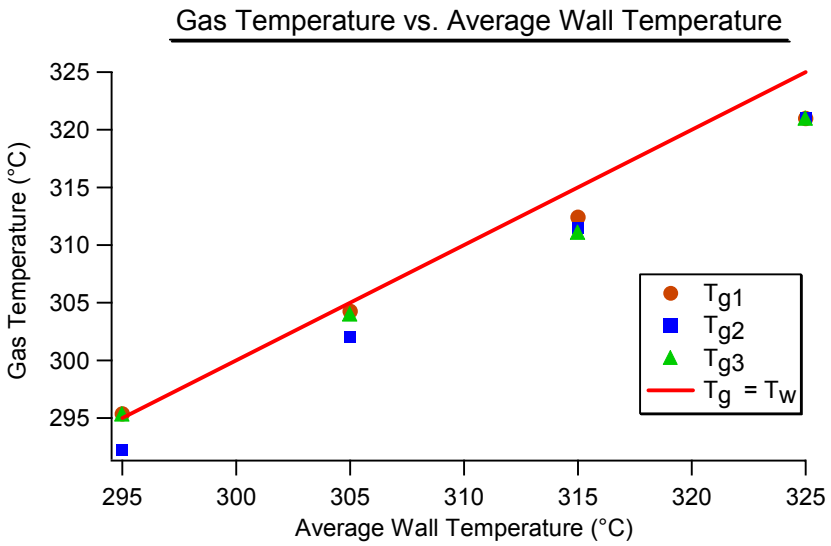

Figure 3-9 Gas temperature response for changes in intake pipe temperature

An Omega CN616 controller is used to control the heater strips. It has the capability of controlling six individual temperature zones. In this setup each of the six heater strips, not wrapped around the runner, is controlled as an individual and independent temperature zone.

The thermocouples denoted $T_{w1} - T_{w6}$ in Figure 3-8 are cemented to the outside of the intake pipes and surge tanks, they monitor the wall temperatures at each of the heater strips and are used by the CN616 to control a temperature zone. The thermocouples denoted T_{g1}, T_{g2} and T_{g3} are located in the center of the gas stream and measure the temperature of the gasses as they flow through the system. The capability of control of the system is shown in Figure 3-9 where the temperature of the intake gases is plotted against the average temperature of the six thermocouples located on the walls of the intake system.

Conduction to the cylinder head causes a significant drop in the intake air temperature as the gas moves through the runner; the rope heaters are wrapped around the runner to counter this heat loss. These heaters also provide the ability to perform fine tuning of the intake temperature just before the gasses enter the engine. They are controlled by an Omega i-series temperature controller. The controller receives an input signal from a thermocouple located in the runner about 14.5 cm (5.75 in) upstream of the intake valves and uses a PID routine to actuate a solid state relay that regulates the flow of electricity to the rope heaters. The heaters are wired together in parallel and controlled together. The PID routine in the Omega controller is only able to maintain the temperature to within three degrees Celsius below the set point temperature and 1 degree Celsius above the set point valve.

3.2.3 Exhaust Air

The exhaust is expelled from the engine and travels through the runner to a mixing diffuser. A portion of the gas is drawn into the emissions bench for analysis, the rest of the gas travels into a surge tank. Another portion of the gas is then drawn back into the intake

system as EGR; the rest of the gas is drawn into a building exhaust fan that directly expels the gasses into the outside atmosphere.

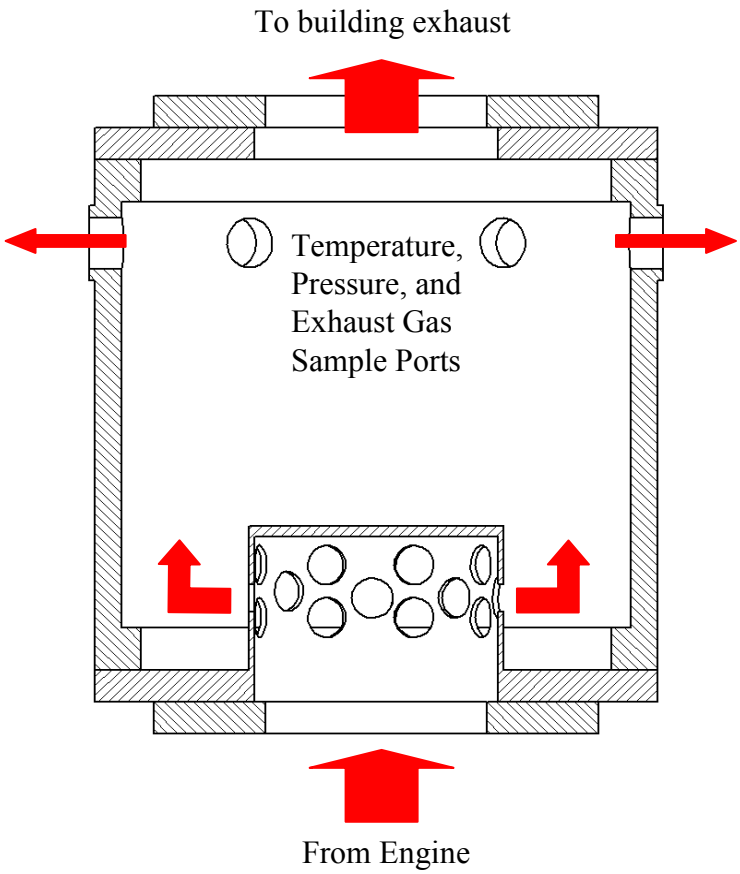

Figure 3-10 Exhaust gas diffuser

The mixing diffuser is installed to cause the exhaust gasses to mix thoroughly before being drawn to the emissions bench; this ensures that the measurement of the emissions is an accurate representation of the emissions being formed in the engine. Figure 3-10 is a diagram of the exhaust mixing diffuser.

The building exhaust system maintains a pressure of approximately 97 kPa absolute (14 PSIA) as measured at the mixing diffuser. For the experiments detailed in this paper, this pressure was not changed, however it is possible to raise the exhaust pressure at the engine.

The gate valve installed just after the surge tank normally acts as a shut off when the engine is not running, however it is possible to use the valve as a coarse control of the exhaust pressure. There is also a pneumatically controlled butterfly valve installed in the system that can also be used to control the exhaust system pressure. This valve is currently manually controlled but it would be possible to control this valve with a Parker Pneumatics control board and Omega PID controller system similar to the one that is used to maintain the upstream pressure of inlet critical air flow orifices constant.

3.2.4 Exhaust Gas Recirculation (EGR)

It is often desirable to mix exhaust gas with the fresh intake charge, the exhaust gas can be used to dilute the fuel concentration which slows reaction rates. Also due to its higher specific heat the exhaust gas will reduce the temperature rise in the engine.

In order to induct external EGR into the intake system a venturi is installed in the intake pipes. The venturi has a reduction in area of 95 percent. The system was sized to induct 50% EGR at a speed of 3000 RPM and atmospheric inlet air conditions. EGR levels greater than 60% were achieved at lower speeds and fueling conditions. A diagram of the venturi is shown in Figure 3-11. The fresh air enters the tee from above and moves into the reduced area where it accelerates, the acceleration causes the pressure at the exit of the EGR tube to be lower which induces EGR to flow from the left hand side towards the lower pressure area and mix with the fresh air. The mixed EGR and fresh air then move to the surge tanks.

The venturi is installed in the portion of the inlet system that is constructed of copper pipe therefore the exhaust gas must be cooled prior to moving into the copper pipes or else

the hot gasses would melt the solder in the joints between the pipes. A spare EGR cooler from a Ford Motor Company engine was retrofit to be installed in the experiment, the original ends have been removed and flanges were welded to the heat exchanger's body, steel pipes connect the cooler to the exhaust surge tank and copper tubes lead from the cooler to the venturi. The heat exchanger is cooled with city water pulsed on and off by a solenoid valve that is controlled by an Omega i-series controller. The i-series controller receives a temperature signal from a thermocouple installed immediately after the EGR cooler, the set point temperature of the controller is 85 °C, which is well below the solder's melting point. The EGR is then heated with the rest of the intake air as it travels into the engine, thus the external EGR does not alter the inlet charge temperature. There is no water trap installed in the EGR line so the combustion generated water vapor is brought back into the intake of the engine.

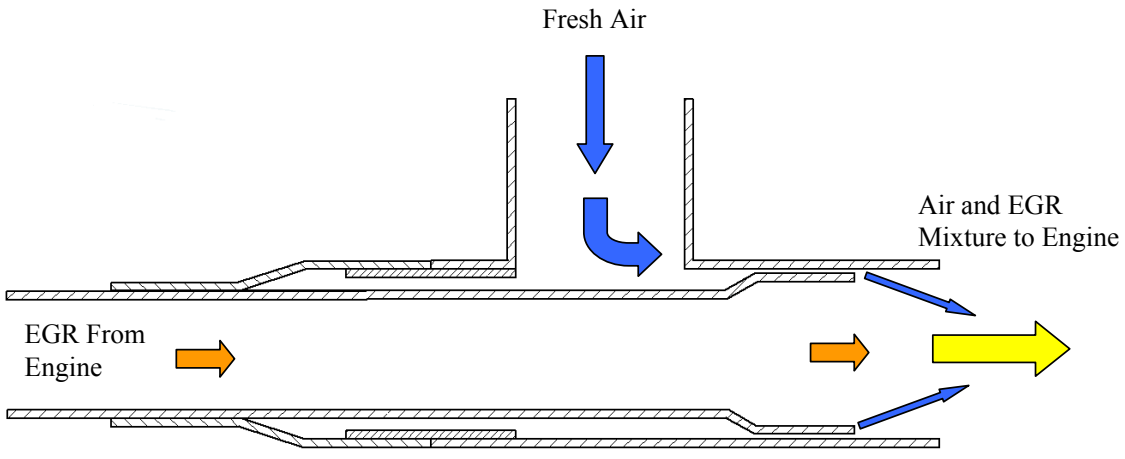

Figure 3-11 Venturi configuration

The percentage of external EGR inducted into the engine is defined in equation 3.1. The ambient carbon dioxide volume fraction is measured in the inlet surge tank at the start of the day, before any exhaust has been inducted into the intake, it is then assumed that the amount of ambient CO_2 does not changes through out the course of the day's tests. The emissions bench has two CO_2 analyzers so air is constantly drawn from the inlet surge tank and the EGR fraction is continuously monitored throughout the course of an experiment.

$$EGR\% = \frac{CO_{2,In} - CO_{2,amb.}}{CO_{2,Exh} - CO_{2,amb}} \times 100 \qquad (3.1)$$

3.2.5 Fuel Delivery

Fuel is delivered to the engine through the use of an air assisted fuel injection system manufactured by the Mercury Marine company for use on their OptiMax direct injection two-stroke engines. This system is used because the air assist injector helps to atomize the fuel as it is injected, this causes the fuel to mix with the air very effectively. The OptiMax fuel delivery system consists of a low pressure fuel pump, a high pressure fuel pump, a fuel injector, and an air assist injector. Two fuel flow meters have also been installed in the system. Figure 3.2 is a diagram of the fuel delivery system.

The fuel is removed from a storage tank and pumped through the fuel flow meters by a low pressure carburetor pump, it then enters the high pressure pump which sends the fuel to the injectors. When the fuel injector opens it discharges the fuel into a cavity in the air injector, when the fuel injector has closed the control system waits a period of 4 ms and then opens the air injector, the fuel and a small amount of air then flow through the air assist injector into the primary air stream.

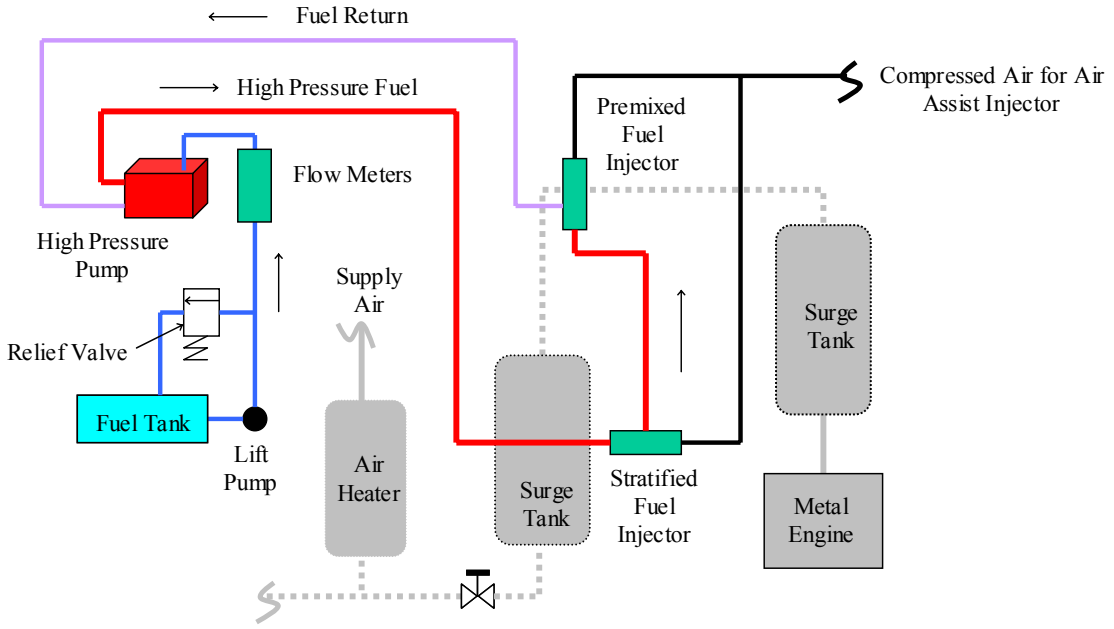

Figure 3-12 Fuel flow schematic

The high pressure fuel pump consists of a fuel filter, a float bowl, a medium pressure pump, and a high pressure pump. The fuel leaves the lift pump and flow meters and enters the filter in the high pressure pump assembly where it is immediately deposited in the float controlled reservoir. The medium pressure pump draws fuel from the reservoir and sends it to the high pressure pump. Fuel is constantly circulated between the high pressure pump and the fuel injector, thus the high pressure pump has a supply of fuel from the injector rail and from the medium pressure pump, the mixture of the two streams is pressurized again and then sent back to the fuel rail. The injector rail has a differential pressure regulator that maintains the fuel pressure 70 kPa (10 PSI) higher than the pressure of the air supplied to the air assist injector, typically 550 kPa gauge (80 PSIG), in other words the fuel pressure is typically 620 kPa (90 PSIG). A diagram of the fuel pump is shown in Figure 3-14 and a diagram of the fuel rail is depicted in Figure 3-13.

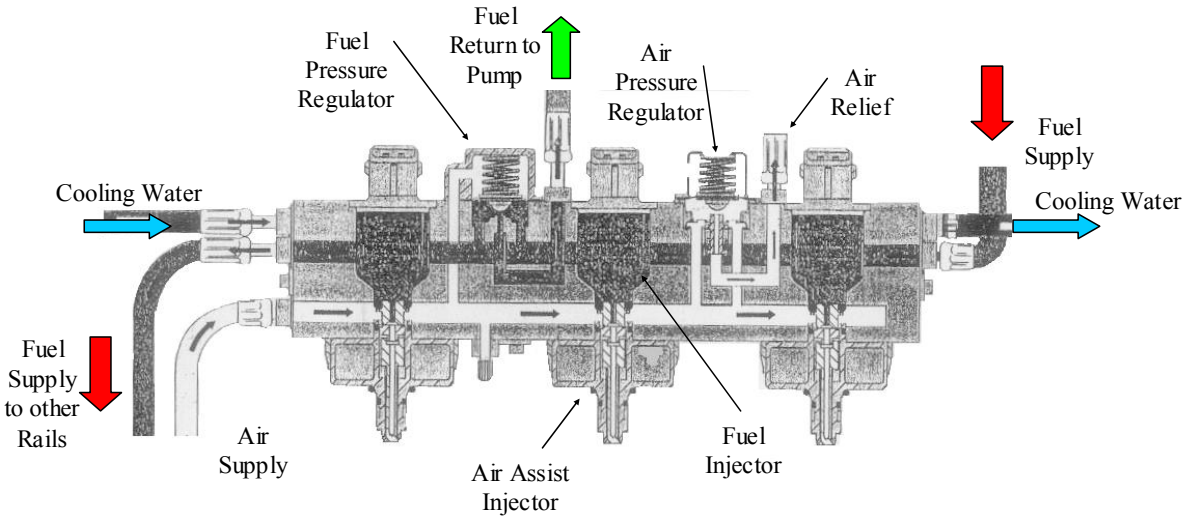

Figure 3-13 OptiMax fuel rail

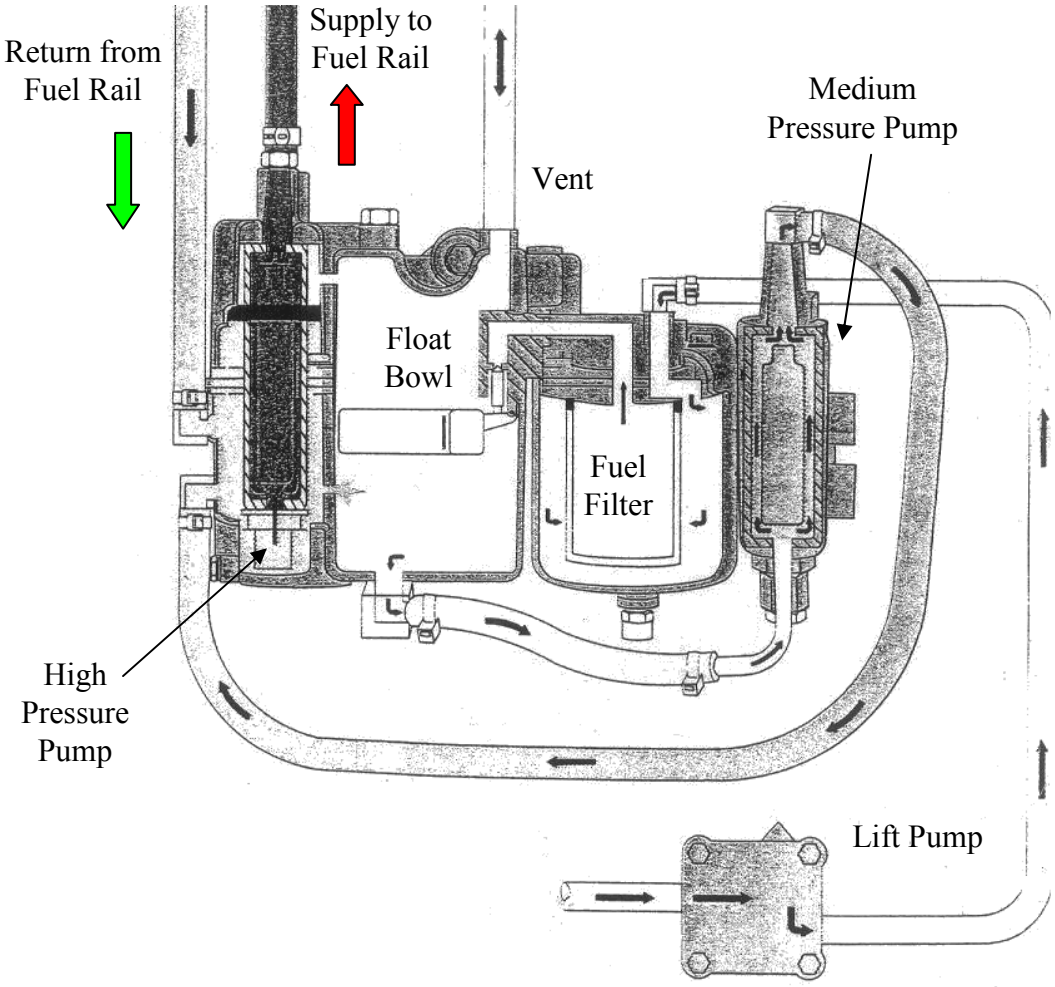

Figure 3-14 OptiMax fuel pump

The amount of air that travels through the air assist injector depends on several factors including the length of time the injector is open, the amount of fuel being injected, and the supply pressure, which isn't always constant. The amount of air injected along with the fuel is not always negligible and will affect the measured air/fuel ratio, therefore an Omega PMA-A2309 mass flow meter is installed in the supply line. The meter outputs a voltage signal proportional to the mass flow through the meter, this signal is supplied to the data acquisition system and monitored throughout all tests.

As is shown in Figure 3-14 the high pressure fuel pump assembly has a float bowl installed in it. The float will prevent flow from the low pressure lift pump into the high pressure pump assembly when the level in the pump's storage tank is too high. This means that the low pressure pump has a significant amount of time where it is dead headed and builds up pressure in the line leading to the fuel pump. To prevent damaging the lift pump a relief valve has been installed in the line. The relief valve directs the flow of fuel back into the supply tank whenever the float bowl in the pump assembly has shut off the fuel flow.

3.2.6 Premixed Fuel Delivery

The premixed fuel is delivered to the engine by utilizing the OptiMax fuel injection system, without any modifications, as it is shown in Figure 3-13. The goal of this setup is to generate the most homogeneous mixture as possible. To ensure thorough mixing of the fuel with the incoming air, the fuel injector is mounted in the intake pipe between the two surge tanks, a distance of over 1.5 meters from the intake valves. The fuel injectors are also pointed against the direction of the air flow.

3.2.7 Stratified Fuel Delivery

In order to investigate the effects of fuel stratification in the intake air on HCCI combustion a second fuel injector system was constructed. The setup consisted of a standard OptiMax fuel injector rail injecting fuel into a heating chamber. The fuel is heated above the vaporization temperature so a gas phase fuel injector was used to regulate the flow of fuel vapor into the cylinder. In order to achieve the highest possible levels of stratification of the fuel and air, a hypodermic tube was used to direct the fuel to a specified location in the intake system.

Figure 3-15 Clean Air Partners injector

The flow of fuel vapor into the intake system is controlled by a Clean Air Partners SP051D1 model gaseous injector, which is shown in Figure 3-15. This injector is a solenoid actuated poppet valve and is designed to control the flow of fuel in natural gas fueled engines. The injector opening time and duration is controlled by a 12 volt pulse-width modulated signal.

The gaseous injector is mounted in an adaptor installed into the standard port fuel injector opening in the cylinder head. The adaptor has a 3.175 mm (1/8 in) tube with a 2.362 mm (0.093 in) ID installed in it that allows the fuel injected to be directed to the place in the

intake where the beginning of the fuel and air mixing is desired. The tube has a length of approximately 63 mm (2.5 in.). Figure 3-16 is a diagram of the mounting block for the CAP injector. The mounting block is designed to allow for different hypodermic tips to be installed in the system. Different tips allow for several different levels of fuel air stratification to be generated and the fuel flow to be directed at either of the intake valves, or almost any other point in the intake port.

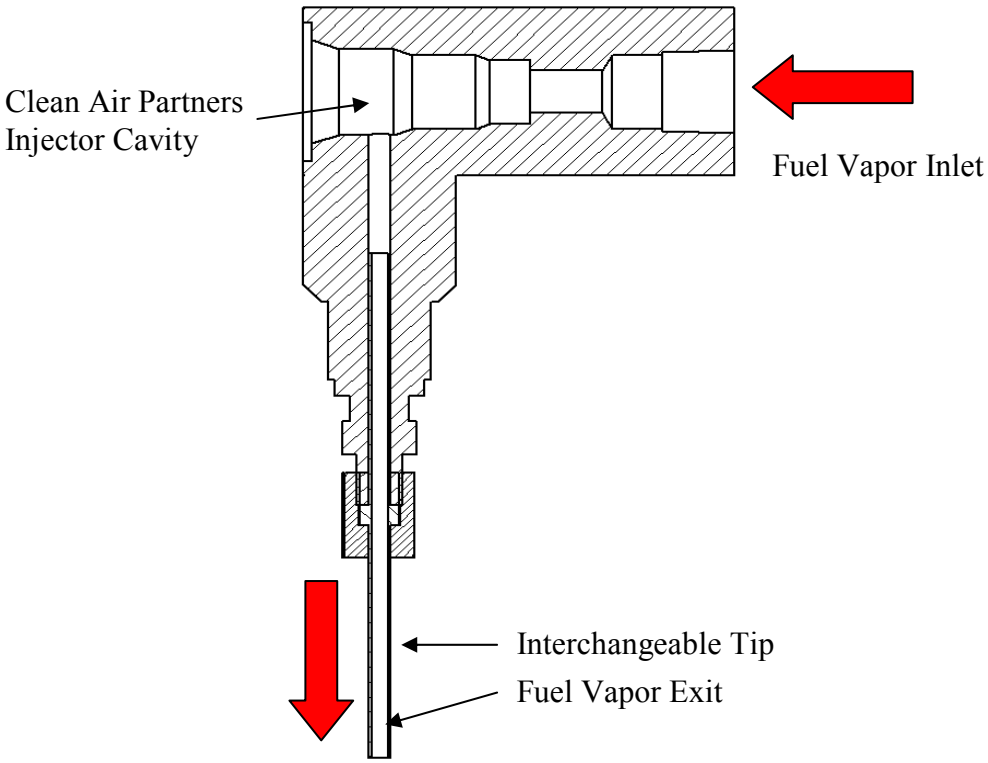

Figure 3-16 Stratified fuel injector mounting adaptor

An air assisted OptiMax injector system, identical to the system used for the premixed fuel injection, is used to inject fuel into a heating chamber. The control algorithm is configured so that the amount of air in the heating chamber is equal to or less than the

amount of fuel in the system, this is to minimize the chance of a fire occurring in the heating chamber.

The primary goal of these tests was to study the affect of gaseous fuel stratification without thermal gradients. The fuel was heated in the chamber so that the fuel injected into the cylinder was ideally at the same temperature as the bulk air flow. Equalizing the temperatures of the two streams decouples the effects of fuel and thermal stratification. The heating is accomplished with three 2.4 m (96 inch) long, 400 Watt rope heaters that are controlled by an Omega i-series controller. The temperature of this mixture is measured by a thermocouple placed in the gas stream and located at a point just prior to entering the adaptor block shown in Figure 3-16.

The pressure in the mixing chamber and upstream of the gaseous injector is maintained at a constant value of 250 kPa absolute (36.2 PSIA). This is accomplished using a lab view program to measure the pressure in the heating chamber and control the power to the OptiMax fuel and air injectors that inject the fuel and assist air into the heating chamber. The timing and duration of the OptiMax injectors is controlled by the MotoTron engine control system which is described in 3.3.1.

The MotoTron software is what tells the upstream air and fuel injectors when to actuate. The power, 12 volts DC, is turned on and off by a LabView program that is monitoring the pressure in the heating chamber. If the pressure is above 250 kPa gauge (36 PSIG) the power to the injectors is cut and the system waits for the pressure to drop below 250 kPa before turning the power back on. The downstream Clean Air Partners injector, however, is actuated each cycle in order to maintain constant fueling. The pressure control scheme can be seen in Figure 3-17. The system is designed to maintain the pressure in the

system at the set point of 250 kPa plus or minus 2.5 kPa. This limits the variation of the fuel flow into the engine to plus or minus 1% when the base fuel flow rate is 10 mg/cycle.

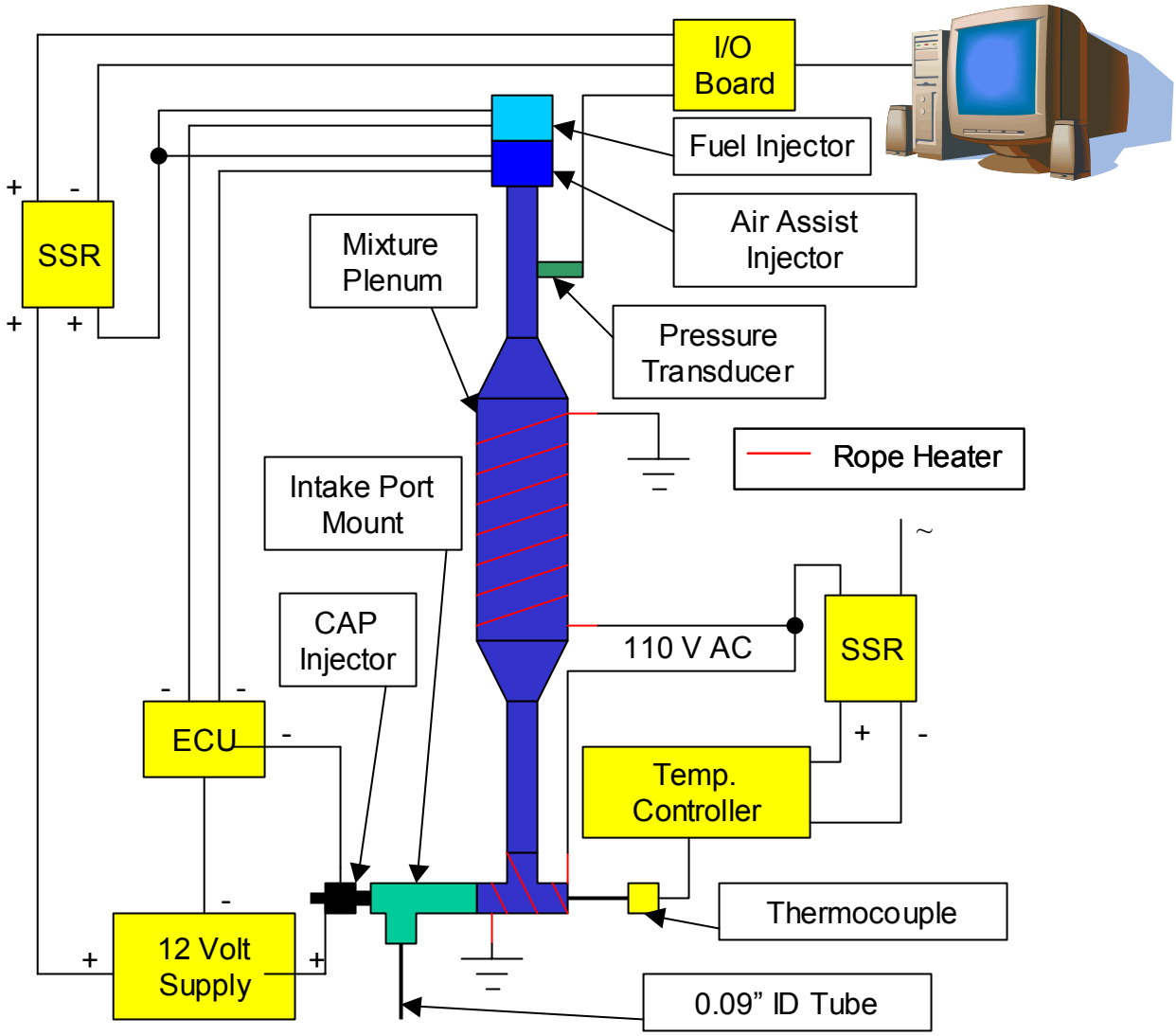

Figure 3-17 Stratified injection system

3.2.8 Fuels

Several different fuels were investigated in these experiments. Research was conducted with both primary reference fuels and a more typical gasoline. The two primary reference fuels were pure isooctane which is defined to have an octane number of 100 and a volumetric mixture of 87% isooctane and 13 % n-Heptane, which is defined to have a research and motor octane number equal to the percentage of isooctane in the mixture or 87 for this case. The isooctane and normal heptane are supplied by Alfa ÆSAR. Properties of these fuels are listed in Table 3-3. Isooctane and n-heptane are both parafins and most typical gasoline used in automotive applications contain significant amounts of olefins and aromatics, the inclusion of which change the auto-ignition characteristics of the fuel. In order to study these "real fuel" effects a research fuel was obtained from Halterman Products which is a Dow Chemical subsidiary. The fuel has a trademark name of EEE and is very similar to the B.P. Amaco product Indolene. EEE has a Research Octane Number of 96.6 and a Motored Octane Number of 88, its properties are detailed in Table 3-4.

Fuels	Isooctane	n-Heptane
Chemical Formula	C_8H_{18}	C_7H1_6
Chemical Structure	$CH_3C(CH_3)_2CH(CH_3)_2$	$CH_3(CH_2)_5CH_3$
Purity	> 99%	> 99%
Molecular Weight	114.23 g/mol	100.20 g/mol
Boiling Point	99.2 C	98.5 C
Lower Heating Value	44.5 MJ/kg	44.93 MJ/kg
Specific Heat	2.09 kJ/kg-K[a] (1.59 kJ/kg-K)[b]	2.24 kJ/kg-K[a] (1.61 kJ/kg-K)[b]
Auto-ignition Temp.	418 C	204 C
Min. Ignition Energy	27.0 mJ	14.5 mJ
Octane Number	100	0

[a] as a liquid at 25 °C [b] as a vapor at 25 °C

Table 3-3 PRF fuel specifications

Test	Units	ASTM Method	Result
Density	Kg/l	D4052	0.742
Initial Boiling Point	C (F)		28.3 (83)
10 % Evaporation	C (F)		50.5 (123)
50 % Evaporation	C (F)		103.9 (219)
90 % Evaporation	C (F)		160.6 (321)
Maximum			207.2 (405)
Lead in Gasoline by AA	g/gal	D3237	<0.01
Olefins	% Volume	D1319	29.6
Aromatics	% Volume	D1319	0.6
Saturates	% Volume	D1319	69.8
Research Octane # (RON)		D2699	96.6
Motor Octane # (MON)		D2700	88
(RON + MON) / 2		Calculated	92.3
Octane Sensitivity		Calculated	8.6
Carbon Weight Fraction		D3343 / E191	0.8659 / 0.8605
Hydrogen Weight Fraction		E191	0.1329
Net Heating Value	kJ/kg	D3338 / D240	
Net Heating Value	BTU / lb	D3338 / D240	18459 / 18618

Table 3-4 Halterman EEE fuel properties

Section 3.3 Controls and Data Acquisition Systems

3.3.1 Engine Operation Controls

The engine is controlled by a MotoTron electronic control unit. The system was developed to operate Mercury Marine OptiMax engines, which was ideal for this experiment since the fuel delivery system utilizes the Mercury Marine fuel delivery system. The ECU is a development unit which means that changes in the engine operation and ECU control settings can be made while the engine is running. This makes it easy to change parameters during the experiments like the amount of fuel injected, or the timing of the injection. Wiring schematics for the controller can be found in **Error! Reference source not found.** in

the appendix and the procedures for controller setup and operation are included in **Error! Reference source not found.** of the appendix.

Interface with the ECU is provided by a software package called MotoTune. The software can be used to turn the injectors, logic signals, and other outputs on and off during engine operation. Overall the system can handle up to eight different spark signals, fuel injectors, and air assist injectors, a total of twenty-four output signals. The system is currently configured with two fuel injector signals, one for the premixed fuel injector and one for the stratified system. The controller is also configured with three air assist injector signals, two of these injectors are located at the two fuel injectors, and the third actuates the Clean Air Partners gaseous fuel injector. There are also three 5 Volt logic output signals being used in the system. The first signal is for a spark plug installed in the engine, this signal is never used. The second logic signal is used as a trigger for the ringing index analysis program, the last signal is used as a trigger for the stratified injector heating chamber pressure control program. The real advantage of the MotoTune software is that each of these output signals can be manipulated separately, the duration of each signal as well as their phasing in relation to each other and the engine position can be changed independently of each other.

3.3.2 Non Engine Specific Controls

In a research laboratory there are a number of parameters that must be controlled which are easier to monitor and control without using an engine controller. Operating conditions such as the coolant and air temperatures, the oil stratified system pressures, and the surge tank pressures. These parameters are monitored and controlled at a control panel

mounted near the engine, each is controlled by one of several 1/16 DIN temperature and process controllers. These controllers consist primarily of Omega i-series controller units however a couple of Omega CN7700 series controllers are also used. The i-series controllers have two control outputs most the controllers are configured with a 0-12 V proportional DC output as well as a solid state relay (SSR) output, there are, however, a couple of dual SSR output controllers. The CN7700 controllers are used in a few cases because they have a 4-20 mA proportional output as well as a SSR output. Table 3-5 lists the controlled parameters, the controller number, the type of output performing the control action, as well as the input type for the standard engine control panel. The controllers are wired together in parallel and communicate with a computer through the RS-485 communications protocol. Acquisition and storage of this data is performed with a LabView program which is describe in 3.3.5. The program collects thirty readings from each device and averages them in order to get a good representation of the parameter during the engine operating period. The parameters read by the data logging system are noted in Table 3-5 with a * after the controllers communications identification number.

Parameter	Units	Instr. Comm. ID #	Input Type	Output Signal
Coolant Temp	C	0003*	Thermocouple	SSR – Heater SSR – Solenoid Valve
Oil Temp	C	0002*	Thermocouple	SSR – Heater SSR – Solenoid Valve
Heated Filter Temp	C		Thermocouple	SSR
Oil Pressure	PSI	0040	Pressure Transducer	SSR – Cutout Relay
Stratified Injector Temp	C	0001*	Thermocouple	0-12 V DC – Relay
Stratified Injector Pressure	kPa	0041*	Pressure Transducer	SSR – Injector Pwr
Intake Air Temp	C	0004*	Thermocouple	SSR – Heater
Orifice Upstream Temp	C	0042	Thermocouple	NA
Exhaust Surge tank Pressure	kPa	0005	Pressure Transducer	NA
Orifice Upstream Pressure	kPa	0006	Pressure Transducer	4-20 mA – Pneumatic Controller
Fuel Temp	C	0007	Thermocouple	NA
EGR Temp	C	0008	Thermocouple	SSR – Solenoid Valve
Heated Line #2 Temp	C	0009	Thermocouple	SSR
Heated Line #1 Temp	C	0010	Thermocouple	SSR
General Temperature Reading	C	0011	Thermocouple	NA
Engine Coolant	C	0012*	Thermocouple	NA
Air Assist Injector Flow rate	SLPM	0013*	Mass Flow Meter	NA

Exhaust Port Temperature	C	0014*	Thermocouple	NA
Inlet Surge Tank Pressure	KPa	0015	Pressure Transducer	NA

* Values read and recorded by the LabView data acquisition program

Table 3-5 Control panel input and output signals

3.3.3 Exhaust Gas Emissions Analysis

The engine generated emissions are sampled with an emissions bench manufactured by Horiba Instruments Inc. This bench uses Nondispersive Infrared (NDIR) analyzers to measure carbon dioxide and carbon monoxide volumetric concentrations, a Magnetopnuematic (MPA) analyzer to measure oxygen concentrations, a Flame Ionization Detector (FID) to measured the unburned hydrocarbon emissions, and a Chemiluminescent (CLA) analyzer to measure the NO. The CLA uses a special converter to chance NO_2 into NO, which means the CLA measures all of the oxides of nitrogen emitted by the engine. In order to quantify the amount of external EGR being inducted into the engine the bench has a second NDIR sampler to measure Carbon Dioxide from the intake surge tank closest to the engine inlet runner.

The emissions bench was donated by General Motors Research. Prior to using the instruments for data collection the instruments were calibrated using a Horiba SGR-710C model gas divider. These calibration curves were used in calculating exhaust emissions concentrations instead of the factory generated calibrations. New calibrations were performed because of the age of the instruments. The calibration curves for these instruments can be found in **Error! Reference source not found.**. At the start of each day of operation the different analyzers in the bench are zeroed and spanned to the calibration value for the reference gas's concentration. It is assumed that the instruments do not drift

from the span points once they have been set. Procedural steps for zeroing and spanning the emissions bench can be found in **Error! Reference source not found.**.

In the Horiba Emissions bench the exhaust gas sample is passed through a chiller bath before being routed to the individual gas analyzers; this causes the water generated in the combustion to condense and allows the water to be filtered out of the gas stream before it enters the emissions analyzers. The water is separated from the gas stream because it will adversely affect the various analysis devices.

In order to add an extra layer of protection for the gas analyzers water is also removed from the sample line prior to being routed to the emissions bench. The exhaust sample is routed into a heat exchanger immediately after it leaves the exhaust surge tank, the condensed water is then separated from the gas sample with a Parker Corporation Balston Division 33G filter before the gas is sent to the emissions bench. The system also has a heated filter and a heated line running from the Balston filter to the emissions bench. However due to the use of the heat exchanger and filter these accessories are not currently in use.

Each of the gas analyzers in the emissions bench have a 0-10 V DC proportional output that is read into the desk top computer. The exhaust species signals are continuously monitored to get real time air/fuel ratio data for the engines operating condition. When the operator desires to collect data for analysis the exhaust species concentration are collected for 1 minute and then averaged. The air/fuel ratio is calculated from these average values using the calculations listed in **Error! Reference source not found.**. For more information on these calculations and their derivation the reader is directed to the work by Stivender [46]

3.3.4 Cylinder Pressure Recording

The cylinder pressure is measured with a Kistler 6125B quartz pressure transducer. The pressure signal is then sent to a Kistler 5010B dual mode charge amplifier. After the charge amplifier the signal is filtered with an 8 kHz with a low pass filter, the signal is then sent to an eight channel DSP 4012 data acquisition system. The signal is collected from the DSP 4012 and analyzed by the computer software program Redline ACAP.

The Kistler 6125B pressure transducer has a range from 0 to 25,000 kPa with an overload pressure of 30,000 kPa. Kistler claims that the transducer pressure sensitivity varies ≤±2 % over a temperature range of -50 – 350 ºC, this makes thermal shock a small concern when looking at the pressure data. The transducer also has a ground insulated design that is meant to eliminate electrical interference in the output signal. The transducer has a linear response to changes in pressure over its operating window; the slope of this line is measured with a dead weight pressure tester. The calibration curve can be seen in **Error! Reference source not found.** of the appendix. Further information on the pressure transducer can be found in Table 3-6.

Range	0 to 250 bar
Calibrated Partial Range	0 to 50 bar
Overload	300 bar
Sensitivity	≈ -16 pC/bar
Natural Frequency	≈ 75 kHz
Linearity, all ranges	≤ ±0.5 % FSO
Acceleration sensitivity	
axial	< 0.002 bar/g
radial	< 0.003 bar/g
Operating Temperature	-50 to 350 °C
Sensitivity Shift	
20 to 350 °C	≤ ± 2 %
50 ± 35 °C	≤ ± 1 %
Thermo shock: at 1500 min^{-1}, 9 bar IMEP	
ΔP	≤ -0.3 bar

ΔIMEP	< -2 %
ΔP_{max}	< -1 %
Insulation Resistance, at 20 °C	$\phi 10^{13}\ \Omega$
Ground Insulation	$\phi 10^{6}\ \Omega$
Shock Resistance	2000 g
Tightening Torque	10 N-m
Plug, ceramic insulator	10-32 UNF

Table 3-6 Kistler 6125B pressure transducer specifications

The signal from the transducer is in pC and must be converted to Volts in order to be read by the data acquisition system. This conversion is performed using a Kistler 5010B charge amplifier. Full specifications for the amplifier can be found in Table 3-7. For all of the experiments conducted, the charge amplifier is always operated in "Charge Mode" with the Transducer Sensitivity set to 15.5 pC/MU, the Scale was set to 10 MU/V, and the time constant was set to "Short".

The pressure signal is captured by a DSP data acquisition system which consists of a model 4012 TRAQ controller module, an 8 channel 12 bit 100 kHz input module, and an 8 megasample memory module. The data is acquired in the DSP system and then analyzed and stored in a desktop computer operating the Redline ACAP v4.0 software. The ACAP software calculates parameters including the IMEP, COV_{IMEP}, the value and location of the peak pressure. Further information about the ACAP software and DSP hardware can be found in the ACAP 4.0 user's manual. [47] The equations and parameters calculated by the software package can be found in **Error! Reference source not found.**.

Measuring Pressure Range	± 10 to 999,000 pC
Sensor Sensitivity	0.01 to 9990 pC/MU or mV/MU*
Scale	0.0002 to 10,000,000 MU/Volt
Output Voltage & Current	± 10 Volts or 5 mA
Output Impedance	100 Ω
Input Insulation Resistance	$10^{14}\ \Omega$

Frequency Response with standard 5311 (-3 db) filter	180 kHz
Time Constant for Long: Medium: Short	Up to 100,000 s: 1 to 10,000 s: 0.1 to 100 s
Amplitude Linearity	< ± 0.05 % FSO
Accuracy	< ± 0.5 %
Sensor Power Voltage Mode	4 mA
Drift (due to leakage current)	< ± 0.03 pC/s
Operating temperature range	0 to 50 °C

*MU = Mechanical Unit (e.g., PSI, kPa, etc)

Table 3-7 Kistler 5010B dual mode charge amplifier specifications

In order to relate the engine pressure signal to the engine's crank angle position a BEI model H25 optical encoder was coupled to the engine crankshaft. The encoder has a resolution of 720 pulses per revolution or one pulse every one half degree. The encoder's "A" pulse, or every half degree, is sent to the DSP system and used to correlate the pressure signal with the engine volume. The DSP system also receives a "Z" pulse from the encoder, which marks the top dead center location of the encoder. The encoder top dead center signal is aligned with the engine crankshaft top dead center position using the methods detailed in the paper by Lancaster et al. [48]

The DSP system also samples signals from pressure transducers located in the intake and exhaust surge tank once each cycle. The signal from the intake surge tank is used as the reference or "pegging" pressure. The DSP system reads a value from the transducer in the intake surge tank and calculates the pressure in the tank from a calibration curve. The voltage value from the cylinder pressure signal that was taken at the same time as the intake surge tank pressure is assigned the same pressure value as the surge tank. All of the other pressure values recorded in the cycle can be determined from knowledge of the pegging pressure and the slope of the calibration curve of the transducer. The pressure transducer located in the exhaust system is sampled following the same procedure, purely for

completeness, but could be used as the pegging device instead of the intake signal. For more information about cylinder pressure pegging the user is directed to the ACAP 4.0 user's manual. [47]

The sensitivity of the crank angle encoder gives 1440 pressure samples every cycle. The storage capabilities of the DSP system and the desktop computer being used to acquire this data limit the maximum number of sequential cycles that can be captured to just over 500. For this reason, all of the cylinder pressure data acquired in the experiment is an average of 500 cycles. It is desirable to average a large number of cycles in acquiring pressure data in order to average out the cycle-to-cycle variations and obtain a good representation of the engine's behavior at the recorded operating condition. Along with the cycle averaged values ACAP also provides statistical data that can be used to quantify the variation of the engine's performance.

3.3.5 LabView Data Acquisition

A LabView data acquisition program has been created that will sample control parameters, the exhaust emissions, and quantify the knock in the cylinder from an analysis of the pressure trace. These signals are captured by a National Instruments BNC 2090 16 channel input panel that along with a National Instruments PCI-6014 data acquisition card collects these signals in a desk top computer located in the laboratory. This program samples and averages 30 readings from each of the specified Omega controllers; the controllers that are read by this program are noted in Table 3-5. While the program is recording readings from the controllers it takes 1 minute worth of emissions samples and averages those as well.

These parameters are sampled concurrently with the cylinder pressure being logged in the ACAP software. After the emissions and control parameters are collected the system collects 500 cycles of pressure data and analyzes the amount of engine ringing or knock that is being generated at the operating condition. Finally the data acquisition program collects five minutes of fuel flow data from the MAX meter to calculate an average fuel flow rate. These values are all written to a text file for analysis later with another LabView program.

When data is not being actively collected the LabView program is constantly monitoring the engine. Air/fuel ratio data is constantly being monitored and output to graphs in the user interface window. The operator can use this information to adjust the input parameters to get the engine to the desired operating condition without spending a lot of time sampling data. Also every 30 seconds the system displays the inlet airflow, the average air/fuel ratio, and the calculated the fuel flow rate on the computer screen. At the same time 50 engine cycles are analyzed to calculate the ringing index. If the ringing index rises above 12 volts a warning message is displayed to alert the engine operator of a potential problem. These values are not recorded, they are displayed for only thirty seconds and then replaced with updated information, the purpose is only to let the operator know how the engine is behaving.

Due to limitations the computer's ability to access signals through the National Instruments data card only emissions and control input data can be sampled concurrently. The engine ringing index and the fuel flow data must be sampled on their own with no other non cylinder pressure data being collected at the same time. It should be noted that once data recording has begun all real time displays are inactive and the operator has no way of obtaining knowledge of how the engine is performing other than listening to it. Fluctuations

in the intake temperature can cause some small inaccuracies in the ringing index value; however, this is not too big of a concern since the ringing index is only used as an indicator of dangerous operating regimes. Care must be taken to make sure that the engine performance does not change too dramatically while the ringing index and fuel flow measurements are being taken.

3.3.6 Ringing Index (Engine Knock) Analysis

In HCCI combustion there are regimes of operation where severe cylinder pressure oscillations can be detected. These pressure oscillations are very similar to knock in a spark ignition engine but due to the differences between HCCI and SI combustion are termed "ringing". These pressure oscillations generate a very large amount of noise in the engine structure. Also experience in this laboratory has shown that high fueling rates coupled with high ringing index values led to destruction of several engine components. In order to prevent damage to the engine and to prolong the amount of time that the operator could spend collecting data a cutoff ringing index value of 8 volts was used as an upper limit to the engines operational window.

The LabView program collects pressure data from 500 sequential engine cycles. The data of interest is from 30 crank angle degrees before top dead center until approximately 100 degrees after top dead center. The voltage signal from the charge amplifier for this period of the cycle is collected by the software and is filtered with a band pass filter built into the program. This filter was set with the high and low pass cutoff frequencies both set at 6.3 kHz. The filtered signal is multiplied by a factor of 500. The computer then takes the filtered and amplified pressure signal and looks for the point in the signal where the pressure

oscillation was the highest. The difference between the highest and lowest voltage for each cycle is collected and averaged, this value is the ringing index. A cutoff ringing index of 8 Volts means that on average the difference between the highest and lowest points in the filtered pressure signal is 0.016 volts. Neglecting any losses in the signal intensity due to filtering the amplification of the signal by 500 times means that, a cutoff voltage of 8 translates into a maximum allowable peak-to-peak variation in the pressure of 16 kPa. For more information on the ringing index metric and the sources of audible combustion noises from an engine the reader is directed to the paper by Eng which was used extensively in the establishment of the ringing index metric for this work. [34]

3.3.7 Fuel Flow Measurement

There are two fuel flow meters installed in the system, the first meter is an Endress & Hauser Promass 83A coriolis effect meter, however the accuracy of this meter decreases dramatically when the flow rates through it are small (less than .200 g/s). Because of the low speed and fueling rates commonly used in HCCI combustion and the inaccuracy of the coriolis affect meter at these flow rates, a Max Machinery Co. model 284 512 flow meter was installed in the system. The Max meter is a positive displacement meter with an extremely small displacement volume which makes the meter much more accurate in the low flow rates seen during these experiments.

Measuring the flow rate through the fuel system is difficult since the OptiMax system utilizes a fuel return line and the float bowl in the high pressure pump system. These devices cause the flow from the lift pump to pulsate from a high flow rate to almost nothing. To control the direction of the flow pulses through the flow meters, check valves were installed

in the flow lines to prevent reverse flow of the fuel through the meters. The line from the lift pump to the high pressure pump is also throttled in order to help dampen the pressure pulses in the line. A final step to help increase accuracy is that the flow rate measured by the Max meter is averaged over a period of five minutes in order to accommodate the variations in the flow measurement caused by the pulsating flow.

Chapter 4 - Experimental Parameters, Trends, and Repeatability

Section 4.1 Operating Parameters and Experimental Conditions

The first step in this research was to setup and construct the laboratory facilities, the results of which have been detailed above. The second step was to work out any and all of the issues relating to operation of the engine and the collection of data. Through the course of establishing operating procedures it was necessary to determine parameters that needed controlling and the appropriate settings for those parameters. In narrowing down the scope of the project it was essential to determine which parameters would be held constant and which would be treated as variables in this research.

4.1.1 Constant Independent Parameters

Several parameters are maintained at a constant value throughout all of the tests. These include the coolant temperature, oil temperatures, fresh air to fuel ratio, intake pressure, and exhaust pressure. Table 4-1 shows the values of these constantly maintained parameters.

Parameter	Set point
Intake Pressure	97 kPa
Exhaust Pressure	100 kPa
Coolant Temperature	95 °C
Oil Temperature	90 °C
Fresh Air to Fuel Ratio	20:1

Table 4-1 Constant engine parameters

Intake Pressure

The intake pressure is maintained at a constant value corresponding to wide open throttle. This is done in order to capture the thermal efficiency benefit that comes from running unthrottled. Higher intake air pressures mean that the engine does less work to pump to charge into and out of the engine and that work can be directly applied to the wheels, which increases the engine's thermal efficiency. A constant intake pressure also keeps the pressure effects on the chemical kinetics constant.

Exhaust Pressure

The exhaust pressure is maintained at a constant value just above the intake air pressure in order to force external EGR to flow into the intake system.

Coolant and Oil Temperatures

The temperature of the fluids flowing through the engine is kept constant as well. These parameters will greatly affect the cylinder head and liner wall temperatures. The wall temperatures will have a large influence on the thermal gradients and boundary layer thickness in the cylinder. In order to keep these parameters constant for all of the tests it was necessary to keep the fluid temperatures constant.

Air/Fuel Ratio

The air/fuel ratio is defined as the ratio of the mass of fresh air inducted each cycle to the mass of fuel inducted each cycle. The ratio of air and fuel that was selected was chosen because it is near the rich limit of HCCI engines but had enough excess oxygen to allow for complete combustion of the fuel. Since the amount of fuel inducted into the engine is the

major limit to the power output of an HCCI engine it was decided that richer air/fuel ratios should be studied before leaner ratios. Later on in this work this fixed value will become a variable. There the air/fuel ratio will be moved to leaner ratios in order to study engine operating conditions near idle.

4.1.2 Variable Independent Parameters

The primary independent parameter in this research is the temperature of the intake charge measured in the intake runner about 13 cm (5.5 in) away from the intake valve. This temperature is referred to as the intake air temperature and is controlled to the desired value by the engine operator. It was decided that this parameter would be used as the main independent parameter because HCCI combustion has been shown to be very dependent on the mixture temperature. The temperature in the runner at this location was chosen because it is the closest to the engine inlet that a thermocouple could be placed.

There are several other parameters that are controlled independently in the experiments. The other independent variables include engine speed, fuel type, fueling rate, fuel introduction location, and stratified fuel injection timing and stratified fuel temperature when the stratified system was employed. The dependent variables changed with the experimental conditions being investigated, therefore each one will be discussed in more detail in subsequent sections.

4.1.3 EGR as a Dependent Parameter

In many cases it was necessary to add EGR to the inlet to maintain the intake air pressure at 97 kPa and keep the fresh air/fuel ratio at 20:1. The EGR is brought into the engine through the use of a venturi that is described in 3.2.4. A series of valves are installed in the EGR line to throttle the flow rate of EGR into the engine. The valves can be wide open which will short circuit the exhaust to the intake. The pressure differential between the two systems will drive the flow rate into the intake system. The mass of EGR drawn into the system is driven by the changes in the density of the fresh air in the inlet system. As the inlet air temperature increases it expands and displaces the EGR in the intake. If the fresh air temperature decreases the density decreases and more EGR is drawn into the engine. Figure 4-1 is a typical plot of how the EGR fraction changes with the intake air temperature.

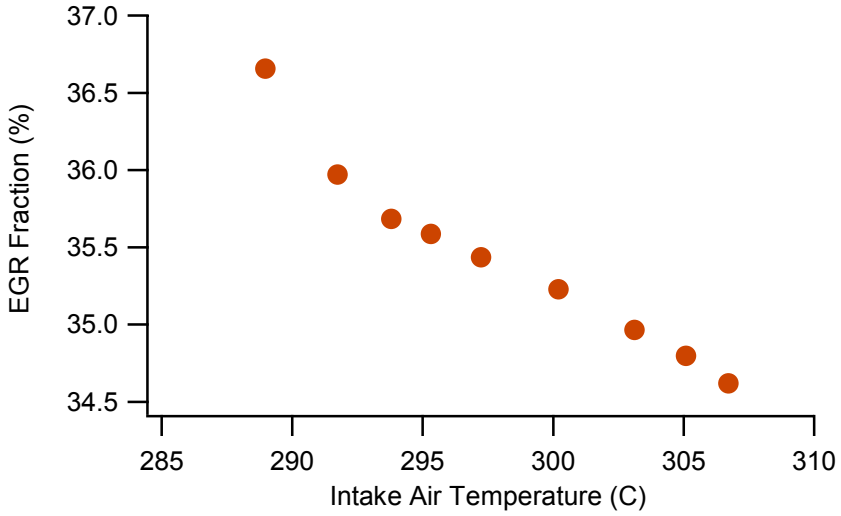

Figure 4-1 EGR flow rate as a function of the intake air temperature

4.1.4 Defined Window of Acceptable HCCI Combustion

In order to investigate HCCI combustion it is necessary to identify the limits of acceptable operation. The operating window was defined using the ACAP pressure analysis and the LabView Ringing Index evaluation described in 3.3.6. The acceptable operating window was defined to be the intake air temperatures where the COV of IMEP was less than 3.0 % and the Ringing Index was less than 8 Volts.

The COV limit was chosen because it is the value that is used by General Motors as the drivability limit of automotive engines. If the COV increases above 3 % then the operator will notice. In general the COV increases quite dramatically once the temperature has moved past the defined low intake temperature limit.

The maximum Ringing Index value was defined simply from having run the engine and by listening to the combustion noises. In general the noise is noticeable when the RI has increased above 4.0 Volts and the noise increases significantly once it has passes 6.0 Volts. Above 7.0 Volts the pressure oscillations are noticeable on an oscilloscope.

The typical performance of the engine through an intake temperature regime is shown in Figure 4-2. It is important to note that the window of intake temperature where acceptable combustion is to be found will vary as parameters such as fuel type and engine speed are changed. One final note is that in the upper portions of the operating window the Ringing Index has a standard deviation of about 3.5 Volts. While the 8 Volt cutoff is used as the maximum value that can be attained during operation, generally any value above 7.5 is deemed high enough.

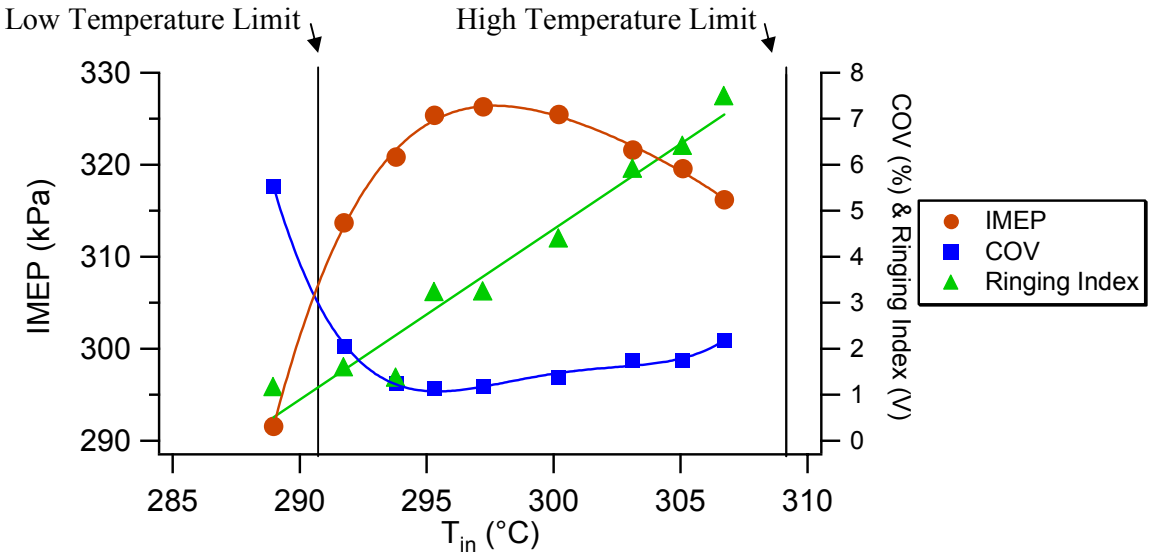

Figure 4-2 Typical HCCI operating window

4.1.5 Operating Notes

Parameter	Setting
Fuel	Isooctane
Speed	1000 RPM
Fueling Rate	10 mg/cycle
Fuel Introduction Method	Premixed

Table 4-2 Experimental parameters for repeatability test

It was also important to establish the limits of repeatability and the consistency of the results both through the course of a single test and on a day-to-day basis. To address this issue of repeatability a base condition was chosen for repeated operation over several days. This operating condition is detailed in Table 4-2. The engine was run at this operating condition for a period of five consecutive days and the results were compared to identify how well the performance could be repeated. Each time the test was run the intake temperature was swept through the range of intake temperatures that yielded acceptable combustion as it

was defined above. Also to address the consistency of the results through the course of the test the points were collected randomly in order to look for inconsistency in the trends.

As was mentioned earlier the engine's behavior was measured against changes in the intake air temperature. Most of the data in this thesis is displayed with the engine's performance indicators plotted against intake air temperature. A number of plots of HCCI data from the repeatability analysis are displayed and discussed in this section. Operating conditions, such as those that include thermal stratification in the cylinder, have proven to be easier to analyze when plotted as a function of the combustion efficiency. For reference purposed some of the data that is presented this section, is plotted as a function of combustion efficiency in Section A.1.

Section 4.2 HCCI Trends and Repeatability

4.2.1 Cylinder Pressure Behavior

The cylinder pressure traits are typically described in terms of the Indicated Mean Effective Pressure (IMEP) which is an indicator of the amount of power generated in the cylinder due to the combustion. IMEP values, collected during the repeatability investigation, are shown in Figure 4-3. The plot shows that the IMEP has the same trends and general shape each day, but the absolute values on a day-to-day basis show more variability than is desirable. The differences between the peak IMEP value from April 9, 2004 and the peak IMEP value for April 11, 2004 is approximately 20 kPa or about 7% of the values measured on April 9. This issue will be discussed later on in this chapter.

At the low temperature end of the operating window there is relatively little initial energy in the cylinder, the gas temperatures near TDC are just sufficient to trip the fuel into auto-ignition and thus the heat release occurs very late in the cycle. Late combustion, therefore, does not generate significant amounts of power in the cylinder. As the intake air temperature increases the higher initial temperatures yield higher compression temperatures which help to accelerate the reaction rates and advance the combustion. At an intake air temperature of about 307 °C the combustion phasing reaches the ideal crank angle and the maximum amount of power is generated inside the cylinder. As the intake air temperature increases, the combustion phasing enters a regime where a significant amount of the energy is released during the compression stroke. As the heat release begins to occur during the compression stroke, the increased pressure pushes down on the piston while the piston is still traveling upwards which leads to a loss of work from the engine.

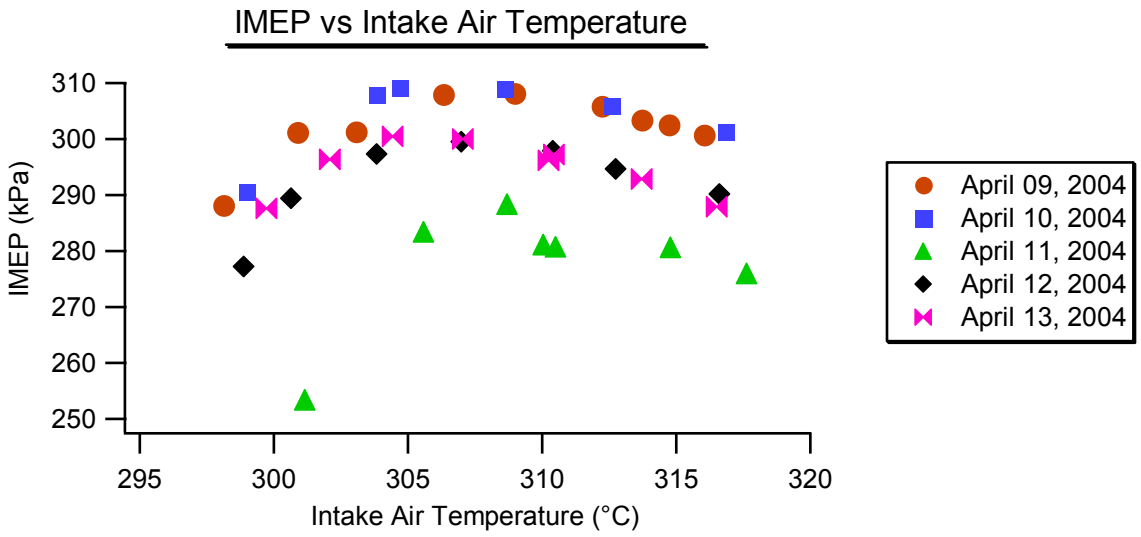

Figure 4-3 IMEP vs. intake air temperature

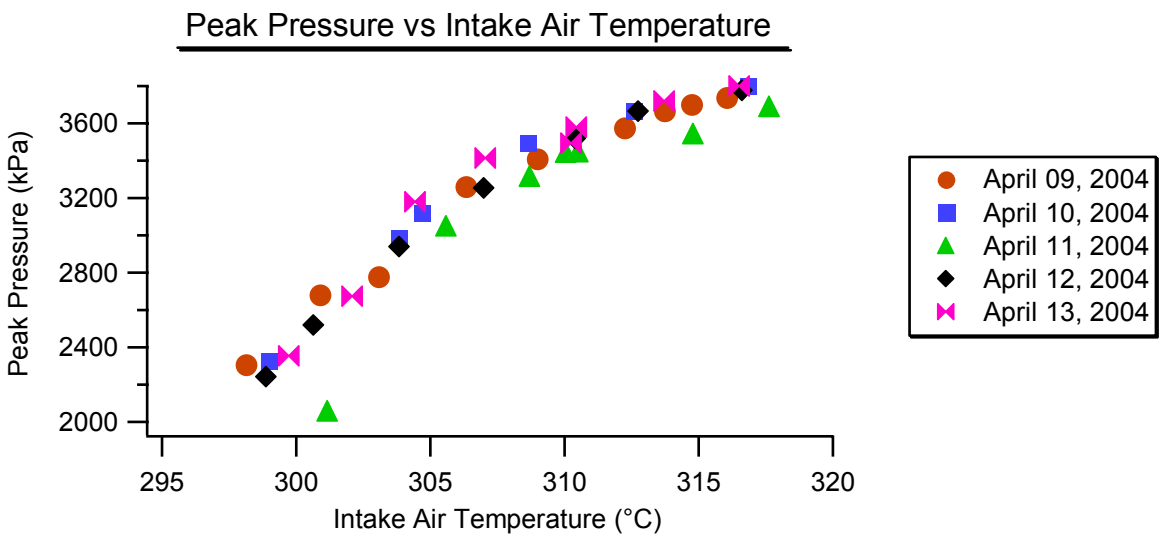

Figure 4-4 Peak pressure vs. intake air temperature

The peak cylinder pressure, which is shown in Figure 4-4, details how the peak pressure increases slowly from a value of about 1900 kPa to a maximum value of about 3900 kPa. At the low temperature limit the peak pressure is what a charge initially at 100 kPA would be reached due solely to compression, without any heat release. The value of 3900 kPa, at the high temperature limit, is not a fundamental upper limit but instead a function of the amount of fuel introduced to the cylinder. If more fuel were introduced to the cylinder the maximum peak pressure would be well above 4000 kPa, and for lower fueling rates the peak cylinder pressure would be much lower than this value. It is important to note, however, that the peak cylinder pressure is limited by the construction of the components of the engine.

The magnitude of the peak pressure data collected over the five days is more consistent than the IMEP values. If the peak pressure had the same variation as the IMEP data showed then the pressures at each temperature would have shown a variation of 270 kPa. These variations are not seen in the peak pressure data. The peak pressure values

appear to be very consistent but more indicators need to be reviewed to determine if the engine's behavior is consistent or not.

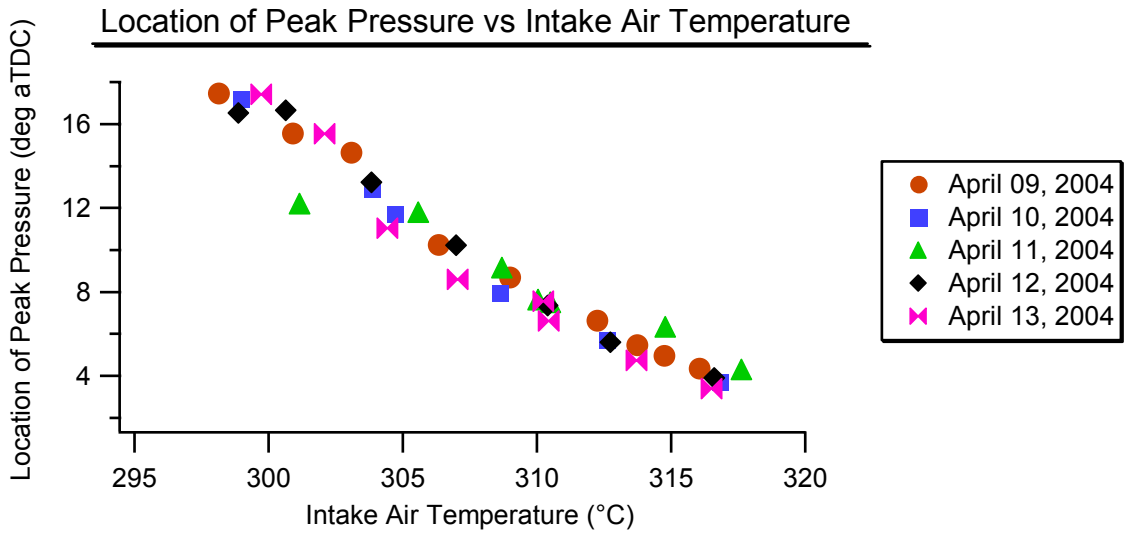

Figure 4-5 Location of peak pressure value

The crank angle at which the location of the peak pressure (LPP) occurs is also observed to be consistent day-to-day. This parameter can be seen in Figure 4-5. As in the other plots it can be seen that, at low intake air temperatures, the fuel doesn't get to its auto-ignition point until very late in the cycle and the combustion often occurs late in the expansion stroke. The peak pressure is, therefore, reached at a crank angle very late in the cycle. As the intake air temperature increases the location of the peak pressure begins to move closer to TDC. Recall that the maximum amount of power was noted at a temperature of about 307 °C, this corresponded to a LPP of approximately 10 degrees ATDC.

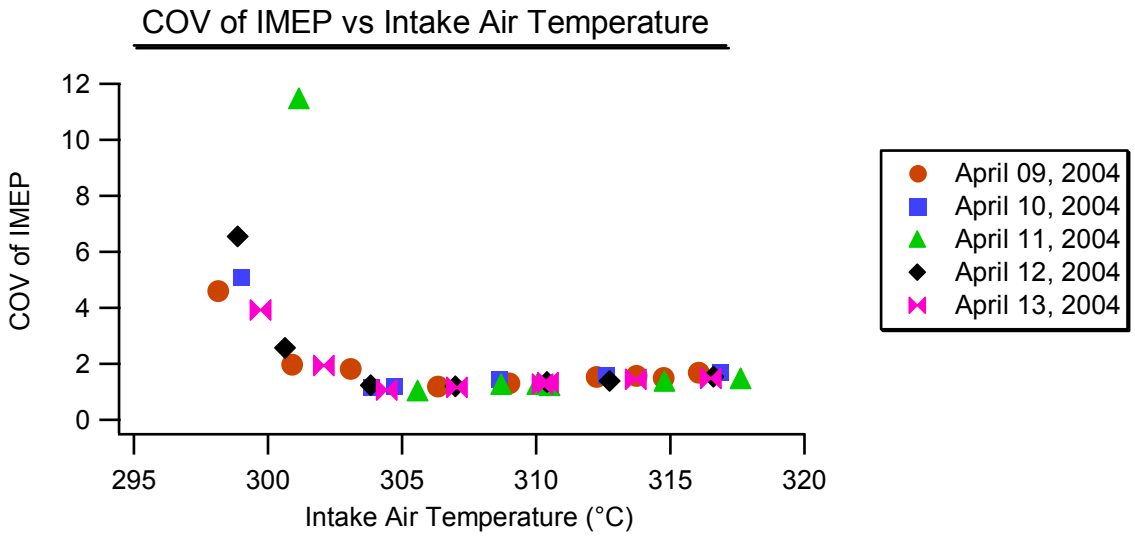

Figure 4-6 COV vs. intake air temperature

As was noted earlier, for this work COV was used as the definition for the lower temperature limit. For non-idle operating conditions an upper limit on the value of the COV was established at 3%. In Figure 4-6 the changes in the behavior of the COV for changes in the intake air temperature can be observed. At temperatures below 300 °C the combustion shows too much variability to be acceptable. As the temperature increases the COV reaches a value of about 1.5% and it stays near that point for the rest of the defined window of acceptable operating temperatures. It is interesting to see that the combustion goes from acceptable to almost non-existent with a high amount of variability with a temperature drop of just 5 °C.

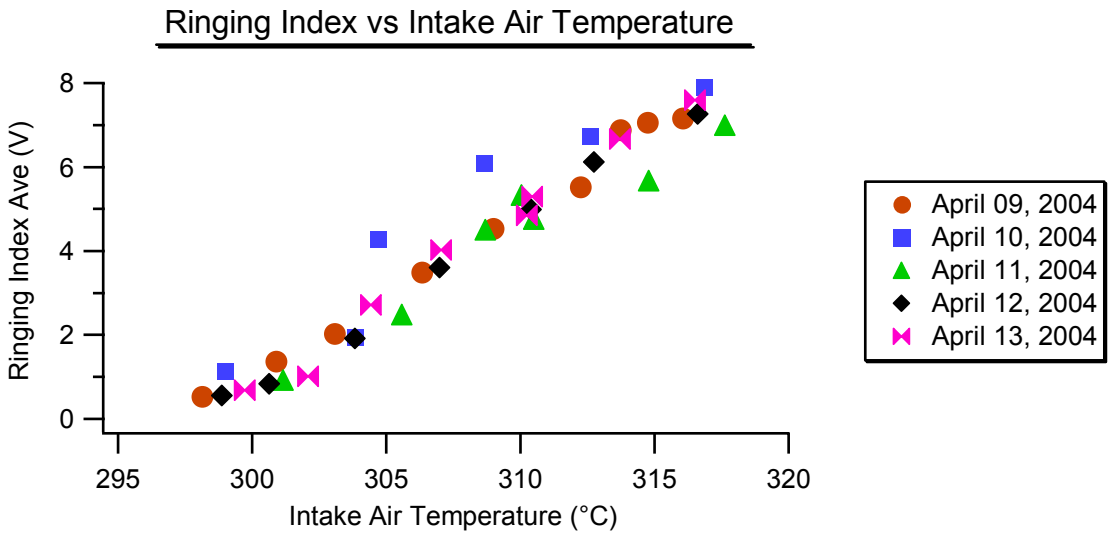

Figure 4-7 Engine generated noise (ringing index) vs. intake air temperature

The upper limit on the acceptable window of intake air temperatures was defined using the ringing index standard. Ringing index is a measure of the combustion noise and the cylinder pressure oscillations that result from auto-ignition. The method of analyzing the combustion noise was originally developed by researchers at General Motors. [34] This metric measures the peak to peak oscillations in the pressure signal, the value was compared to audible combustion noise and an absolute upper limit is arbitrarily established. Experience in this laboratory has shown that any ringing index values greater than 10 volts are very irritating, also any ringing index value above 20 volts has proven to be detrimental to the engine structure, even when run over short periods of time. Figure 4-7 shows how the ringing index value evolves over the intake temperature operating window. The value increases in a fairly linear manner from the point where the COV becomes acceptable to the arbitrarily defined upper noise limit.

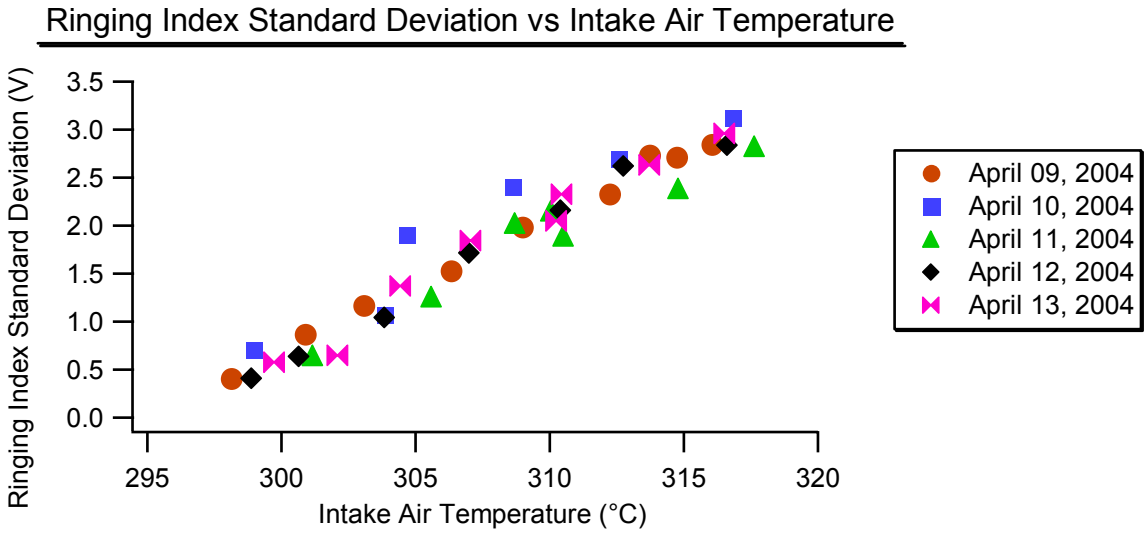

Figure 4-8 Ringing index standard deviation vs. intake air temperature

One characteristic of the ringing index that needs to be kept in mind, when using it as a metric for determining the upper limit of engine operation, is the variability inherent in the ringing index value itself. The index is an average value of the largest peak to peak pressure oscillation seen each combustion event for 500 cycles. The standard deviation of the data collected is shown in Figure 4-8. As can be seen in the plot, as the intake temperature and the combustion related pressure oscillations increased, the standard deviation in the ringing index value also increased. This shows that while from a global viewpoint the HCCI combustion was very uniform cycle-to-cycle, at small scales the combustion exhibited a significant variability. It is important, when running the engine, that the operator be aware of this variability in the ringing index and that they do not try push the intake temperature to levels that will cause the index to increase too far above 8 V or else they might cause damage to the engine. Experience has shown this to be a particular concern at fueling rates greater than 10 mg/cycle.

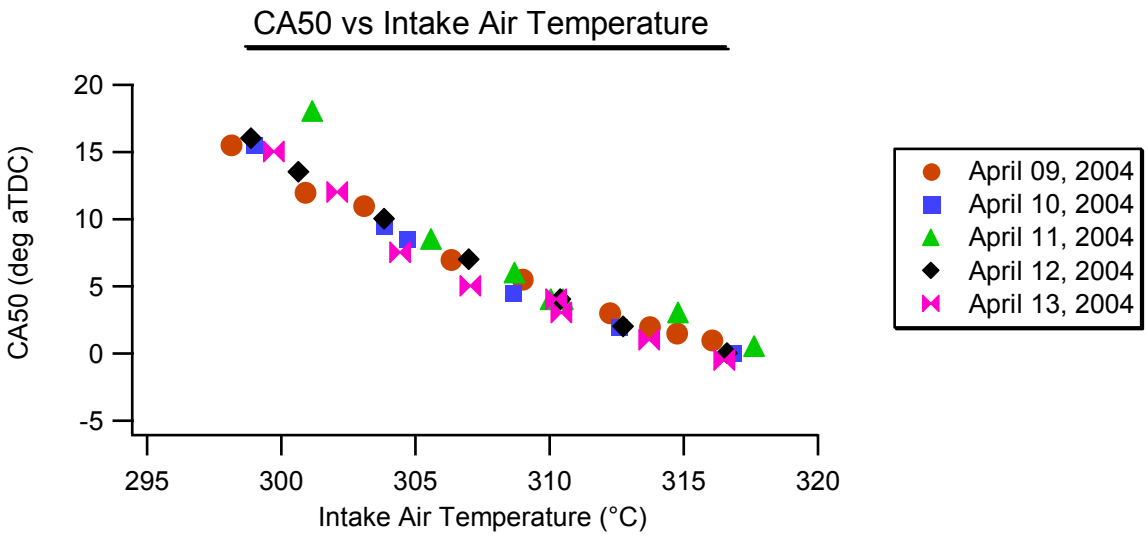

Figure 4-9 CA50 vs. intake air temperature

The location of the peak pressure was used above in demonstrating that the combustion behavior was more consistent than the IMEP values indicated. But in most of the analysis presented in this thesis LPP was not reviewed. Instead of LPP the value of CA50 point was more often reviewed when looking for changes or consistency in the engine's operation. The behavior of CA50 as a function of intake air temperature is shown in Figure 4-9. The plot the value of CA50 changes in the same manner as the LPP, in fact the value of LPP just slightly lags the value of CA50. The point where the IMEP was at its maximum corresponds to a CA50 value of approximately 6 degrees ATDC.

The combustion duration values are shown in Figure 4-10. Because it is difficult to determine precisely when the combustion beings and ends, the burn duration is defined, here, as the number of crank angles between the values of 10 and 90% fuel mass fraction burned. In a typical SI engine the burn duration is between about 20 and 40 crank angle degrees, as can be seen in Figure 4-10 at this operating condition, HCCI combustion lasts for between 4 and 12 crank angle degrees. A short duration of the combustion event is typical in HCCI

combustion and is a result of the fact that most of the fuel mixture in the cylinder is near its auto-ignition point at the time that the combustion begins. The heat release, from the first portions of the cylinder to burn, then helps to trip most of the rest of the gasses into auto-ignition. The near instantaneous release of energy from the fuel to the cylinder, if phased correctly, is very close to the ideal Otto Cycle where the energy is released at a constant volume, this helps to increase the thermal efficiency of the combustion process.

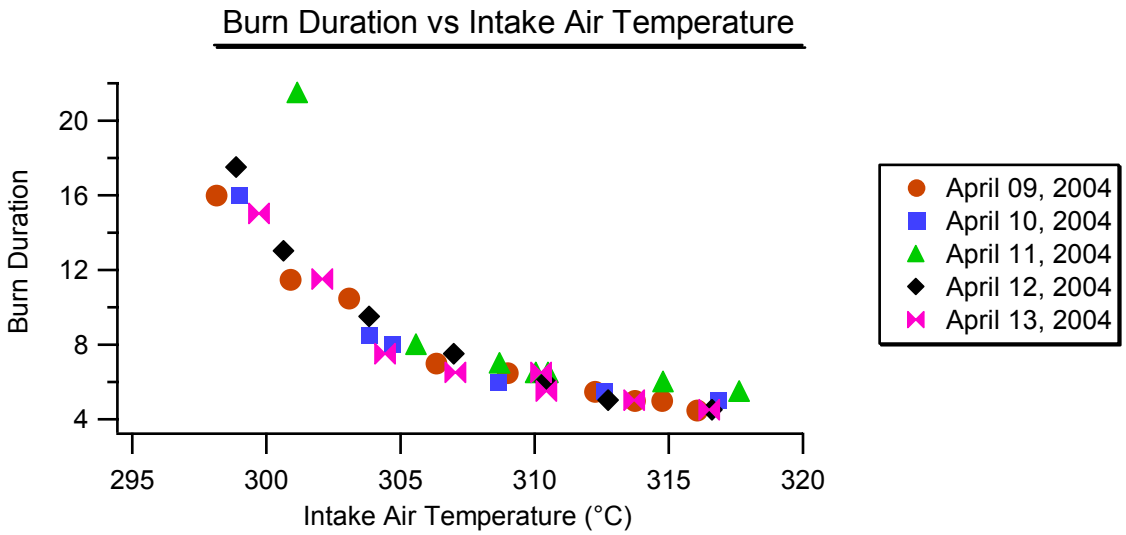

Figure 4-10 Burn duration vs. intake air temperature

The data presented in Figure 4-11 shows pressure traces and heat release results from the data collected on April 12, 2004. This plot shows how these two parameters respond to changes in the intake air temperature. The combustion tendencies that can be picked out of this plot have all been described earlier in this section, however, they become more obvious when looking at this graph.

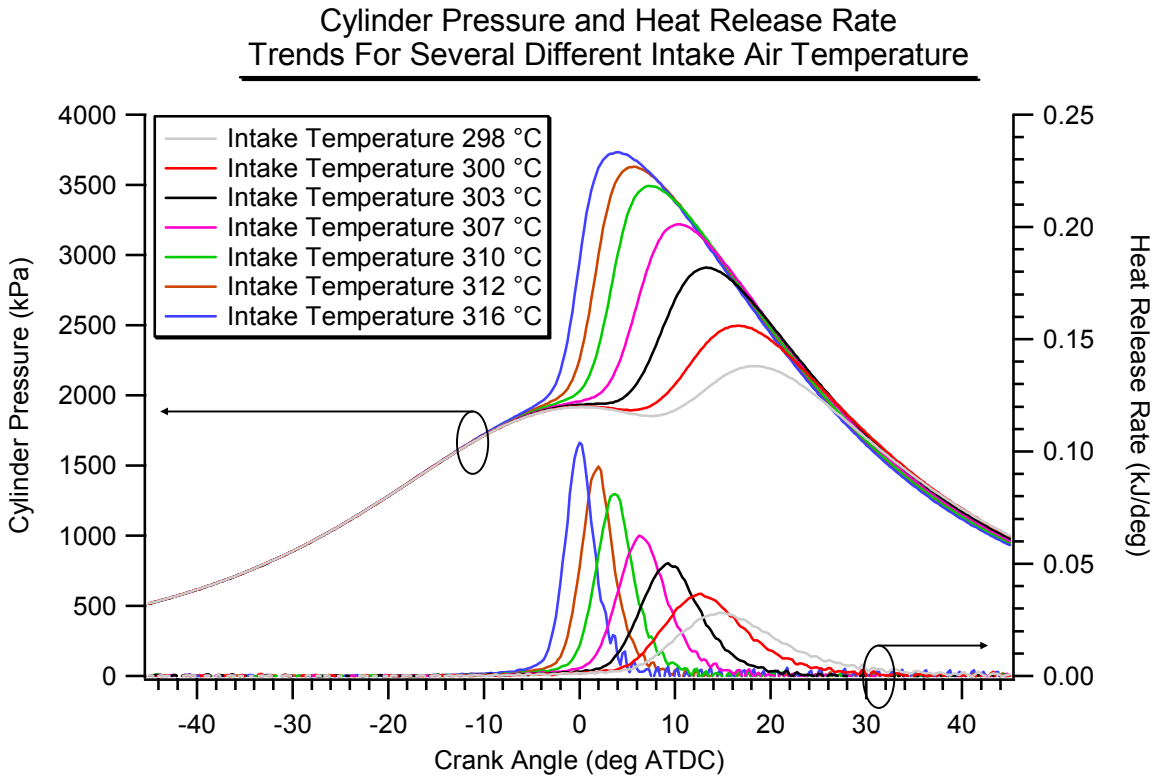

Figure 4-11 Cylinder pressure and heat release rates over intake air temperature sweep for data collected on April 12, 2004.

It is important to discuss why the IMEP data shows more variability that the rest of the pressure data indicates that is should. Looking at the polytropic expansion coefficient, Figure 4-12, it can be seen why the IMEP data is inconsistent. To calculate the polytropic expansion coefficient the value of the cylinder pressure from 20 degrees ATDC to 110 degrees ATDC is plotted on a logarithmic scale against the cylinder volume at those same crank angles, which is also plotted on a logarithmic scale. The pressure then appears as a straight line, the slope of this line is the value of the polytropic expansion coefficient.

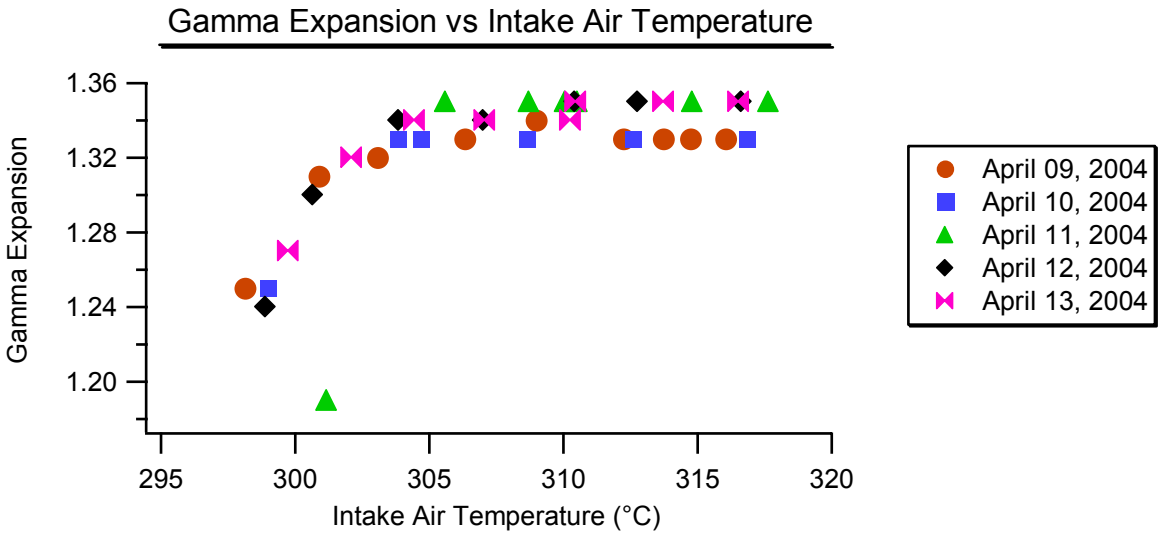

Figure 4-12 Polytropic coefficient of expansion

A review of the engine operation notes indicates that the pressure transducer was cleaned on April 11, 2004. It can be seen in the IMEP data that the data collected on the two days before the cleaning are consistent with each other and the data from the two days after the cleaning are also consistent with each other. The data from April 9 and April 10 have a lower expansion coefficient which means that the pressure doesn't drop as quickly in relation to the cylinder volume as the data taken on April 11 through April 13 this gives the higher IMEP values for those days. The mechanism for this difference can only be speculated at. Since all of the other pressure indicators are consistent the day-to-day variation in the IMEP and polytropic expansion data will be ignored. With a few exceptions the IMEP data will not be presented in the rest of the data analysis, instead the peak cylinder pressure will be used as the primary indicator of the engine's behavior in terms of cylinder pressure.

4.2.2 Engine Emissions Behavior

Several times through the course of this thesis it has been stated that one of the primary for investigating HCCI is the potential for the generation of almost no nitrogen oxide emissions. This potential is demonstrated in Figure 4-13. For intake temperatures below about 305 °C the engine produces no significant amount of NO_x, however, as the temperature increases towards the upper limit and the combustion phasing moves closer to TDC, the amount of NO_x generated in the cylinder begins to increase in an almost linear manner. These values are considerably lower that those currently generated in a spark ignition engine, but if an HCCI engine is to be run at a relatively high fueling rate near the upper end of the intake air temperature window, then the engine will still need a 3-way catalyst to remove the NO_x generated in the cylinder, particularly as government regulations continue to tighten.

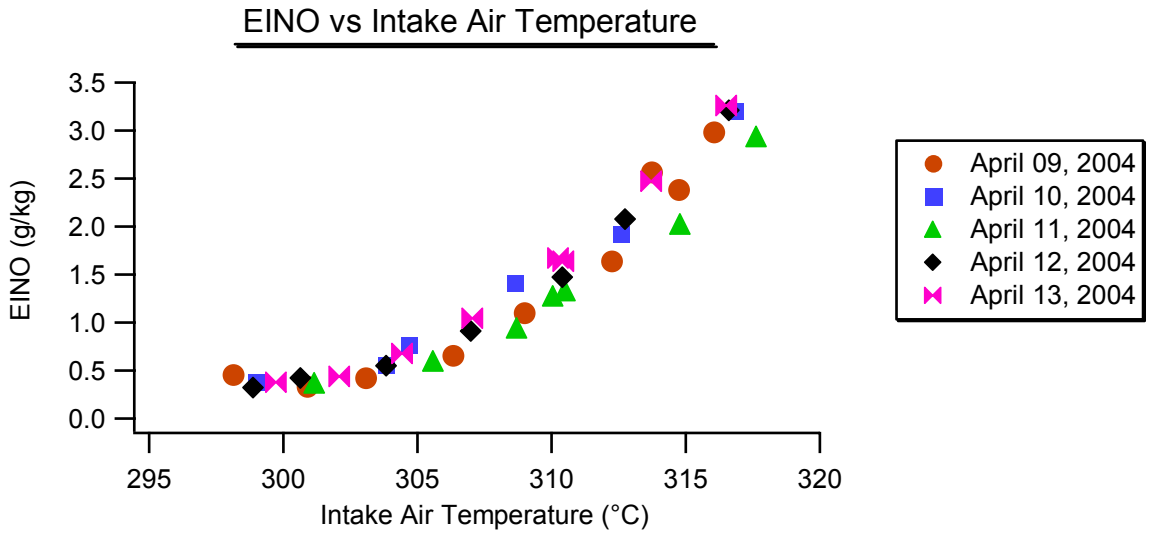

Figure 4-13 NO_x emissions vs. intake air temperature

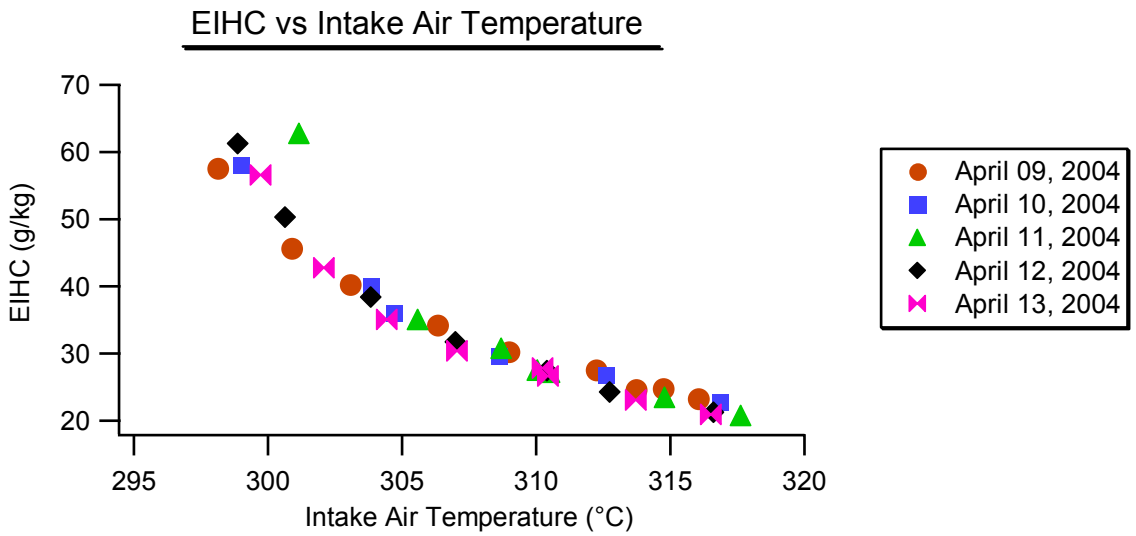

Figure 4-14 Unburned hydrocarbon emissions vs. intake air temperature

Figure 4-14 and Figure 4-15 show the emissions of unburned hydrocarbons and carbon monoxide from the engine respectively. These plots show how as the intake air temperature increases, and the combustion phasing begins to move closer to TDC, the emissions of both pollutants decrease. This is indicative of higher combustion temperatures and more complete reactions inside the cylinder. High levels of CO and HC emissions are symptoms of poor combustion efficiency. Low combustion efficiency means that a large amount of the chemical energy available in the cylinder, was not released or utilized, therefore, it is ideal to run the engine in regimes with high combustion efficiencies. Recent work by Dec has implied that the high amounts of CO and HC emissions, at low cylinder temperatures, is due to incomplete combustion in the bulk of the gasses. The combustion simply occurs too late in the cycle and the expansion due to piston motion cools the gasses before the reactions can move to completion. [26]

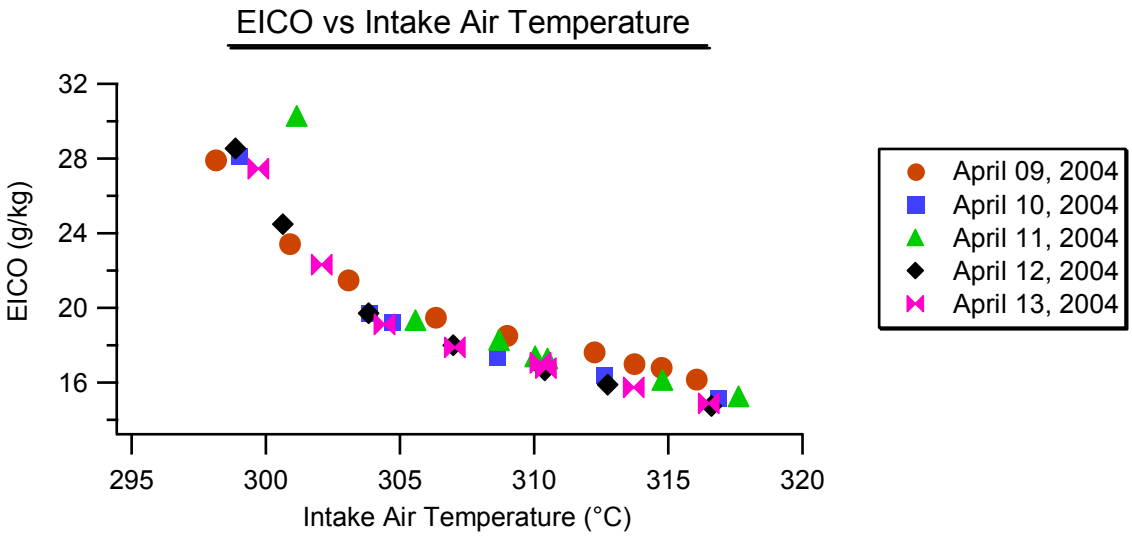

Figure 4-15 Carbon monoxide emissions vs. intake air temperature

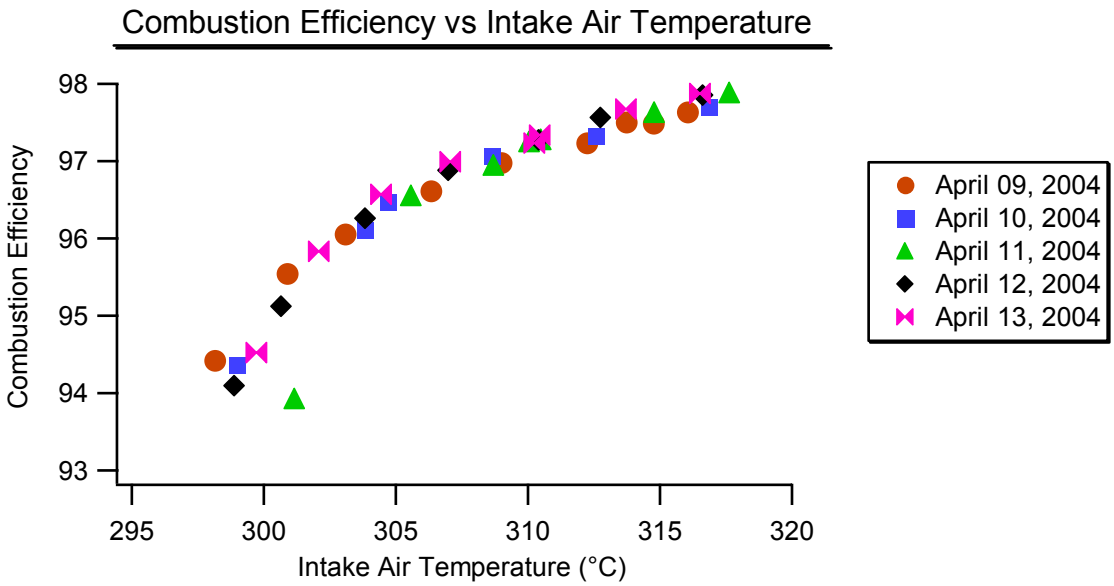

Figure 4-16 Combustion efficiency vs. intake air temperature

Figure 4-16 shows the calculated values of the combustion efficiency and how it changes as the intake air temperature increases. The combustion efficiency appears to have an asymptotic limit of approximately 98%. This is because a homogeneous mixture ensures that there will always be a certain fraction of the fuel trapped that is in the crevice volumes.

This portion of the charge remains too cold to react. Also you can see that the combustion efficiency seems to drop off very quickly near the low temperature limit, which shows that temperatures lower than 300 °C do not generate any significant amount of work in this engine at the chosen operating conditions.

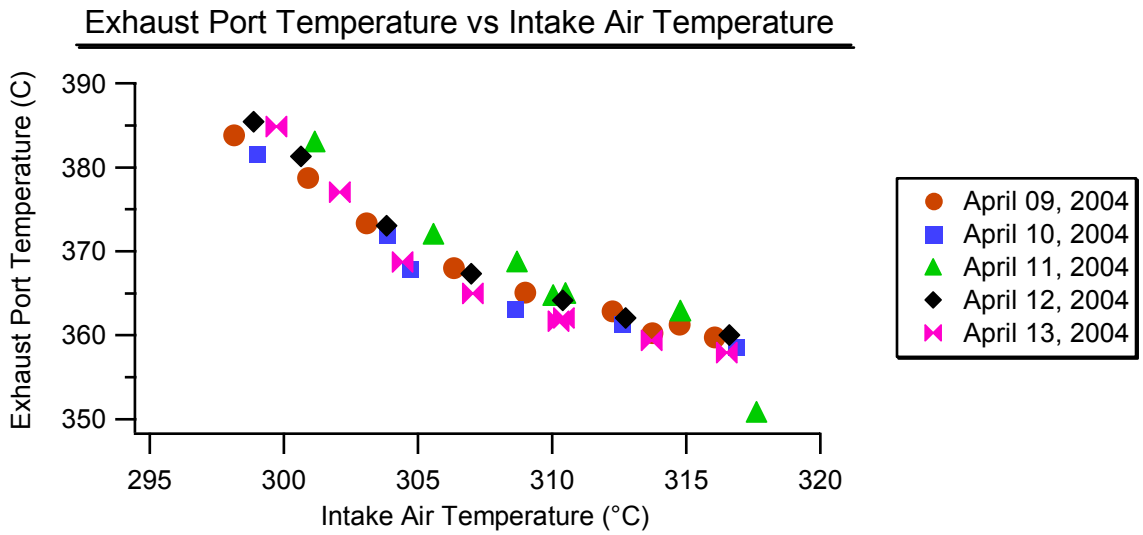

Figure 4-17 Exhaust port temperature vs. intake air temperature

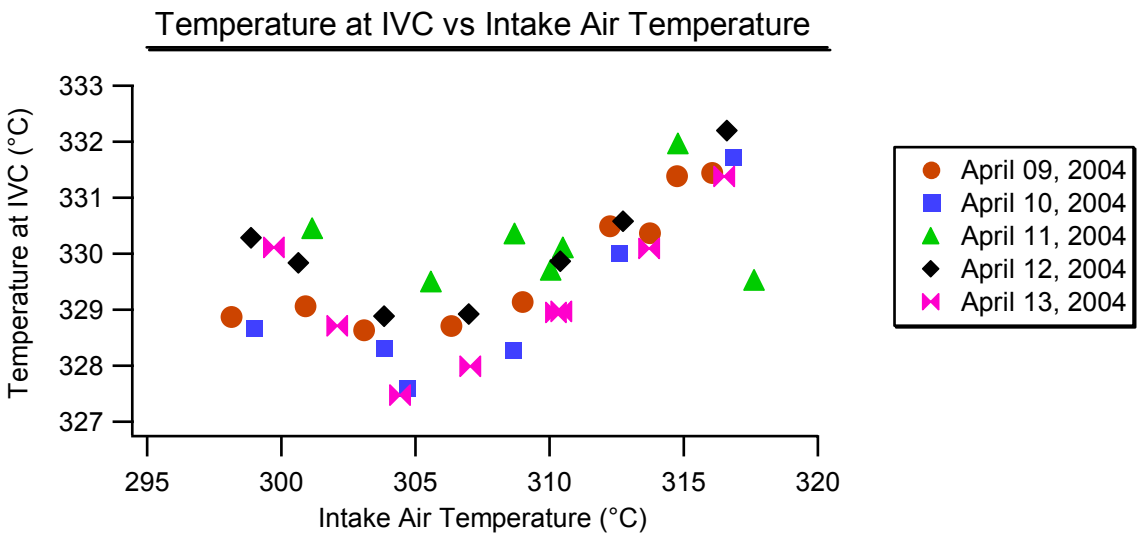

Figure 4-18 Temperature at IVC vs. intake air temperature

The exhaust temperature is another indicator of the combustion phasing. The exhaust temperatures can be seen in Figure 4-17. As the combustion begins to move closer to TDC the hot cylinder gasses have more time available for heat transfer, this lowers the exhaust temperatures. Also as the phasing moves closer to the best IMEP point the engine extracts more work from the gasses in the cylinder; this also yields lower exhaust temperatures. The plot also indicates that as the combustion phasing reaches TDC the exhaust temperatures will reach an asymptotic value of approximately 355 °C.

Figure 4-18 shows the values of the average temperature of the gasses inside the cylinder at the time that the intake valves close. This value is important to know because it indicates the amount of energy that it is necessary at the start of the compression process in order to successfully achieve auto-ignition. This parameter is a much more important indicator in a setup that utilizes exhaust gas rebreathing to achieve auto-ignition instead of external charge heating. The trend that the plot shows helps to confirm that to advance the combustion phasing the initial thermal energy of the charge inside the cylinder must be increased.

4.2.3 Repeatability of Controlled Engine Parameters

The plots in this section show the level of repeatability in the controlled operating parameters that can be achieved in the laboratory with the current setup. Figure 4-19 shows the repeatability of the fuel flow rates for each day. The fuel flow is calculated using the air/fuel ratio measured with the emissions bench and the airflow calculated using the critical flow orifice. Over all of the operating points collected the fuel flow is between 9.90

mg/cycle to 10.10 mg/cycle, these points would be within an error band of ±1% from the desired value of 10 mg/cycle. And as can be seen the band is even tighter for the majority of the points collected. The fuel flow calculation is also checked against a physical measurement of the fuel flow rate, these two values always agreed to within 0.3 mg/cycle. However, for the reasons discussed in 3.3.7, the fuel flow is hard to directly measure accurately and the direct measurements vary considerably more than those calculated using the air/fuel ratio measurement from the emissions bench.

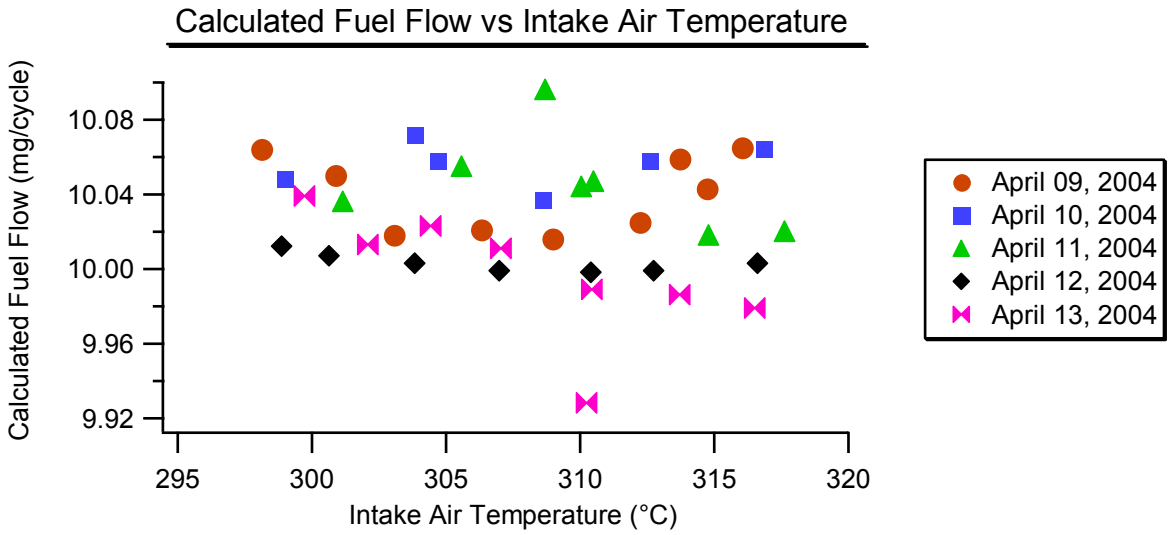

Figure 4-19 Calculated fuel flow rate vs. intake air temperature

The plot of the intake manifold absolute pressure (MAP), Figure 4-20, shows that the manifold pressure doesn't change considerably over the course of the test and the total day-to-day variation was approximately 1.2 kPa which is just a variation of about ±0.5% from the average value of the absolute pressure in the manifold. Since the pressure at the end of the compression process will be sensitive to changes in the starting pressure, the intake MAP, it

is important this pressure be kept constant so that the combustion behavior remains consistent.

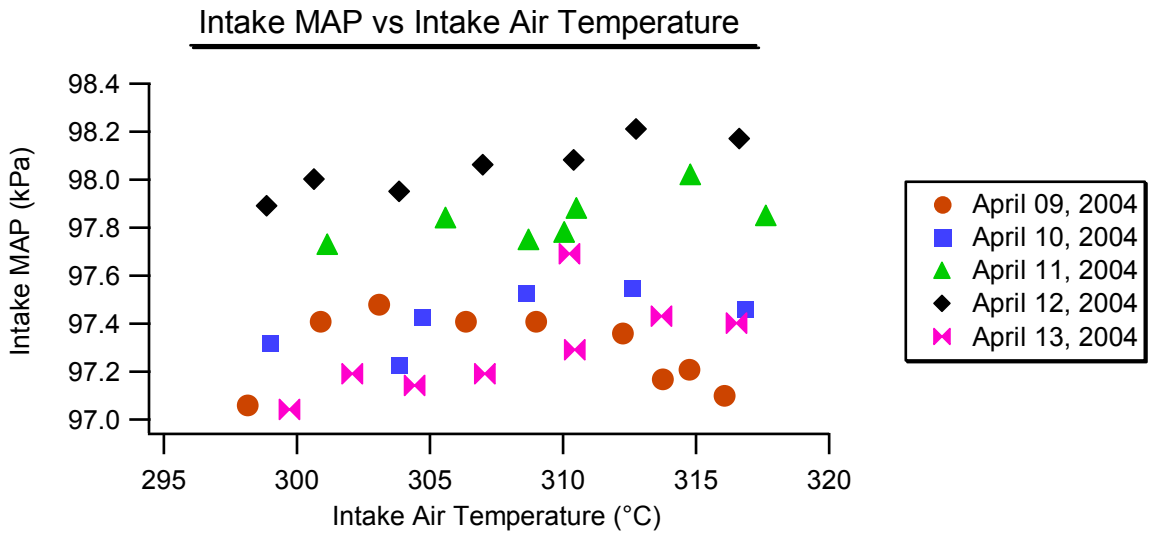

Figure 4-20 Intake manifold pressure vs. intake air temperature

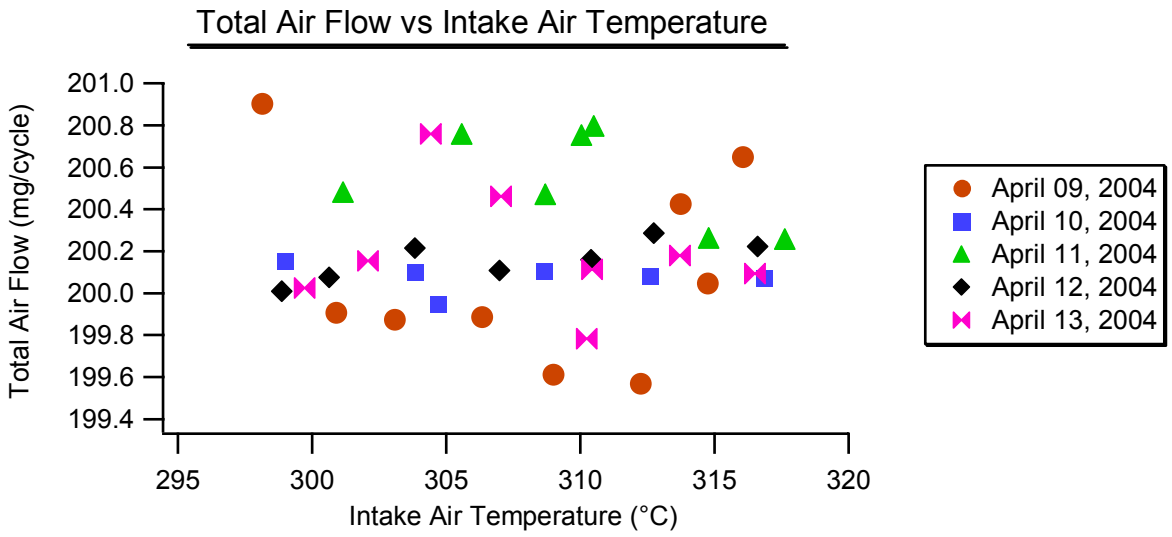

Figure 4-21 Measured air flow per cycle vs. intake air temperature

The recorded temperatures of the cooling water are shown in Figure 4-22. Fluctuations in the temperature of the cooling water will change the amount of heat transfer

from the gasses inside the cylinder to the head. If the heat transfer characteristics change day-to-day, or through the course of a test, then there would be no consistency in the cylinder pressure behavior. This is especially true since the thermal energy of the gasses in the cylinder is what determines the phasing of the combustion.

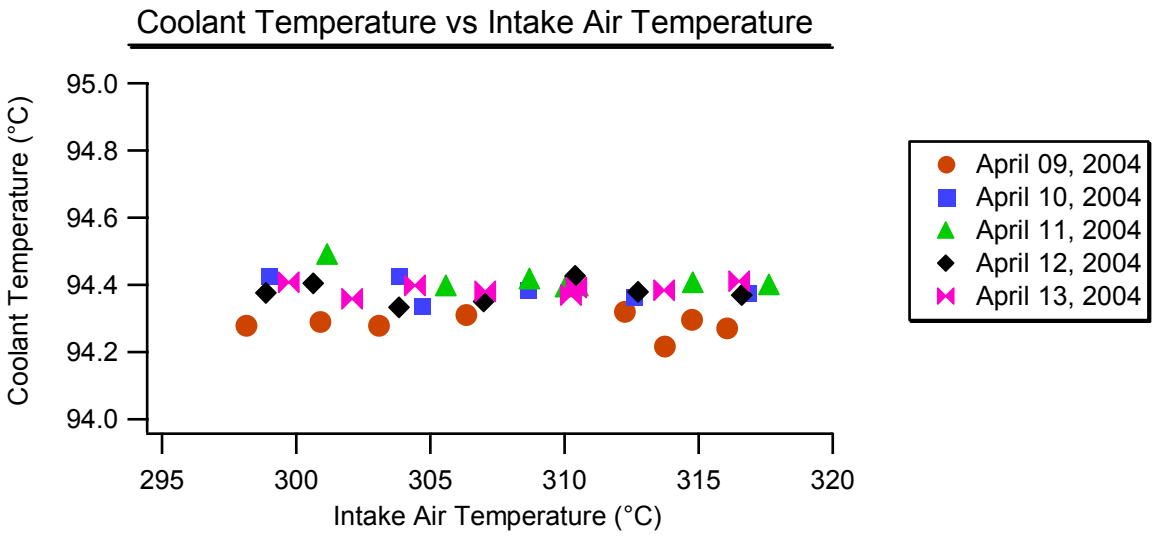

Figure 4-22 Coolant temperature vs. intake air temperature

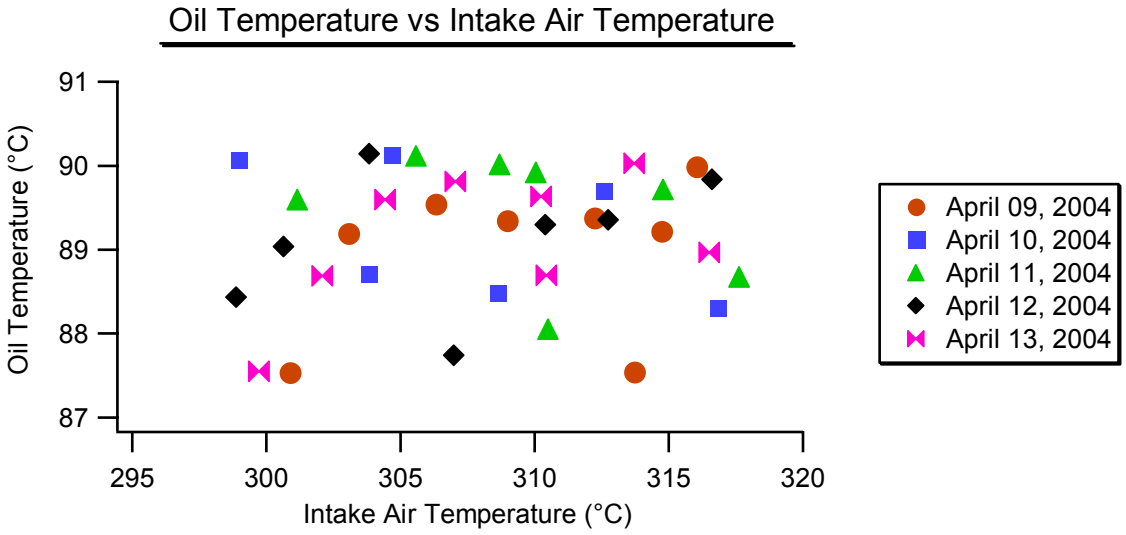

Figure 4-23 Oil temperature vs. intake air temperature

The recorded temperature of the lubricant as it entered the oil gallery is shown in Figure 4-23. This demonstrates that the oil temperature showed more variation than the cooling temperature. However, a K-type thermocouple has a quoted accuracy of ±1.6 °C. Therefore, the variability in the oil temperature is primarily within the quoted level of accuracy for the thermocouple and is ignored. The other reason for ignoring this variability is that the construction of the engine ensures that the oil is, for the most part, thermally isolated from the gasses inside the cylinder. There is a little bit of oil that travels up and down the cylinder walls with the piston, but otherwise the lubricant does not interact with the combustion chamber or the engine components in a way that would alter their temperature.

The results of this experiment show that the combustion is very stable on a day-to-day basis. The work also shows that HCCI combustion is very sensitive to changes in the temperature of the charge inside the cylinder prior to the onset of compression. The combustion shows low cyclic variability over most of the intake air temperatures investigated. At lower intake air temperatures the combustion shows high amounts of variability coupled with a large amount of CO and unburned hydrocarbon emissions. As the intake air temperature increases the combustion becomes more robust and the phasing moves closer to TDC. The only parameter of the data that showed a significant variability is the IMEP. The IMEP values exhibited sensitivity to differences in the polytropic coefficient of expansion, which can not be easily explained.

Chapter 5 - Sensitivity to Intake Charge Heating

There are several things in the engine setup that cause concern about the state of the fuel entering the cylinder. The engine installed in this laboratory has a relatively low compression ratio. Low compression ratios coupled with the employment of high octane fuels, and a lack of internal EGR, meant that the intake charge temperatures had to be in excess of 500 K. Also when running in premixed mode at 1000 RPM the intake charge has a residence time of about 9 seconds in the intake system.

Air/fuel mixtures at temperatures near 500 K often participate in low temperature reactions, this suggests that the fuel entering the engine could be isomerized or partially reacted. While the fuels used in this experiment were not expected to exhibit cool flame behavior participation in these reaction types is still a concern that needs to be addressed.

A series of experiments were performed in order to determine if the fuel was reacting in the intake system due to the long residence times at high temperatures. The following sections present the experimental matrix for these tests as well as the results of the experiments.

Section 5.1 Experimental Notes and Conditions

The volume of the intake system between the premixed fuel injector and the intake valves, which includes the pipes, the surge tank, and the intake runner, is approximately 40 liters. This is equal to approximately 80 times the individual cycle

consumption of fresh charge. At 1000 RPM that volume of premixed charge has a residence time of approximately 9 seconds. To counteract heat loss all of this volume is heated to a temperature above the desired engine inlet temperature. The residence time and the temperature of the charge may be sufficient for the mixture to begin reacting in the intake system. If the fuel is reacting in the intake system it would be expected that the fuel molecules would under go hydrogen abstraction reactions as well as some oxygen addition reactions. The result of undergoing these steps would most likely be to lower the auto ignition resistance of the fuel. If this were the case, as the gas temperatures in the surge tank were increased the combustion would advance, even though the final intake air temperature was held constant.

In order to determine if low temperature reactions were, in fact, occurring the intake system was configured to allow independent control of the temperature of each heater strip in the intake system and the control system was configured to maintain the surface temperature at each of the heater strips at a constant temperature. This configuration also maintained the gas temperatures through the intake system at a constant value. Referring to Figure 5-1, the control system was setup so that $T_{w1} = T_{w2} = \ldots = T_{w6}$ and $T_{g1} = T_{g2} = T_{g3}$. The gas temperatures, T_{g1} through T_{g3}, were one of the independent variables in this experiment.

The actual engine inlet air temperature, T_{in} in Figure 5-1, was adjusted to maintain acceptable HCCI combustion as the temperature in the upstream portions of the intake system was changed. T_{in} was manipulated by allowing heat transfer, in the runner, to cool the charge below $T_{g1} = T_{g2} = T_{g3}$, or using the rope heaters to add extra heat causing T_{in} to be above $T_{g1} = T_{g2} = T_{g3}$. In these tests the engine was swept over the range of acceptable HCCI combustion for different values of $T_{g1} = T_{g2} = T_{g3}$.

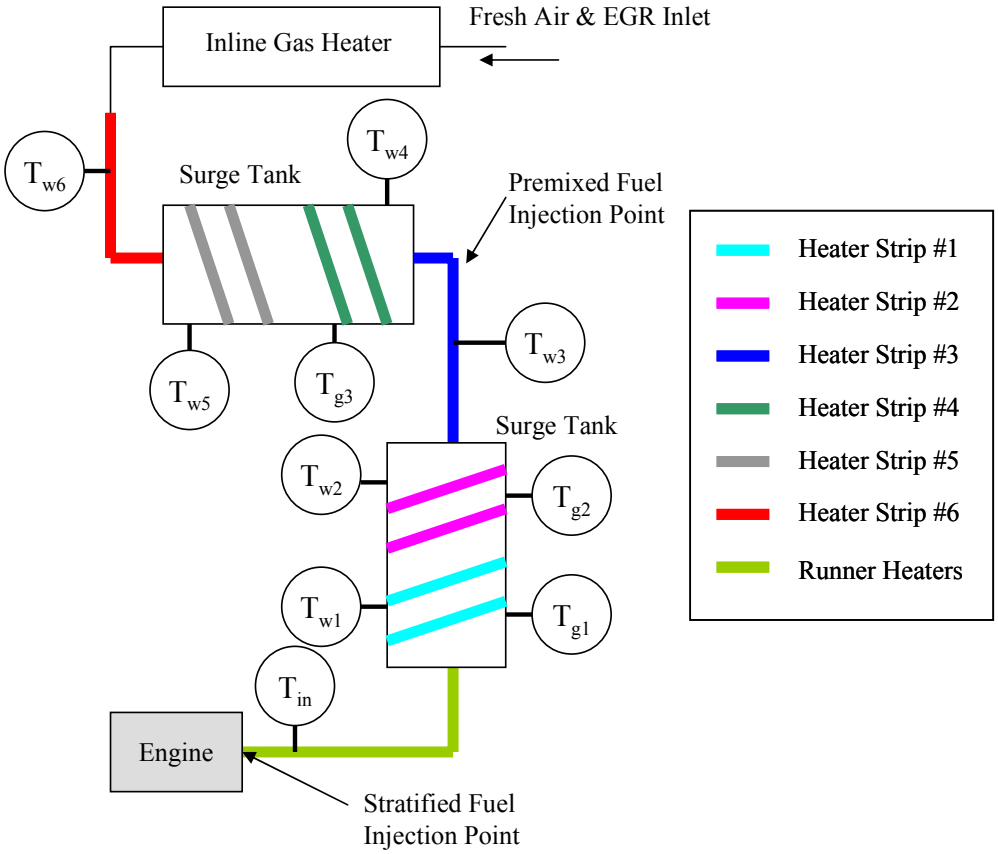

Figure 5-1 Intake heating system

In order to get an indication of the extent of low temperature reactions occurring in the intake system, different fuels were used in these experiments. A fuel with a higher initial resistance to auto ignition would be expected to show less tendency to participate in the low temperature reactions than a fuel with less resistance to auto ignition. The fuels employed in this experiment were PRF87, EEE, and Isooctane. If low temperature reactions were occurring in the intake system then the PRF87 would be expected to exhibit more sensitivity to changes in the upstream temperatures than isooctane or EEE. The temperatures at which

auto ignition occurs is different for each fuel, therefore the final intake air setting changes with each fuel. The experimental matrix for these conditions is shown in the tables below.

Speed	1000 RPM
Surge Tank Gas Temperature	276, 280, 285, 290
Engine Inlet Temperature	245 – 295
Fueling Rate	10 mg/cycle
Fuel Type	PRF87

Table 5-1 Intake air thermal history sensitivity experimental matrix for PRF87

Speed	1000 RPM
Surge Tank Gas Temperature	280, 290, 300, 310
Engine Inlet Temperature	255 - 295
Fueling Rate	10 mg/cycle
Fuel Type	EEE

Table 5-2 Intake air thermal history sensitivity experimental matrix for EEE

Speed	1000 RPM
Surge Tank Gas Temperature	295, 305, 315, 325
Engine Inlet Temperature	285 - 315
Fueling Rate	10 mg/cycle
Fuel Type	Isooctane

Table 5-3 Intake air thermal history sensitivity experimental matrix for Isooctane

Section 5.2 Fueling with PRF87

Figure 5-2 shows the IMEP for each of the various values of $T_{g1} = T_{g2} = T_{g3}$ in the surge tank plotted as a function of the final intake runner air temperature, T_{in}. In the figure it can be seen that as the temperature in the surge tanks increases the window of temperatures over which successful HCCI combustion can be achieved shifts to lower values of T_{in}.

The range of actual engine intake air temperatures shown in Figure 5-2 span the range of intake temperatures that could be achieved with the current intake heating setup. The rope

heaters wrapped around the intake runner where capable of heating the intake air about 20 ºC above the temperature of the gasses upstream of the runner, this is why the lowest surge tank temperature is 276 ºC. Heat transfer in the intake runner is capable of decreasing the gas temperatures by approximately 45 ºC. This is why no upstream temperatures greater than 290 ºC were investigated in this work.

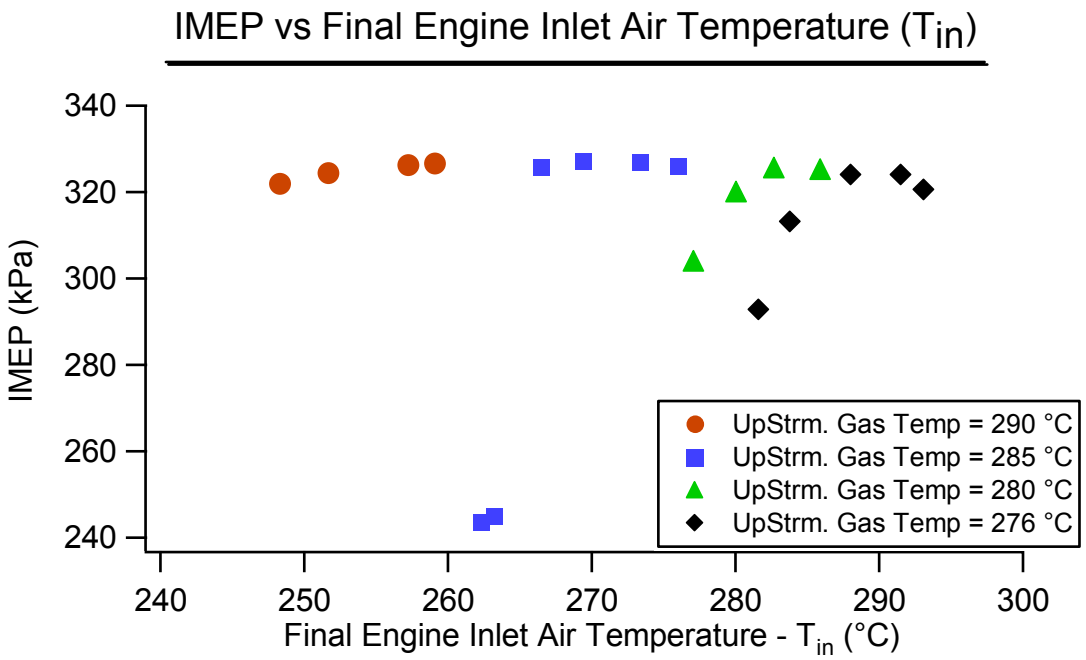

Figure 5-2 IMEP vs. final engine inlet air temperature for PRF87 fuel

For the operating conditions where the surge tank gas temperature was maintained at 276 ºC the HCCI operating window was entirely above the temperature of the gasses in the surge tank. As the gas temperature in the surge tanks increased the HCCI operating window shifted towards lower inlet temperatures. It is also interesting to note that the differences in operating windows between the case with the 276 ºC surge tank temperature and the 280 ºC temperature is relatively small, however, once the surge tank temperatures rise above 280 ºC

the operating window seems to shift to lower final engine inlet temperatures in 10 ºC increments.

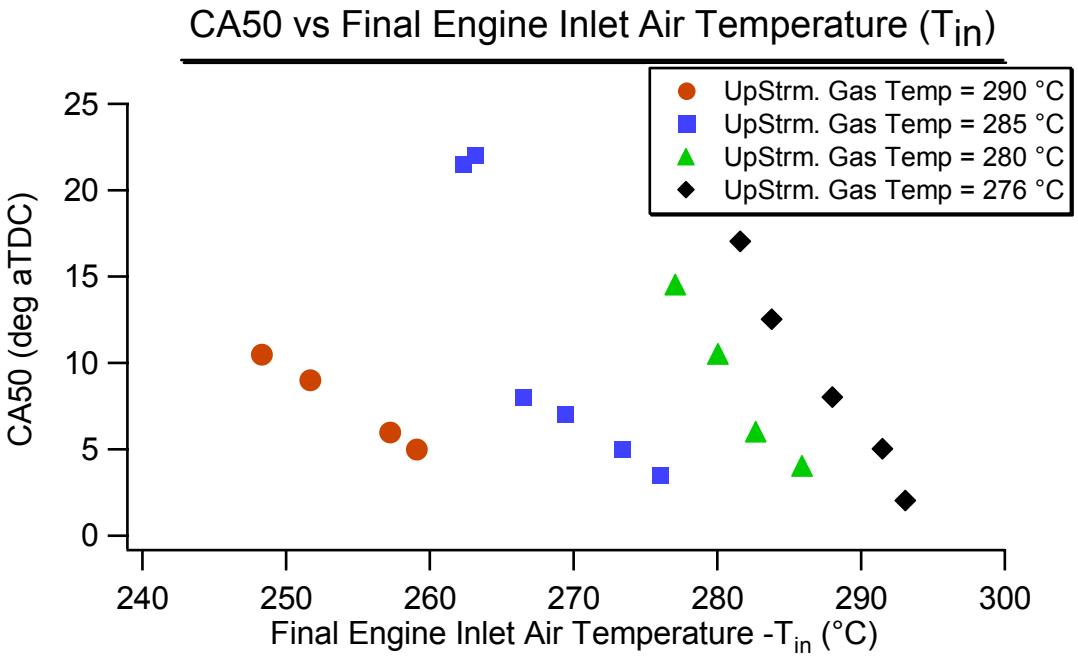

Figure 5-3 CA50 vs. final engine inlet air temperature for PRF87 fuel

An examination of the combustion phasing as a function of the engine inlet air temperature, seen in Figure 5-3, shows that as the temperature of the gasses in the surge tank increases the 50% mass fraction burned point shifts to lower temperatures. This plot indicates that the HCCI operating window is not being extended by raising the upstream gas temperatures in the surge tank; instead the window is being offset towards lower engine inlet temperatures with increases in the surge tank temperatures. Another way of stating the trends indicated in this plot is, in order to maintain the combustion phasing at a given crank angle the actual temperature of the air entering the engine has to be decreased as the temperature of the air in the heating chambers upstream of the intake valves increases.

A look at the plot of the combustion phasing as a function of the combustion efficiency, Figure 5-4, shows all of the data collapsed down to a single curve. This means that for a given total amount of fuel reacted, (combustion efficiency) the point where 50% of the fuel mass has reacted always occurs at the same crank angle. However, the actual engine inlet temperature, at which this combustion efficiency occurs, decreases with the increase in the gas temperature in the surge tanks.

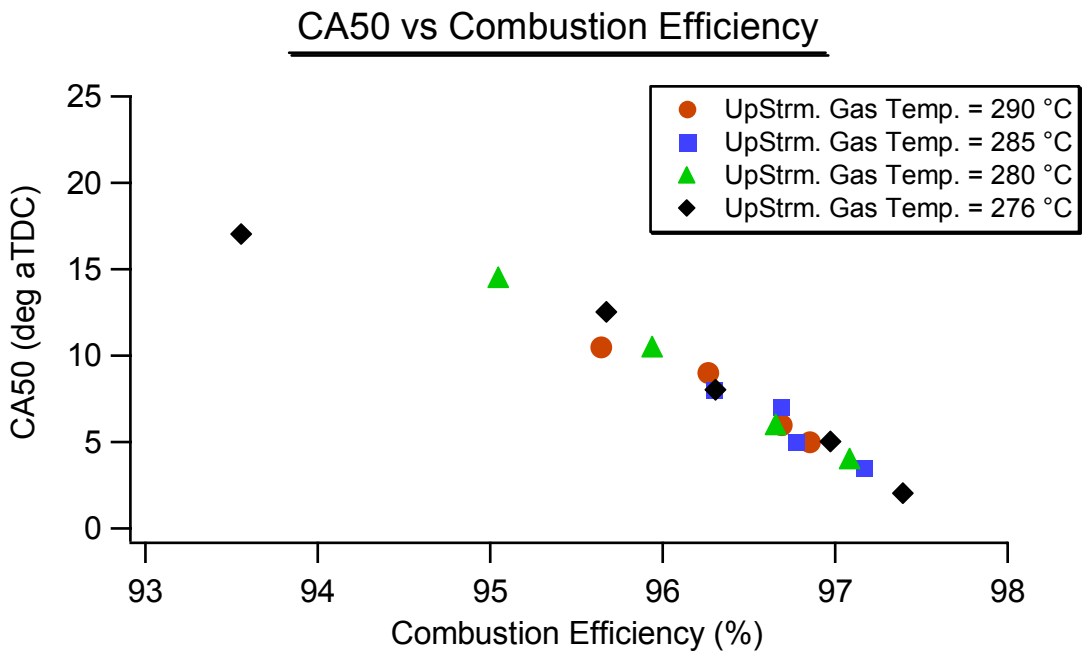

Figure 5-4 CA50 vs. combustion efficiency for PRF87 fuel

An examination of the NO_x emissions as a function of combustion efficiency, seen in Figure 5-5, provides an interesting look at how the different engine intake temperatures affect the generation of NO_x. From the plot it can be seen that for a given amount of fuel reacted the most NO_x is generated with the operating conditions where the temperature of the gasses in the surge tank is 276 ºC, this is the case where the actual temperature of the gasses entering the engine are in the range from 280 to 295 ºC. When the temperature of the gasses

in the surge tank is increased to 290 ºC the amount of NO_x emissions generated in the engine at a given combustion efficiency are noticeably lower than is observed in the cases with lower upstream gas temperatures. This indicates that as the actual engine inlet temperature is decreased the combustion temperatures decrease which acts to reduce the NO_x emissions from the engine.

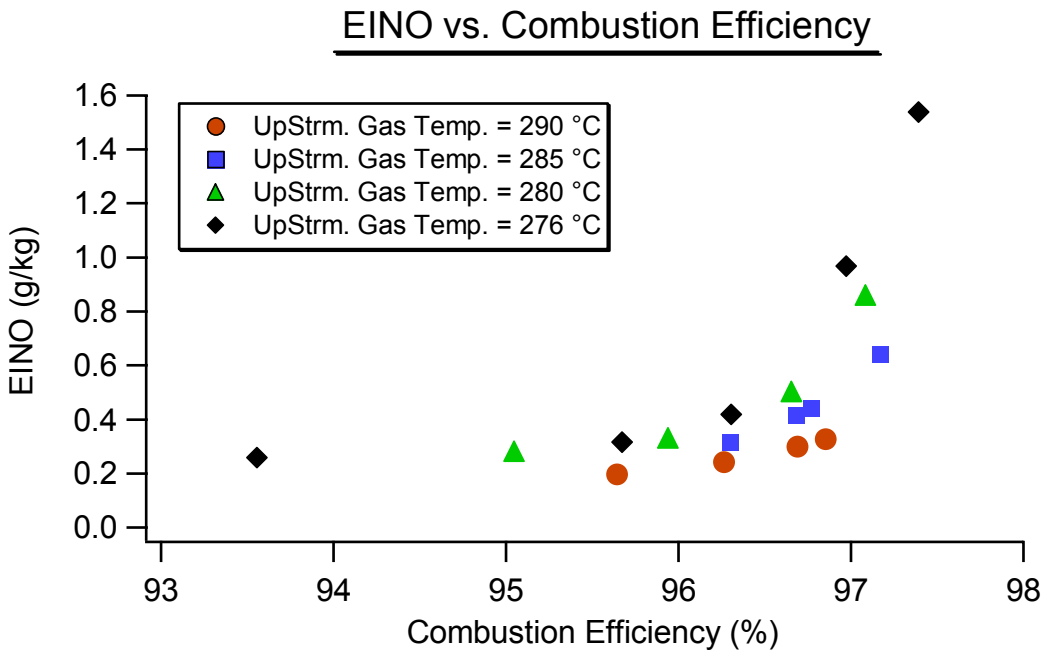

Figure 5-5 NO_x emissions vs. combustion efficiency for PRF87 fuel

The conclusion that the combustion temperatures are lower for the cases where the surge tank temperature is 290 ºC can be verified by looking at the plot of CO as a function of combustion efficiency, Figure 5-6. This plot shows that for a given amount of fuel reacted, the highest CO emissions are emitted when the gasses in the surge tank are heated to 290 ºC and the temperature of the charge as it actually enters the engine is between 250 and 260 ºC.

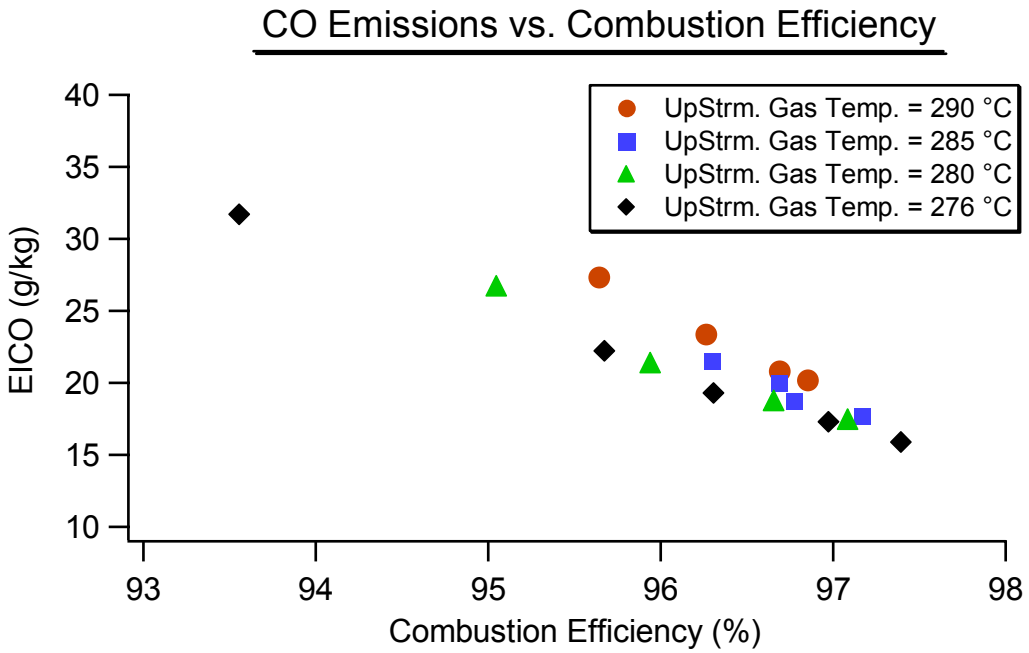

Figure 5-6 CO emissions vs. combustion efficiency for PRF87 fuel

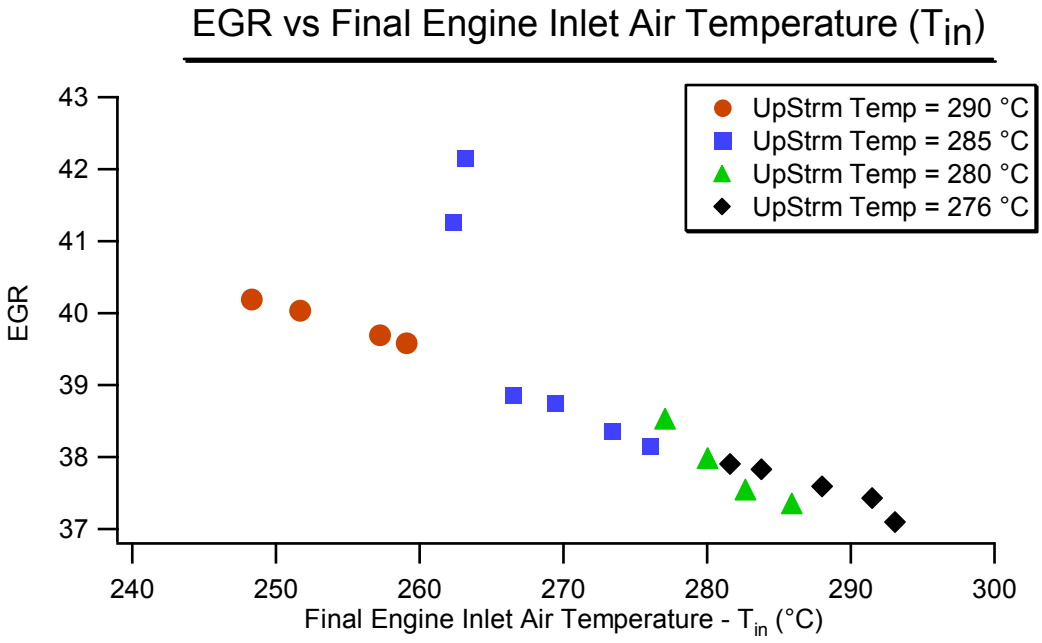

Figure 5-7 EGR fraction vs. final engine inlet air temperature for PRF87 fuel

As would be expected, for reductions in the value of T_{in} the amount of EGR inducted into the engine increases. For the range of surge tank gas temperatures tested in this work the

EGR increased by a total of approximately 3%. This increase can be seen in Figure 5-7. Since the actual engine inlet temperature is lower for the cases with higher upstream temperatures the density of the gasses at the inlet is higher which means that more mass enters the engine each cycle for these cases. However, since the mass of fresh air entering the cylinder each cycle is fixed, and so is the mass of fuel entering the engine, the extra mass inducted into the engine is EGR. The reasons for this laboratory configuration were discussed in section 4.1.3 and were a result of the decision to maintain a constant inlet pressure.

What is most interesting about the observation that the EGR increases as the final inlet temperature decreases, is that the combustion does not seem to be affected by this increase. EGR typically dilutes the mixture and thus slows down the combustion rates; this is not detected in these results. It is most likely that the act of increasing the diluents, and decreasing the charge temperature both work to slow down the combustion and counter the trend of advancing combustion phasing with increased surge tank gas temperatures.

Examination of these results quickly leads to the hypothesis that the fuel is beginning to break down in the intake system prior to entering the engine. Since the PRF87 fuel is composed of 13% normal heptane, which is a molecule that isomerizes quite easily it is most likely that this molecule is the one that is degrading in the intake system. It is probable that the n-heptane is participating in some of the initiation reaction steps in the intake prior to entering the engine. As the upstream temperature increases the amount of n-heptane that participates in these initiation steps increases thus generating larger radical pools whose higher reactivity helps to lower the temperature threshold of auto-ignition. The radicals will have more time to react during the compression stroke which means that the system will

reach its auto-ignition criteria at an earlier point in the cycle. To counter the advancing combustion phasing the actual inlet temperature must be lowered which slows the kinetic rates, this works to keep the combustion phasing at the same point in the cycle. As can be seen in Figure 5-8, the temperature at which the combustion is 5% complete decreases as the upstream temperature increases. This plot reinforces the hypothesis that the fuel is reacting in the intake and this action works to advance the ignition point of the air/fuel mixture one it is inside the engine.

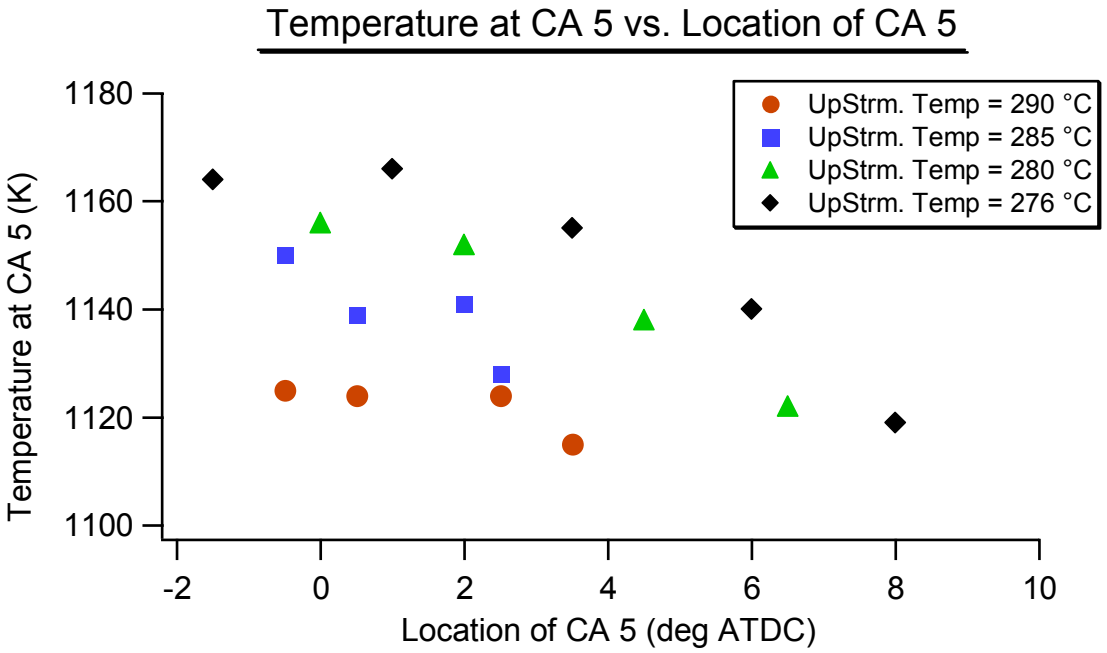

Figure 5-8 Temperature at CA5 vs. location of CA5 for PRF87 fuel

It is instructive to look at the cylinder pressure and heat release characteristics of the combustion events recorded in this work, examples of which can be seen in Figure 5-9. Each curve on the plot represents the ensemble average of 500 combustion events. The data points presented in this graph were selected because their combustion phasing was such that the location of the 50% burn point (CA50) was between 5 and 6 deg ATDC. The curves for each

of the upstream heating conditions show almost identical pressure and heat release curves for the selected combustion phasing. It is also interesting to note that there is no indication of cool flame activity for any of the heating conditions. This plot also reinforces the idea that the amount of upstream heating only changes the starting point of the kinetics mechanism not the actual characteristics of the combustion itself.

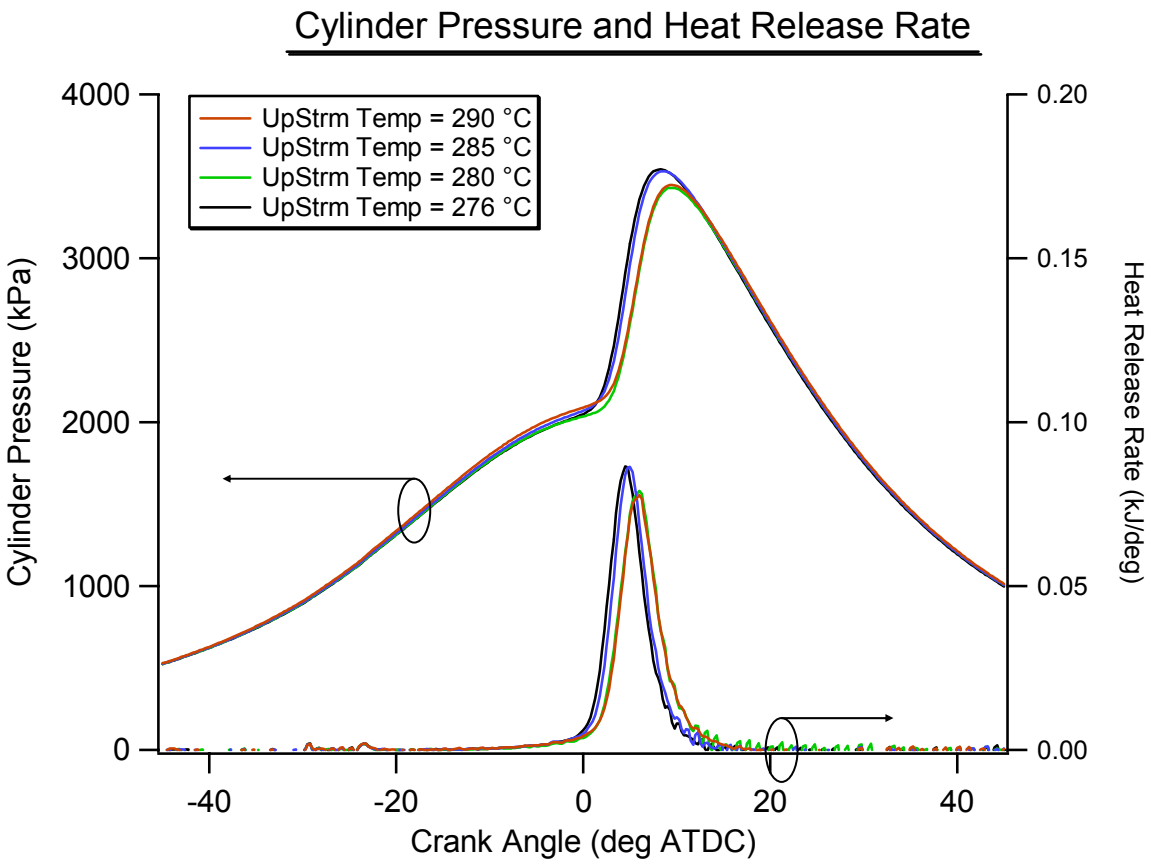

Figure 5-9 Cylinder pressure and heat release rate for PRF87 fuel, CA50 values for each upstream temperature data set are between 5 and 6 dATDC.

The temperatures of the gasses inside the cylinder are shown in Figure 5-10. These values are calculated using the ideal gas law and the measured cylinder pressure, with the volume being calculated using the slider crank mechanism. The equations are also shown in **Error! Reference source not found.** of the appendix. The peak in-cylinder temperatures

due to combustion become lower as the upstream heating increases, corresponding to the decrease in the intake runner temperature that was necessary to keep the combustion phased correctly. This result is one more indicator that upstream heating is changing the intake air/fuel mixture in some way that decreases its resistance to auto-ignition.

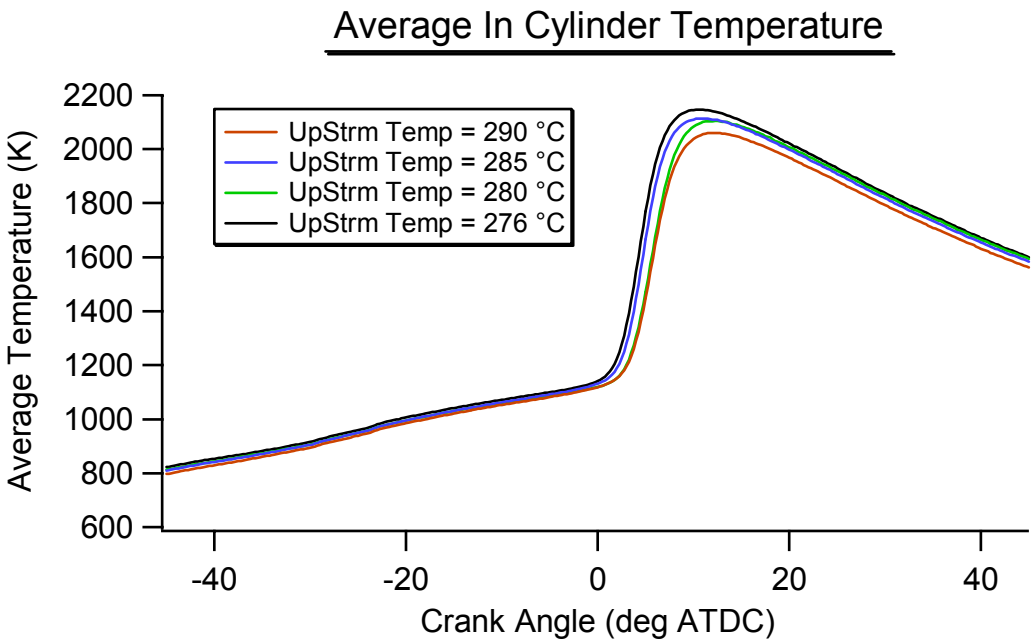

Figure 5-10 Average in-cylinder temperature for PRF87 fuel, CA50 values for each upstream temperature data set are between 5 and 6 dATDC.

In order to verify the hypothesis of intake system fuel reformation, the same tests were rerun with isooctane as the fuel. It is believed that pure isooctane, with its high octane number, will not be as susceptible to thermal cracking in the intake system as was the n-heptane in the PRF87. Thus the results from these new experiments should show little sensitivity to the temperature of the gasses upstream of the inlet valves.

Section 5.3 Fueling with Isooctane

The results for the experiments performed with the isooctane fuel can be seen in Figure 5-11 through Figure 5-14. These experiments were performed so that the experimental conditions were as close of a match to the PRF87 experiments as possible. The only differences were the composition of the fuel and the intake temperature set points. The results of these experiments provide a sharp contrast to the experiments performed with the PRF87.

The first thing to note is the total lack of sensitivity to the temperature of the gasses upstream of the engine inlet, which can be seen in the plot of IMP as a function of the actual engine inlet air temperature, Figure 5-11. Over the complete set of upstream temperatures investigated the engine's performance did not exhibit any significant behavior changes.

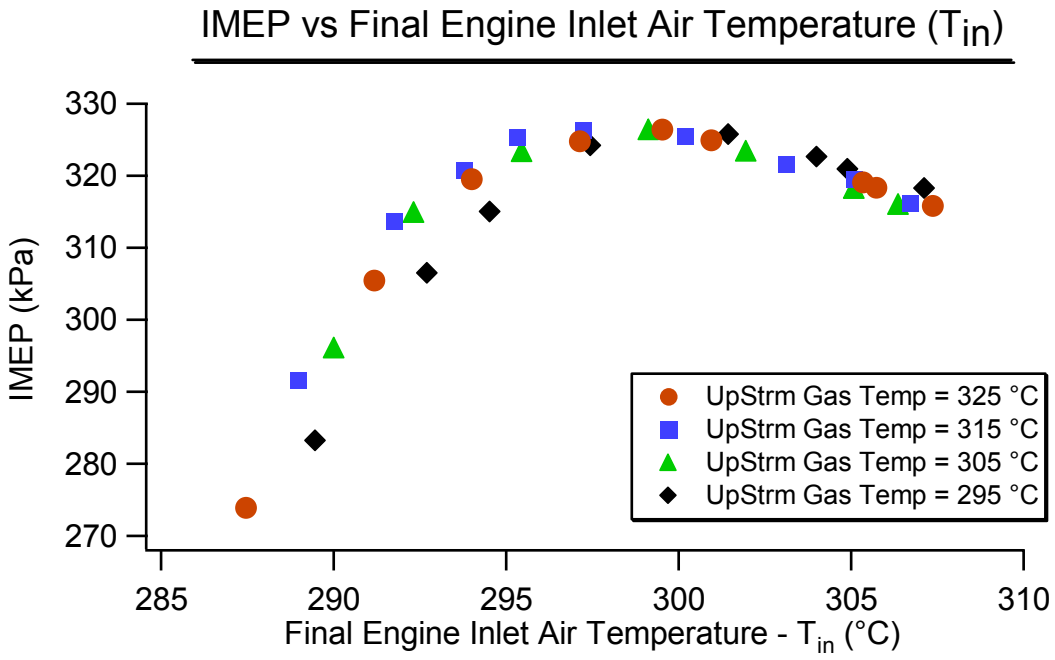

Figure 5-11 IMEP vs. final engine inlet air temperature for isooctane fuel

The other trend that can be seen in these plots is that the actual engine inlet temperature operating windows for all of the isooctane cases are higher than for the PRF87 cases. This is due to the higher octane number of pure isooctane, which reflects the tendency of the fuel to resist auto ignition. However, the width of the operating window of the actual engine inlet air temperature is not significantly different from the results of the PRF87 experiments, and the shape of the curves is consistent with the previously presented experimental results.

The plot of the location of the 50% burn point as a function of the actual intake air temperature, Figure 5-12, shows that the combustion phasing for the pure Isooctane experiments also does not show any significant sensitivity to temperature of the gasses upstream of the intake runner. This is consistent with the results shown in Figure 5-11 and with the expectations presented above.

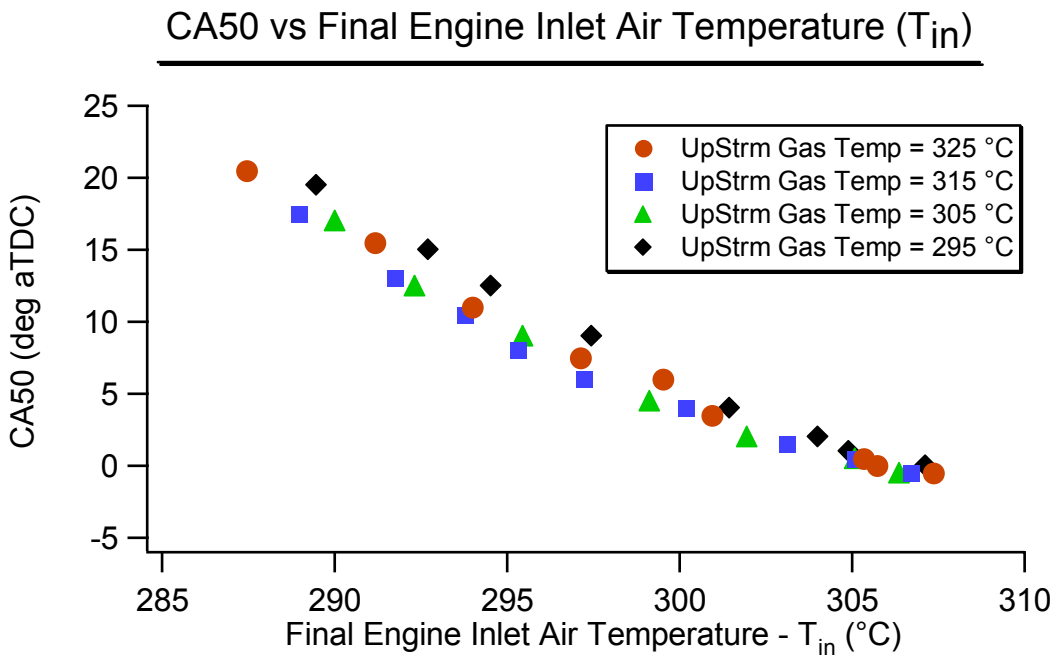

Figure 5-12 CA50 vs. final engine inlet air temperature for isooctane fuel

The data presented in these plots lead to the conclusion that the Isooctane fuel is not breaking down in the intake system. It further reinforces the hypothesis suggested in the previous section that it is the n-heptane in the PRF87 beginning to react in the intake prior to entering the engine that is responsible for the shift in operating windows with the increase upstream temperatures.

An investigation into the engine out emissions for this case shows that the emissions are also not sensitive to the upstream temperature of the mixture. The NO_x emissions are plotted as a function of combustion efficiency in Figure 5-13 and the carbon monoxide emissions are plotted as a function of combustion efficiency in Figure 5-14. For both of these plots the data shows only one trend line for all of the upstream gas temperatures investigated, unlike the PRF87 data presented earlier. This implies that for isooctane the driving parameter for the auto-ignition phenomenon is only the temperature of the intake charge just prior to entering the engine. Using these data for a reference it was decided that until rebreathing cams are installed in the engine, which will lower inlet temperatures, all future experiments would be performed using pure isooctane as the fuel.

All of the data, taken with isooctane as the fuel, show that the trends detailed in the previous section must be a fuel related effect. Since all of the other operating conditions were the same, if the trends described previously were not fuel related then they should also have been observed in the data presented in this section where pure isooctane was run in the engine.

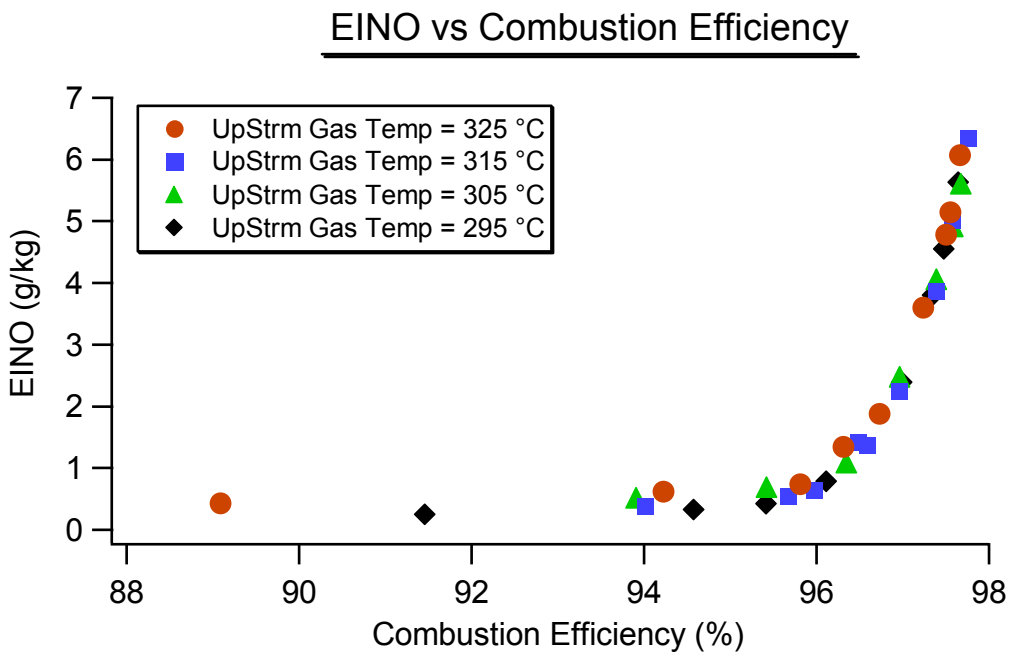

Figure 5-13 NO_x emissions vs. combustion efficiency for isooctane fuel

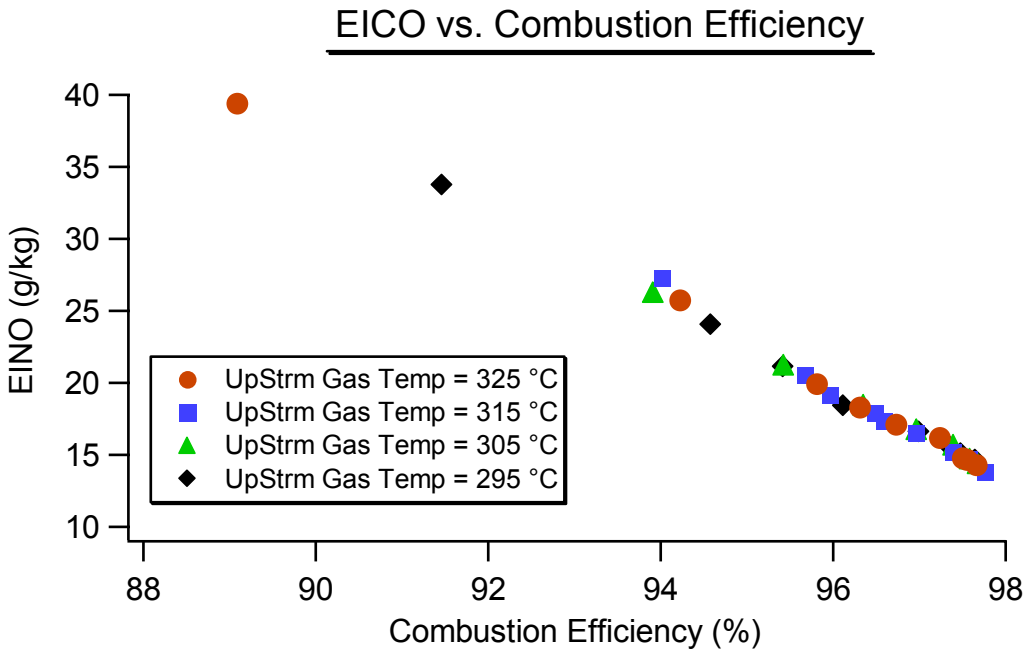

Figure 5-14 CO emissions vs. combustion efficiency for isooctane fuel

Section 5.4 Fueling with EEE

The results presented in the last section are for pure fuels that are paraffinic in nature, however real gasolines are composed of many different types of components including paraffins, olefins and aromatics. A typical gasoline fuel will also have molecules of many different lengths and varied auto-ignition characteristics. Therefore it is also instructive to investigate if a real gasoline would be susceptible to the same operating window shift that the PRF87 fuel was. Therefore EEE reference gasoline was also run in the engine at the same operating conditions as described in the previous sections. The objective of this series of tests was to determine how a real gasoline would respond to various upstream inlet heating conditions.

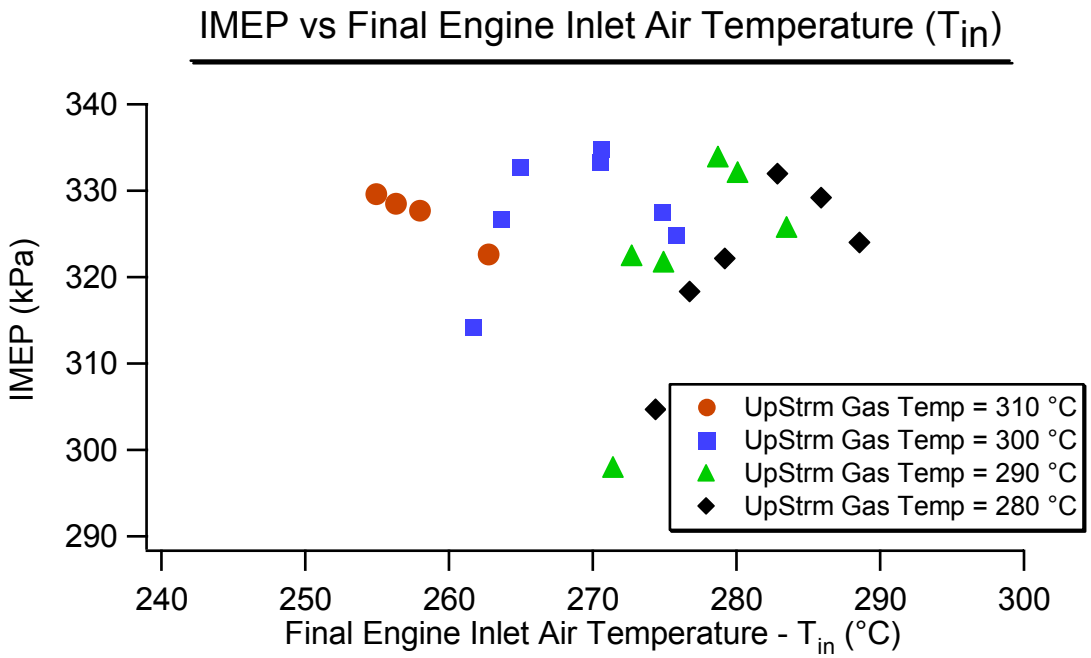

Figure 5-15 IMEP vs. final engine inlet air temperature for EEE fuel

The results from operation with EEE fuel are shown in Figure 5-15 through Figure 5-20. From a global standpoint the trends shown in these figures are the same as those shown in Section 5.2 where the engine is run with the primary reference fuel blend. The major difference between the EEE results and the PRF87 results is that in order to shift the engine's performance to intake temperatures 10 °C lower than the previous upstream heating condition, the upstream gas temperatures have to be increased by 10 degrees as opposed to the observed 5 degree changes for the PRF87. This observation would indicate that for the EEE fuel there is a smaller number of light molecules that are capable of reacting in the intake and therefore enhancing the combustion. This is consistent with its higher octane number relative to the PRF87.

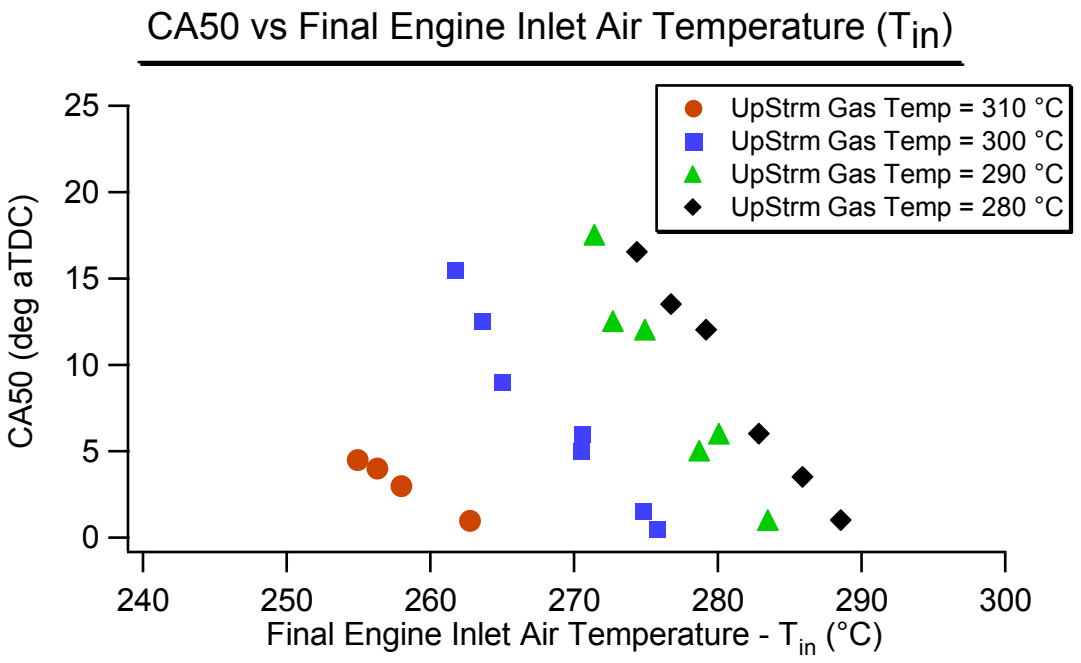

Figure 5-16 CA50 vs. final engine inlet air temperature for EEE fuel

The plots also indicate that the fuel degradation in the intake does not become a significant factor until the upstream temperature has increased above 280 °C. This is evident from the observation that the change in the HCCI operating window is insignificant when the upstream gas temperatures increase from 270 to 280 °C. However, for the higher upstream gas temperatures investigated the shift in the operating window to lower values of T_{in} is more noticeable. As in the previous results the combustion behavior with respect to phasing, such as CA50, collapse when plotted as a function of combustion efficiency.

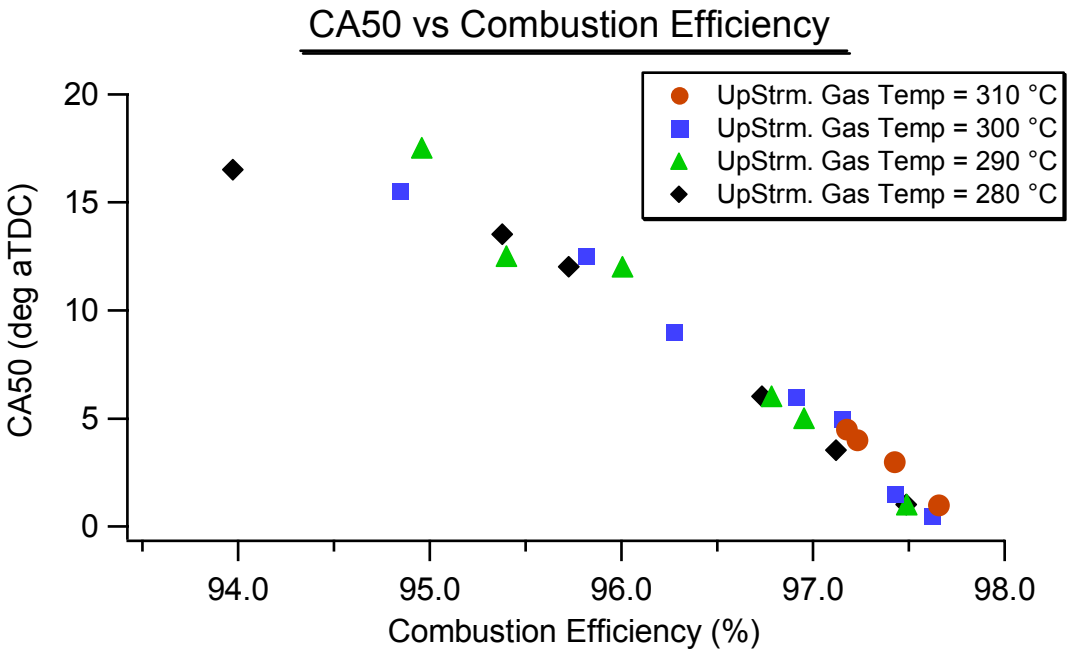

Figure 5-17 CA50 vs. combustion efficiency for EEE fuel

The data also clearly demonstrates the fact that the combustion temperatures become lower as the engine's inlet temperature decreases. This can be seen in the plot of the NO_x as a function of combustion efficiency, Figure 5-18, where for a given combustion efficiency the amount of NO_x generated in the cylinder decreases as the upstream gas temperature is

increased corresponding to a lower final inlet temperature to achieve acceptable HCCI combustion.

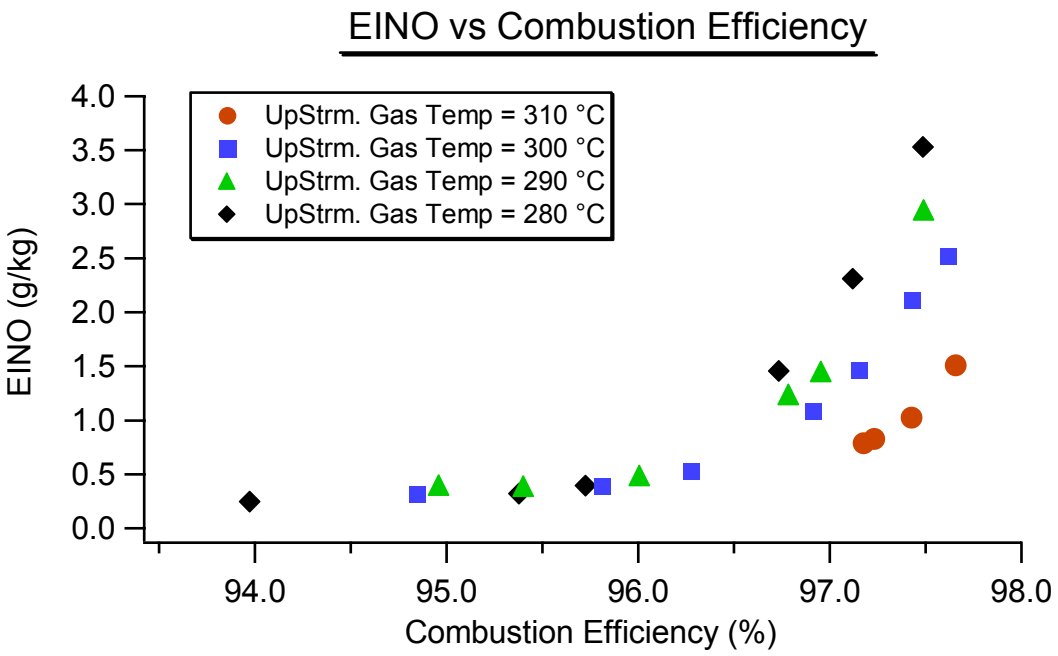

Figure 5-18 NO_x emissions vs. combustion efficiency for EEE fuel

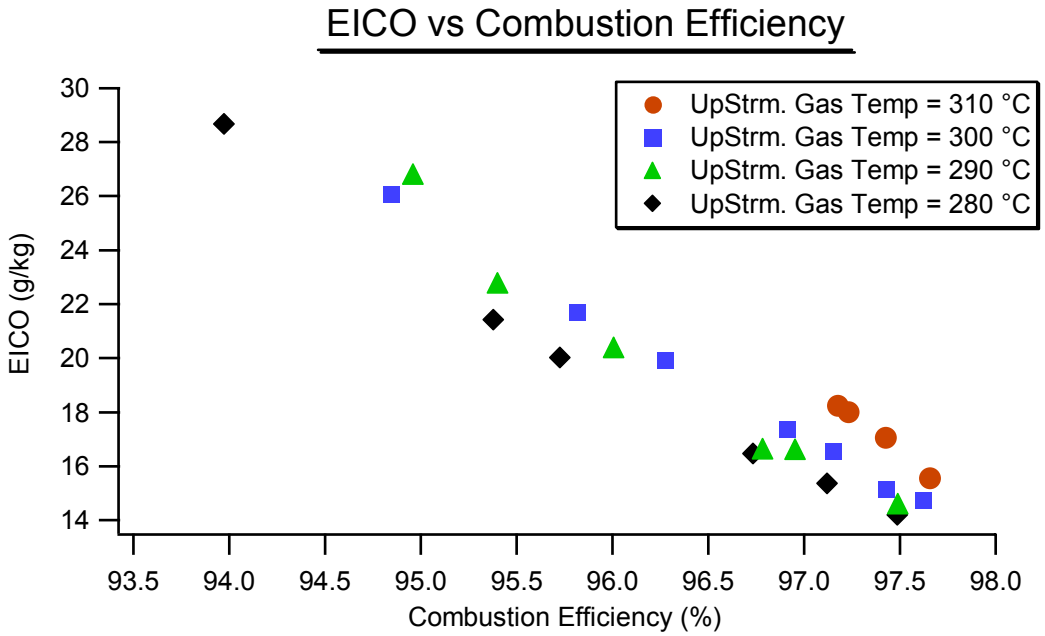

Figure 5-19 CO emissions vs. combustion efficiency for EEE fuel

The plot of the carbon monoxide emissions as a function of combustion efficiency, Figure 5-19, clearly shows the increase in the CO emissions, for a given combustion efficiency, as the upstream gas temperatures is increased. This is consistent with lower combustion temperatures resulting in incomplete combustion that were hypothesized earlier. CO emissions also represent poor thermal efficiency since a significant amount of energy is released in the oxidation of carbon monoxide.

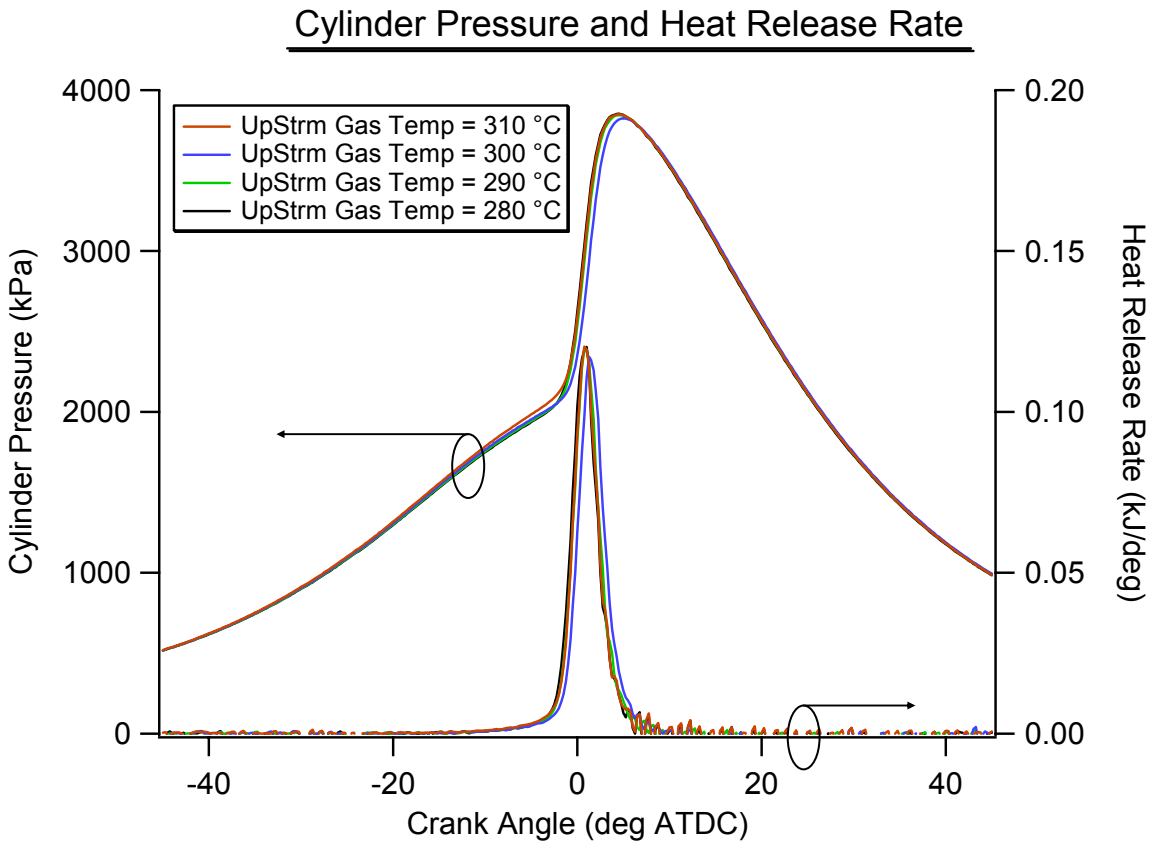

Figure 5-20 Characteristic cylinder pressure and heat release rate for EEE fuel, CA50 values for each upstream temperature data set are between 1 and 2 dATDC.

A typical plot of the cylinder pressure and heat release is shown in Figure 5-20. The cases selected for this plot were those where the CA50 point was between 1 and 2 degrees ATDC. Again, as with the PRF87 cases, there is no indication of any cool flame activity for

the various upstream gas temperatures investigated here. This further reinforces the hypothesis that the changes in the inlet mixture created by increased upstream heating only serve to reduce the number of reaction steps necessary for auto-ignition to occur once the gasses are inside the cylinder, thus lowering the temperature at which auto-ignition will commence. Again it should be pointed out that upstream heating appears to only reduce the temperature requirement for auto-ignition to occur, the general combustion behavior does not appear to be affected by the changes in the gas temperature upstream of the engine's inlet.

Section 5.5 Gas Chromatograph Mass Spectrogram Results

In order to get a handle on how exactly the mixture is changing with increased upstream intake air heating a series of samples of the gasses immediately before entering the cylinder were taken. The samples were then analyzed using a HP 6890 Model Gas Chromatograph and Mass Spectrometer. The goal of these tests was to look for differences in the intake mixture's composition that might indicate what species would be acting to advance the combustion as the temperature of the intake gasses in the surge tanks was increased.

The gas sampling tests were conducted using the same methodology as the tests outlined above. The upstream heating temperature was maintained at a given upstream temperature and the intake runner temperature was adjusted until the combustion phasing was the same for each of the test points. A sample of the intake gasses was then taken from the intake approximately 15 cm (6 inches) from the engine's inlet valves. It was decided to maintain a fixed combustion phasing instead of a fixed engine intake temperature because the

combustion could not be maintained in regimes that were deemed safe for all of the upstream heating conditions of interest. The tests were conducted for the PRF87 fuel as well as the isooctane fuel. Also as in the previous experiments, the engine was run with cooled external EGR inducted into the inlet This was done in order to meet the same mixture conditions as in the previous work as well as to keep the inlet pressure at 100 kPa. The engine operating conditions for which gas samples were taken are described in Table 5-4.

Condition	1	2	3	4	5	6
Speed	1000	1000	1000	1000	1000	1000
Fuel	PRF87	PRF87	PRF87	PRF87	Isooctane	Isooctane
Engine Inlet Air Temp.	288	273	264	258	308	308
Upstream Gas Temp.	275	285	290	295	303	325
EGR Percentage	38	38.4	40.3	39.6	36.4	36.7
CA50	4	3	7	2	7	6

Table 5-4 Engine operating condition for gas chromatograph mass spectrogram tests

The results of the G.C. Mass Spec. tests conducted in the current work can be seen in the following figures. The graphs show a mass spectrograph as a function of the time in minutes. This is the time that the gas sample has been in the analysis device. Each of the abundance peaks is specific to a certain gas species.

Figure 5-21 shows the mass spectra plots for the samples collected when the engine was run on the PRF87 fuel. The peaks between zero and four minutes correspond to the oxygen and nitrogen from the air, the two major peaks between sixteen and eighteen minutes correspond to the fuel molecules, the left hand peak is for normal heptane and the right hand peak is isooctane. The considerably smaller peaks in the time periods between five and twenty-five minutes are the ones that are most interesting for this work. In order to look at these plots the data presented in Figure 5-21 are broken up into smaller time segments and

the y-axis is scaled appropriately to show changes in these small species. These results are presented in Figure 5-22 through Figure 5-26. The plots also include identification of many of the peaks in the spectrum; however, not all of the peaks were identifiable.

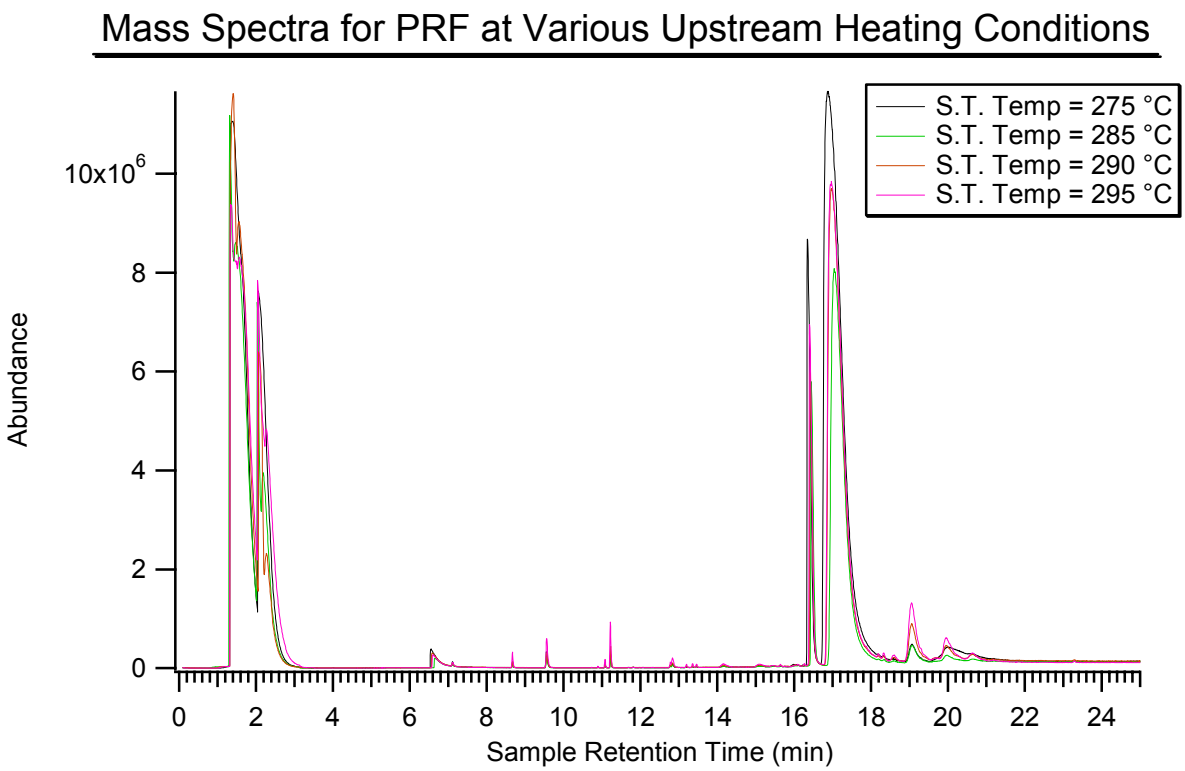

Figure 5-21 Mass spectra for the PRF87 fueling conditions

In the period between five and 10 minutes shown in Figure 5-22, there are several observations in the spectra which should be discussed. Of note is that the species acetaldehyde and 2-methyl-1-propene both steadily increase as the temperature of the gasses in the surge tank is increased. This would be consistent with the original suggestion that the fuel is breaking down in the intake as the amount of upstream heating is increased. The concentration of the water in the mixture does not show any trends with upstream temperature, which is most likely a result from the amount of water in the mixture being due

to the relative humidity of the fresh air or the EGR gasses before they are mixed. Acetaldehyde is also observed to increase between the lowest and the higher upstream temperatures, however since acetaldehyde is a precursor of low temperature reactions for both isooctane and n-heptane, the increasing trend can not easily be attributed to low temperature reactions of the n-heptane in the fuel as was originally hypothesized.

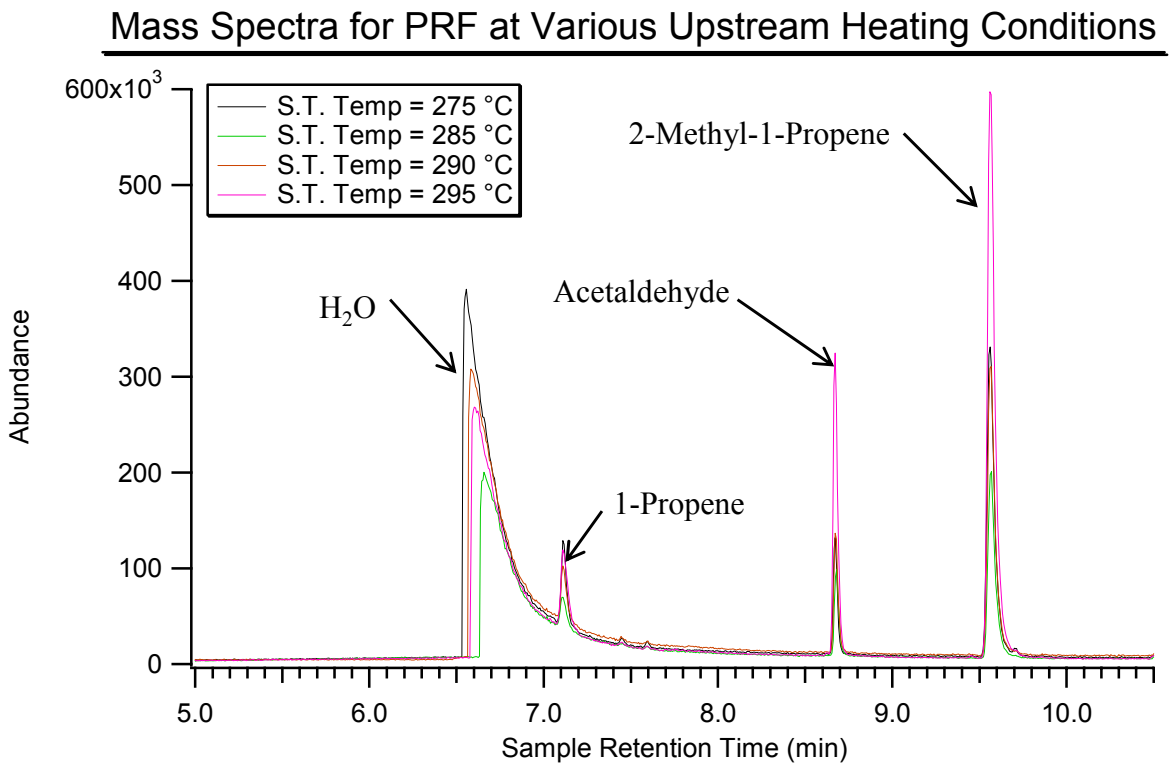

Figure 5-22 Partial mass spectra for the PRF87 fueling conditions

The rest of the spectra, Figure 5-23 through Figure 5-25, show and identify the other chemical species that were detected while analyzing the intake charge. There are a number of species that appear through the rest of the spectra plots that are of interest. These include Propanal, Butanal, 2-Butanone, 2-methyl-2-propanone, 2-methyl-2-propanone, 2,2 dimethyl-propanal, and to a lesser extent the 2,2,4,4-tetramethyl-tetrahydrofuran. Another species that is observed to change is the unidentifiable peak seen immediately before Butanal is detected.

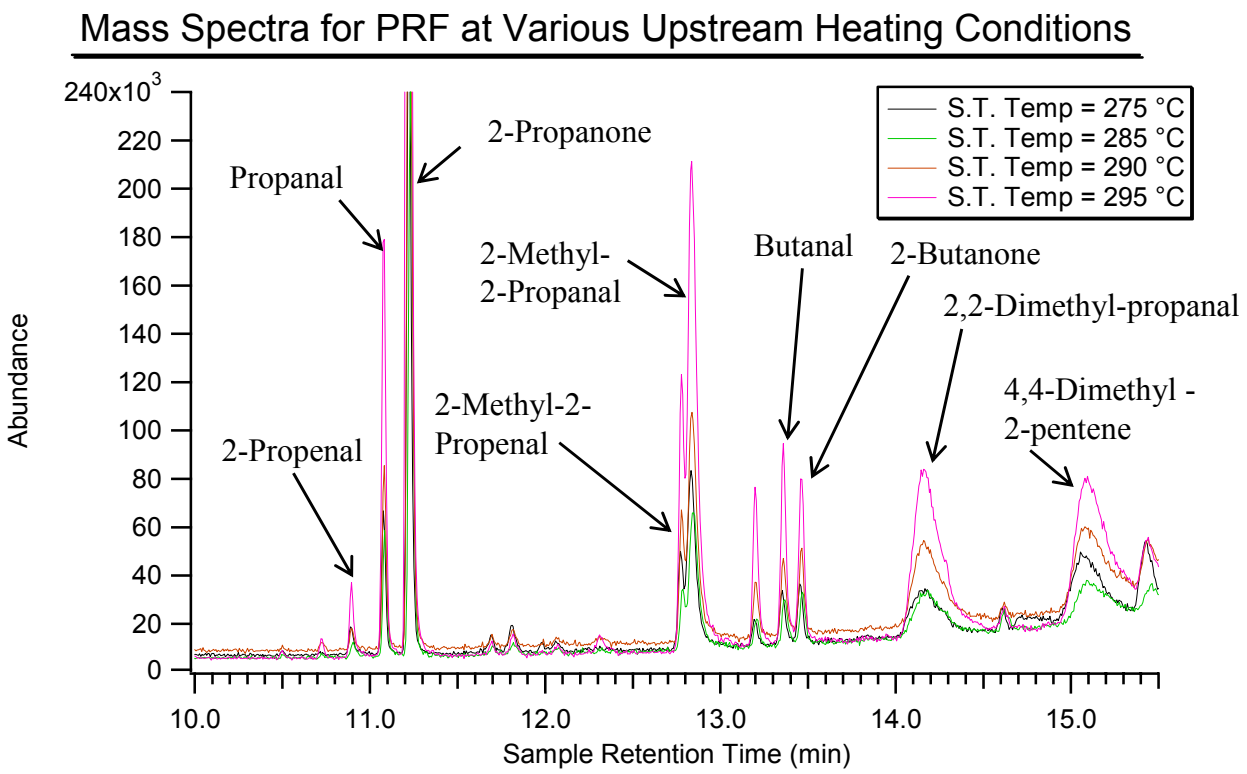

Figure 5-23 Partial mass spectra for the PRF87 fueling conditions

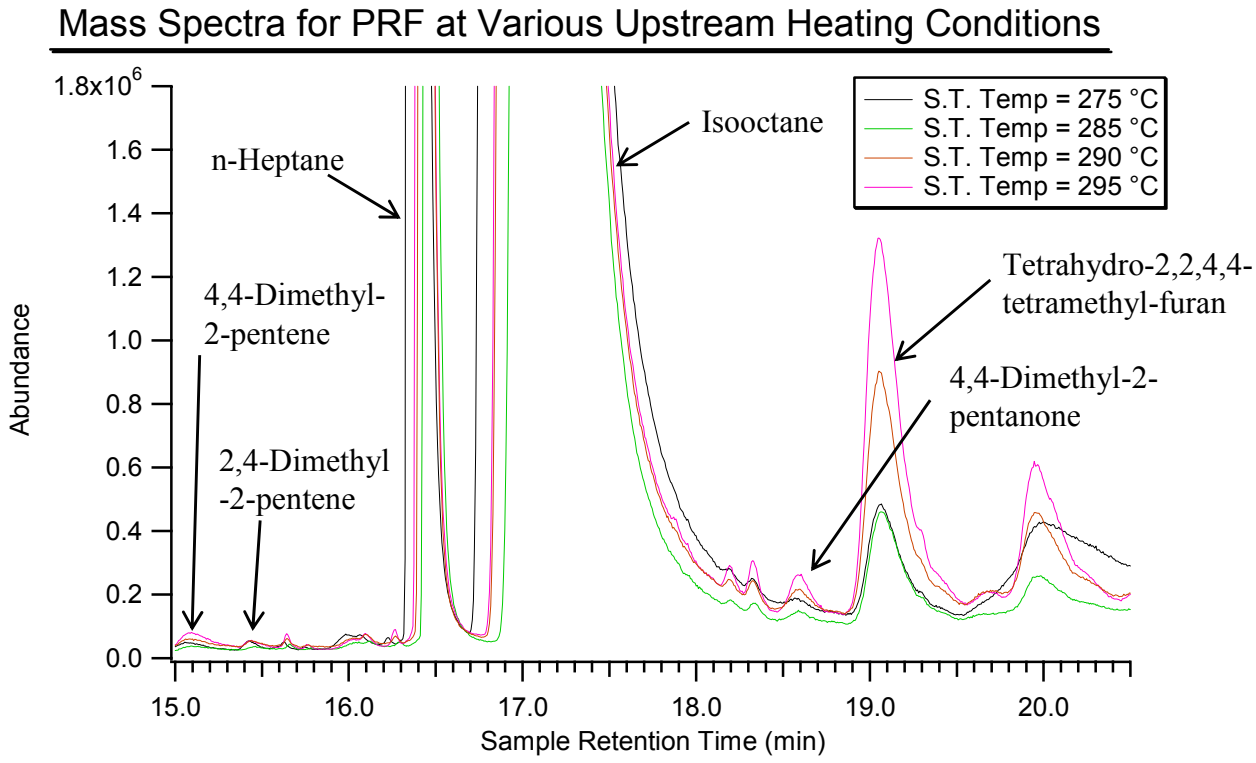

Figure 5-24 Partial mass spectra for the PRF87 fueling conditions

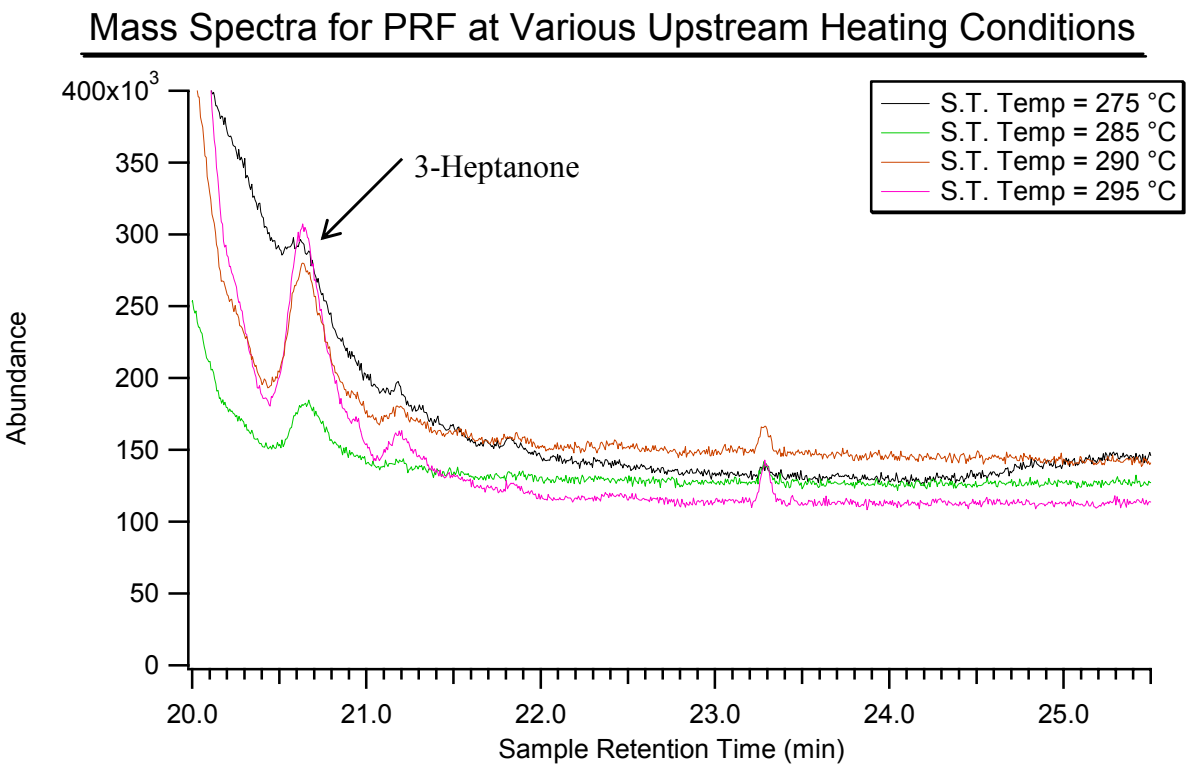

Figure 5-25 Partial mass spectra for the PRF87 fueling conditions

One point that should be considered before continuing on with this analysis is that as the upstream temperature is increased the actual engine inlet temperature is decreased which yields an increase in the mixtures density at the inlet. This density increase will increase the amount of mass in the intake, as well as the amount of mass in the sampling syringe, which could cause the GC Mass Spec to read the species in higher concentrations, this could be expected to cause the data collected at the higher upstream temperatures to have an abundance that would be scaled by the increased density. This scaling could give problems in determining changes in the quantity of the sub-species generated in the inlet. However, an examination of the mass spectra plots indicates that it is most unlikely that this change in the amount of mass in the sample was significantly affecting the relative magnitude of the

various peak heights for the different upstream temperature conditions. This conclusion is draw by noticing that all of the peaks do not scale linearly, as would be expected if increased density was scaling the observed magnitudes. Also looking closely at the plots there are a number of peaks such as 4,4-dimethyl-2-pentene that do not show any changes with temperature, which indicates that the major driving factor for the increase in the species concentrations with increased upstream heating is low temperature reactions of the fuel in the intake.

One final point that should be made before continuing to investigate these results is that the intake mixture sampled and analyzed in this work includes externally recycled EGR gas at a fraction of approximately 38%. Among many different components the EGR includes a large amount of hydrocarbon species. Individual samples of the exhaust gas were not taken, but based on the work by Ciajolo et al we can label a number of the components that appear in the GC Mass Spec plots as being the results of recycled EGR. [18] The species that are most likely present because of the EGR are 2-Propanone, 4,4-dimethyl-2-pentene, 2,4-dimethyl-2-pentene, 4,4-dimethyl-pentanone, and 2,2,4,4-tetramethyl-tetrahydrofuran. These are all species that are products of low temperature reactions of isooctane and would be the likely forms that the unburned hydrocarbons would assume. [18]

In order to quantify the amount of hydrocarbons inducted into the engine through the EGR a series of calculations were performed to identify the mass flow rate of hydrocarbons into the engine. The results of these calculations can be seen in Figure 5-26. The plot shows the mass of unburned hydrocarbons inducted into the engine for the conditions described in Section 5.2. It can be seen in this plot that the mass flow rate of hydrocarbons is not increasing with the increase in EGR that resulted from the increase in upstream temperatures.

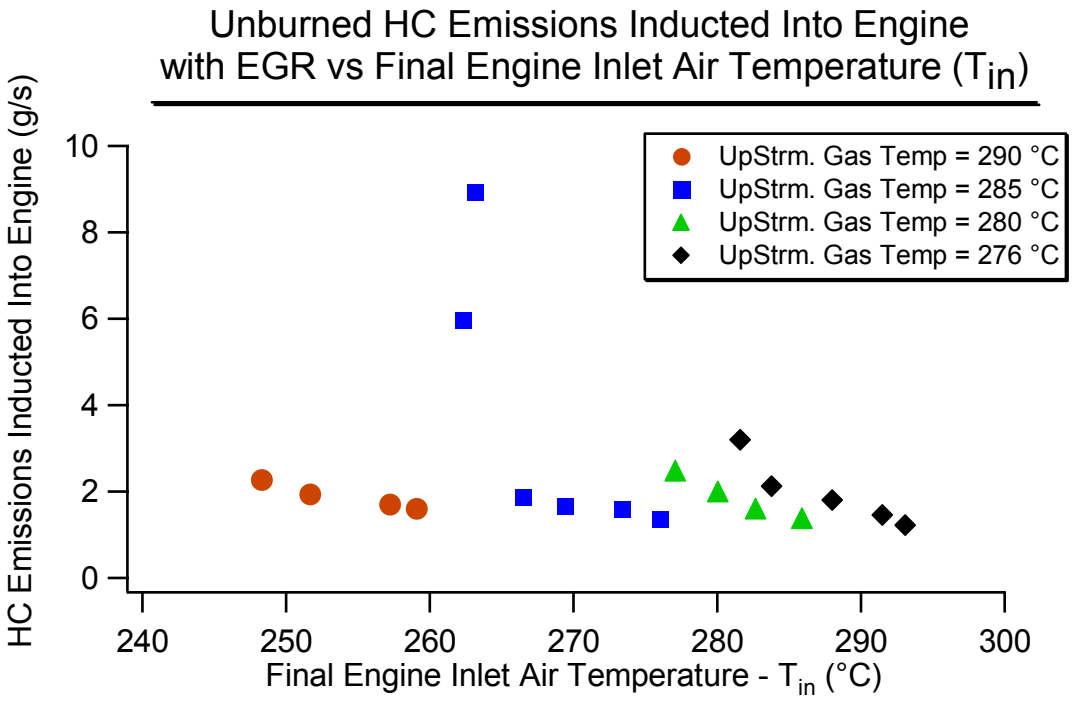

Figure 5-26 Mass flow rate of unburned hydrocarbons due to EGR flow

It is interesting to note that in the spectra plotted in Figure 5-22 through Figure 5-25 the amount of species that are assumed to be the result of EGR induction also increase with the change in upstream gas temperatures. There is no immediate explanation for this increase, as was noted before it is unlikely that differences in the mass of each sample are affecting these results. However as was noted above, and can be seen in Figure 5-26, the mass flow rate of unburned hydrocarbons is not increasing which means that the increase in EGR fraction is not an explanation for this observation. Further work should be conducted to study this issue.

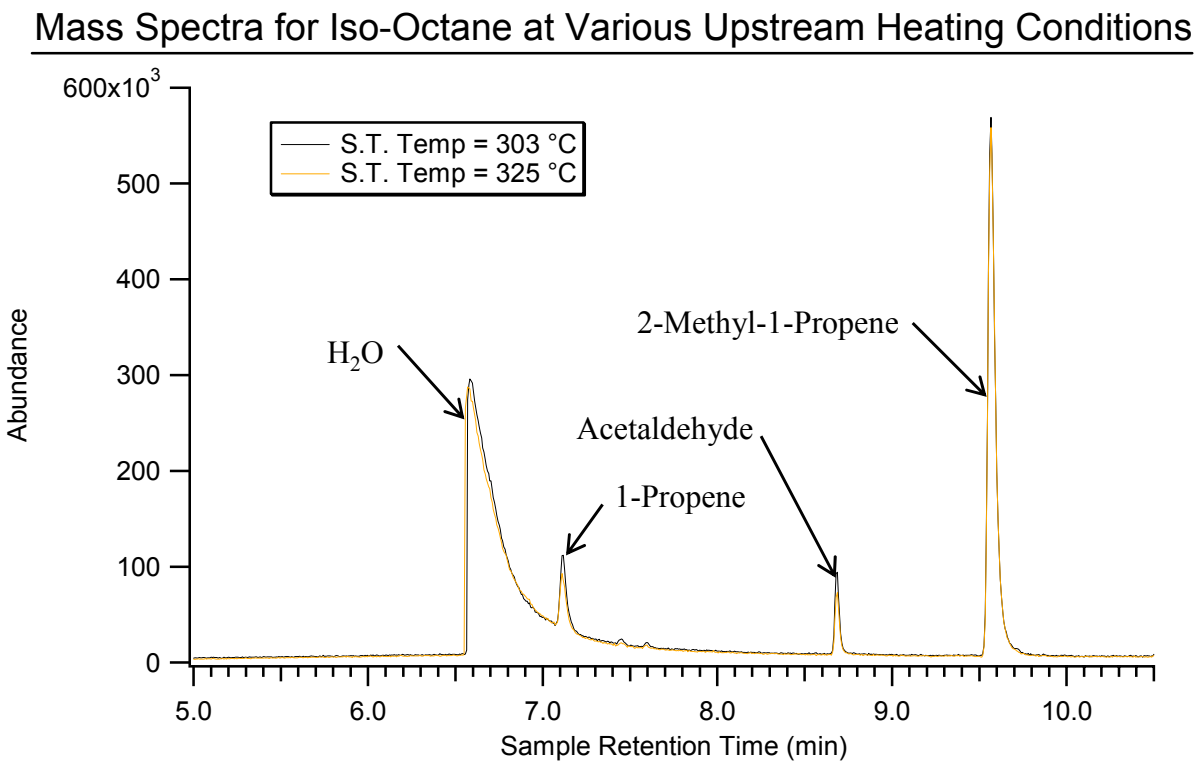

Figure 5-27 Partial mass spectra for isooctane fueling conditions

The mass spectra curves for the data collected when the engine was run on pure isooctane are shown in Figure 5-27 through Figure 5-29. One thing to note is that there are trace amounts of n-heptane and normal C_7 conjugates detected in this gas sample. This is believed to be due to contamination of the fuel through the fuel pump. For the pure isooctane cases the entire fuel system was drained, flushed, and drained again, as well as run for over 8 hours prior to sampling of the gasses, however, it doesn't appear to have eliminated all of the n-heptane from the fuel pump. The contamination, however, is deemed to be minimal sufficiently small to allow us to draw conclusions about the changes in the intake gas compositions due to increased upstream heating.

These plots do not show any significant increase in the concentrations of any of the species, detected in the gas sample, for any increase in the upstream gas temperature. In fact

the differences detected point to higher concentrations in a number of species at lower upstream temperatures. This difference is mostly negligible and is likely due to a subtle shift in the relative concentration of species in the EGR gas. Another explanation for the change in concentrations is that the lower upstream temperature case was collected early in the day and the engine was run for several hours before the higher upstream temperature case was collected. Therefore the changes in detected species concentration could be the result of the small amount of fuel contamination.

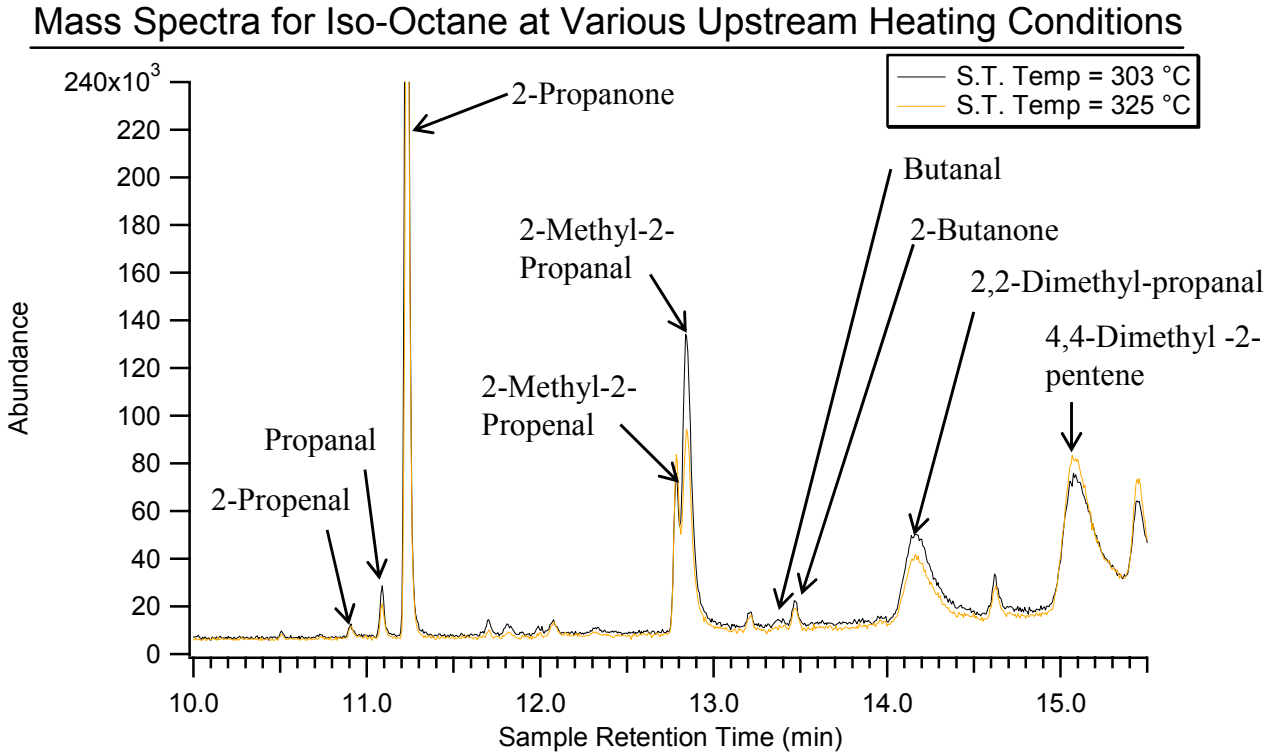

Figure 5-28 Partial mass spectra for isooctane fueling conditions

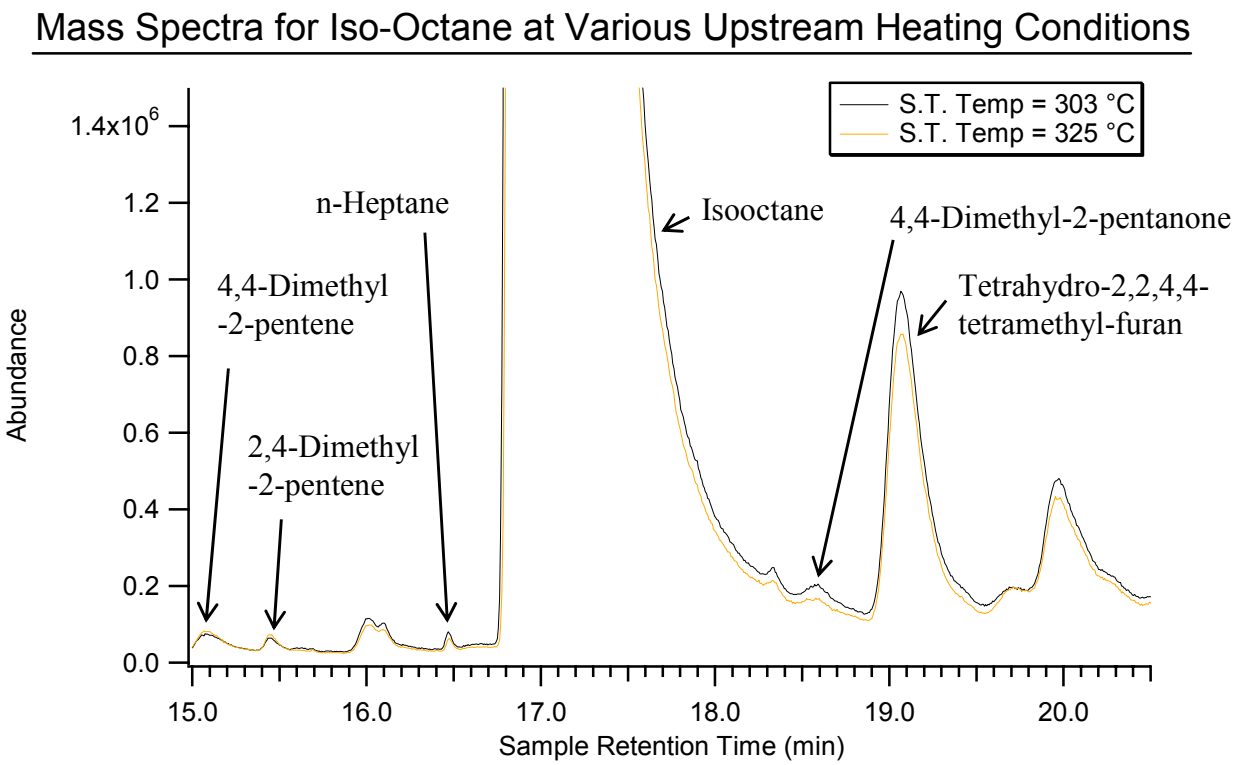

Figure 5-29 Partial mass spectra for isooctane fueling conditions

Finally in order to get a good idea of the differences between the results from the PRF87 fueling condition and the isooctane fueling condition the highest upstream temperature for the PRF87 was plotted against the lowest temperature for the isooctane on the same graph. These correspond to a surge tank temperature of 295 °C for the PRF87 case and 303 °C for the isooctane case. These plots are shown in Figure 5-30 to Figure 5-32. On these graphs it is quite easy to see which species are most likely being drawn into the engine with the EGR and which are most likely being generated in the intake.

The species that are most likely brought into the engine through the EGR induction include 2-methyl-1-propene, 2-Propanone, 2-methly-2-propenal, 2-methyl-2-propanal, 4,4-Dimethyl-2-pentene, and 2,4-Dimethyl-pentene. The species that are being generated in the intake itself are most likely 2-propenal, propanal, butanal, and 2-butanone.

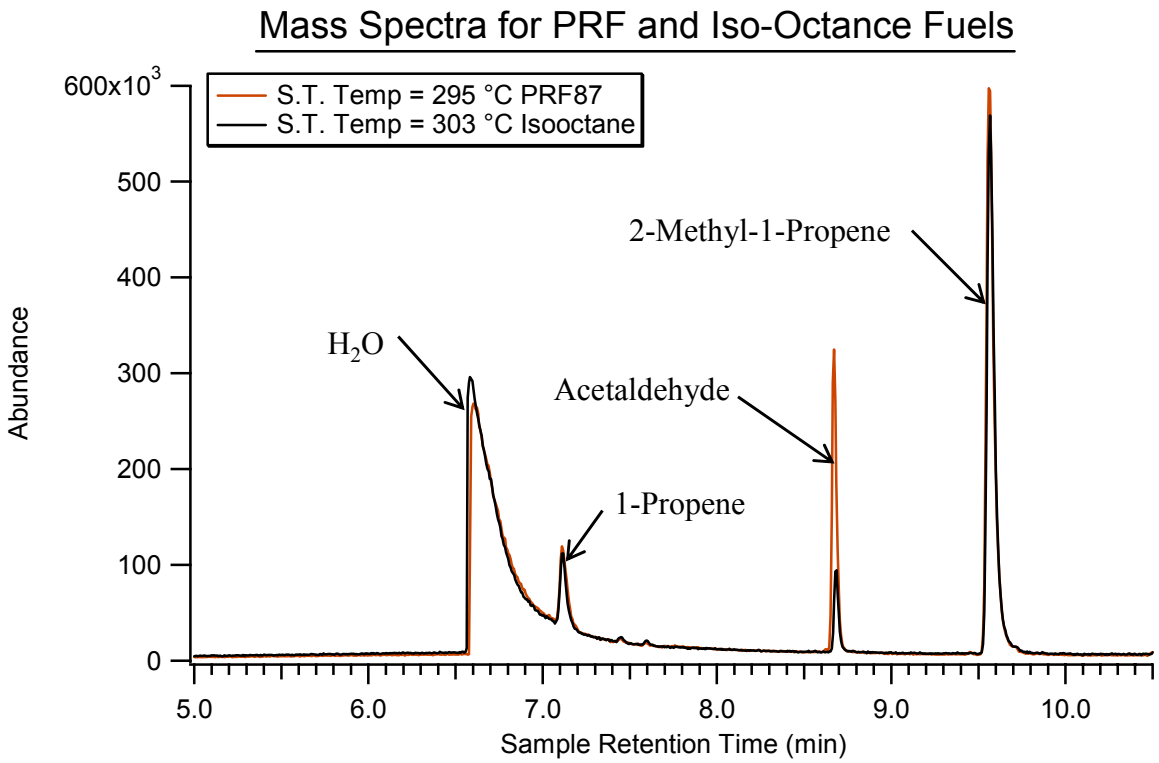

Figure 5-30 Partial mass spectra comparison for isooctane and PRF87 fuels

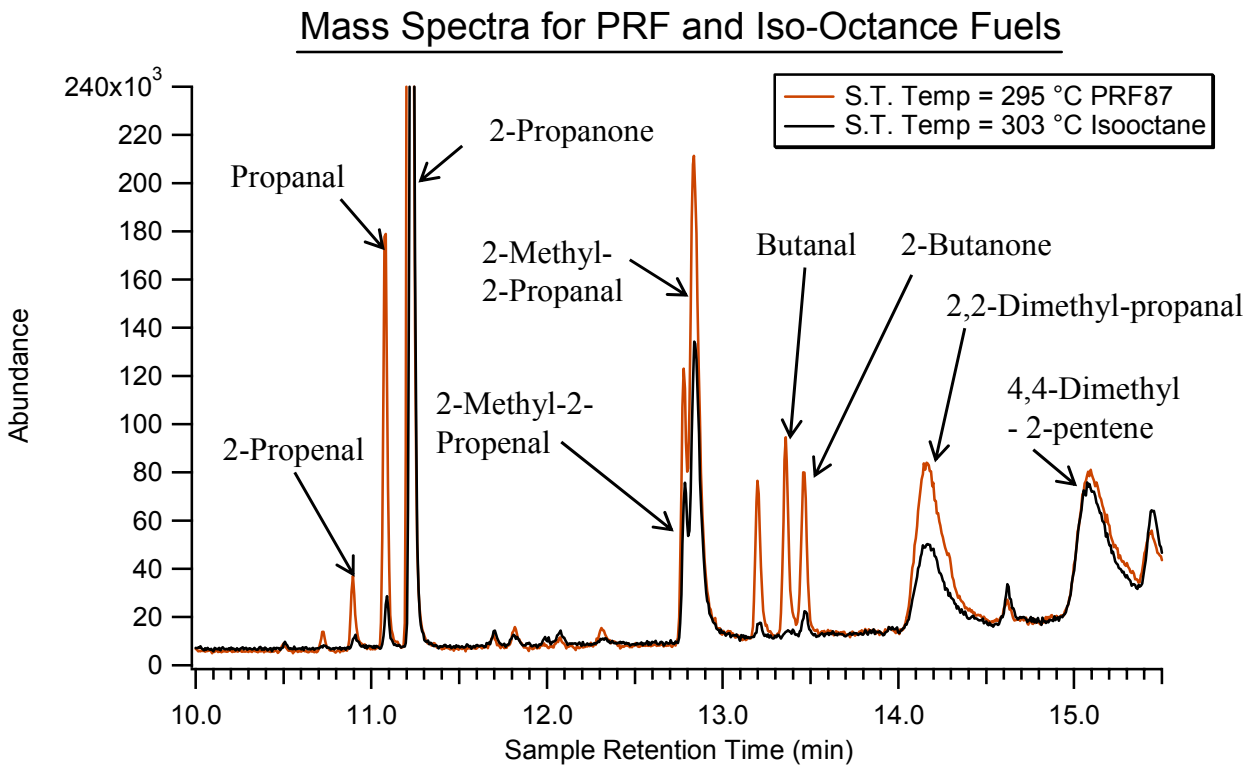

Figure 5-31 Mass spectra comparison of isooctane and PRF87 fuels

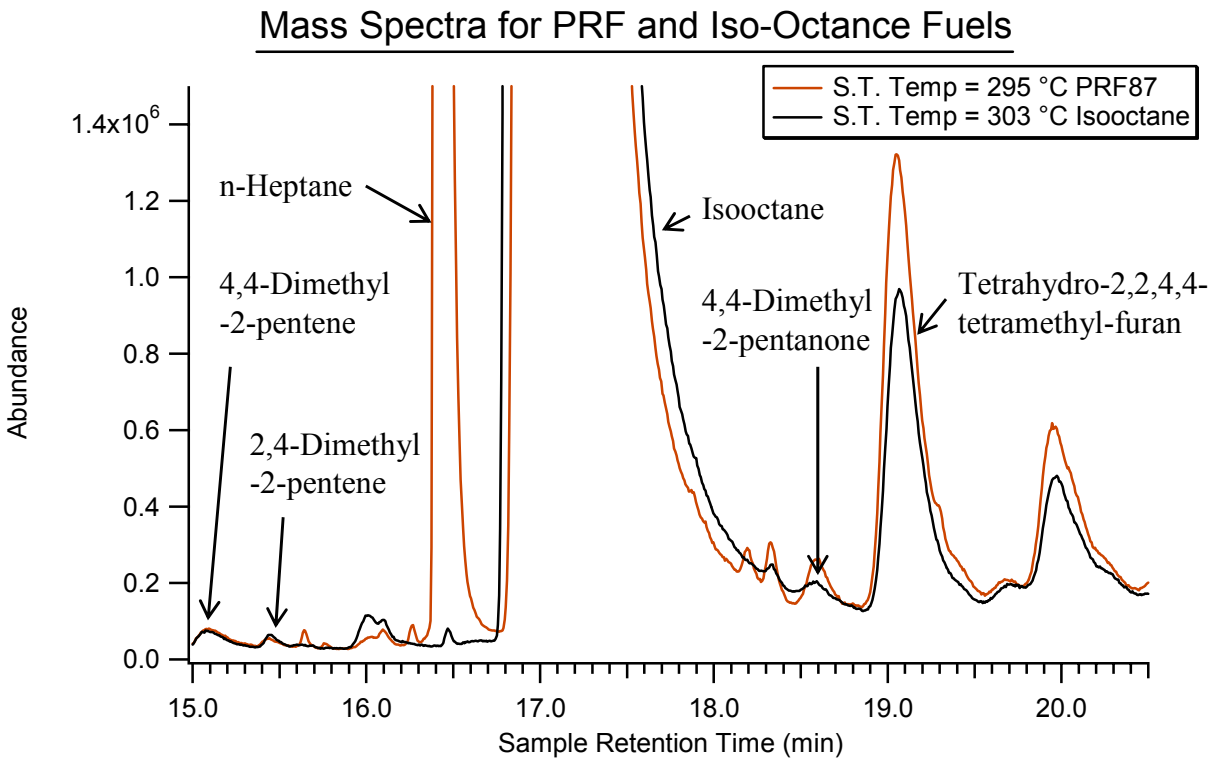

Figure 5-32 Mass spectra comparison for isooctane and PRF87 fuels

There are three molecules that appear in these data that suggest a very interesting behavior. These are acetaldehyde, 2,2-dimethyl-propanal, and 2,2,4,4-trimethyl-tetrahydrofuran. These species each show up in significant quantities when the engine was run with pure isooctane as the fuel and they did not show any significant changes when the upstream temperatures were increased. Both the 2,2-dimethyl-propanal and the 2,2,4,4-Trimethyl-tetrahydrofuran are only possible as products of isooctane oxidation, yet they are noted to be increasing as the upstream temperatures increase for the PRF87 cases, in fact the amount, of these three specific species, detected in the highest temperature PRF87 case is significantly higher than is detected in the pure isooctane cases. It is possible that when the PRF87 fuel is in the intake system the high temperatures cause the n-heptane to begin

breaking down and that the sub-species generated in these steps then promote reactions of the isooctane which generates these three particular species, and possibly other species that were either undetectable or unidentifiable.

Section 5.6 Conclusions

A study was conducted of the effects of heating of a fuel/air mixture prior to entering an HCCI engine on the behavior of the combustion in such an engine. When operating an engine with an 87 octane primary reference fuel blend it was observed that the engine could be run at many different actual engine inlet air temperatures by simply altering the temperature the fuel was at prior to entering the intake runner. The combustion was shown to be viable at progressively lower final engine intake temperatures as the temperature of the preheating chamber was increased. The ability to operate the engine at lower inlet temperatures lowered the amount of NO_x generated in the engine but increased the amount of CO generated. These trends were also observed when the engine was run with a full boiling range reference gasoline, but they were not observed when the engine was run on pure isooctane.

The intake charge was analyzed using a G.C. Mass Spec. This analysis showed that for the PRF87 oxygenated fuel fragments such as butanol, 2-butanone, and propanal were entering the engine, and that the amount of these molecules generated increased as the preheating temperature was increased. For the pure isooctane case the gas samples did not show any significant quantities of butanol, 2-butanone, or propanal, nor did the components of the gas show any sensitivity to changes in the preheating temperature.

It is currently believed that for the fuels composed of molecules that are easily isomerized, a portion of the fuel is undergoing some low temperature chemical reactions while the fuel is in the surge tanks. These reactions appear to involve hydrogen abstraction and oxygen addition. While the extent of the work is not sufficient to determine which species in particular are causing the advancement of the combustion it is most likely that the oxygenated derivatives of butane and propane as well as the higher acetaldehyde, 2,2-dimethyl-propanal and 2,2,4,4-Trimethyl-tetrahydrofuran concentrations are responsible for the change in the combustion.

Chapter 6 - Air/Fuel Stratification

Section 6.1 Experimental Notes and Conditions

As was noted in Chapter 2, one fundamental question that needs to investigation is what effects, if any, does the level of uniformity in the spatial distribution of the fuel and air have on HCCI combustion. This question was the primary focus for this laboratory. In order to answer the question the fuel delivery systems described in Chapter 3 was developed. It was decided to utilize a port injection fueling system because a duel mode SI and HCCI engine is most likely to be only receive fuel from a port injector. For the purposes of this research any spatial gradient in the distribution of the fuel inside the cylinder is termed stratification. This term is also used interchangeably with unmixedness.

In an HCCI engine, stratification of fuel and air is expected to affect the combustion, but then so is any thermal gradient that exists inside the cylinder. It is most desirable to quantify how much each type of stratification affects HCCI. In order to achieve this, it is necessary to separate the two types of in-cylinder variation. For this work it was decided to focus on the effects of spatial variations in the fuel's distribution.

The fuel delivery system was set up so that the fuel in the heating chamber could be heated to the same temperature as the engine intake air temperature at a point upstream of the stratified injector. The fuel then traveled through the injector and a hypodermic tube and finally into the inlet port. Heating the fuel to the engine intake air temperature should remove thermal stratification such as the type that is related to fuel evaporation, which would

be present in a direct injection engine. The only thermal gradient in the engine will be due to the cold cylinder walls, which can not be removed from this engine.

There are many ways for stratification of the air/fuel mixture to be generated and many different levels of stratification that can be generated. This work was mostly performed to prove that the experimental setup was valid, i.e. that charge stratification could be generated and that the effects could be detected. It was decided that the maximum amount of stratification possible would be investigated. To that end all of the fuel delivered into the engine was delivered through stratified injector.

The injector system was designed so that several different hypodermic tubes could be installed which enabled the operator to direct the flow of fuel into the intake at almost any location. One configuration tested in this work, had the hypodermic tube set so that the fuel was delivered at one of the intake valves just a few millimeters from the back of the valve. This configuration is intended to keep the fuel and air streams separated for as long as possible to minimize mixing and maximize the stratification. The fuel should only enter the engine through the valve at which the hypodermic tube is located. These configurations are referred to as either “Left” or “Right” intake valve fueling depending on the valve, the designations refer to the valve placement when looking through the port.

The system was setup so that the tube could be pointed at either valve. The injector was also configured without a hypodermic tube. In this configuration the fuel left the injector shortly after it entered the intake port, and the fuel was then free to mix with the air and to enter the cylinder through either of the intake valves. This configuration is referred to as the “No Flow Direction” case from here on out.

The amount of stratification generated could be controlled by manipulating the length of time that the fuel and air had to mix. This is accomplished by changing the timing of the fuel injection into the intake port. A total of five different injection timings were used, these injection timings can be seen in Figure 6-1. There were two injection timings outside of the valve open period. These were chosen to generate the most mixing and provide a direct comparison to the premixed data. The timings inside the valve event were selected so that one injection started as the valve opened, another ended as the valve closed, and the third injection was centered on the middle of the valve open event.

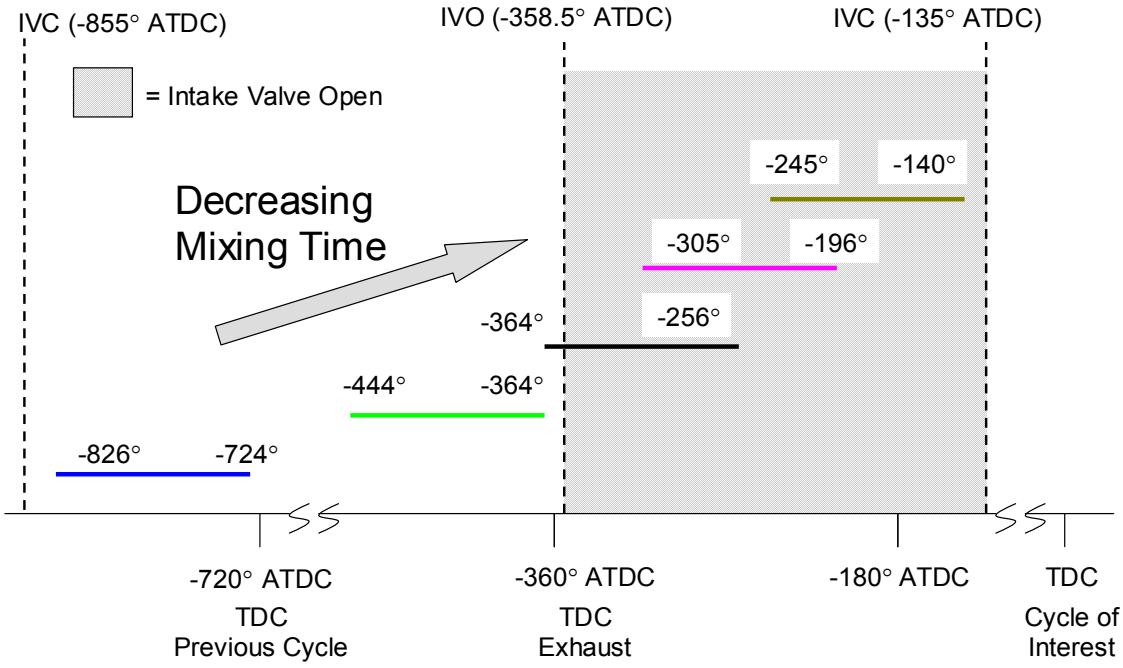

Figure 6-1 Stratified system injection timings

The original experimental matrix was designed so that the independent variables were the hypodermic tube configuration, the injection timing, and the temperature of the engine intake air. For these tests the fuel was controlled so that the temperature of the fuel vapor

upstream of the CAP injector was the same as the bulk inlet air. The experimental matrix is detailed in the following table.

Speed	1000 RPM
Engine Inlet Temperature	290-340 C
Fueling Rate	10 mg/cycle
Fuel Type	Isooctane
End of Stratified Injection Timing	-724, -364, -256, -196, -140 ATDC
Stratified Injection Hypodermic Tube Configuration	Left Intake Valve, Right Intake Valve, Undirected

Table 6-1 Initial stratified injection baseline matrix

After reviewing the data from the engine tests it was determined that the fuel was not entering the intake at the same temperature as the bulk inlet air stream. In order to quantify the extent of this thermal gradient a series of experiments were designed to measure the temperature of the fuel jet as it exited the hypodermic tube. These tests led to a new design of the hypodermic tube that was attached to the injector body. The redesign was performed to allow heat transfer to the fuel jet from the bulk gasses. The goal was to get both streams at the same temperature prior to mixing in the cylinder thus removing the thermal stratification from the cylinder. After the redesign a new set of baseline conditions were examined. These new baseline conditions are shown in Table 6-2 below. Like before the major parameter investigated was the timing of the fuel injection.

Speed	1000 RPM
Engine Inlet Temperature	300-330 C
Fueling Rate	10 mg/cycle
Fuel Type	Isooctane
End of Stratified Injection Timing	-724, -364, -256, -196, -140 ATDC
Stratified Injection Hypodermic Tube Configuration	Left Intake Valve

Table 6-2 Second stratified injection baseline matrix

After the baseline experiments confirmed that the new stratified injection tube configuration succeeded in removing the thermal stratification from the cylinder a series of tests were conducted to determine how stratification of the air/fuel mixture in the cylinder affected the HCCI combustion. The tests compared engine operation for a fixed air/fuel ratio with several different fueling rates, a fixed fueling rate with several air/fuel ratios, and finally several points at a lower speed. The low speed condition was chosen after considering a limitation of the laser that will be used in the optical engine; the laser will only pulse at a frequency of 10 Hz. This made it necessary to get some data at either 600 or 1200 RPM in order to compare optical engine data with metal engine data. It was decided to perform experiments at 600 RPM, which is closer to idle conditions than 1200 RPM. The final experimental matrix is shown in the following tables.

For all of these tests the engine was run with isooctane as the fuel. The stratified tests were conducted such that all of the fuel entering the cylinder was delivered through the injector at the port in the head. Finally the only operating condition where significant amounts of combustion ringing could be detected was the condition where 10 mg of fuel per cycle was delivered. Therefore for all of the lower fueling rates, the cutoff for any temperature sweep was an intake temperature of 375 °C. This temperature was chosen as the upper limit due from safety considerations, as well as the fact that raising the intake air temperature above 375 °C becomes exceedingly difficult in the current laboratory setup.

For all of these tests the engine was run in premixed mode and then shifted into totally stratified mode. Each set of points collected and presented for a given configuration were taken on the same day and with the same engine setup.

Speed (RPM)	λ	Fueling Method	Fueling Rate (mg/cycle)
1000	1.33	Premixed	10
1000	1.33	100 % Stratified	10
1000	1.33	Premixed	7
1000	1.33	100 % Stratified	7
1000	1.33	Premixed	5
1000	1.33	100 % Stratified	5

Table 6-3 Matrix of experimental conditions for fueling sweep tests

Speed (RPM)	λ	Fueling Method	Fueling Rate (mg/cycle)
1000	1.33	Premixed	5
1000	1.33	100 % Stratified	5
1000	1.66	Premixed	5
1000	1.66	100 % Stratified	5
1000	2.00	Premixed	5
1000	2.00	100 % Stratified	5

Table 6-4 Matrix of experimental conditions for air/fuel ratio tests

Speed (RPM)	λ	Fueling Method	Fueling Rate (mg/cycle)
600	1.33	Premixed	10
600	1.33	100 % Stratified	10
600	1.66	Premixed	5
600	1.66	100 % Stratified	5
600	2.00	Premixed	5
600	2.00	100 % Stratified	5

Table 6-5 Matrix of experimental conditions for low speed tests

It should be noted here that it is unknown exactly how much stratification is being generated inside the cylinder. That question will be answered with the optical engine experiments that are to be performed in the future. This work is meant to lay the ground work in detailing areas of engine operation where the stratified injector system can be observed to be generating combustion effects inside the cylinder.

Section 6.2 Initial Air/Fuel Stratification Tests

The results of the initial stratification tests are show in Figure 6-2 through Figure 6-17, the matrix of experimental conditions is shown in Table 2-1. Reviewing the results from the tests, there were no discernable differences between the configurations where the flow was directed to the right hand or the left hand intake valves. Due to this observation only the condition where the fuel is inducted through the left hand intake valve will be shown here. A comparison of the two injector configurations can be found in Section A.2 of the appendix. The engine's behavior for the left hand intake valve fueling setup will be compared and contrasted with the condition where the fuel is sprayed into the intake port with no flow direction.

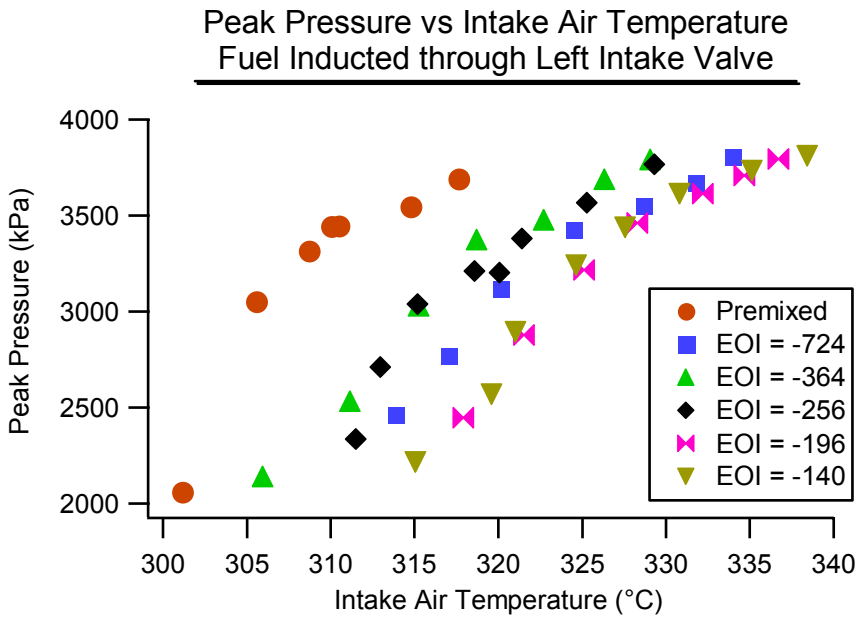

Figure 6-2 Peak pressure vs. intake temperature for directed stratified fueling at 10 mg/cycle

Figure 6-2 shows the peak cylinder pressure for the condition where all of the stratified fuel is introduced through the left intake valve. The pressure is plotted as a function

of the intake air temperature. All five of the stratified fueling injection timings are plotted on the graph along with a set of premixed data. The data series show that the stratified fueling conditions require higher intake air temperatures to achieve HCCI combustion than does the premixed fueling condition does.

Figure 6-3 shows the same tests for the experimental configuration where the tube leading to the intake valves was removed and the fuel was injected into the intake without any flow direction. Running without any direction on the fuel flow jet was expected to increase mixing of the fuel and air relative to the directed flow cases and give results that more closely match the data collected when running premixed. It can be seen in this figure that the stratified fuel system still needs higher intake air temperatures for acceptable combustion. The interesting thing about the results from these experiments is the response of the engine to the changes in the injection timing for the directed and the undirected configurations.

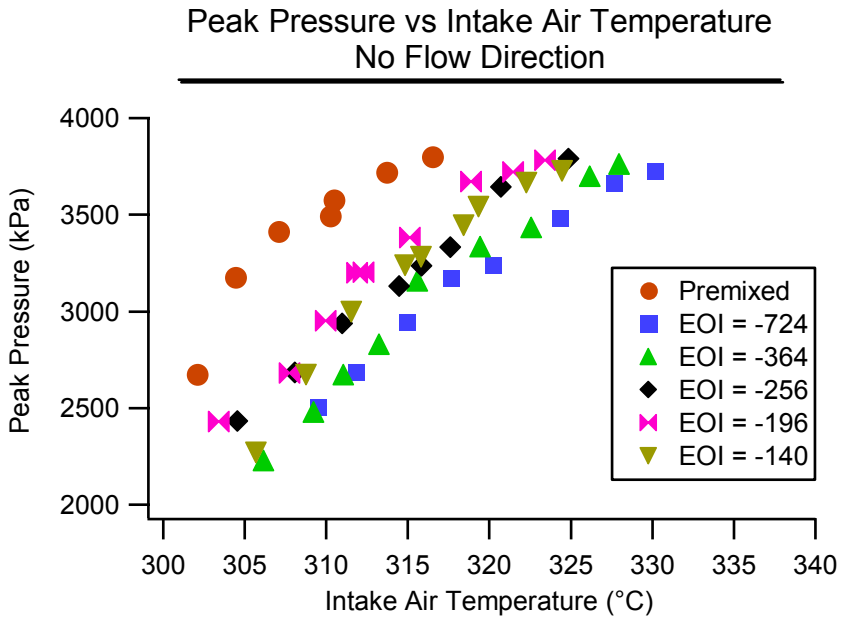

Figure 6-3 Peak pressure vs. intake temperature for undirected stratified fueling at 10 mg/cycle

When there is no direction to the flow of the fuel into the engine, the injection timing for which the highest intake temperatures are required was the -724 ATDC injection timing, or the point where the fuel had the most time available to it to mix with the incoming air. As the injection timing was moved closer to TDC the window of temperatures that yield acceptable HCCI combustion move closer to those of the premixed data.

For the directed fuel flow case, the injection timing that resulted in the most mixing does not have the highest range on intake temperatures. The timing where the fuel is injected into the intake immediately before the valve opens gives the operating window that is the closest to the premixed operating condition, indicating close similarity to premixed operation. As the timing moves closer to TDC the temperature operating window begins to move away from the premixed window. Figure 6-4 and Figure 6-5 show the results for the location of 50% burn (CA50) for these two injector configurations. These results and all of the other cylinder pressure data are consistent with what was shown in the peak pressure data.

Looking at the plots shown in Figure 6-6 and Figure 6-7 it can be seen that when plotted as a function of combustion efficiency, the peak cylinder pressure collapses down to a single trend line. The fact that this data collapses with combustion efficiency shows that the engine's behavior in terms of pressure phenomenon is consistent for a given amount of fuel reacted, no matter what the timing is of the fuel injection. This is true regardless of what the inlet gas temperature is. This shows that the data can be plotted against combustion efficiency as a way to look for differences generated by air/fuel stratification.

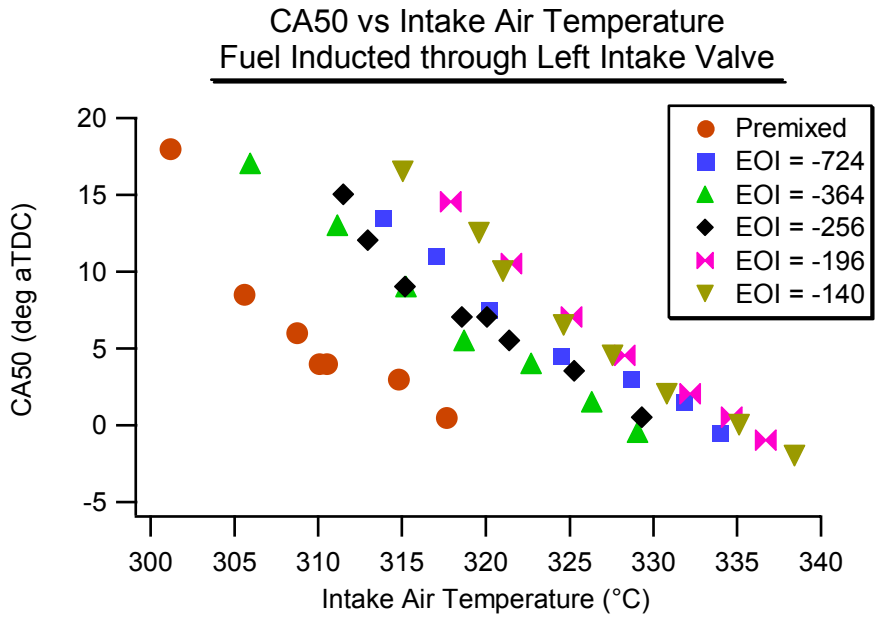

Figure 6-4 CA50 vs. intake temperature for directed stratified fueling at 10 mg/cycle

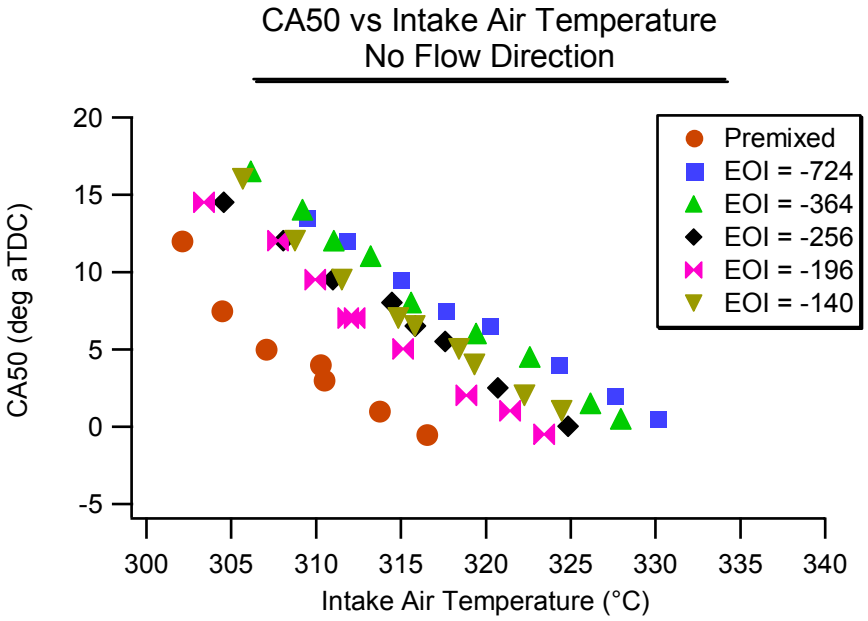

Figure 6-5 CA50 vs. intake temperature for undirected stratified fueling at 10 mg/cycle

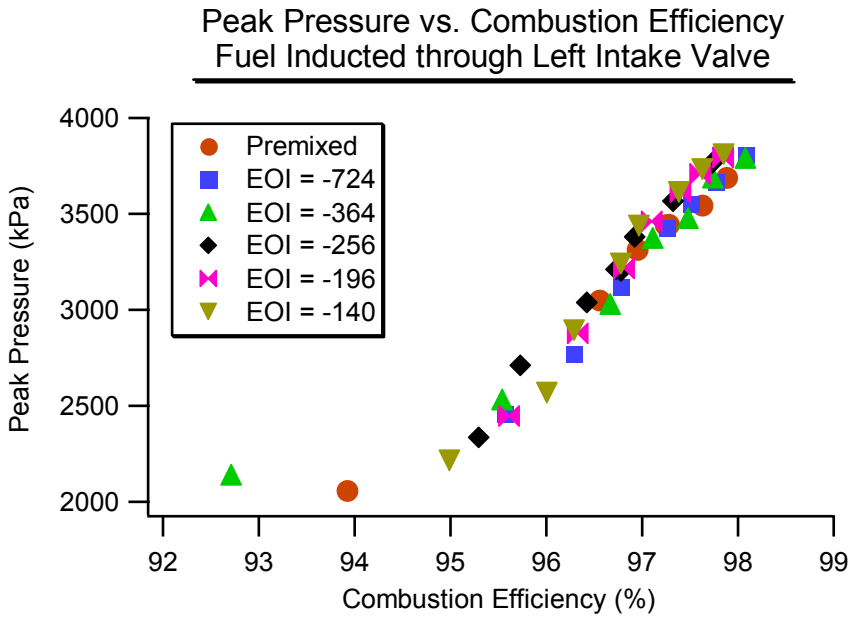

Figure 6-6 Peak pressure vs. combustion efficiency for directed stratified fueling at 10 mg/cycle

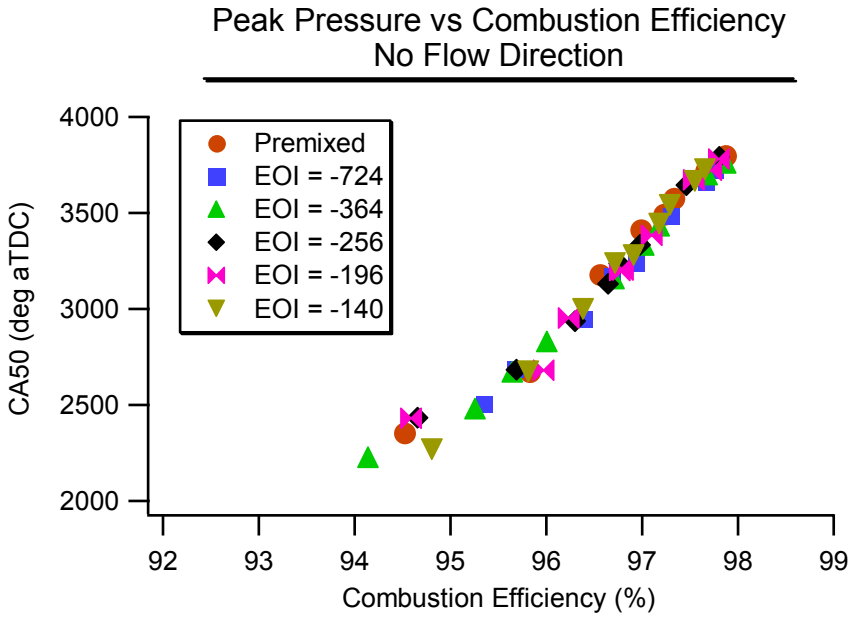

Figure 6-7 Peak pressure vs. combustion efficiency for undirected stratified fueling at 10 mg/cycle

To confirm the conclusion that the engine's behavior doesn't change significantly with charge stratification, one can look at the plots of COV and Ringing Index as functions of combustion efficiency. Figure 6-8 and Figure 6-9 show the COV values and Figure 6-10

and Figure 6-11 show the Ringing Index values for the two selected injector configurations. Looking at these values it can be seen that from a global standpoint, the trends of the COV and combustion generated noise (the defined metrics of acceptable HCCI combustion) do not change at all with respect to combustion efficiency. For all cases the COV values tail up towards unacceptable combustion variability when the combustion efficiency drops below about 96%. Looking at the plots, it can be seen that when the stratified fueling system is run without any flow direction the combustion shows much more variability than the premixed or the directed flow operating conditions. This variability is the worst at the injection timing in the middle of the valve event. It is most likely that the higher COV values are due to stratification and possibly exaggerated by variability in the flow rate of fuel from the stratified injection system, which is inherent to the design of the system.

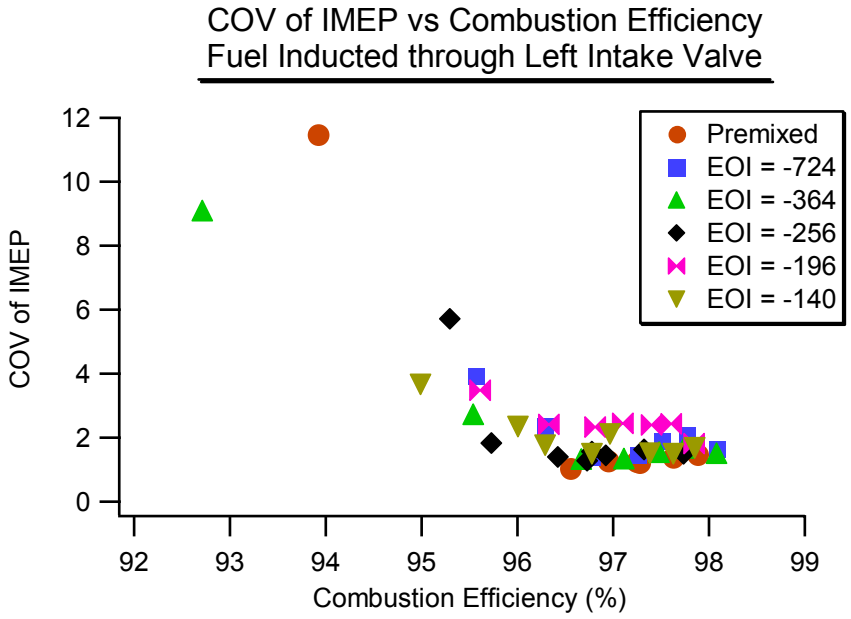

Figure 6-8 COV vs. combustion efficiency for directed stratified fueling at 10 mg/cycle

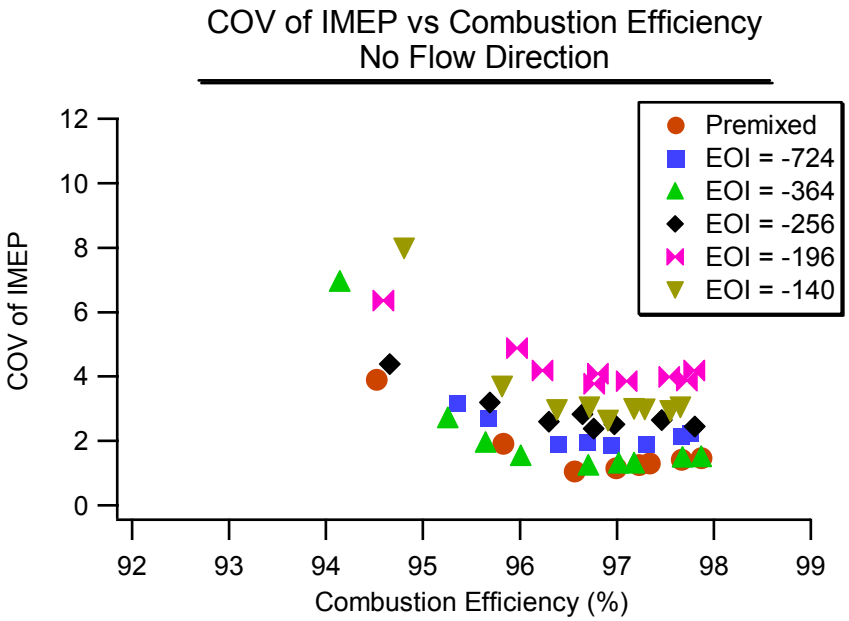

Figure 6-9 COV vs. combustion efficiency for undirected stratified fueling at 10 mg/cycle

The plots of the ringing index, or combustion generated noise, as a function of combustion efficiency show the same trend as the COV. The noise, emitted from the engine for all configurations and timings investigated, begins to increase as the combustion efficiency passes 96%. This is about the same time that the COV metric enters acceptable levels. The scatter seen in Figure 6-10 is characteristic of the variability in the noise emitted from the engine and the high standard deviation in the ringing index metric. Looking at all of these plots, we can see that in terms of cylinder pressure behavior, as a function of the amount of fuel reacted in the cylinder, the performance of the engine does not change with either stratified injection timing or intake air temperature. The reasons for the required change in the intake air temperature under stratified injector operation will be discussed in the next section, but before moving to that discussion it is insightful to look at the emissions trends from the engine while running in stratified mode.

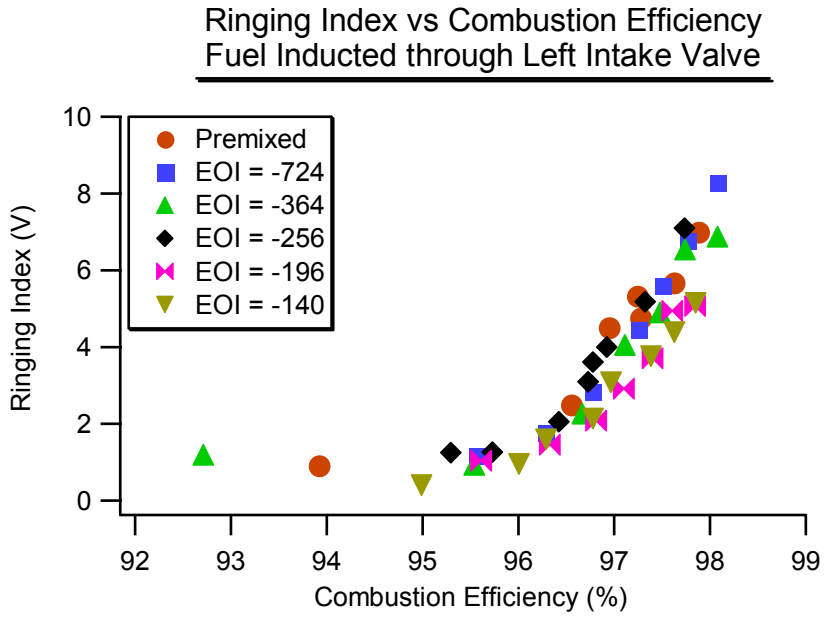

Figure 6-10 Ringing index vs. combustion efficiency for directed stratified fueling at 10 mg/cycle

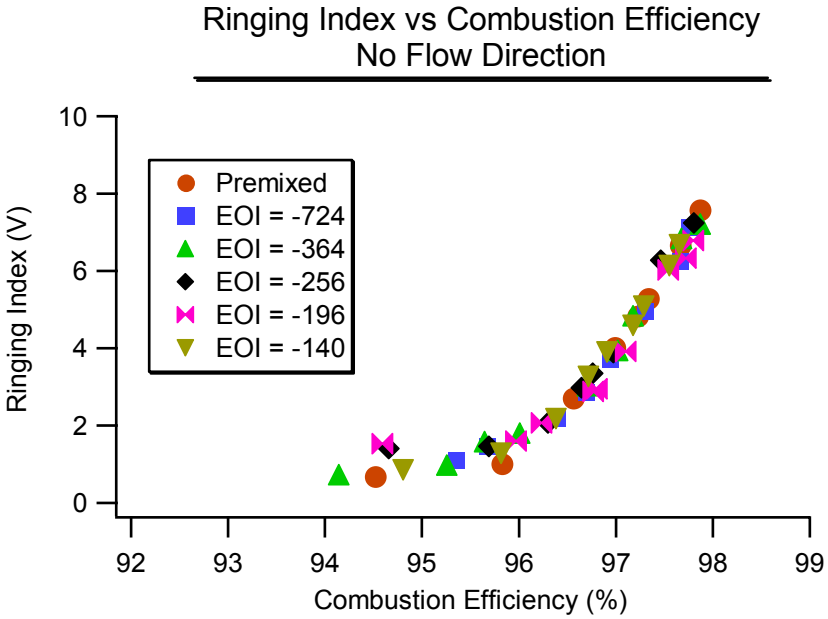

Figure 6-11 Ringing index vs. combustion efficiency for undirected stratified fueling at 10 mg/cycle

The emissions from the engine indicate a different assessment of stratified HCCI combustion than was obtained from the cylinder pressure. Figure 6-12 and Figure 6-13 show the plots of NO_x as a function of combustion efficiency. These plots show that more NO_x is

generated as the injection timing moves closer to TDC. This occurs for both of the configurations; or stated another way, as the amount of time available for mixing decreases the NO_x emissions increase. The largest amount of NO_x is generated for the left intake valve directed system it is over three times higher than the amount generated with the premixed system.

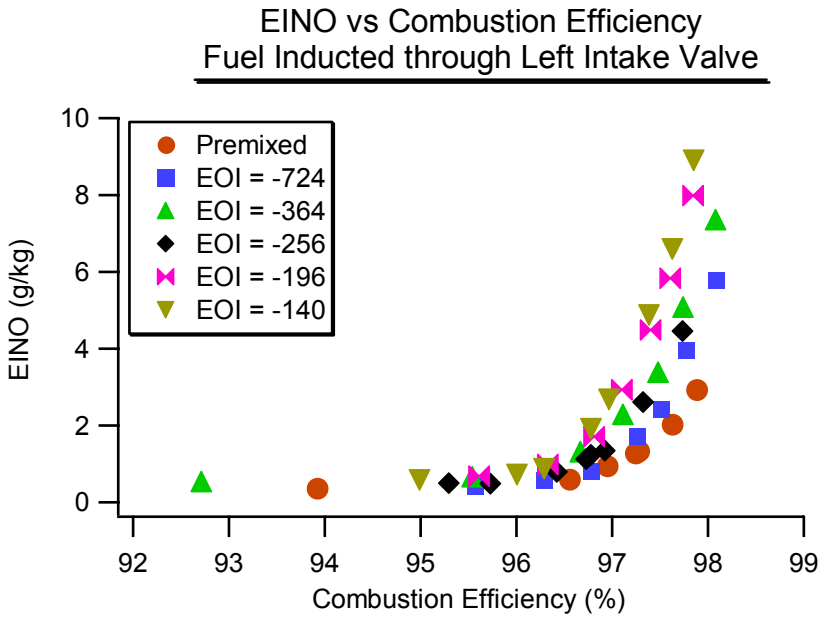

Figure 6-12 NO_x emissions vs. combustion efficiency for directed stratified fueling at 10 mg/cycle

There are two possible mechanisms for the increased amount of NO_x emissions when running with the stratified system. The first explanation is that the system being stratified has portions of the cylinder gasses at air/fuel ratios richer than the global air/fuel ratio. These rich zones would burn hotter locally than a uniform mixture and therefore would generate more NO_x. The other explanation is that to achieve acceptable HCCI combustion higher intake air temperatures were required for the stratified runs than for the premixed runs. These higher temperatures might increase the peak combustion temperatures to levels

sufficiently high to generate the increased NO_x detected when running the stratified fueling system.

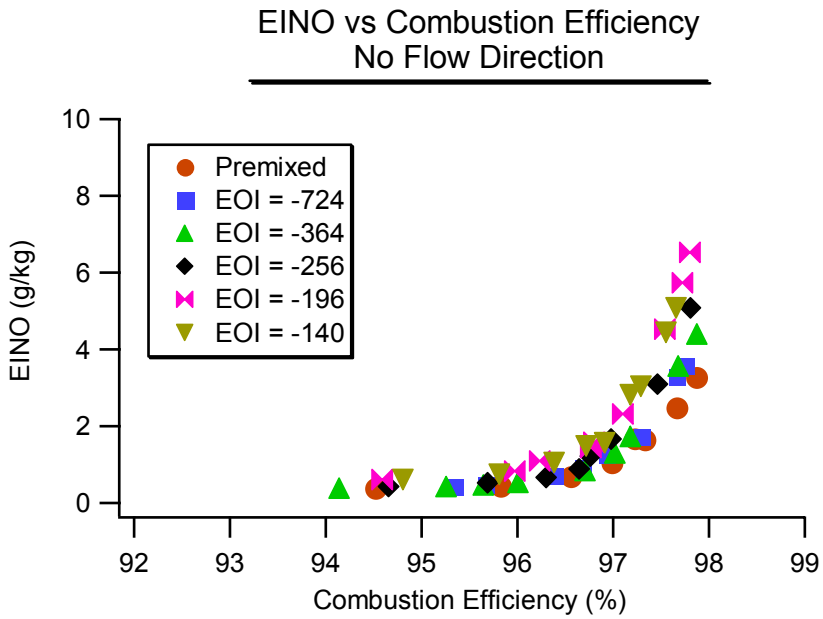

Figure 6-13 NO_x emissions vs. combustion efficiency for undirected stratified fueling at 10 mg/cycle

It is surmised that it is most likely that both factors were influencing the combustion in the engine. This conclusion can be drawn by looking at several indicators. First, the amount of NO_x is progressively higher as the fuel injection moves closer to TDC; this is despite the fact that the operating temperature windows for the left hand valve injection configuration did not have a trend of progressively higher temperature windows with fuel injection timing. Also the undirected configuration has the highest window of temperatures for the injection timing of -724 degrees ATDC, yet this timing does not show the highest levels of NO_x emissions, which would be expected if the intake temperature effect is the only mechanism controlling the NO_x emissions. However, note that the intake temperatures for the undirected flow are 10 °C or more lower than the directed flow. This fact implies that the

reason the peak NO_x emissions, for the undirected case, are about 2/3 of the directed emissions is most likely due to a scaling effect generated by the slightly lower intake temperatures.

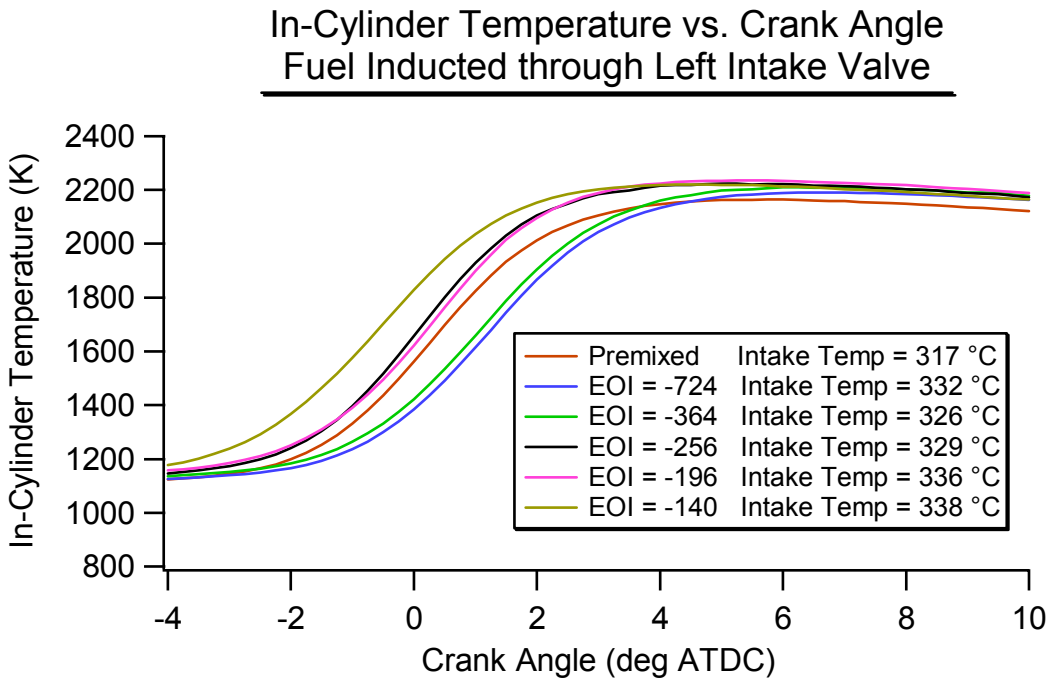

Figure 6-14 In-cylinder temperature for directed stratified fueling at 10 mg/cycle, the combustion efficiency of each curve is approximately 98%

The average temperature of the gasses in the cylinder was calculated using a single zone heat release analysis program. The results of these calculations are shown in Figure 6-14 and Figure 6-15. The cylinder temperature for each crank angle is plotted for both injector configurations and all of the injection timings tested, the data presented was selected so that the combustion efficiency for each point was around 98%. As can be seen in these plots, the peak gas temperatures only track weakly. This data helps reinforce the idea that the higher levels of NO_x emissions are not solely a function of the intake air temperature for these data sets.

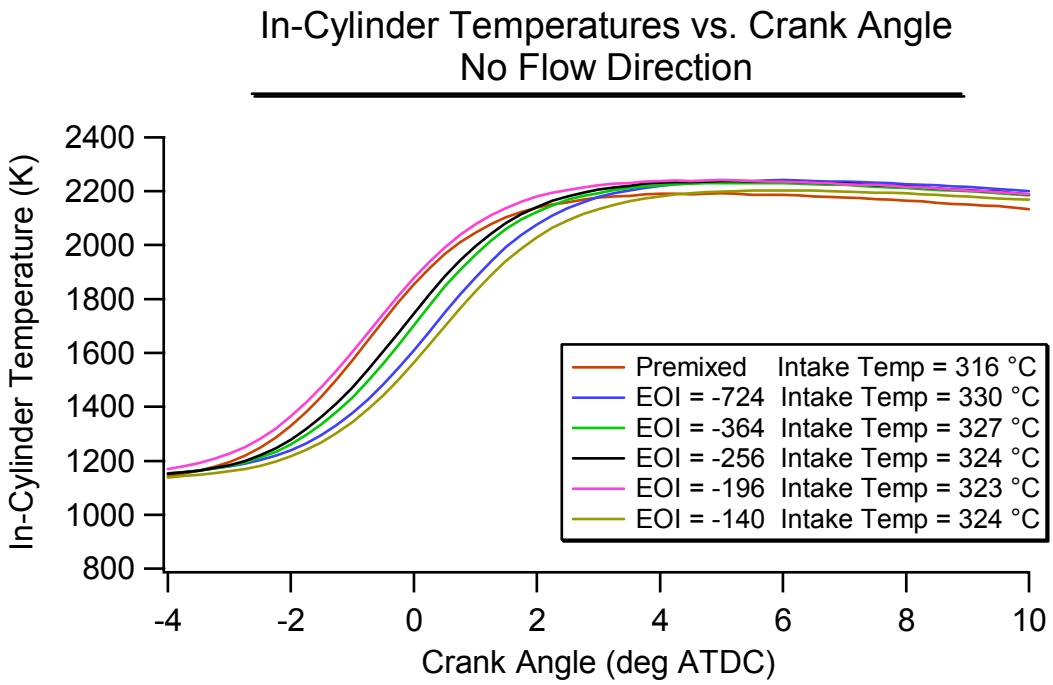

Figure 6-15 In-cylinder temperature for undirected stratified fueling at 10 mg/cycle, the combustion efficiency of each curve is approximately 98%

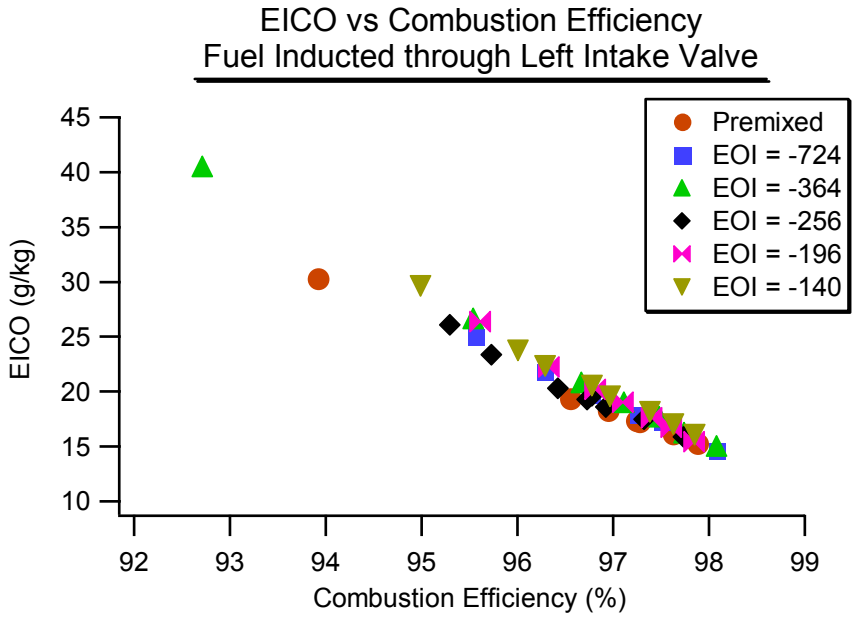

Figure 6-16 CO emissions vs. combustion efficiency for directed stratified fueling at 10 mg/cycle

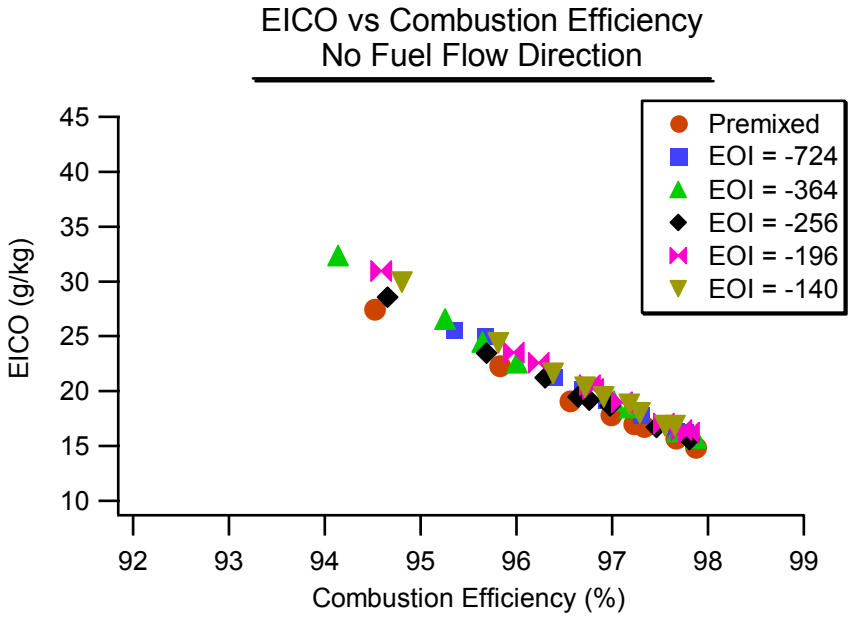

Figure 6-17 CO emissions vs. combustion efficiency for undirected stratified fueling at 10 mg/cycle

A review of the carbon monoxide emissions shows a trend of slightly increasing CO emissions as the injection timing moves closer to TDC; these results can be seen in Figure 6-16 and Figure 6-17. This increase in CO emissions is most likely due to incomplete bulk gas reactions in the portions of the cylinder that are locally lean due to the stratification generated in the cylinder. The lean areas will not reach the same temperatures as the rich zones, which leads to less complete bulk gas reactions. Recall that the oxidation of CO to CO_2 is where much of the combustion related heat is released, this means that increased CO emissions could equate to lost work from the engine and therefore increased thermal inefficiency.

Section 6.3 Measurements of the Fuel Jet's Temperature

A review of the data from the engine, which was presented in Section 6.2, leads one to believe that there is a level of thermal stratification generated in the inlet charge. Remember that the original goal of these experiments was to develop a level of fuel/air stratification in the intake charge that did not have any thermal stratification coupled to it. It would be best if a way could be found to decouple the thermal and spatial stratification effects. Before attempting to decouple these two stratification modes it is a good idea to quantify the amount of thermal stratification that was actually generated in the inlet. This was accomplished with a series of tests devised to measure the temperature of the fuel jet as it exited the stratified fuel injector system.

There are three mechanisms through which the temperature of the fuel jet can be altered from the temperature upstream of the injector. The first mechanism is a temperature drop associated with expansion of a sonic flow through a critical flow orifice. Calculations suggest that this mechanism will lower the exit temperature, of the jet, approximately 20 °C below the temperature upstream of the injector. A second mechanism that can alter the fuel jet's temperature is heat transfer to the cylinder head and cooling water. The coolant temperature is maintained at 95 °C and the fuel jet and intake air were to be maintained at 300 °C thus the head is considerably colder than the intake air or the fuel jet. This means that the fuel jet will loose energy to the cylinder wall and exit the hypodermic tube at a temperature lower than it entered the injector assembly. Finally it is possible that the bulk air could transfer heat through the hypodermic tube to the fuel jet, thus raising the jet's temperature. These three mechanisms are all coupled together in a complex and nonlinear

manner; this means that it was necessary to measure the jet's temperature instead of attempting to calculate it.

The temperature measurements were conducted using a bare wire K-type thermocouple with a diameter of 0.127 mm (0.005 in). The thermocouple has a calculated response time of 0.26 ms. The diameter of the thermocouple's wire was chosen for the fast response capability. A thermocouple with even smaller wires which would have had better response times was tested, but turned out to not be sufficiently durable to survive the testing procedures. The signal from the thermocouple is input into an Analog Devices model AD5595CD amplifier chip which converts the signal to a voltage with a scaling of 10 mV/°C.

A calibration of the thermocouple and amplifier chip assembly was performed using an ice bath and boiling water as reference points. The thermocouple read a value of 0.8 °C in the ice bath and a value of 98.8 °C in the boiling water. Both values are accurate to within the K-type error bands as quoted by Omega Instruments, Inc. These values were deemed acceptable.

A special ceramic holder was designed to be installed in the intake runner. This holder slipped over the hypodermic tube attached to the injector body. The thermocouple was held in the ceramic holder, centered over the hypodermic tube with the wires being isolated from any metal contact. The wires were then insulated and run out of the intake port to the amplifier chip. The signal from the amplifier was read by the computer using the LabView software package. Electrical interference from the dynamometer was picked up by the thermocouple when the engine was running so these experiments were performed with the engine stationary and positioned at the crank angle where the intake valves were fully

open. Air was then directed through the intake valve and out of the cylinder through the spark plug hole and finally dumped into the building exhaust.

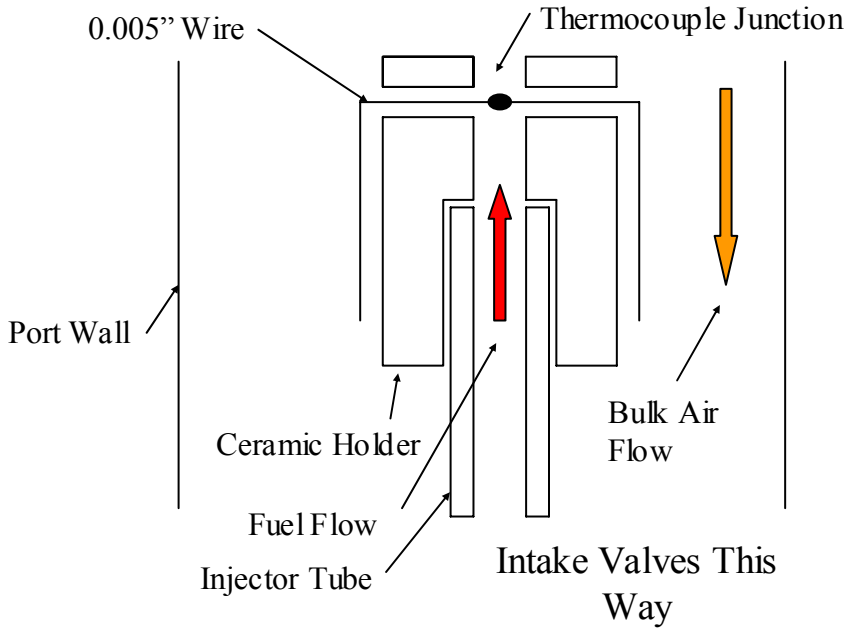

Figure 6-18 Stratified fuel jet temperature measurement apparatus

To measure the temperature of the spray jet, a special hypodermic tube was constructed to turn the flow of fuel so that it exited the injector tube moving away from the inlet valve. This was necessary in order to gain enough space to install the thermocouple. A diagram of the mounting system is shown in Figure 6-18.

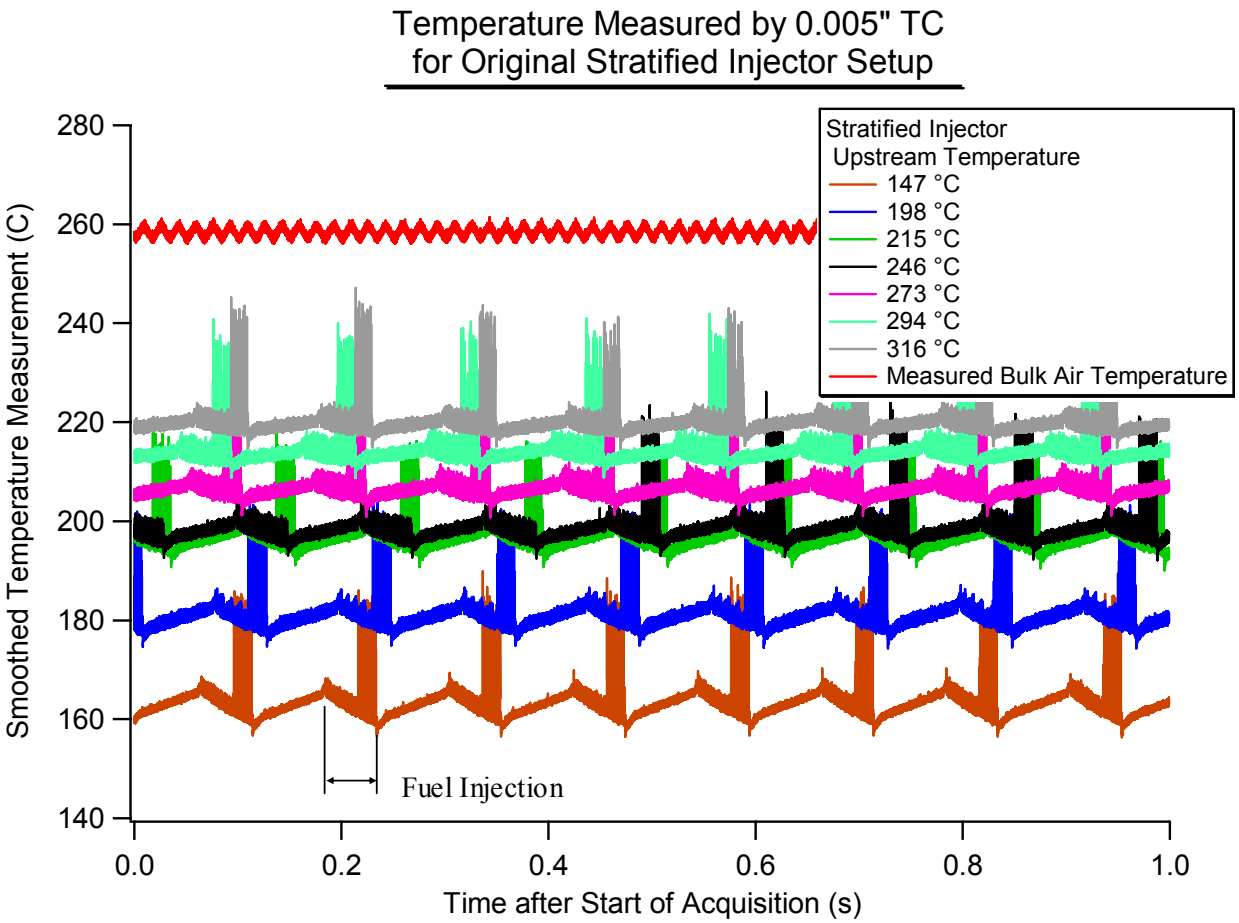

Figure 6-19 Stratified fuel temperature measurements

The results of the temperature measurements can be seen in Figure 6-19. Measurements were taken of the temperature of the gas for a number of temperatures upstream of the Clean Air Partners injector. The objective of these experiments was to determine if the jet's exit temperature scaled linearly with the upstream temperature. For all of these points the coolant was maintained at 95 °C and the temperature of the bulk air was held constant at about 300 °C, which was measured five inches away from the intake valve. The value of the bulk air temperature read by the thermocouple at the hypodermic tube end is shown on the plot as well, the two thermocouples are approximately three inches apart. Also

on the plot is a set of marks that denote a typical injector open cycle. The jet's temperature reaches a steady state value just a few milliseconds before the injector closes. The large spikes that appear at the end of the injection are electrical noise associated with the closing of the CAP injector.

As can be seen in the figure, the temperature of the fuel stream as it exits the stratified system is lower than the temperature of the bulk air for all fuel temperatures. The upstream temperatures at which the stratified system is run during engine operations are between 300 and 340 °C. Based on these results, it appears that the fuel is entering the cylinder at temperatures at least 40 degrees lower than the bulk air. The fuel traveling through the stratified system is about 6% of the mass entering the engine. Calculations show that this mass, at the temperatures measured in the figure, can decrease the mixture's temperature by 15 to 20 degrees. This is enough to mandate the increase in the intake air temperature to achieve the operating windows that was observed in the previous sections.

Section 6.4 Redesigned Hypodermic Tube Assembly

Reviewing the data presented in Figure 6-19, it is interesting to note that the temperature at the tube's exit does not change linearly with the temperature ahead of the injector. Looking at the rate of increase in the temperature of the fuel jet as it exits the injector body, lead one to the assessment that heat transfer plays an important role in controlling the exit temperature of the fuel jet. This can be seen by noting that when the temperature of the gasses upstream of the CAP injector is held at 150 °C the fuel exits the injector at a temperature of about 160 °C.

As stated before the goal of the experiments performed in this laboratory was to explore fuel/air spatial stratification without any thermal stratification in the cylinder. This means that the fuel must enter the intake port at the same temperature as the bulk air. Based on the conclusion that heat transfer was changing the fuel jet's temperature, a simple shell and tube heat exchanger was constructed inside the intake runner to transfer energy from the bulk air to the stratified fuel and bring the two gas streams to the same temperature.

6.4.1 Heat Exchanger Design

The design of the heat exchanger is very simple. The hypodermic tube is brought into the engine through the intake port as it was in the original design but instead of going directly to the valve the tube was run upstream into the runner, it looped back down to the intake valve. The exit of the tube was aligned with the axis of the valve stem. The total length of the hypodermic tube is approximately 0.76 m (30 in). Also as in the original design the tube is a 3.175 mm (0.125 in) outside diameter stainless steel tube with an inner diameter of 2.286 mm (0.090 in).

The original design of the stratified injection system was such that the fuel would have as short of a residence time in the hypodermic tube as possible. This goal was set so that as much fuel as possible would consistently make it into the engine each cycle. As the residence volume increases the shot to shot variation of the fuel delivery increases. For this work it was decided to sacrifice consistency of the shot to shot fuel delivery for higher fuel jet temperatures. In the final embodiment used in the experiment the ratio of the volume of fuel injected to the volume of the tube equals approximately 2.3. Originally the ratio of fuel volume to tube volume was about 18. The layout of the tube can be seen in Figure 6-20.

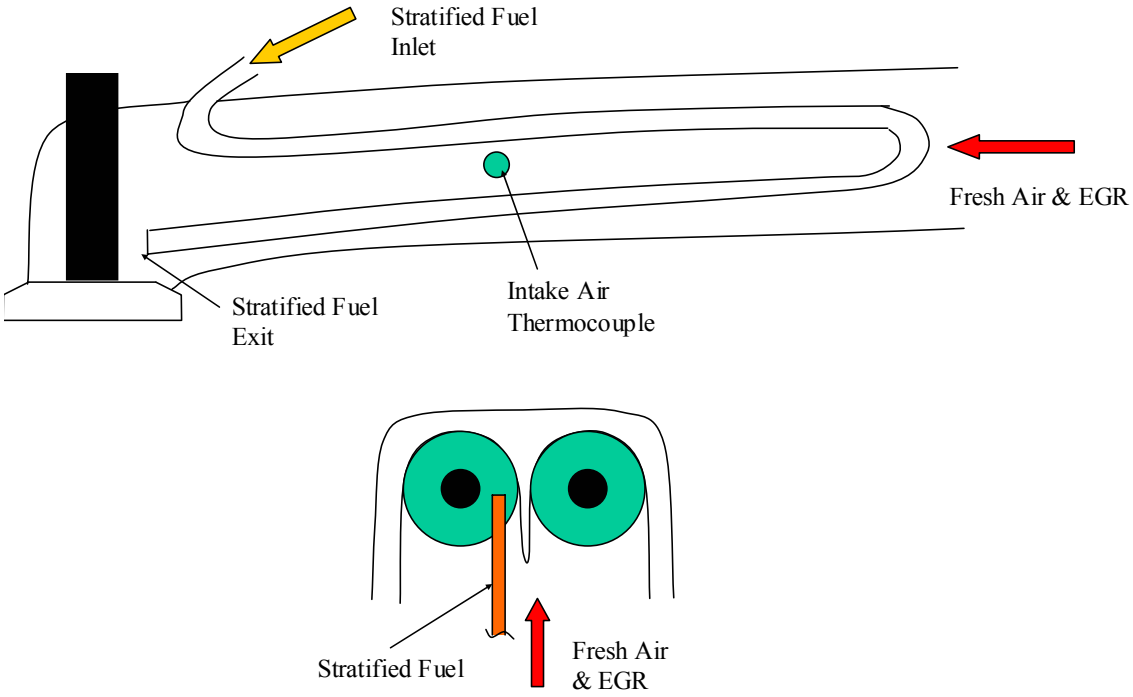

Figure 6-20 Stratified fuel heat exchanger system

The tube was installed so that it points at the left hand valve, but it could also be pointed at the right hand valve. However the intake runner must be removed from the engine in order to change the tube's placement, a procedure that takes a significant amount of time and effort. Also after reviewing the results from the previous experiments, the placement of the tip did not show any significant effect on the results, so it was decided not to run the setup with the injector pointed at the right hand intake valve.

If this heat exchanger was employed in a configuration with no energy addition to the runner and intake air, the device would only serve to lower the temperature of the bulk air. However in the current experimental setup there are heater strips to add energy to the bulk air which makes up for any losses to the fuel stream. By adding energy to the runner and bulk

air and by using the long hypodermic tube to allow the fuel to absorb thermal energy from the bulk air it is possible to control both the fuel and bulk air temperatures to the same value.

6.4.2 Temperature Measurements

In order to ensure that the steps taken to remove the thermal stratification were successful, temperature measurements were again taken of the fuel jet as it exited the hypodermic tube. The same thermocouple assembly as used previously was used for these measurements. The setup was the same as above with a few notable exceptions.

The first difference was that the coolant pump was not always on, so there are several data sets for which the cylinder head was considerably colder than it was in the previous temperature measurements. The second difference was that the injector tip now pointed towards the intake valves (downstream), so the two gas streams were traveling in the same direction.

A final note on the setup is that due to space limitations temperature measurements could not be taken from the 30 inch long hypodermic tube. In order to fit everything into the runner, the tube used for the temperature measurements was about 0.54 m (21 in) in length. This is acceptable because the shorter tube leaves less time and surface area for heat transfer to occur so the measured temperatures will be lower than the temperature of the fuel jet exiting the longer hypodermic tube used in the actual experiments. The results of these temperature measurements can be seen in Figure 6-21.

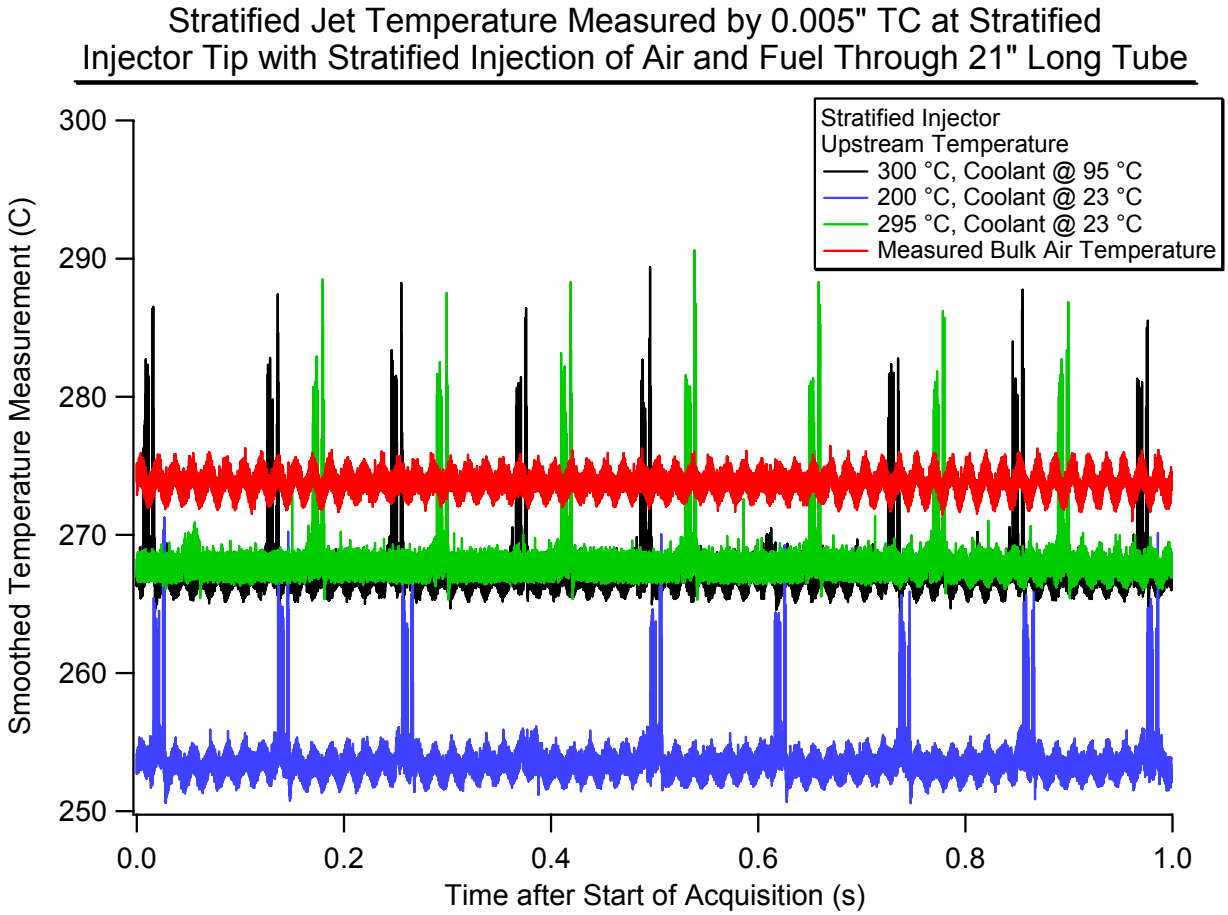

Figure 6-21 Stratified fuel temperatures leaving the long hypodermic tube

From the results shown in Figure 6-21 it can be seen that the new design of the hypodermic tube was successful in removing most of the temperature drop that was observed in the original design. It can be seen that when the gas temperature upstream of the CAP injector is 200 °C the fuel exits the injector body at a temperature greater than 250 °C, also note that this is with the coolant in the cylinder head at room temperature. This confirms the hypothesis that heat transfer has the driving role in the temperature of the fuel jet. You can also see that when the upstream fuel temperature is brought up to 300 °C the fuel exits the injector body within 5 degrees of the bulk air temperature, as measured by the thermocouple

at the hypodermic tube. Also for the 300 °C upstream temperature it can be seen that when the coolant in the cylinder head is heated to 95 °C, the fuel leaves the injector assembly at the same temperature that it did when the coolant was at room temperature. This demonstrates that heat transfer, from the bulk air stream to the fuel jet, is overcoming all of the heat transfer losses from the stratified fuel system to the cylinder head and surroundings.

Section 6.5 Stratification Tests without Thermal Gradients

The five degree temperature difference between the stratified fuel jet temperature and the bulk air temperature was deemed to be small enough to allow us neglect thermal stratification in the subsequent stratified fueling experiments. This allowed us to repeat the investigation described in Section 6.2, only this time without any thermal stratification.

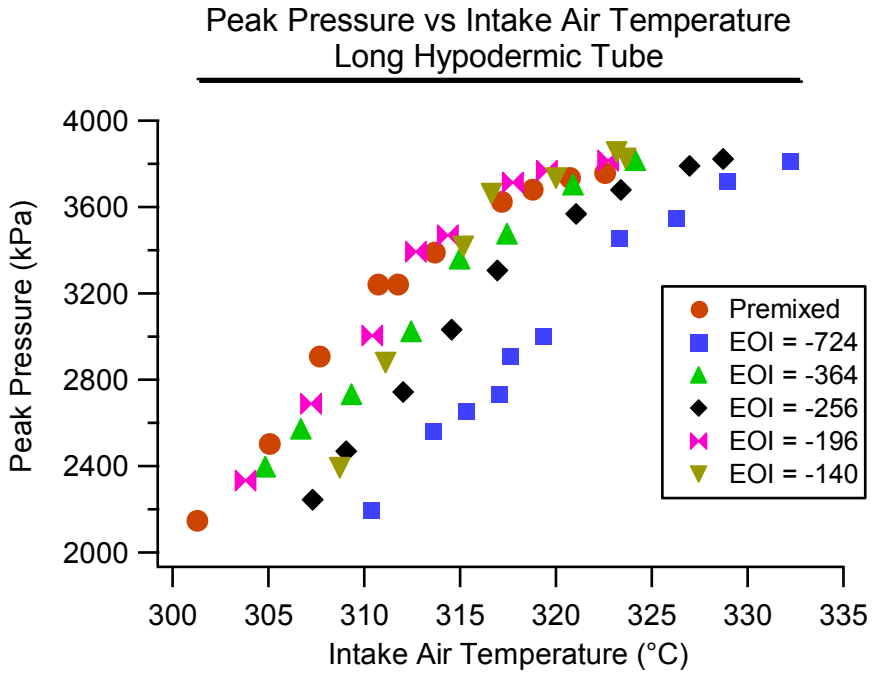

Figure 6-22 Peak pressure vs. intake air temperature for long hypodermic tube at 10 mg/cycle fueling

Experiments were performed with the hypodermic tube pointed at the left hand intake valve. The matrix of experimental parameters is detailed in Table 6-2. Figure 6-22 shows a plot of the peak cylinder pressures for the five stratified injection timings shown in Figure 6-1, as well as premixed operating data. You can see in this plot that the operating windows for all of the data sets are very similar. The one operating condition that has a significantly different temperature operating window is the -724 degree ATDC injection timing. This is interesting because one would expect that the earliest injection timing should give the most uniform mixture of fuel and air and therefore the operating conditions would be expected to be the most close to the premixed data.

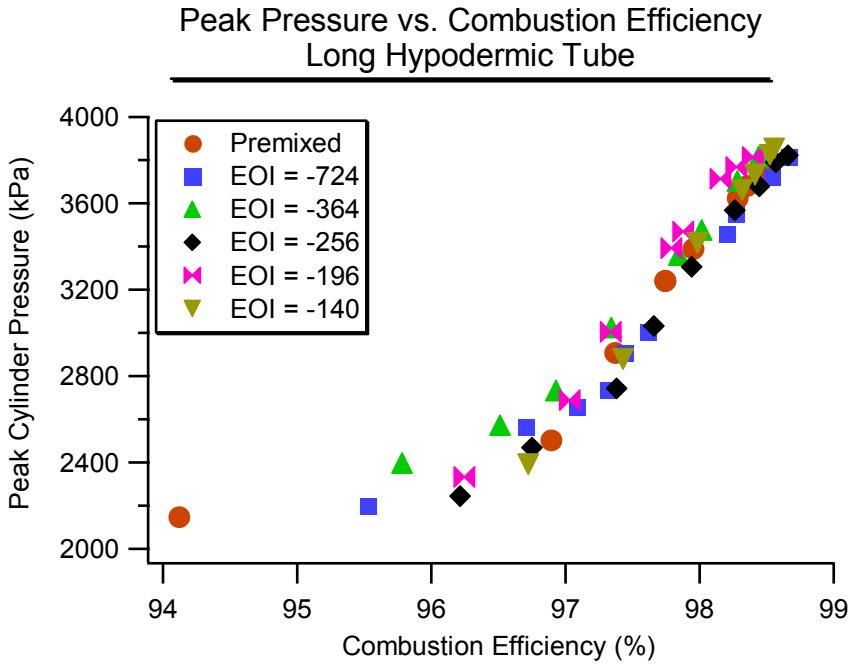

Figure 6-23 Peak pressure vs. combustion efficiency for long hypodermic tube at 10 mg/cycle fueling

The reason for the discrepancy most likely lies in the heat transfer losses to the walls of the port. The fuel is injected right into the port near the back of the intake valve and does

not mix with the air instead it looses energy to the cold cylinder head due to heat transfer. This means that the intake air has to be heated to higher temperatures to overcome the energy loss of the fuel to the intake port walls.

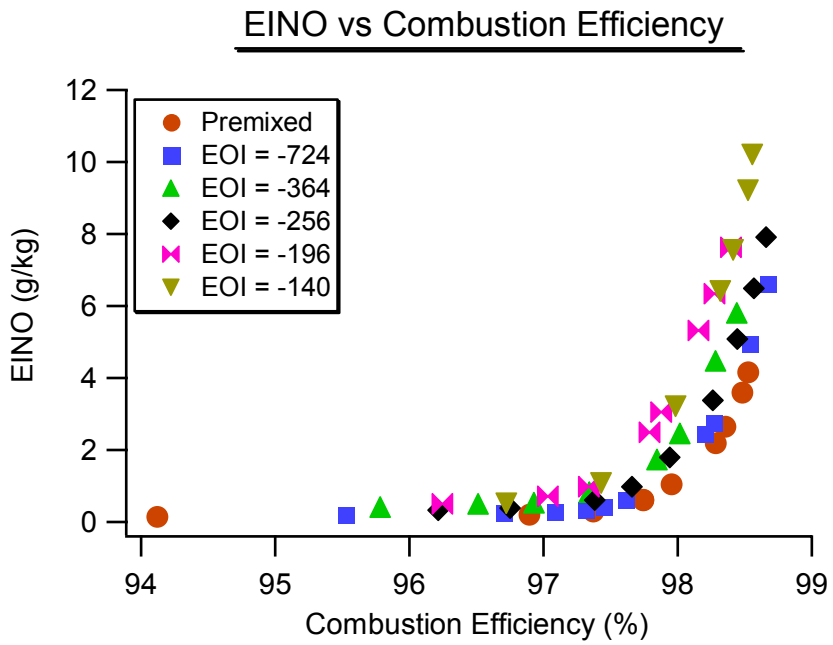

Figure 6-24 NO_x emissions vs. combustion efficiency for long hypodermic tube at 10 mg/cycle fueling

A plot of the pressure data as a function of combustion efficiency shows that the data still collapses to a single trend line, which is show in Figure 6-23. This analysis, however, wasn't really necessary, since the data was fairly well collapsed when plotted against the intake air temperature. The plot does, however, allow us to say with confidence that the results seen at the -724 degrees ATDC injection timing is controlled solely by heat transfer and not the timing of the fuel injection.

The emissions of NO_x and CO are plotted as functions of combustion efficiency in Figure 6-24 and Figure 6-25 respectively. These results are very similar to the data that was

shown in Section 6.2. This data shows that even when the thermal stratification is removed from the experimental matrix, more NO_x is generated when fueling the engine with the stratified injector as opposed to the premixed fueling system. It can be seen that the amount of NO_x generated in the cylinder increases as the injection timing moves closer to TDC. This result shows that indeed locally rich regions are generated in the cylinder and that they tend to burn hotter than does the fully mixed charge. However, the existence of these locally rich regions does not seem to affect the engine's behavior in terms of intake air operating windows or cylinder pressure behavior. Again, in the plot of CO vs. combustion efficiency, Figure 6-25, it can be seen that the CO emissions increase slightly as the injection timing moves closer to TDC. The reason for this trend is believe to be incomplete bulk gas reactions in the areas of the cylinder where the mixture is reacting at a more fuel lean condition than the global air/fuel ratio indicates.

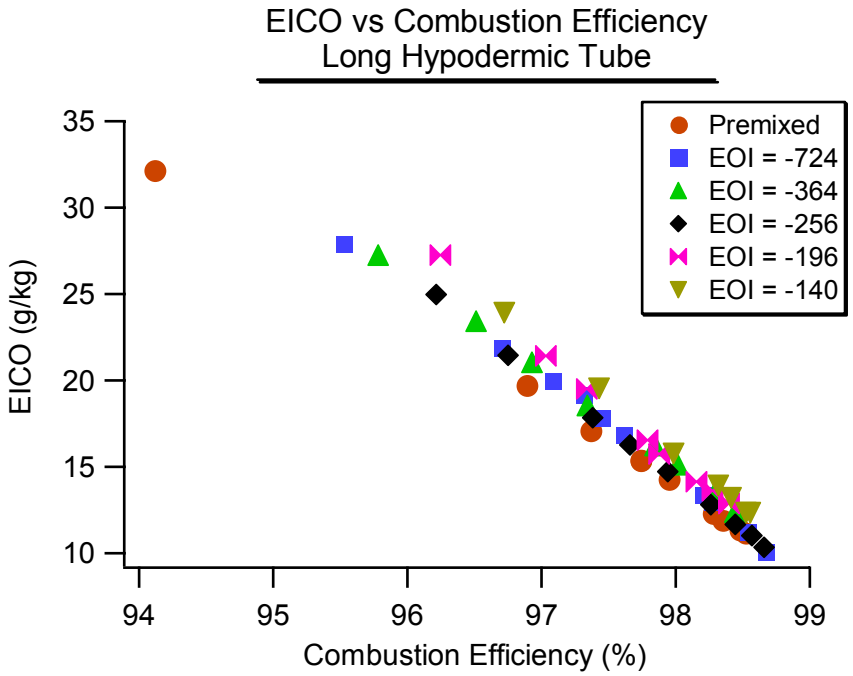

Figure 6-25 CO emissions vs. combustion efficiency for long hypodermic tube at 10 mg/cycle fueling

All of the new stratified injector data indicate that some amount of spatial stratification is actually generated inside the cylinder. However the effects that this stratification generates only appear in the exhaust emissions. Therefore an initial conclusion is that air/fuel stratification alone has only a modest influence over HCCI combustion. One must be careful when stating this since it is unknown how much stratification is actually generated inside the cylinder. Also since these results were only for a single operating point, it is necessary to investigate other engine operating points in order to strengthen the conclusion that stratification is a negligible factor in HCCI combustion. To that end a series of analyses were performed at lower engine speeds, at various air/fuel ratios, and for several fueling rates. For all of these tests the timing of the stratified injection was set to -140 degrees ATDC. This point was chosen since it was the point that appeared to have the most influence over the engine emissions.

6.5.1 Constant Air/Fuel Ratio Variable Fueling Rate Tests

After confirming that the stratified injection system worked as intended and that there was no thermal stratification in the cylinder, the engine was run at a constant air/fuel ratio of 20:1 or a lambda of 1.33. This section presents data for the experimental matrix described in Table 6-3.

The data presented in Figure 6-26 is the peak pressure collected for the three fueling rates and the two different fuel introduction methods. The premixed data is presented with closed symbols and the stratified data is presented with open symbols. The things that are notable in this plot are that the stratified fueling data does not exhibit any major differences from the premixed fueling data. Also the peak cylinder pressure decreases as the amount of

fuel introduced into the engine decreases, this is because a lower fueling rate means that less chemical energy is brought into the cylinder each cycle.

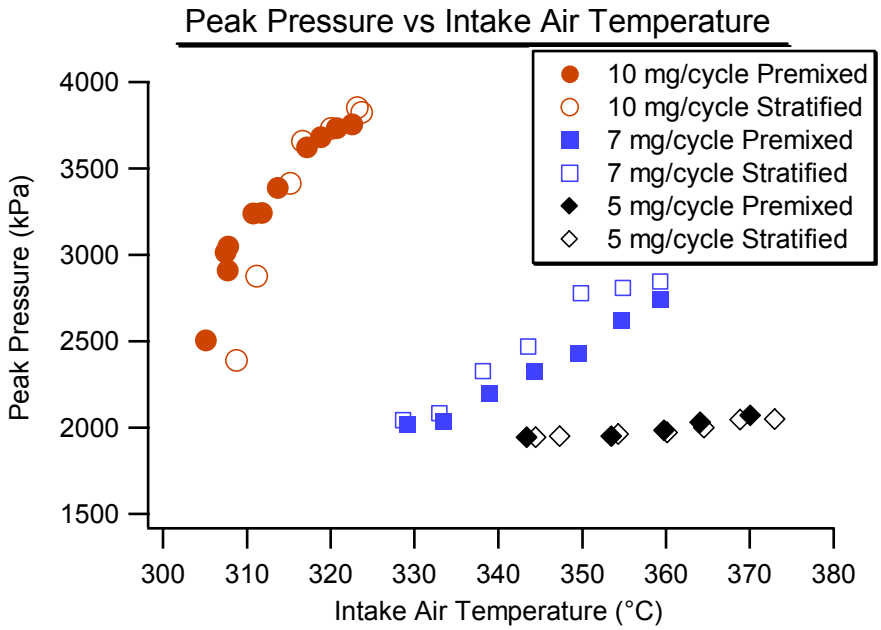

Figure 6-26 Peak pressure for constant air/fuel ratio and variable fueling rates

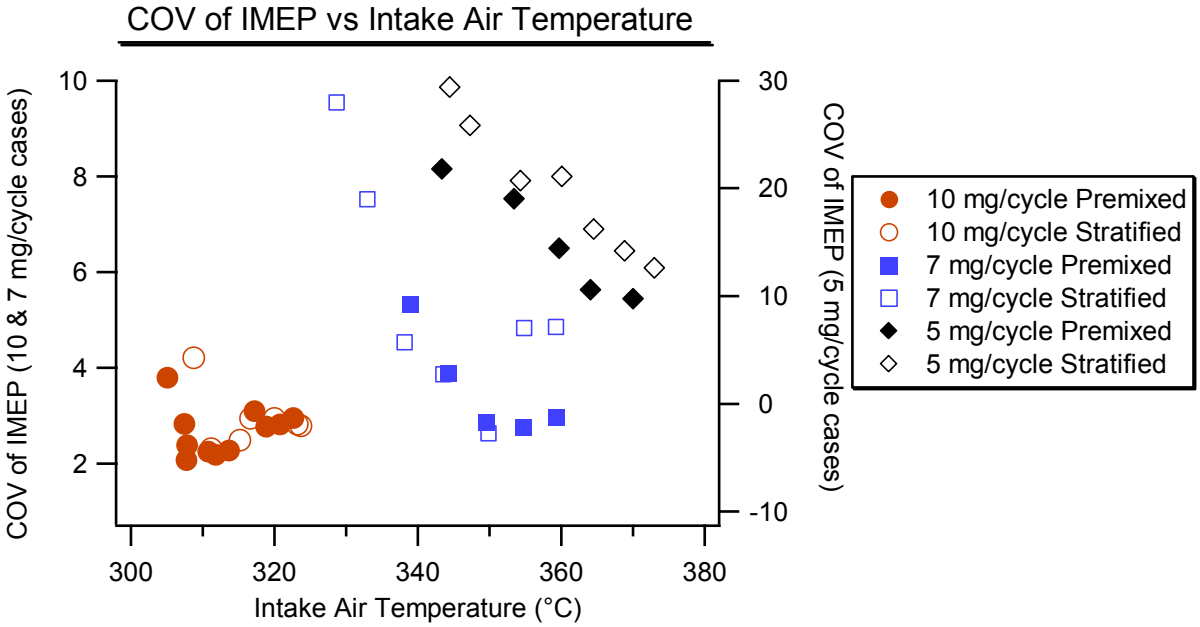

Figure 6-27 COV for constant air/fuel ratios and variable fueling rates

The rest of the plots in this section are presented to emphasize changes in the HCCI combustion behavior that are due to changes in the fuel and air flow rates. They will also continue to emphasize any differences that appear to be the result of air/fuel mixture stratification. Figure 6-27 shows the COV results for the examined engine operating conditions. The axes on this plot are configured so that the 10 and 7 mg/cycle fueling rates are shown on the left hand axis and the 5 mg/cycle fueling rate is shown on the right hand axis. The plot shows that as the fueling rate decreases the COV increases. This is primarily due to the decrease in the mean value of the IMEP, which is the result of the lower fueling rates. The definition of COV is shown in Equation (6.1). As the average IMEP is decreased the value of COV will increase for a given standard deviation. This is the reason that for idle conditions the high COV limit is typically set to 6%.

$$COV = \frac{StdDev_{IMEP}}{Mean_{IMEP}} \bullet 100\% \qquad (6.1)$$

It should also be noted that when the engine was fueled at 5 mg/cycle the COV never reached acceptable levels with either the premixed or the stratified fueling methods. Therefore it is unlikely that such a low fueling rate will be achievable in HCCI without a mechanism to lower the required intake temperatures.

The plot of combustion efficiency also shows an interesting HCCI characteristic which can be seen in Figure 6-28. Looking at the combustion efficiency for the three fueling rates it can be seen that it decreases with the fueling rate. Interestingly the 5 mg/cycle fueling rate has combustion efficiencies well below 90%. This is totally unacceptable in a practical roadworthy engine. The lower combustion efficiencies are due to the lower amount of chemical energy brought into the cylinder. Lower amounts of initial chemical energy in

the cylinder yield lower combustion temperatures and therefore incomplete combustion. This plot also shows that there is very little difference between the premixed and stratified fueling methods, and the few detectable differences between the two fueling methods are primarily due to the high amount of variability shown in the COV plot.

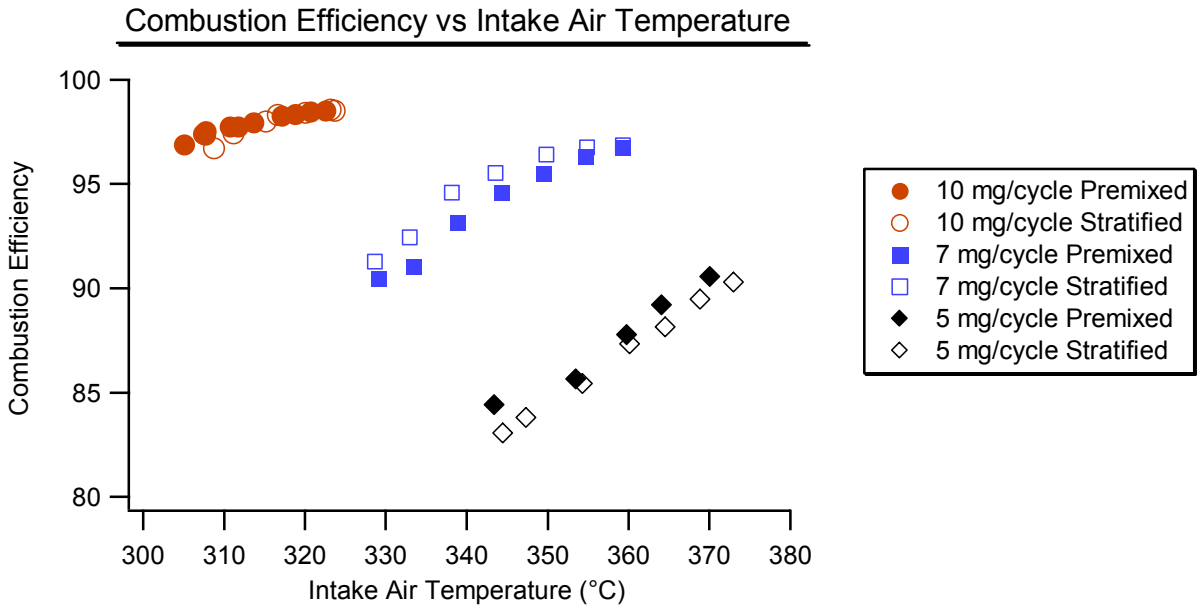

Figure 6-28 Combustion efficiency for constant air/fuel ratios and variable fueling rates

Figure 6-29 shows the crank angle where 50% of the fuel mass has burned (CA50). This plot again shows no differences between the stratified and premixed fueling methods. This is not surprising since no differences were noted in the peak pressure and COV plots. The other thing that can be seen on this plot, which is interesting, is the difference in the slopes for the three fueling rates. The data indicates that increasing the intake air temperature has less ability to advance the combustion as the fueling rate decreases. This trend is an artifact of the way the tests were performed. As the fueling rate is decreased, the airflow is decreased to keep lambda constant. As a result the EGR flow rate is increased to keep the

intake manifold pressure fixed at atmospheric pressure. The high amounts of EGR brought into the cylinder each cycle will act as a thermal absorber, the energy that the EGR absorbs does not act on the fuel in the cylinder which slows down the chemical reaction rates. This means that as the EGR fraction increases it takes more and more initial thermal energy input to advance the combustion phasing.

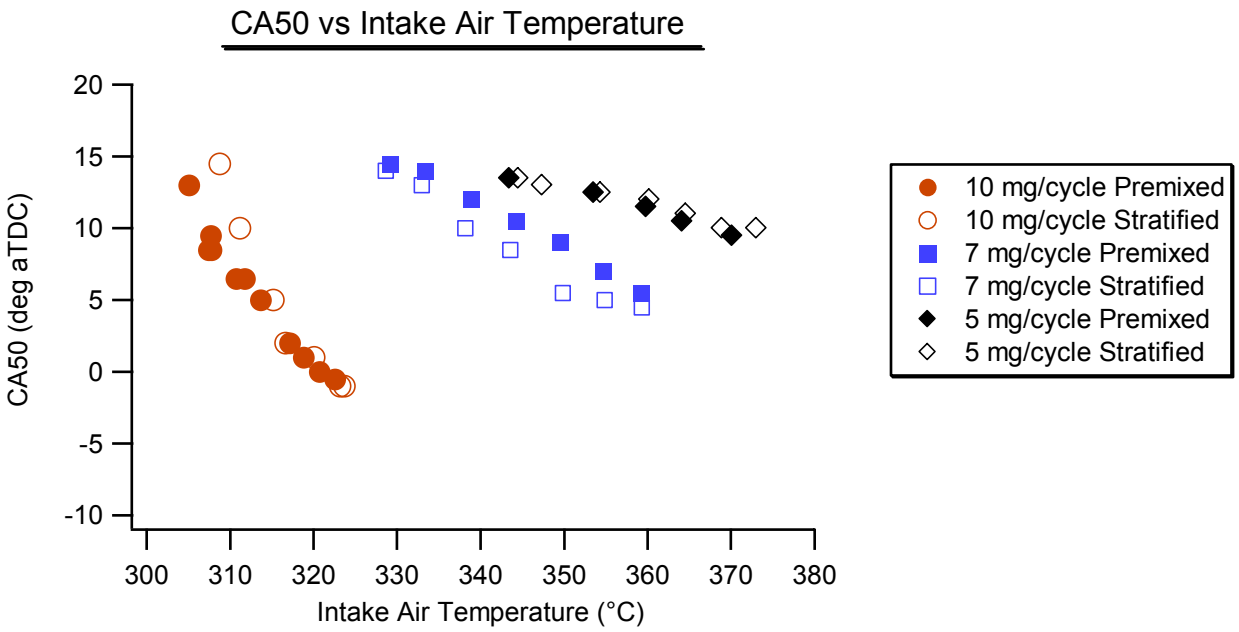

Figure 6-29 CA50 for constant air/fuel ratio and variable fueling rates

The amount of initial thermal energy required for combustion can be seen in Figure 6-30 which shows the temperature at Intake Valve Closure (IVC) as a function of the location of CA50. The plot clearly shows that for each progressively lower fueling rate, the amount of initial thermal energy required for combustion phasing at or near TDC increases significantly. This demonstrates that while dilution is important for inhibiting the formation of nitrogen oxides it has a negative impact on the requirements for proper combustion phasing.

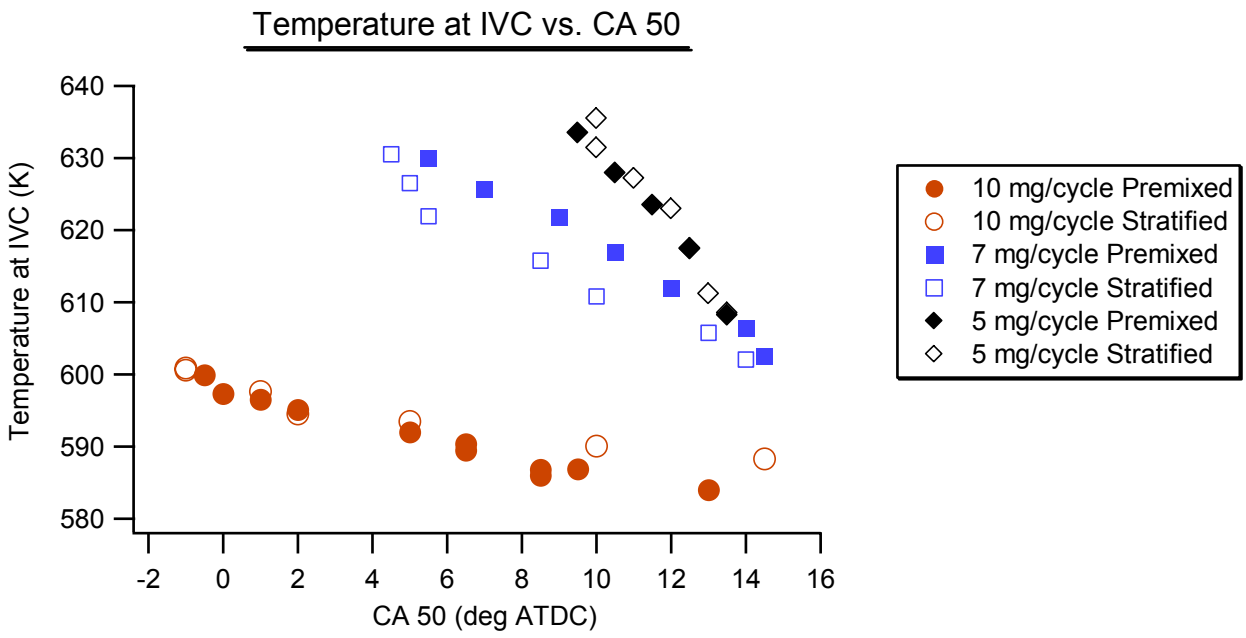

Figure 6-30 Temperature at IVC for constant air/fuel ratio and variable fueling rates

One other point that should be made is that the exhaust temperatures decrease with the fueling rate. This is due to the high amounts of dilution and the lower amount of chemical energy present in the cylinder at these conditions. Lower exhaust temperatures indicate that there is a fundamental lower limit on the range of fueling rates for which exhaust rebreathing will be practical. The exhaust rebreathing strategy attempts to capture the thermal energy in the exhaust by retaining the exhaust in the cylinder or rebreathing the exhaust during the intake stroke. This helps to raise the initial charge temperature and lessen the need for preheating of the intake charge. But, if the thermal energy of the exhaust is not high enough to raise the initial charge temperature to the auto-ignition point then the strategy will not be useful. This indicates that a different strategy will be required to bring about auto-ignition in an HCCI engine at idle conditions.

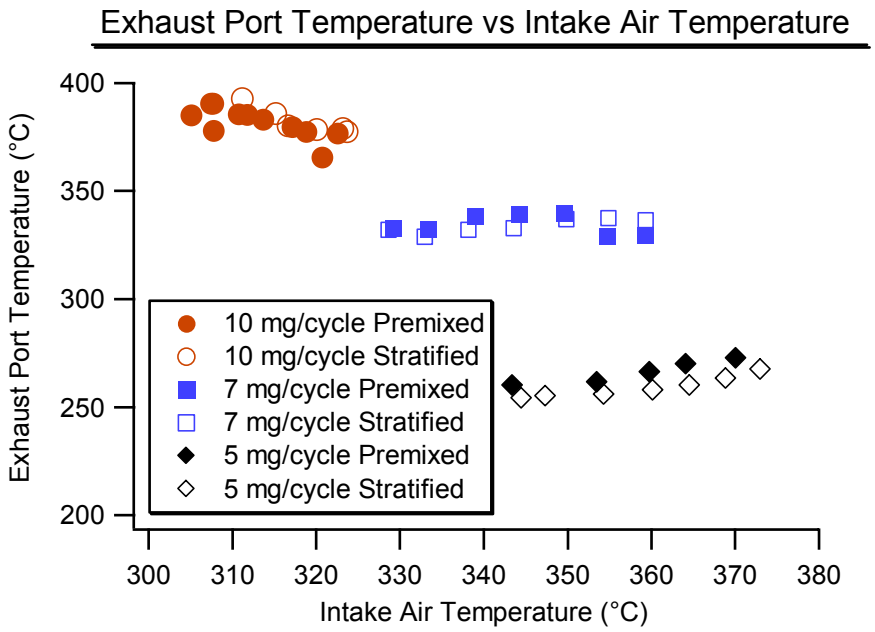

Figure 6-31 Exhaust temperature for constant air/fuel ratio and variable fueling rates

An investigation into the emissions from the engine shows again similar trends to what was seen during the injection timing sweeps described above. Figure 6-32 shows the emissions of nitrogen oxides measured for the three fueling rates. The axes are configured so that the 10 mg/cycle fueling rate is shown on the right hand y-axis and the 5 and 7 mg/cycle fueling rates are both shown on the left hand y-axis. In this plot we can see that generally the stratified fueling system leads to higher emissions of NO_x. The exception to this rule is the fueling rate of 5 mg/cycle, but as was noted earlier, this fueling rate does not have very high combustion temperatures, which tends to result in low NO_x emissions. Also since at this fueling rate the stratified system's NO_x emissions are lower than the premixed system's, we can safely conclude that values around 0.1 g/kg-fuel of NO_x emissions are inside the noise limit for the Chemiluminescent analyzer.

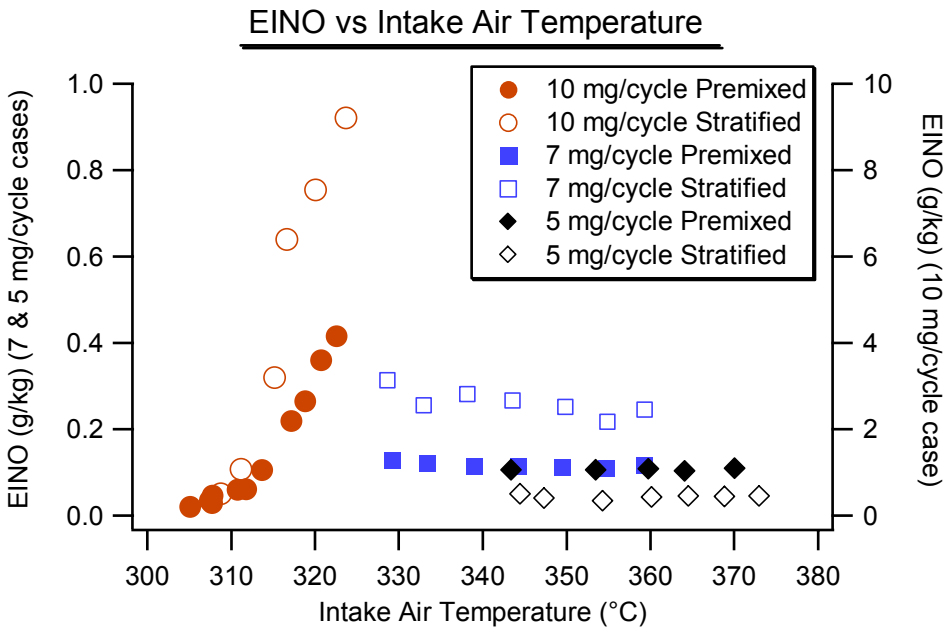

Figure 6-32 NO_x emissions for constant air/fuel ratio and variable fueling rates

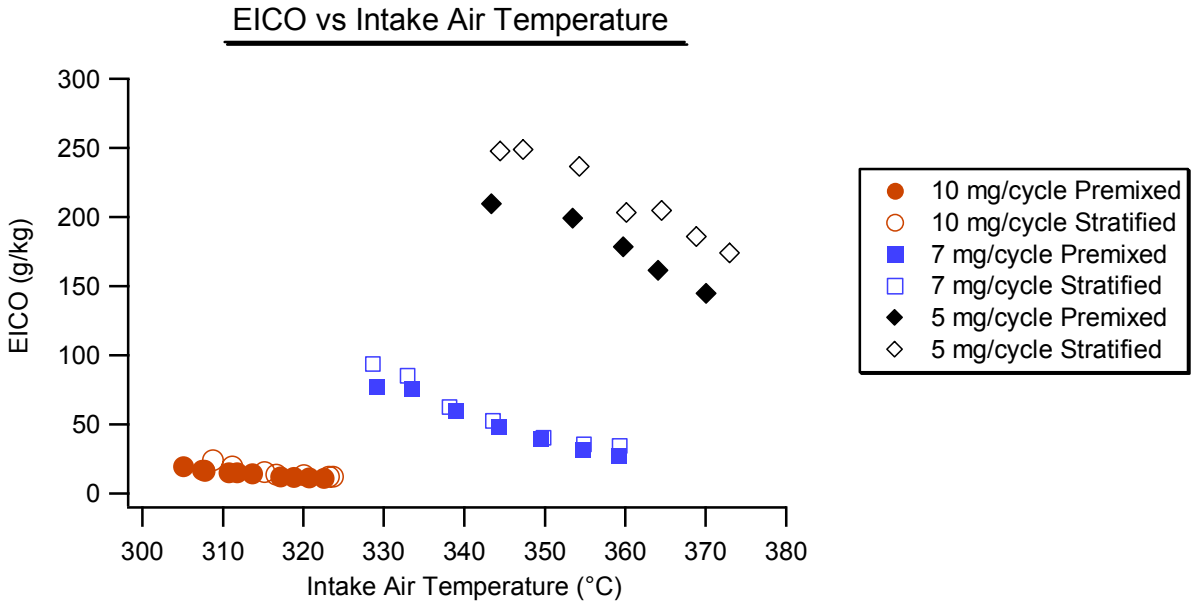

Figure 6-33 CO emissions for constant air/fuel ratio and variable fueling rate

The plot of CO emissions for these operating conditions shows very little sensitivity to the fueling system employed; however, the magnification of the y-axis is vastly different from that of the earlier plots. The CO emissions are shown in Figure 6-33. This shows just

how minor the trend of increasing CO emissions described in the earlier plots truly was. The 5 mg/cycle fueling rate does exhibit significantly higher CO emissions for the stratified fueling condition, but the combustion variability was so high that this is more likely an artifact of the combustion variability than it is a result of the fueling system employed.

These plots have summarized the changes in the engine's behavior when the fueling rate is changed but the air/fuel ratio and speed are maintained fixed. With the exception of the increase in NO_x emissions, no sensitivity to the manner in which the fuel is brought into the engine was detected.

6.5.2 Constant Fueling Rate Variable Air/Fuel Ratio Tests

While mapping the behavior of the engine, a series of tests were performed to investigate if the engine's performance was sensitive to the air/fuel ratio. Idle conditions are of the most interest, so it was decided to see if the combustion at the 5 mg/cycle fueling rate could be improved through the implementation of leaner air/fuel ratios and intake charge stratification. The matrix of experimental conditions is described in Table 6-4.

Figure 6-34 shows how the combustion responded to these operating conditions. It can be seen that when the air/fuel ratio is increased to 30:1 (2.00 Lambda) the combustion improves with higher peak pressures and a wider window of operation in terms of intake air temperature. It is also interesting to note that the effects of charge stratification are still minimal. The plot shows that for these experiments the peak cylinder pressure is not at all sensitive to the manner in which the fuel is introduced to the cylinder. It is currently believed that the explanation for the improvement in the engine's behavior appears is tied to the

increase in the amount of oxygen in the cylinder. Calculations show that the in-cylinder oxygen ratio is about 11% by volume for a lambda of 1.33, it increases to 14% at a lambda of 1.66, and at a lambda of 2.00 the oxygen ratio is near 16%.

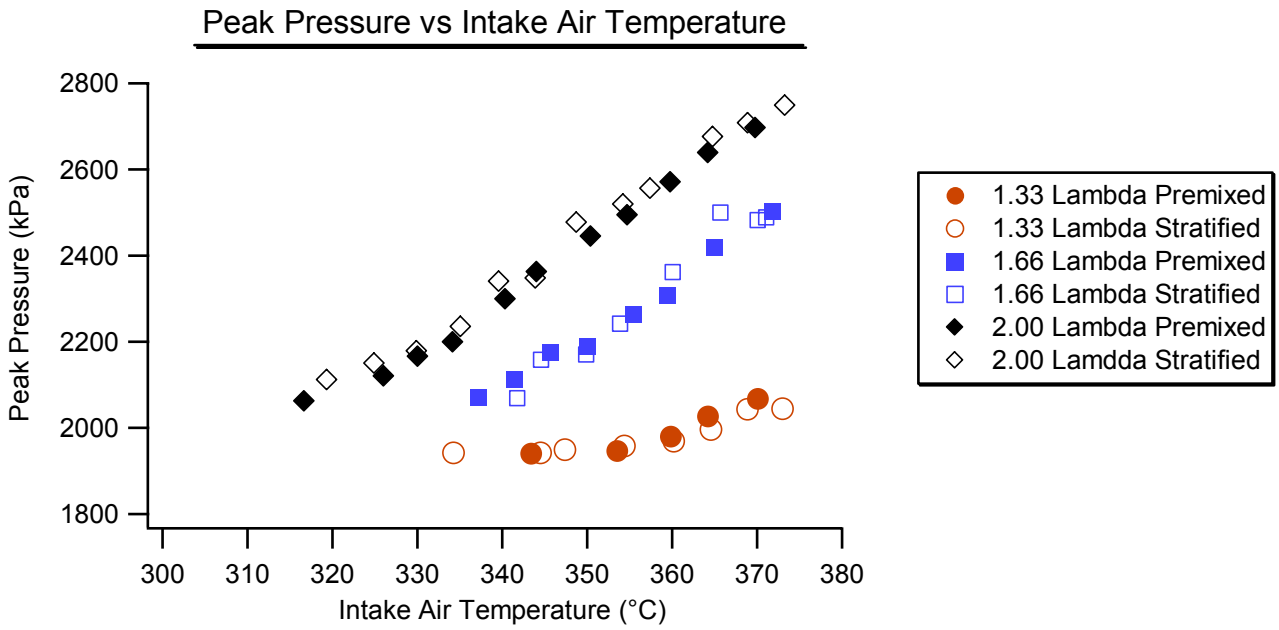

Figure 6-34 Peak pressure for constant fueling rate and variable air/fuel ratios

The plot of the variability of the combustion, Figure 6-35, indicates that increasing the air/fuel ratio decreases that rate at which the combustion variability deteriorates. It is interesting to note that for lambda values of 1.66 and 2.00 the variability is about 5% for all intake temperatures greater than 360 °C. This implies that 5-6% COV is the best that can be achieved at this fueling rate, but this value is in the range of acceptable variability for idle conditions.

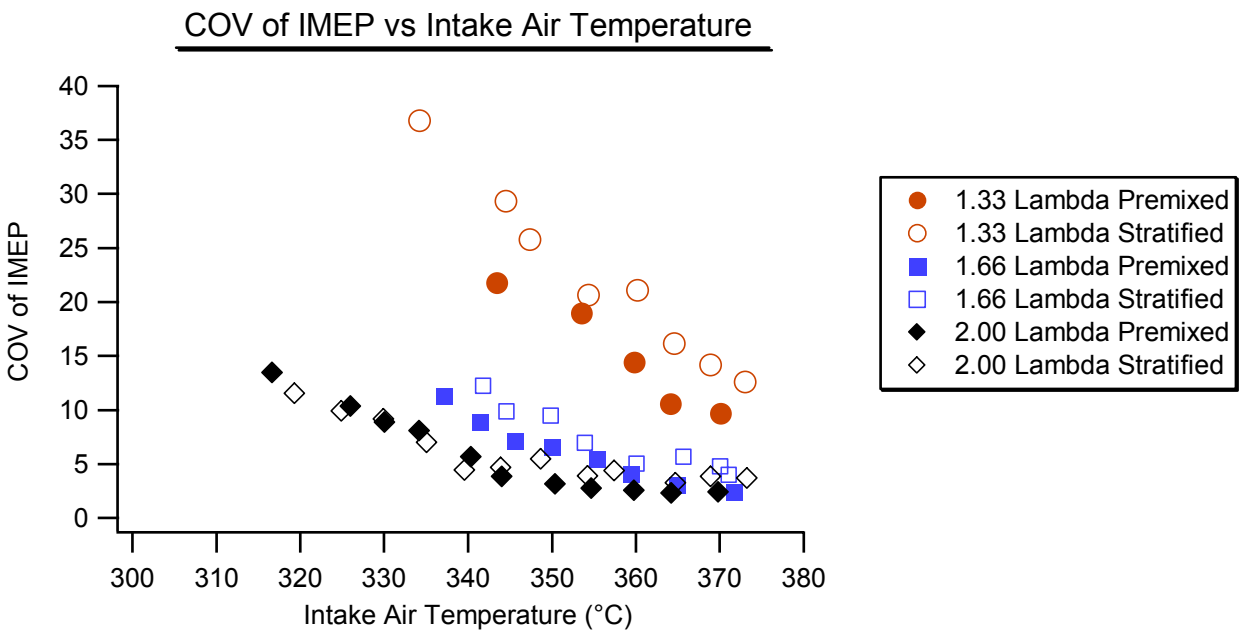

Figure 6-35 COV for constant fueling rate and variable air/fuel ratios

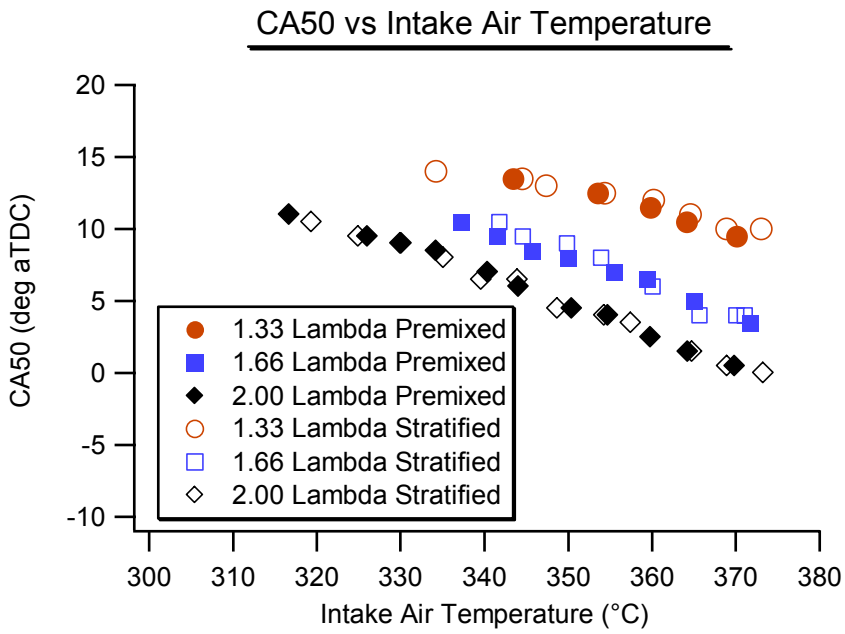

Figure 6-36 CA50 for constant fueling rate and variable air/fuel ratios

The location of the CA50 point is shown in Figure 6-36. In this plot it can be seen that for a fixed intake temperature the combustion phasing moves closer to TDC as the

mixture becomes leaner. This shift in the combustion phasing is part of the reason that the peak pressure increases for a fixed intake temperature.

Figure 6-37 shows pressure and heat release characteristics for the three air/fuel ratios for premixed and stratified fueling conditions for a fixed intake temperature of 359 °C. The stratified fueling data sets are plotted with dashed lines. This presentation again shows that as the air/fuel ratio becomes leaner the heat release rates increase and the phasing moves closer to TDC. It is also interesting to note that the stratified fueling conditions do not show any appreciable differences from the premixed fueling conditions.

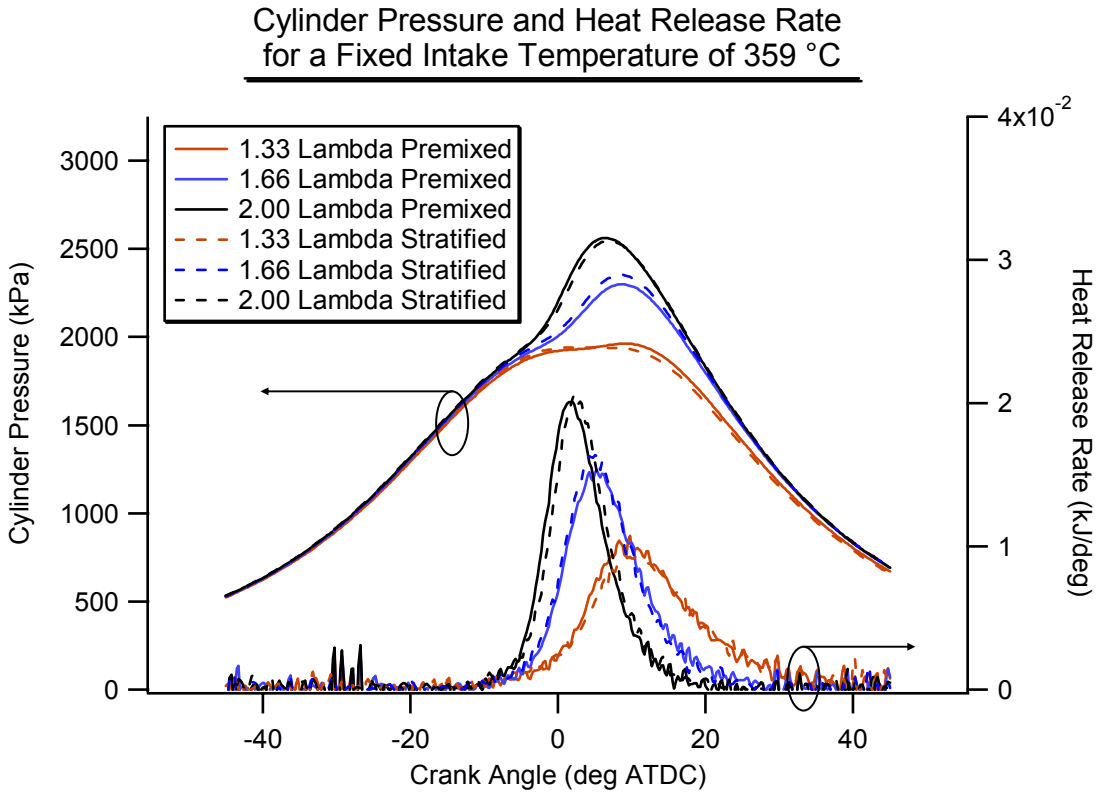

Figure 6-37 Comparison of cylinder pressure and heat release rate results for premixed and stratified fueling conditions at a fixed fueling rate of 5 mg/cycle and variable air/fuel ratios

The most significant indicator that can be used to demonstrate that the combustion has improved with leaner air/fuel ratios is the combustion efficiency, which is shown in Figure 6-38. The plot shows higher combustion efficiencies as the mixture becomes leaner. This is particularly noteworthy at the lower intake air temperatures. At intake air temperatures of approximately 360 °C the combustion efficiency for the 1.66 and 2.00 lambda air/fuel ratios approach the same value. Table 6-6 shows data of how the combustion efficiency and intake air temperatures at which the COV has deteriorated to 10% continually decreases as the value of lambda is increased. This flexibility in intake air temperature ranges for acceptable operation with increasing lambda could be very useful in trying to control HCCI.

Lambda	1.33	1.66	2.00
Temperature of 10% COV	370 °C	340 °C	325 °C
CA50 of 10% COV	9.5 deg ATDC	9.5 deg ATDC	9.5 deg ATDC
Combustion Efficiency at 10 % COV	92%	89%	86%

Table 6-6 Summary of engine behavior at idle for variable air/fuel ratios

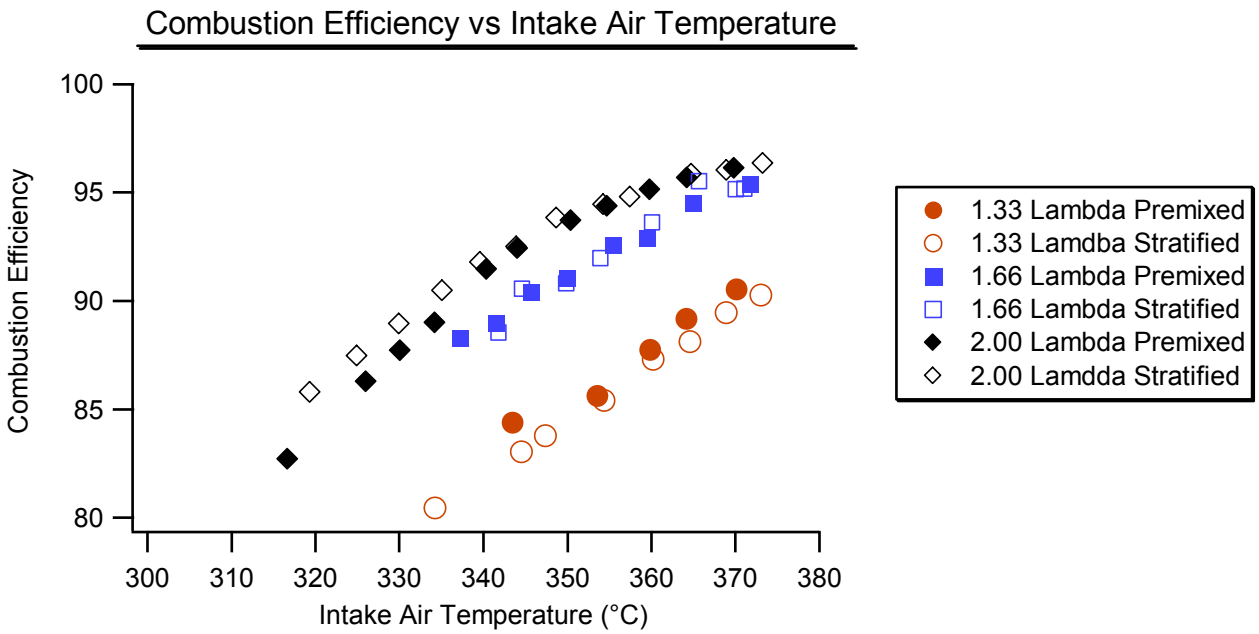

Figure 6-38 Combustion efficiency for constant fueling rate and variable air/fuel ratios

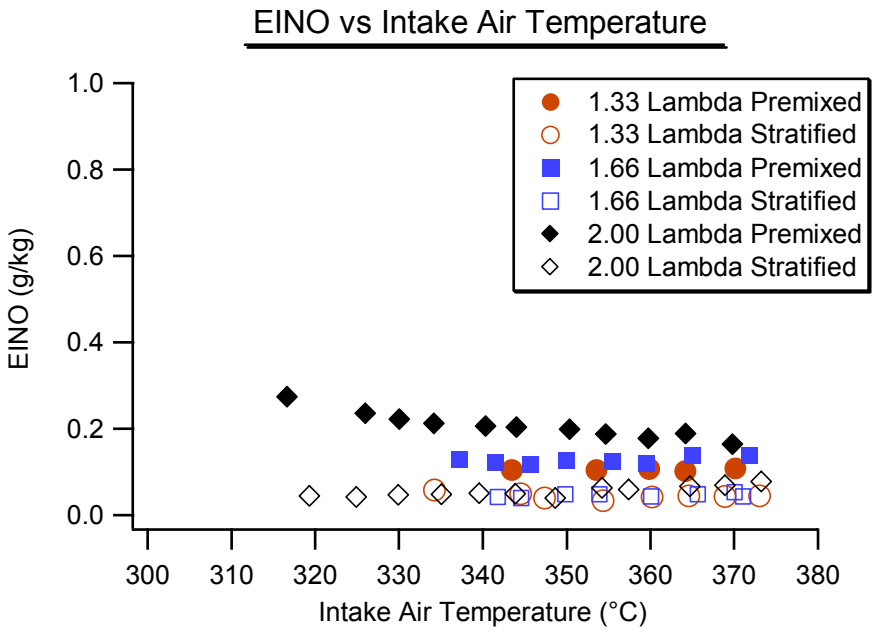

Figure 6-39 NO_x emissions for fixed fueling rate and variable air/fuel ratios

The emissions of nitrogen oxides are shown in Figure 6-39. This plot shows that for all three air/fuel ratios the engine emits no discernable amount of nitrogen oxides. These values are all within the noise limits of the detection equipment. As a result the author does not attribute any significance to the observation that the stratified fueling rates all exhibit lower NO_x emissions than the premixed operating conditions which, is contrary to all previously recorded and presented results.

One last plot of interest is that of the IVC temperature as a function of the location of CA50, which is seen in Figure 6-40. This plot clearly indicates that by increasing the air/fuel ratio manipulation of the combustion phasing can be achieved at lower IVC temperatures, which is the equivalent of lower intake air temperatures. This suggests the possibility of raising the air/fuel ratio to enable HCCI combustion at idle conditions, at intake temperatures

that are achievable using exhaust rebreathing strategies. This hypothesis has yet to be investigated though.

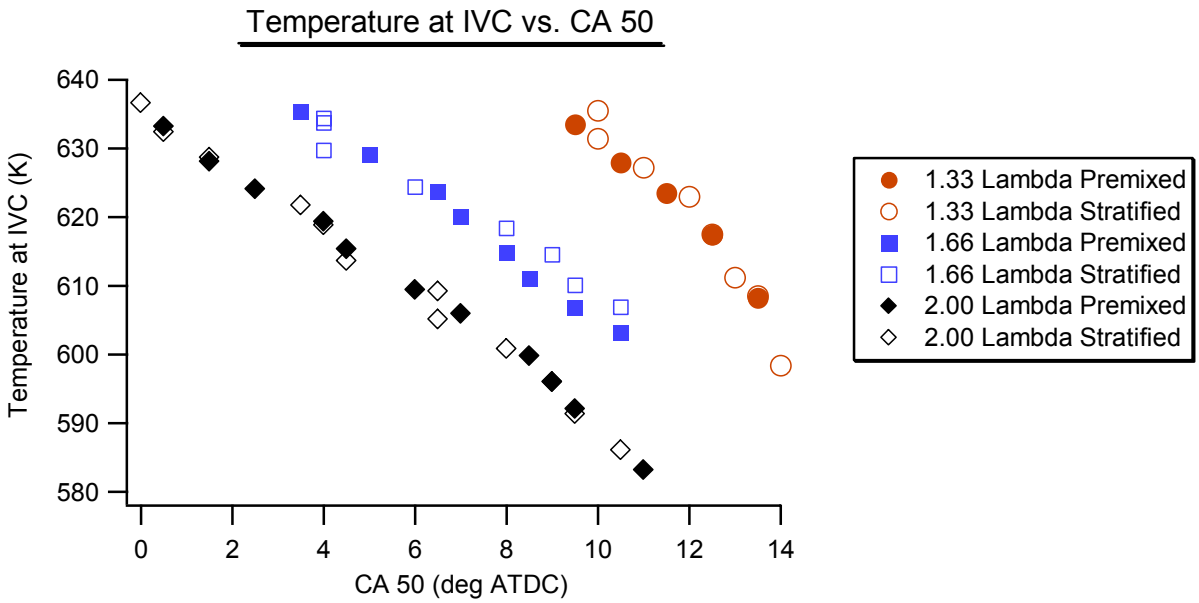

Figure 6-40 Temperature at IVC for fixed fueling rate and variable air/fuel ratios

This concludes the review of the engine's behavior when the air/fuel ratio is changed at a fixed fueling rate of 5 mg/cycle. The data demonstrates that by increasing the air/fuel ratio HCCI combustion behavior at light loads can be improved. These results, however, do not establish if this improvement could be experienced for other fueling rates, nor does it provide any solid evidence as to what physical mechanism is actually providing this improvement, these steps are left to future researchers. In terms of the original goal of the experiments, the major conclusion that can be drawn from this data is that for the port fuel injection configuration examined charge stratification does not appear to improve HCCI combustion at idle conditions, no matter what the air/fuel ratio.

6.5.3 Low Speed Tests

The last step of this experimental work was to generate some results in the standard engine at lower engine operating speeds. The experiments that will be pursued later on in the optical engine will be compared with these results to tie together the HCCI behavior of the two similar engines. Because the laser that will be used in the optical engine experiments only pulses at 10 Hz the speeds at which the engine can be run are limited to 600 or 1200 RPM. For this work it was decided to collect data at a speed lower than 1000 RPM, which meant that the engine had to be run at 600 RPM. The matrix of experimental conditions examined is described in Table 6-5.

For the lower engine operating speed it can be seen that the engine behaves in a similar manner to the way it behaved at 1000 RPM. The plot of peak pressure, Figure 6-41, shows that the stratified fueling condition still does not appear to affect the HCCI combustion. At this speed and for all operating conditions, the peak cylinder pressures are lower than they are at the speed of 1000 RPM. This is because at 600 RPM there is more time for heat transfer to occur from the gasses to the cylinder walls. Increased heat transfer lowers the charge temperatures inside the cylinder which slows down the chemical reaction rates. Lower gas temperatures also keep the gas density elevated which lowers the pressure inside the cylinder for a given volume. The increased heat transfer also caused the range of acceptable intake air temperatures to increase. The author believes the reasons for this are tied to the slower rates of reaction that result from the higher rates of heat transfer.

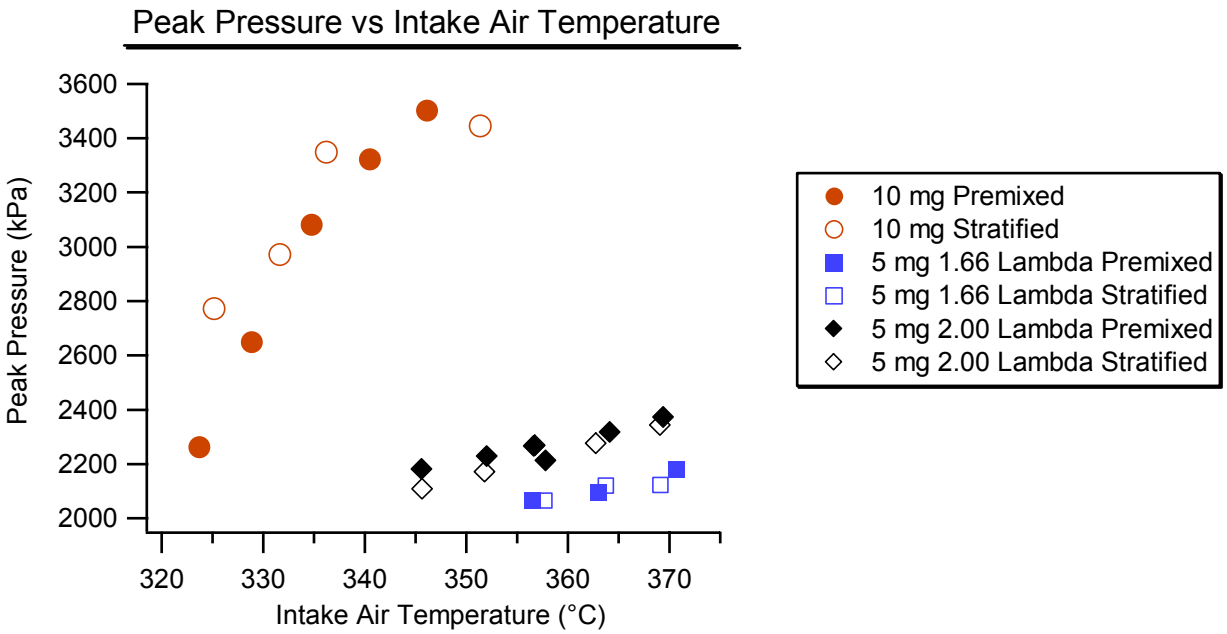

Figure 6-41 Peak pressure for 600 RPM operation at fueling rates of 10 and 5 mg/cycle

The plot of COV for this speed, Figure 6-42, shows that lower engine speeds trend towards higher combustion variability. The 10 mg/cycle fueling rate which is displayed on the right hand y-axis in this plot shows relatively low load variability over the range of intake temperatures investigated, however the COV is closer to the 3% cutoff value than it was at 1000 RPM. For a fueling rate of 5 mg/cycle the engine could not be run at a lambda of 1.33, and, even at a lambda of 1.66 the combustion variability was unacceptable, however, we still see the improvement in the combustion with a leaner air/fuel ratio.

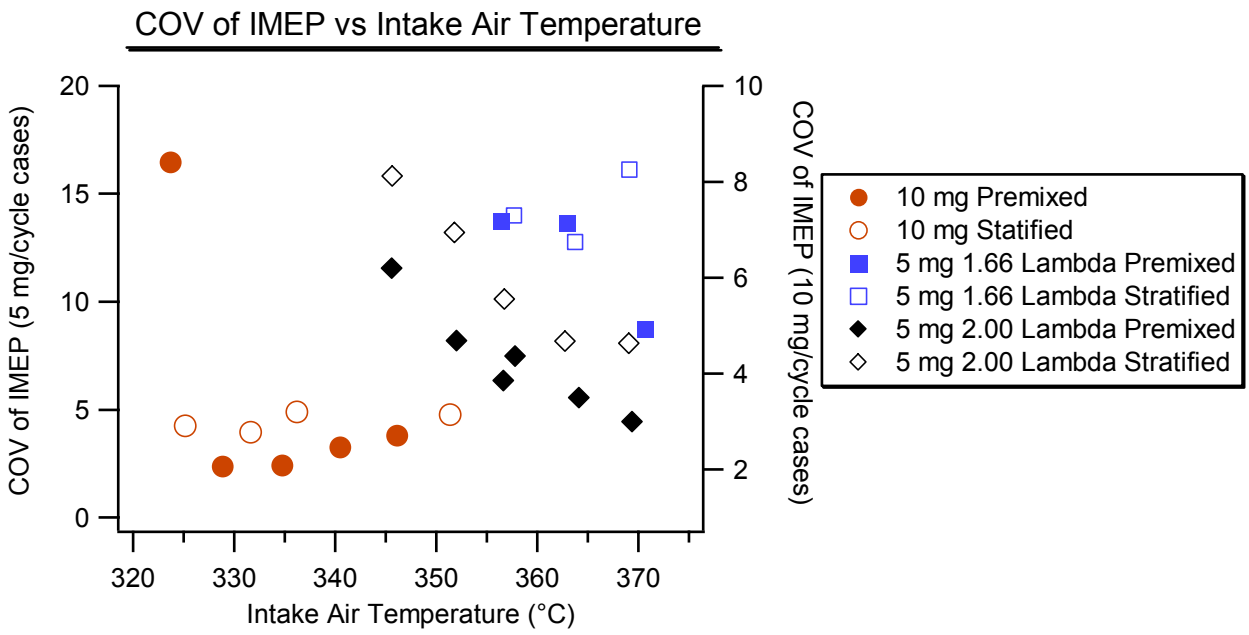

Figure 6-42 COV for 600 RPM operation at fueling rates of 10 and 5 mg/cycle

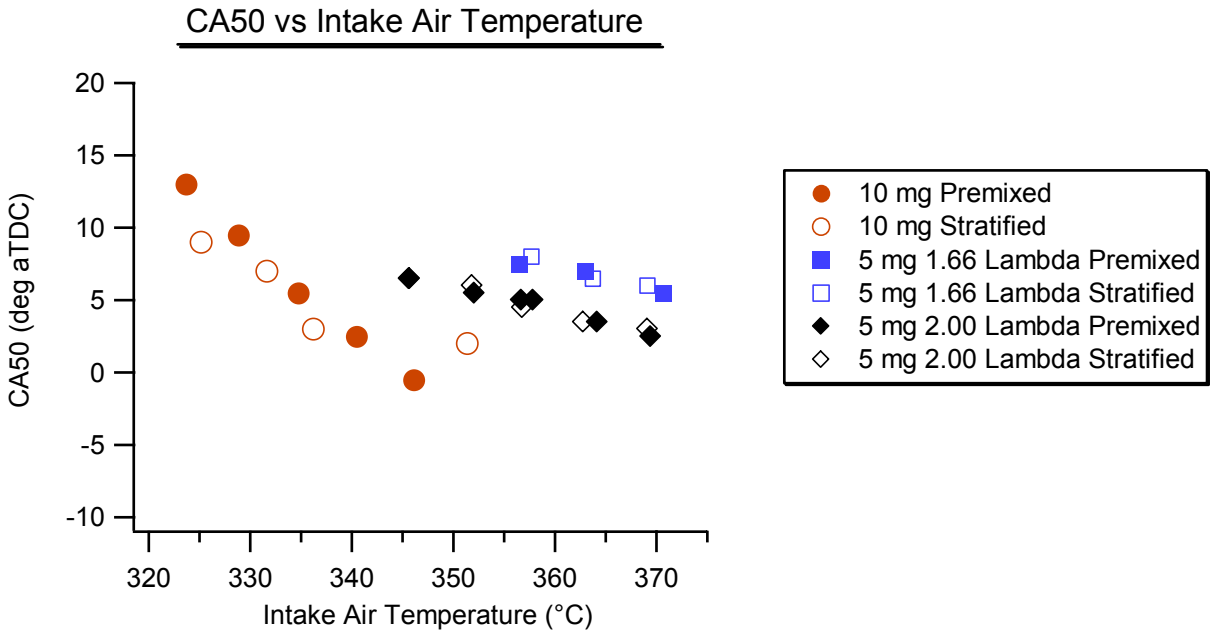

Figure 6-43 CA50 for 600 RPM operation at fueling rates of 10 and 5 mg/cycle

Figure 6-43 shows the location of the 50% burn point for the engine conditions examined. Again this plot shows similar trends to those exhibited at 1000 RPM. The 10

mg/cycle fueling rate shows more sensitivity to the change in the intake air temperature than the does 5 mg/cycle fueling rate. As was mentioned in the previous section, this is due to the increase in the thermal dilution at the fueling rate.

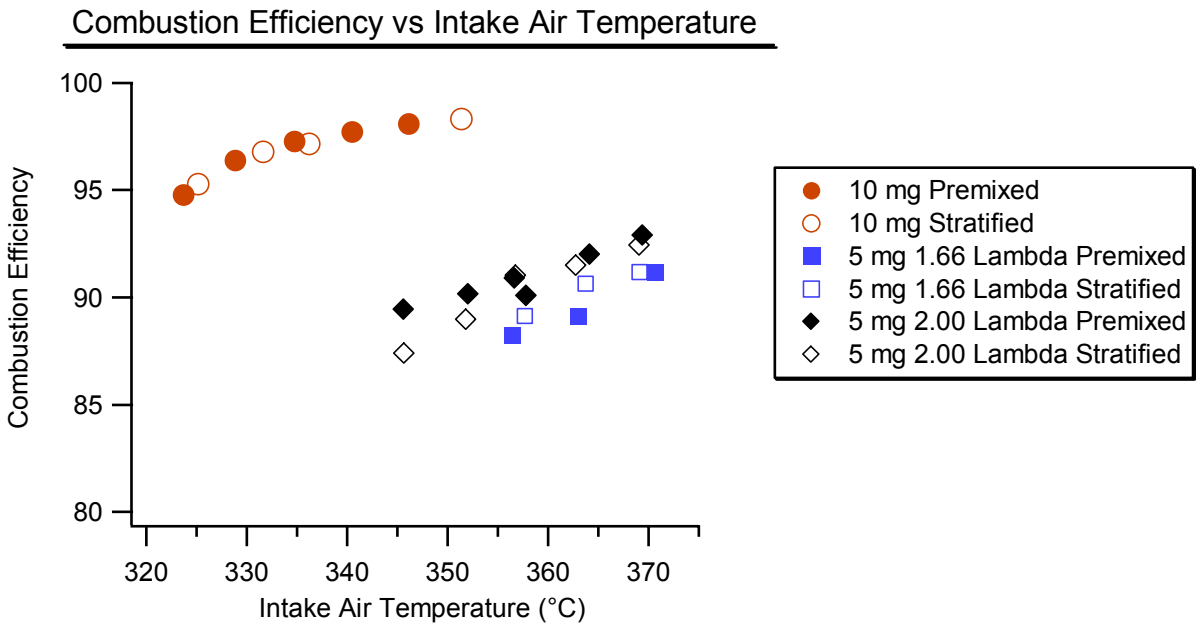

Figure 6-44 Combustion efficiency for 600 RPM operation at fueling rates of 10 and 5 mg/cycle

The combustion efficiency, which can be seen Figure 6-44, shows very little sensitivity to the mechanism of the fuel's introduction. The increase in air/fuel ratio had less of an impact upon the combustion efficiency than it did at 1000 RPM. However, there was an increase in combustion efficiency observed with higher air/fuel ratios. Therefore, increasing lambda to even higher levels might offer additional improvement in the combustion efficiency.

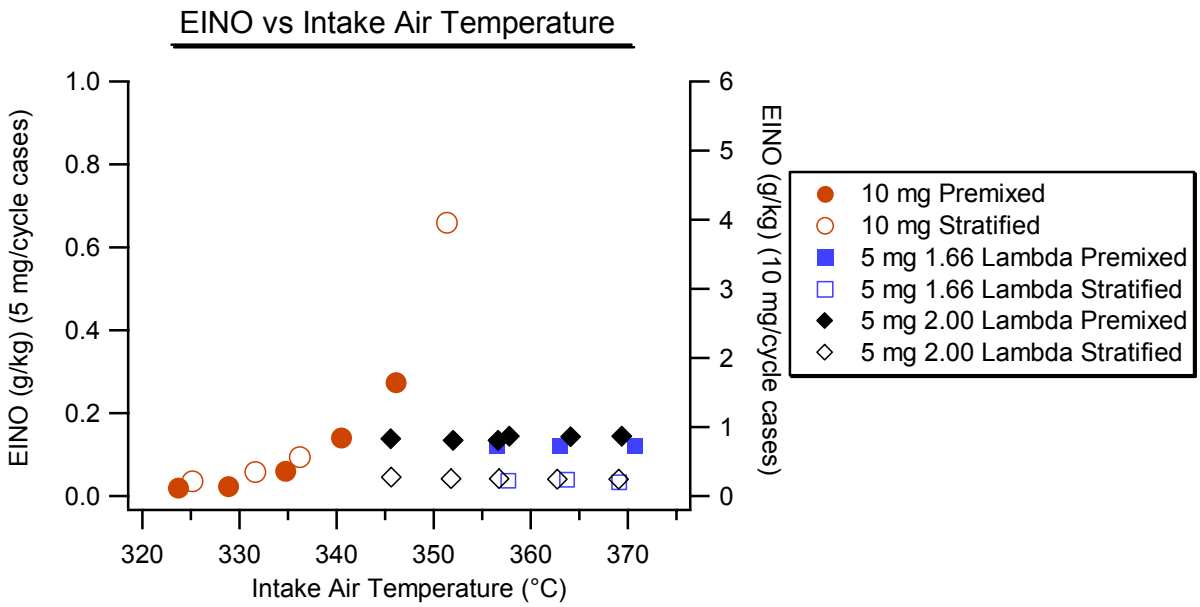

Figure 6-45 NO_x emissions for 600 RPM operation at fueling rates of 10 and 5 mg/cycle

The impact of engine speed is also noticeable in the emissions of nitrogen oxides, which can be seen in Figure 6-45. This plot is setup so that the 5 mg/cycle fueling cases are both plotted on the left hand y-axis and the 10 mg/cycle fueling cases are shown on the right hand y-axis. As happened when the engine was run at 1000 RPM, NO_x measurements for the 5 mg/cycle cases were below the resolution of our measurement devices. However, unlike the results from 1000 RPM, the 10 mg/cycle fueling rate at this speed exhibit very little difference between the stratified fueling cases and the premixed fueling cases. This could be the result of the increased time for mixing due to the slower engine speed, or it could be due to increased heat transfer lowering the cylinder temperatures. While the lower gas temperature hypothesis is interesting it is inconsistent with the magnitude of the NO_x emissions which are observed to be significant. Therefore, it is most likely that the increased mixing time is the reason that the lack of difference in the NO_x emissions for the stratified

and premixed fueling conditions. However, the data set is a little sparse. A more extensive temperature sweep would be needed to confirm this conclusion.

This concludes the review of the effects of stratified fueling on HCCI combustion when the engine is run at slower speeds. The data shows that the engine's behavior did not change at all when run with the stratified fueling system at this speed. We also see the same trends in the engine's performance at 600 RPM that were observed at 1000 RPM.

Chapter 7 - Summary and Conclusions

Section 7.1 Experimental Setup and Validation

A facility was setup and configured in order to perform HCCI research with a single cylinder four-stroke engine. In the laboratory instruments were installed to measure the composition of the exhaust gasses, record the cylinder pressure, and monitor and control the other input and output parameters for the engine.

The primary focus in this research was to study the effects of stratification in the intake charge on HCCI combustion. In this work the terms stratification includes spatial variations in the mixture, thermal gradients in the intake charge and inside the cylinder, and to a lesser extent variability in the chemical composition of the fuel. For the first configuration the engine was setup with an external fueling system. Auto-ignition is achieved through the use of external heating of the intake charge prior to compression by the piston.

One goal of the work was to separate the effects of spatial variations and the thermal gradients due to fuel evaporation, which is a concern in any direct injection HCCI experiments and study only the spatial variation effects. In order to study the effects of spatial stratification of the air and fuel as they mix two fueling systems were developed. The fuel in the stratified system was heated to the same temperature as the bulk of the intake charge in an external heating vessel and then injected into the intake near one of the intake valves while the intake valve was open. The fuel was therefore only allowed to mix with the

air for the amount of time between the end of the fuel injection and the time when the auto-ignition event occurs.

While running these experiments in a completely metal engine it was not possible to be absolutely certain of the extent of the stratification was being generated in the intake charge. The results of the experiments performed with this setup can be used to infer that stratification is being generated, but this inference still needs to be visually verified. To that end, an optically accessible engine has been designed, constructed, and installed in the laboratory. This engine will be used to evaluate if gradients in the fuel distribution actually exist in the cylinder at the onset of combustion, and how large these gradients actually are.

Initial operation of the engine, mapped the characteristics of HCCI operation for the current laboratory configuration. This initial work also defined the limits of repeatability of the results and the controllers. The work showed that, at a given speed and load condition, HCCI combustion had a narrow window of intake air temperatures over which acceptable combustion could be achieved. At the intake temperatures near the lower end of the operating window the combustion showed large amounts of variability and unacceptably high emissions of CO and unburned hydrocarbons. As the intake temperature increased the combustion became more stable and the phasing shifted towards TDC. The high temperature operating conditions were characterized by CO emissions near 15 g/kg_{fuel} and HC emissions of approximately 20 g/kg_{fuel} and also relatively high NO_x emissions around 3 g/kg_{fuel}.

The results all showed good repeatability with the exception of the IMEP data which was observed to be sensitive to slight changes in the polytropic coefficient of expansion. Because the IMEP data was not representative of the repeatability observed in the other parameters of the system it was primarily ignored in the analysis performed on the rest of the

data collected in this research. The controlled parameters of fuel flow rate, intake manifold pressure, air flow rate, coolant temperature and oil temperature all showed repeatability within a level of ±1% or better. This work validated that the experimental setup was operating well and gave a high level of confidence in the validity of the results that were obtained in the experiments.

Section 7.2 Sensitivity to Intake Charge Heating

The first experiment performed in the laboratory, after the validation of the setup, was an investigation of the effects of heating the intake charge on premixed charge combustion. There was concern that the long residence time of the fuel in the intake system (approximately 9 seconds) and the high temperatures of the charge (greater than 500 K) would cause the fuel to react while still in the intake system.

This concern was investigated by establishing two separately controlled heating sections in the intake system. The first heating section was the surge tank just before the intake runner which could be heated to any desired temperature. The second heating section was the intake runner leading to the cylinder; this area could be cooled or heated to any temperature within a window of 50 degrees below to 20 degrees above the temperature of the gasses in the upstream surge tank. The tests were conducted for three different fuels, an 87 octane primary reference fuel blend, a 92.5 octane ((R+M)/2) reference gasoline, and pure isooctane.

Through operation of the engine it was demonstrated that the final engine inlet temperature required to achieve acceptable HCCI combustion could be reduced by increasing the temperature of the gasses in the heating chamber upstream of the runner. As the

temperature leaving the heating plenum in the surge tank increased the intake charge had to be cooled prior to entering the cylinder, in order to maintain a constant combustion phasing point. This result was true for both the PRF87 fuel and the reference gasoline. However, when fueling the engine with isooctane there was no sensitivity whatsoever to the temperature of the gasses in the heating plenum. To maintain the desired combustion phasing for the PRF87 fuel the temperature at the engine inlet had to be reduced by 10 °C for an increase of the plenum temperature of just 5 °C.

G.C. Mass Spec measurements of the intake gasses were taken to determine the composition of the intake charge. The results showed that when the engine was fueled with a PRF87 mixture there were a number of oxygenated compounds present in the intake charge, these included species such a propanal, 2-propenal, butanal, and butanone. As the temperature of the gasses in the heating plenum was increased, the concentrations of the oxygenated species increased, however the change was not particularly large. The G.C. Mass Spec results from the isooctane data did not demonstrate any significant change in the composition of the mixture with increases in the heating plenum temperature, nor were any of the oxygenated compounds listed above detected.

The mechanisms that generate the oxygenated species in the intake plenum are currently unknown. However, the main point of these results is not that the intake charge is observed to react at low temperatures and pressures, however, it is a concern that must be kept in mind. Nor is it to explain the mechanisms through which the intake charge reacts or to identify the dominate reactions taking place. The important point that should be taken from this work is that HCCI combustion can be operated in a very large window of intake temperatures by manipulating the composition of the intake charge.

Section 7.3 Air/Fuel Stratification

An investigation was performed into what effects varying levels of fuel and air mixedness in the intake charge would have on HCCI combustion. The gaseous fuel injector was and a specially designed fuel introduction system was used to generate a stratified mixture of air and fuel. By manipulating the timing of the fuel injection we attempted to generate different levels of stratification, inside the cylinder. The goal of these experiments was to determine if the performance of an HCCI engine could be altered by manipulating the level of mixedness of the fuel. As such, the goal was to establish this air/fuel stratification without generating any thermal gradients due to fuel evaporation inside the cylinder.

It turned out that in the initial design of the stratified injection system, the fuel temperature could not be controlled to the desired value, this lead to thermal stratification inside the cylinder. At the fueling rate chosen for this experiment, the coupling of the two stratification types was shown to alter the intake temperature windows over which HCCI combustion was achievable. The results showed that for a given combustion efficiency value, as the mixing time was decreased, the engine emitted increasingly higher amounts of NO_x and CO. The results also demonstrated that the amount of mixing time available influenced the initial charge temperature requirement.

Measurements were taken of the temperature of the fuel as it exited the hypodermic tube attached to the stratified injector adaptor block. It was determined that the typical engine operating conditions, the fuel was exiting the injector between 40 and 60 °C below the temperature of the bulk air. Mixing of the fuel and the air was calculated to generate a mixture with a temperature about 10 °C lower than the initial temperature of the bulk air.

In order to bring the two streams to the same temperature, the hypodermic tube was redesigned to allow more heat transfer from the bulk air to the fuel stream. With the modified fuel introduction system the heat was transferred from the bulk air stream to the fuel traveling in the hypodermic tube, additional thermal energy was added to the bulk air in the runner with heater strips wrapped around the runner. This maintained all of the gasses in the intake at approximately the same temperature. Measurements of the temperature of the fuel jet as it exited the modified stratified fueling system showed that this new design functioned very well.

An investigation into the operating characteristics of a stratified fueled HCCI engine with no thermal stratification showed that the combustion was achieved over the same range of intake air temperatures for most of the investigated injection timings. The results also showed that the combustion was generally the same for all levels of stratification investigated. The only major stratification induced effect, observed on the combustion was that as injection timing moved closer to TDC, the engine emitted higher amounts of nitrogen oxides and carbon monoxide. The initial conclusion is that for the fueling rate and speed chosen for this investigation, and the amount of stratification generated in the cylinder, the effects were not significant.

A series of tests were also conducted to observe if changing the fueling rate, the speed, or the air/fuel ratio would produce operating regimes where stratification of the intake charge would produce significant and observable effects on the combustion. The results of these experiments did not show any operating condition where stratification could be judged to have a significant impact on the combustion. However, it was observed that increasing the air/fuel ratio for a low fueling rate did improve the combustion. The higher air/fuel ratios

widened the window of acceptable intake air temperatures, and lowered the amount of COV when the combustion efficiency reached lower values.

Section 7.4 Recommendations for Future Research

The results of this work bring about more questions than they answer. This served as a problem in defining at what point exactly this research should end. It is always tempting to look at just one more operating point or to try one more method to get additional results or to clarify older work. This section outlines aspects of the results presented in this thesis that warrant further investigation. It also notes a few investigations that were originally planned at the start of this work.

7.4.1 Fuel Degradation

Studying the effects of the fuel degradation in the intake would be very interesting to continue investigating. G.C. Mass Spec data could be taken for conditions where the fuel used is a full boiling range reference gasoline. It would be interesting to see what species are generated with such a fuel and how they change with upstream heating temperatures and how the species compare with the results from the PRF87 experiments. Also G.C. Mass Spec data could be taken for the exhaust gas composition for each fuel type in order to determine absolutely, which hydrocarbon species leave the engine as unburned hydrocarbons. These results would make analysis of the changes affected in the intake system easier.

Noting the influence that leaner air/fuel ratios had in the stratified fueling experiments is would be useful to see if upstream heating has a different effect on the combustion at other

air/fuel ratios. It would be interesting to observe both leaner and richer air/fuel ratios to see at what air/fuel ratio the largest shifts in the intake air temperature could be achieved.

An investigation could also be performed with a fuel that contained larger fraction of easily isomerized molecules such as a PRF50. If a better method of cooling the gas prior to entering the engine were incorporated in the intake system it would be interesting to see just how low the final intake air temperature can be driven for even higher upstream temperatures.

It would also be useful to try to perform a series of experiments where the radicals observed in the GC Mass Spec experiments are added to the intake system individually. This could allow us to see which of the species are actually advancing the combustion phasing. This experiment is difficult to perform since most of the species observed in the G.C. Mass Spec results are not stable species.

7.4.2 Stratification

The effects of stratification have been fairly well documented; however, there are a couple of points that could be investigated for the purposes of completeness. The most important point here is an investigation of any effects that would be generated at higher engine speeds. At higher engine speeds, the time available for mixing would be less than with the engine speeds investigated in this work. It may be that, at higher speeds, stratification could be observed to be more significant or the existence of turbulent mixing could cancel out the short mixing time. The speeds that should be looked at are 1200 RPM,

in order to give another measurement point for the optical engine, and 2000 RPM to get the full benefit of less fuel mixing time.

The other issue that could be explored is the sensitivity of the combustion to leaner air/fuel ratios. This investigation could be performed for the 1000 RPM 10 mg/cycle condition to see if the operating window can be improved at this condition as well. Also at the 5 mg/cycle operating condition the air/fuel ratio could be increased further to see if the improvement in the combustion continues, and if there is a limit to how much the combustion can be improved. Hopefully, this investigation would shed more light on why increasing the air/fuel ratio actually improves the combustion in a setup that already has more than enough oxygen for complete reaction.

7.4.3 Other Research Ideas

The primary focus of the upcoming HCCI research in this facility will focus on obtaining results from the optical engine. This work is important in order to quantify the extent to which stratification was achieved and maintained throughout the combustion process during the research presented in this thesis. The optical work should be able to show where the locally rich and locally lean zones exist in the cylinder and where the combustion is initiated in relation to these zones. This work should also enable us to track the temperature gradients in the cylinder and try to identify the areas of the cylinder where the larger amounts of NO_x are being generated.

At the time of the writing of this thesis the optical engine had been installed in the laboratory, all of the basic setup had been performed and the engine has been run, but no

optical data had been collected. The majority of the physical setup, plumbing, and wiring of this engine are the same as the setup described in this thesis, however, alterations will have to be made to the setup in order to perform the optical experiments. While the design as well as the installation, of the engine was performed as part of this work, the documentation of the setup and configuration, as well as the design of the engine will be documented in the PhD thesis of Randy Herold where it is more applicable to the research conducted.

Down the road there are a number of ways that the research can be branched and still continue to investigate the effects of variations in the intake charge on HCCI combustion. One of these steps is to begin investigating thermal stratification in the intake. The preliminary results, seen in this work, indicate that this type of stratification is where the largest effects on HCCI combustion are going to be observed. The results of this work suggest that the only requirement for successful HCCI combustion is that the fuel be at the right temperature for auto-ignition. This implies that if the fuel can be brought to the appropriate temperature the rest of the gasses do not need to be at such elevated temperatures. This is something that it may be worth investigating, however, achieving such a state practically will not be easy.

Bibliography

1. Sher, E., Handbook of Air Pollutions from Internal Combustion Engines - Pollution Formation and Control. First ed. 1998, Chestnut Hill, MA: Academic Press.
2. United States Environmental Protection Agency - Office of Mobile Sources, Regulatory Impact Analysis - Control of Air Pollution from New Motor Vehicles - Tier 2 Motor Vehicle Emissions Standards and Gasoline Sulfur Control Requirements, 1999.
3. Heywood, J.B., Internal Combustion Engine Fundamentals. First ed. 1988, New York, New York: McGraw-Hill.
4. Noguchi, M., Y. Tanaka, T. Tamka, and Y. Takeuchi. "A Study on Gasoline Engine Combustion by Observation of Intermediate Reactive Products During Combustion", SAE Paper 790840, 1979.
5. Najt, P.M. and D.E. Foster. "Compression Ignition Homogeneous Charge Combustion", SAE Paper 830264, 1983.
6. Amano, T., S. Morimoto, and Y. Kawabata. "Modeling of the Effect of Air/Fuel Ratio and Temperature Distribution on HCCI Engines", SAE Paper 2001-01-1024, 2001.
7. Noda, T. and D.E. Foster. "A Numerical Study to Control Combustion Duration of Hydrogen-Fueled HCCI by Using Multi-Zone Chemical Kinetics Simulation", SAE Paper 2001-01-0250, 2001.
8. Christensen, M., B. Johansson, and P. Einewall. "Homogeneous Charge Compression Ignition (HCCI) using Isooctane, Ethanol and Natural Gas - A Comparison with Spark Ignition", SAE Paper 972874, 1997.
9. Thring, R.H. "Homogeneous Charge Compression Ignition", SAE Paper 892068, 1989.
10. Turns, S.R., An Introduction to Combustion: Concepts and Applications. Second ed. 1996, Boston, Massachusets: McGraw Hill.
11. Kotz, J.C. and J. Paul Treichel, Chemistry & Chemical Reactivity. Third Edition ed. 1996, Fort Worth, TX: Saunders College Publishing.
12. Aroonsrisopon, T., An Experimental Investigation of Homogeneous Charge Compression Ignition Operating Range and Engine Performance with Different Fuels, Masters Thesis, University of Wisconsin - Madison, 2002.
13. Radkiewicz, J., *Designation of Carbon Atom Types*, in *Chem 307: Organic chemistry for Majors*. 2001: Norfolk, Virginia.
14. Westbrook, C.K., W.J. Pitz, and W.R. Leppard. "The Auto-Ignition Chemistry of Paraffinic Fuels and Pro-Knock and Anti-Knock Additives - A Detailed Chemical Kinetics Study", SAE Paper 912314, 1991.
15. Milovanovic, N. and R. Chen. "A Review of Experimental and Simulation Studies on Controlled Auto-Ignition Combustion", SAE Paper 2001-01-1890, 2001.
16. Westbrook, C.K. "Chemical Kinetics of Hydrocarbon Ignition in Practical Combustion Systems", Twenty-Eighth International Symposium on Combustion, 2000. Edinburgh, Scotland: The Combustion Institute.

17. Najt, P.M., Compression Ignition Homogeneous Charge Combustion, Masters Thesis, University of Wisconsin - Madison, 1981.
18. Ciajolo, A. and A. D'Anna, "Controlling Steps in the Low-Temperature Oxidations of n-Heptane and Isooctane", in Combustion and Flame, The Combustion Institute. 1998, Elsevier Science Inc. p. 617-622.
19. Sohm, V., S.-C. Kong, and D.E. Foster. "A Computational Investigation into the Cool Flame Region in HCCI Combustion", SAE Paper 2004-01-0552, 2004.
20. Sanders, S.T., T. Kim, and J.B. Ghandhi. "Gas Temperature Measurements During Ignition in an HCCI Engine", SAE Paper 2003-01-0744, 2003.
21. Hultqvist, A., M. Christensen, B. Johansson, A. Franke, M. Richter, and M. Alden. "A Study of Homogeneous Charge Compression Ignition Combustion Process by Chemiluminescence Imaging", SAE Paper 1999-01-3680, 1999.
22. Willand, J., R.G. Nieberding, G. Vent, and C. Enderle. "The Knocking Syndrome - Its Cure and Its Potential", SAE Paper 982483, 1998.
23. Onishi, S., S.H. Jo, K. Shoda, P.O. Jo, and S. Kato. "Active Thermo Atmosphere Combustion - A New Combustion Process for Internal Combustion Engines", SAE Paper 790501, 1979.
24. Law, D., J. Allen, and R. Chen. "On the Mechanisms of Controlled Auto-Ignition", SAE Paper 2002-01-0421, 2002.
25. Aoyama, T., Y. Hattori, J.i. Mizuta, and Y. Sato. "An Experimental Study on Premixed-Charge Compression Ignition Gasoline Engine", SAE Paper 960081, 1996.
26. Dec, J.E. and M. Sjoberg. "A Parametric Study of HCCI Combustion - The Sources of Emissions at Low Loads and the Effects of GDI Fuel Injection", SAE Paper 2003-01-0752, 2003.
27. Aroonsrisopon, T., P. Werner, J.O. Waldman, V. Sohm, D.E. Foster, T. Morikawa, and M. Iida. "Expanding the HCCI Operation with the Charge Stratification", SAE Paper 2004-01-1756, 2004.
28. Stanglmaier, R.H. and C.E. Roberts. "Homogeneous Charge Compression Ignition (HCCI): Benefits, Compromises, and Future Engine Application", SAE Paper 1999-01-3682, 1999.
29. Epping, K., S.M. Aceves, R. Bechtold, and J.E. Dec. "The Potential of HCCI Combustion for High Efficiency and Low Emissions", SAE Paper 2002-01-1923, 2002.
30. Chen, R., J.W.G. Turner, and D.W. Blundell. "The Transition Between Controlled Auto Ignition and Spark Ignition", SAE Paper 2004-01-0939, 2004.
31. Aceves, S.M., D.L. Flowers, C.K. Westbrook, J.R. Smith, W.J. Pitz, R.W. Dibble, M. Christensen, and B. Johansson. "A Multi-Zone Model for Prediction of HCCI Combustion and Emissions", SAE Paper 2000-01-0327, 2000.
32. Christensen, M., A. Hultqvist, and B. Johansson. "Demonstrating the Multi Fuel Capability of a Homogeneous Charge Compression Ignition Engine with Variable Compression Ratio", 1999-01-3679, 1999.
33. Iida, M., T. Aroonsrisopon, D.E. Foster, and J. Martin. "The Effect of Intake Air Temperature, Compression Ratio, and Coolant Temperature on the Start of Heat Release in an HCCI (Homogeneous Charge Compression Ignition) Engine", SAE Paper 2001-01-1880, 2001.

34. Eng, J.A. "Characterization of Pressure Waves in HCCI Combustion", SAE Paper 2002-01-2859, 2002.
35. Bradley, D., C. Morley, X.J. Gu, and D.R. Emerson. "Amplified Pressure Waves During Auto-ignition: Relevance to CAI Engines", SAE Paper 2002-01-2868, 2002.
36. Christensen, M., B. Johansson, P. Amneus, and F. Mauss. "Supercharged Homogeneous Charge Compression Ignition." SAE Paper 980787, 1998.
37. Law, D., D. Kemp, J. Allen, G. Kirkpatrick, and T. Copland. "Controlled Combustion in an IC-Engine with a Fully Variable Valve Train", SAE Paper 2000-01-0251, 2000.
38. Kontarakis, G., N. Collings, and T. Ma. "Demonstration of HCCI Using a Single Cylinder Four-Stroke SI Engine with Modified Valve Timing", SAE Paper 2000-2870, 2000.
39. Kaahaaina, N.B., A.J. Simon, P.A. Caton, and C.F. Edwards. "Use of Dynamic Valving to Achieve Residual-Affected Combustion", SAE Paper 2001-01-0549, 2001.
40. Agrell, F., H.E. Angstrom, B. Eriksson, J. Wikander, and J. Linderyd. "Integrated Simulation and Engine Test of Closed Loop HCCI Control by Aid of Variable Valve Timing", SAE Paper 2003-01-0748, 2003.
41. Chen, R., N. Milovanovic, J. Turner, and D.W. Blundell. "The Thermal Effect of Internal Exhaust Gas Recirculation on Controlled Auto-Ignition", SAE Paper 2003-01-0751, 2003.
42. Girard, J.W., R.W. Dibble, D.L. Flowers, and S.M. Aceves. "An Investigation into the Effect of Fuel-Air Mixedness on the Emissions from an HCCI Engine", SAE Paper 2002-01-1758, 2002.
43. Richter, M., J. Engstrom, A. Franke, M. Alden, A. Hultqvist, and B. Johansson. "The Influence of Charge Inhomogeneity on the HCCI Combustion Process", SAE Paper 2000-01-2868, 2000.
44. Marriott, C.D. and R.D. Reitz. "Experimental Investigation of Direct Injection-Gasoline for Premixed Charge - Compression Ignited Combustion Phasing Control", SAE Paper 2002-01-0418, 2002.
45. DyneSystems Co., Dyn-Loc IV: User's Manual, 2001.
46. Stivender, D.L. "Development of a Fuel-Based Mass Emission Measurement Procedure", SAE Paper 710604, 1971.
47. DSP Technology, Redline ACAP User Manual, 1995.
48. Lancaster, D.R., R.B. Krieger, and J.H. Lienesch. "Measurement and Analysis of Engine Pressure Data", SAE Paper 750026, 1975.

Appendix A Supplemental Graphs

Section A.1 Engine Behavior as a Function of Combustion Efficiency

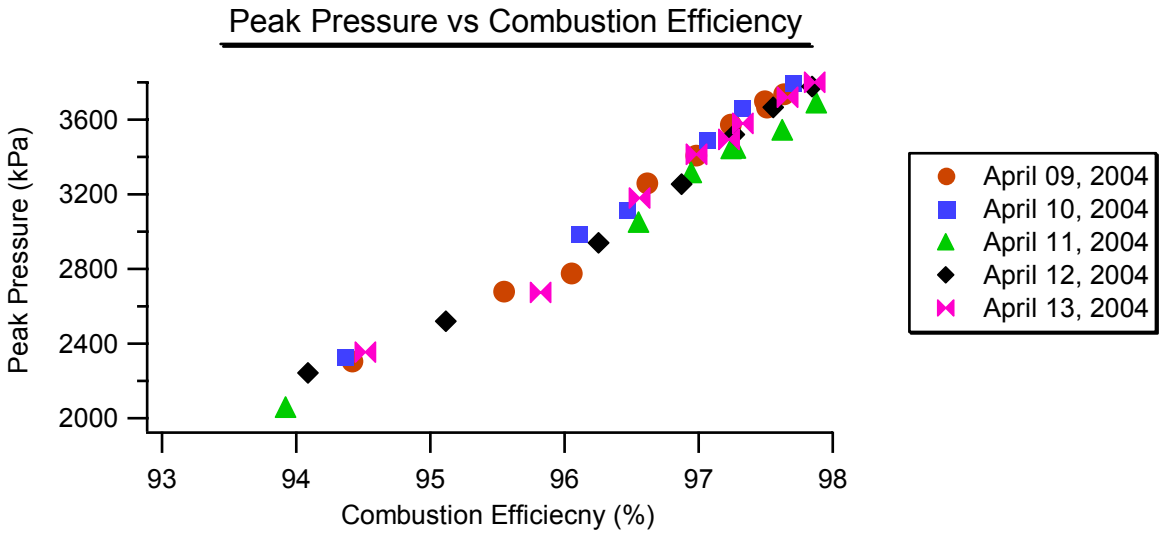

Figure A-1 Peak pressure vs. combustion efficiency

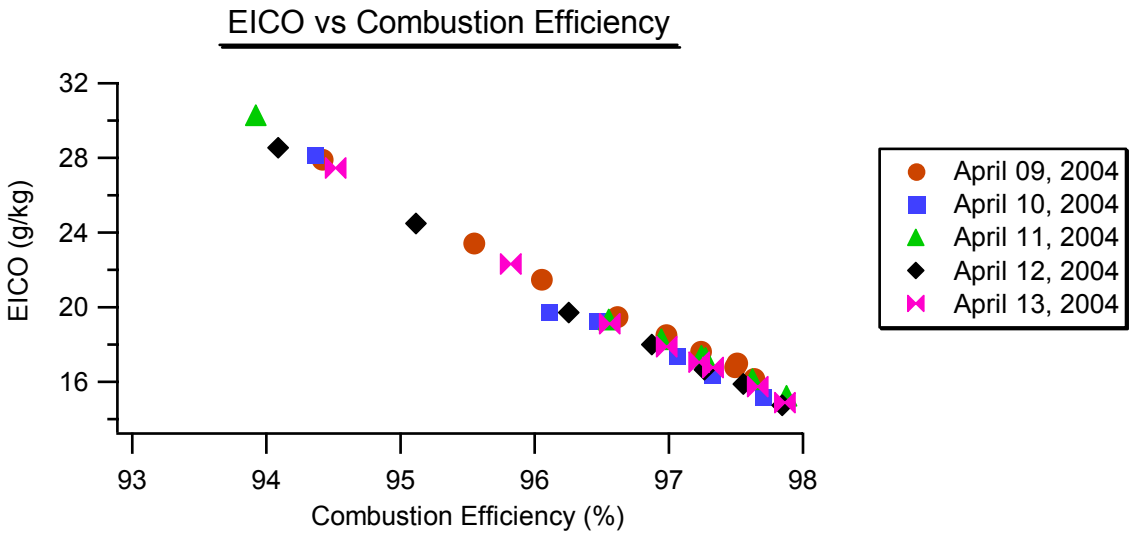

Figure A-2 Carbon monoxide emissions vs. combustion efficiency

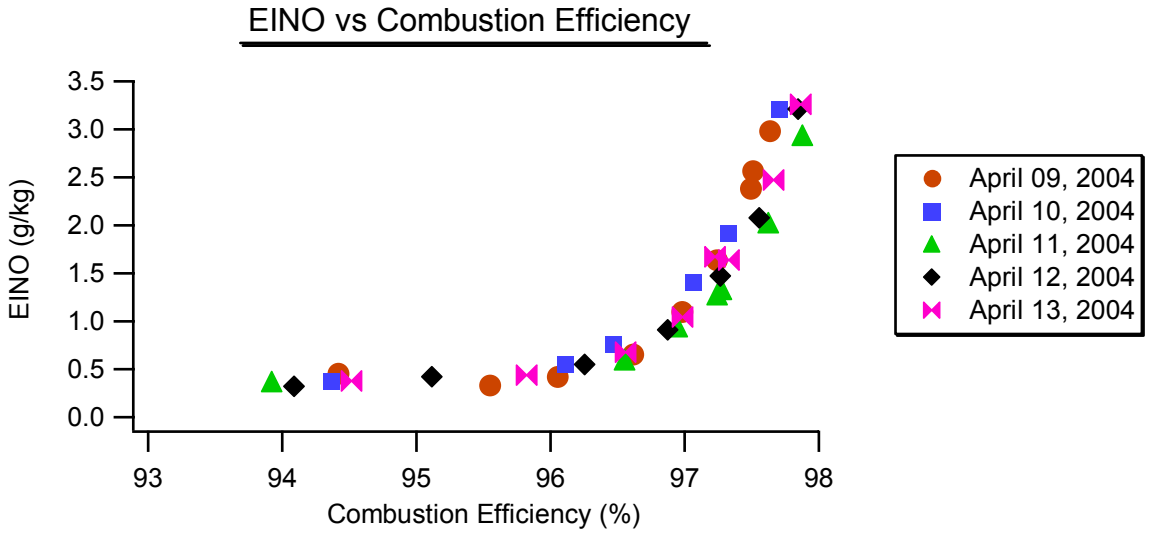

Figure A-3 NO_x emissions vs. combustion efficiency

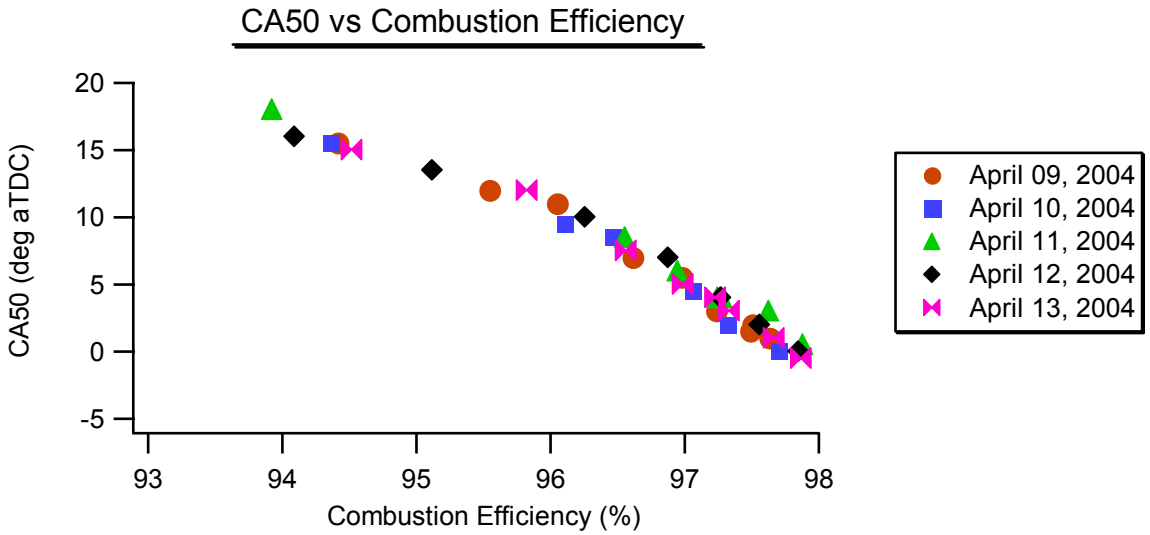

Figure A-4 CA50 vs. combustion efficiency

Section A.2 Comparison of Injector Tip Configurations for Stratified Injector System with Thermal Stratification

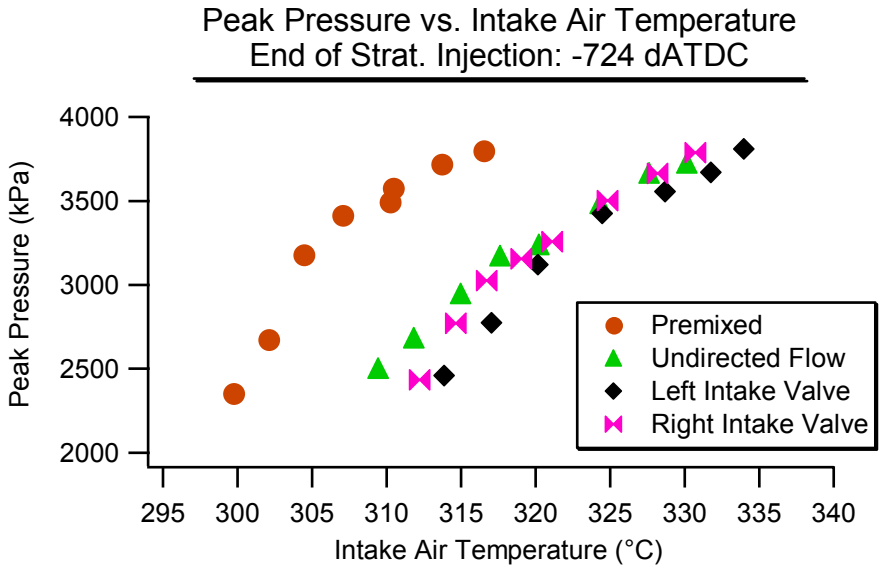

Figure A-5 Tip comparison: peak pressures for stratified EOI = -724 dATDC

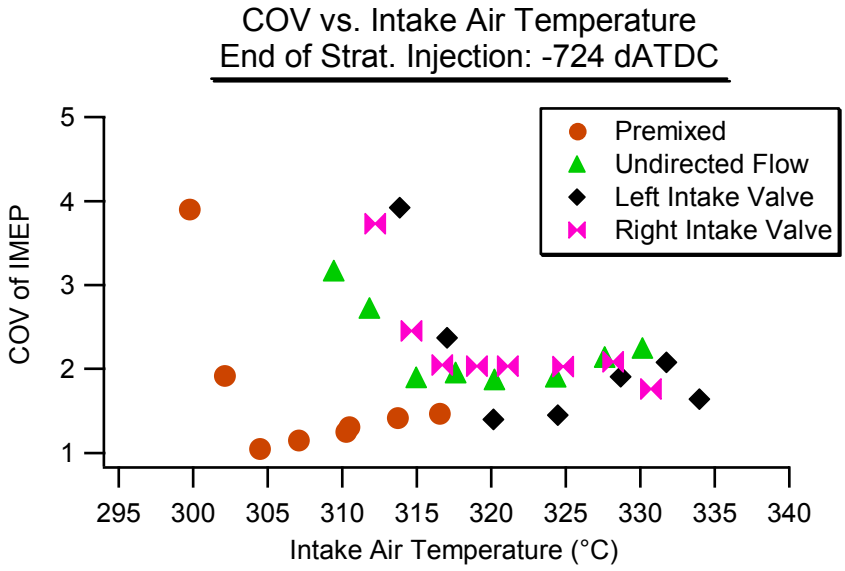

Figure A-6 Tip comparison: COV for stratified EOI = -724 dATDC

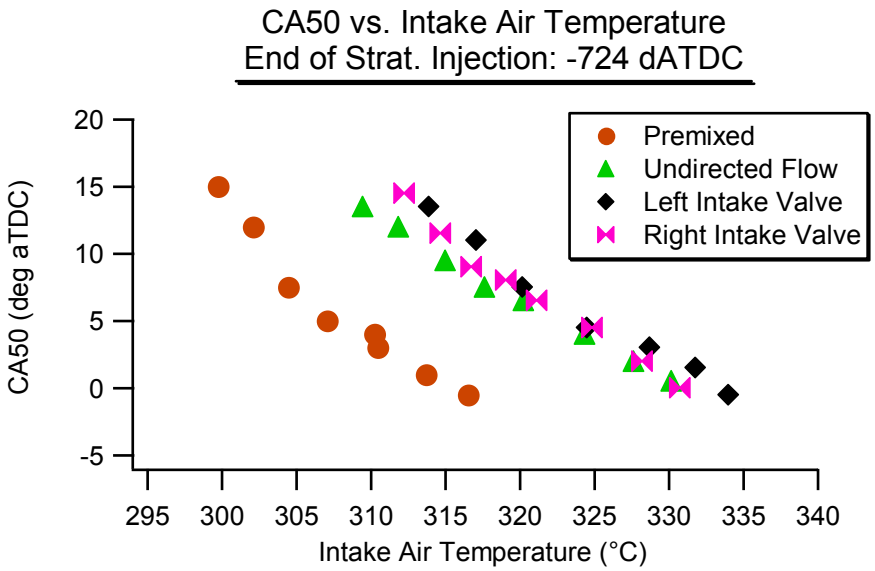

Figure A-7 Tip comparison: CA50 for stratified EOI = -724 dATDC

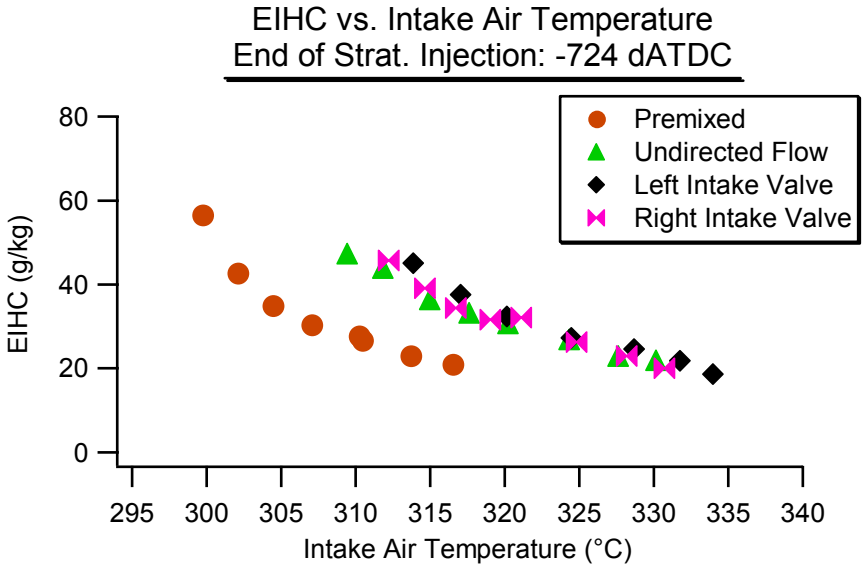

Figure A-8 Tip comparison: EIHC for stratified EOI = -724 dATDC

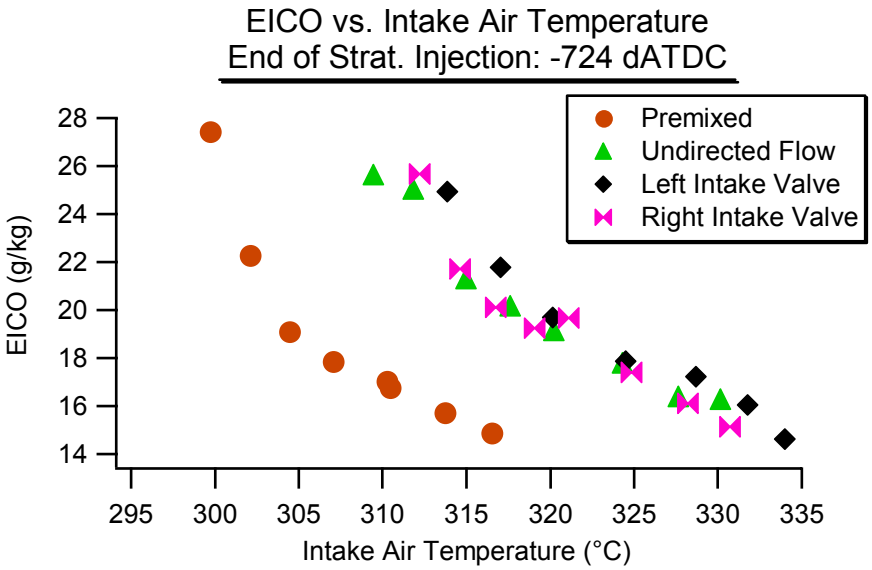

Figure A-9 Tip comparison: EICO for stratified EOI = -724 dATDC

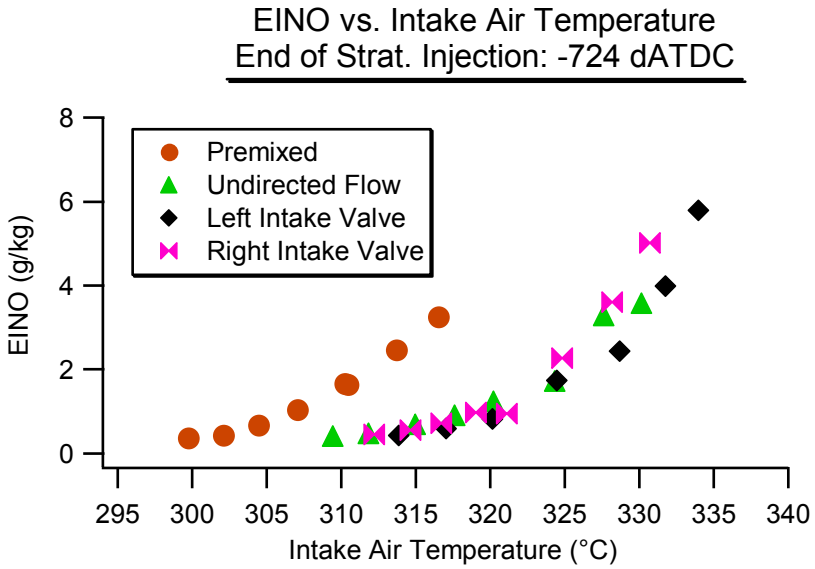

Figure A-10 Tip comparison: EINO for stratified EOI = -724 dATDC

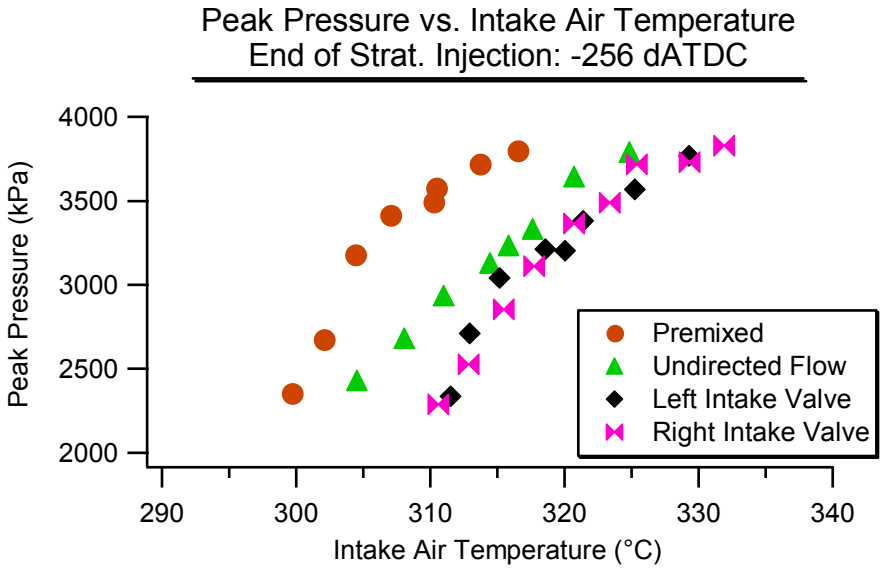

Figure A-11 Tip comparison: peak pressure for stratified EOI = -256 dATDC

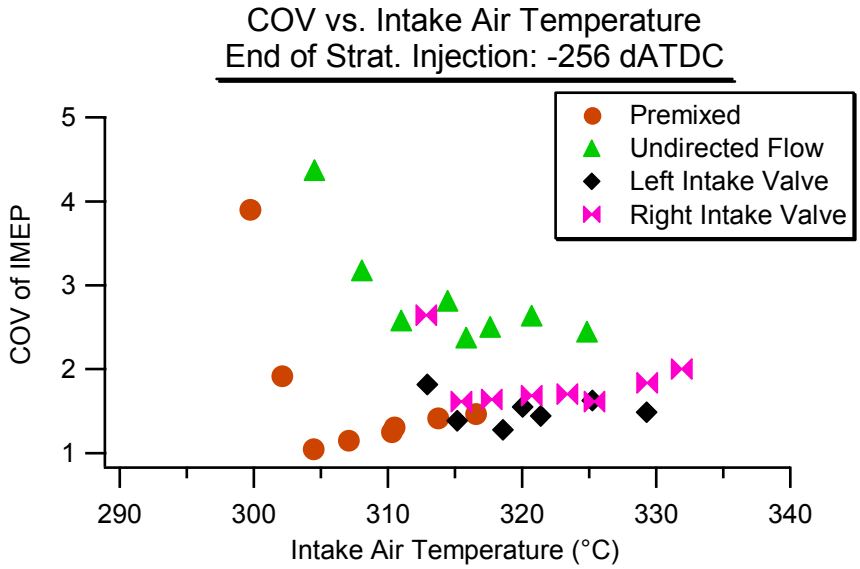

Figure A-12 Tip comparison: COV for stratified EOI = -256 dATDC

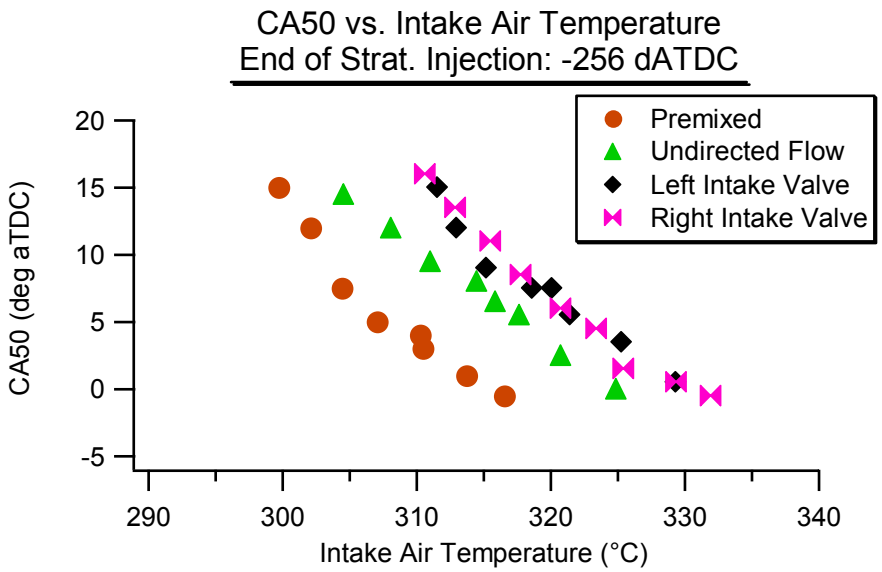

Figure A-13 Tip comparison: CA50 for stratified EOI = -256 dATDC

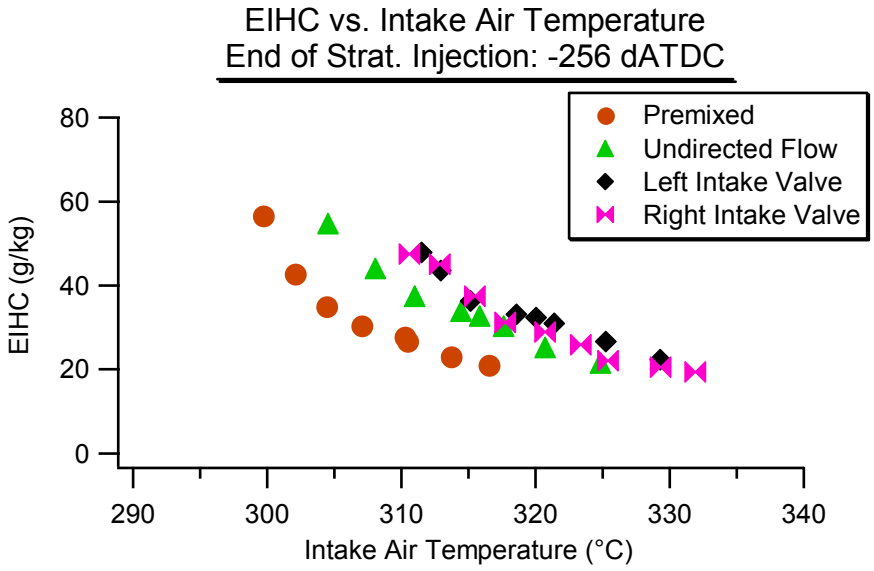

Figure A-14 Tip comparison: EIHC for stratified EOI = -256 dATDC

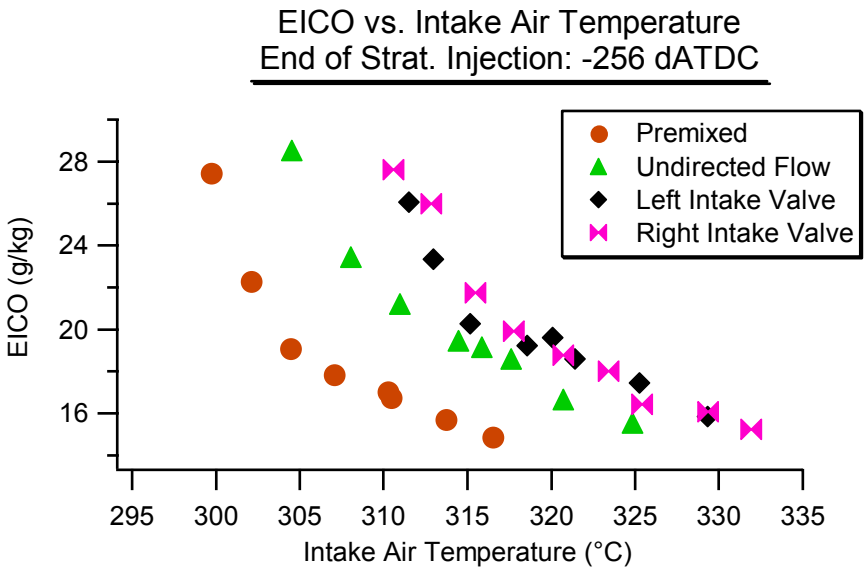

Figure A-15 Tip comparison: EICO for stratified EOI = -256 dATDC

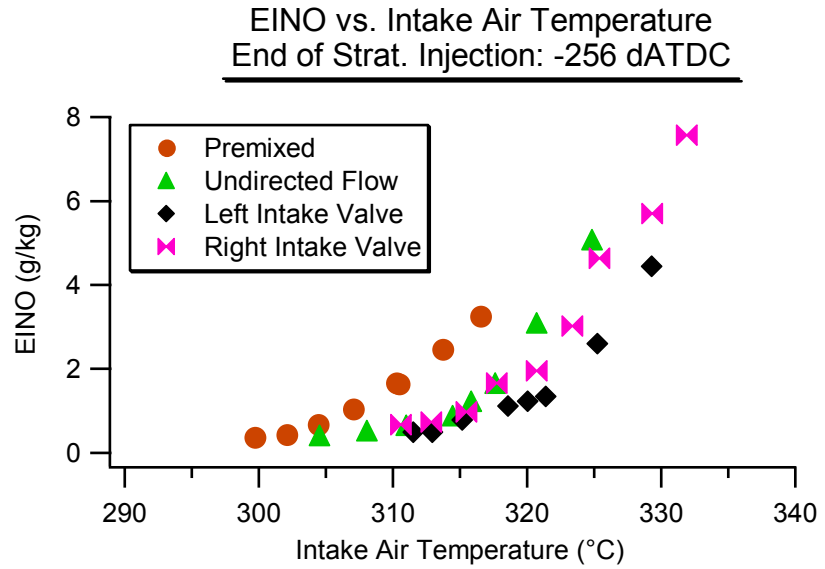

Figure A-16 Tip comparison: EINO for stratified EOI = -256 dATDC

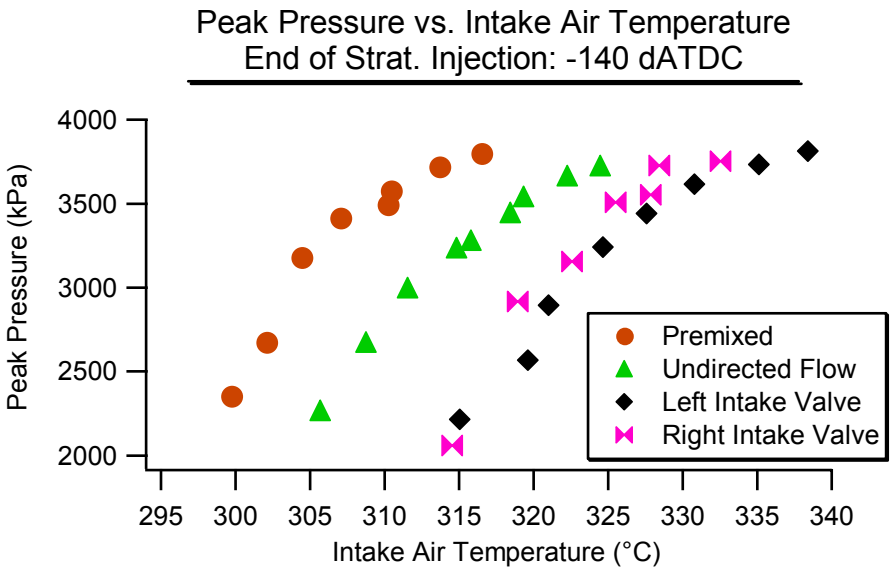

Figure A-17 Tip comparison: peak pressure for stratified EOI = -140 dATDC

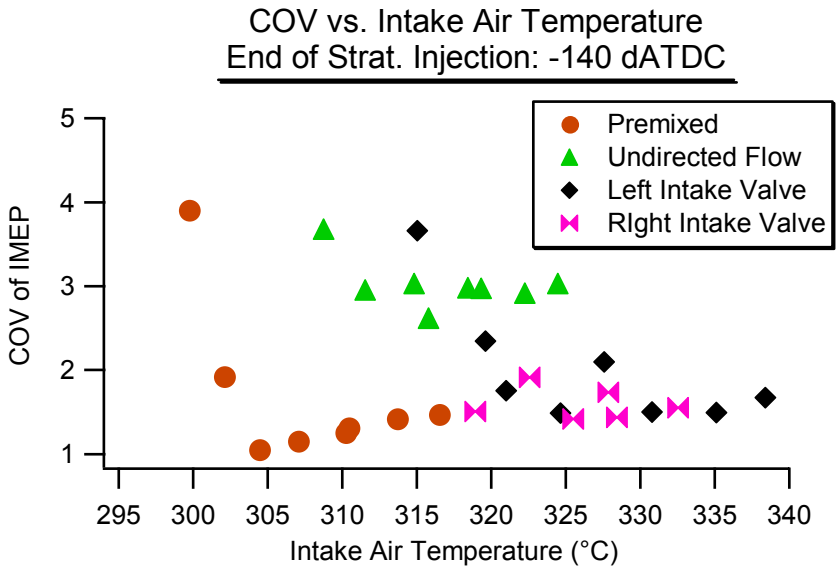

Figure A-18 Tip comparison: COV for stratified EOI = -140 dATDC

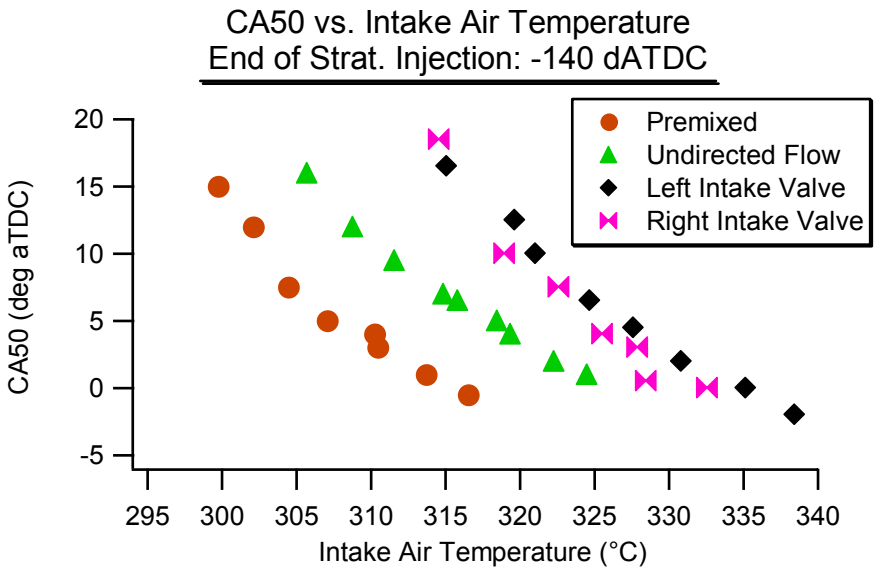

Figure A-19 Tip comparison: CA50 for stratified EOI = -140 dATDC

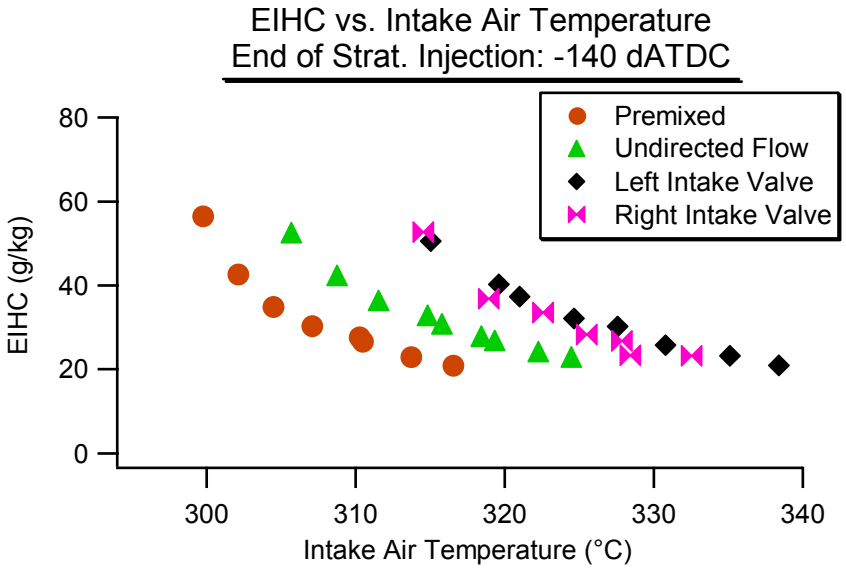

Figure A-20 Tip comparison: EIHC for stratified EOI = -140 dATDC

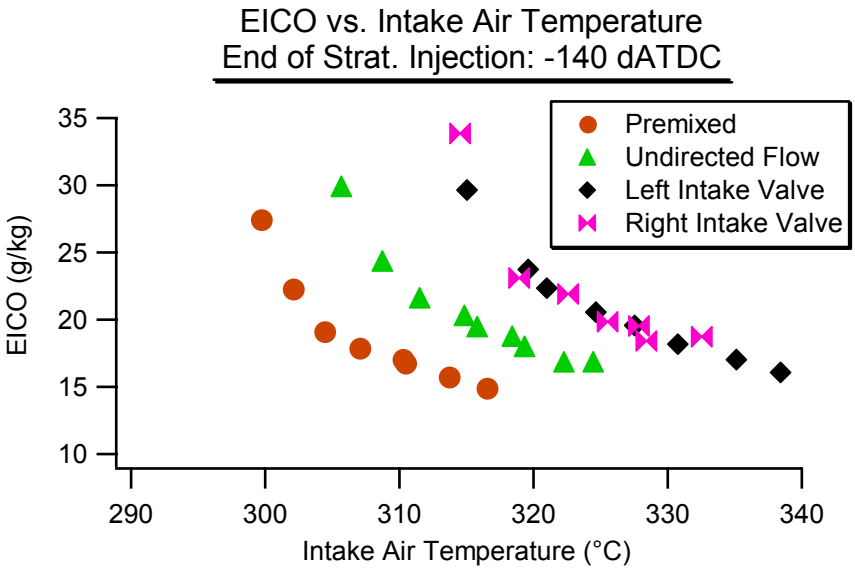

Figure A-21 Tip comparison: EICO for stratified EOI = -140 dATDC

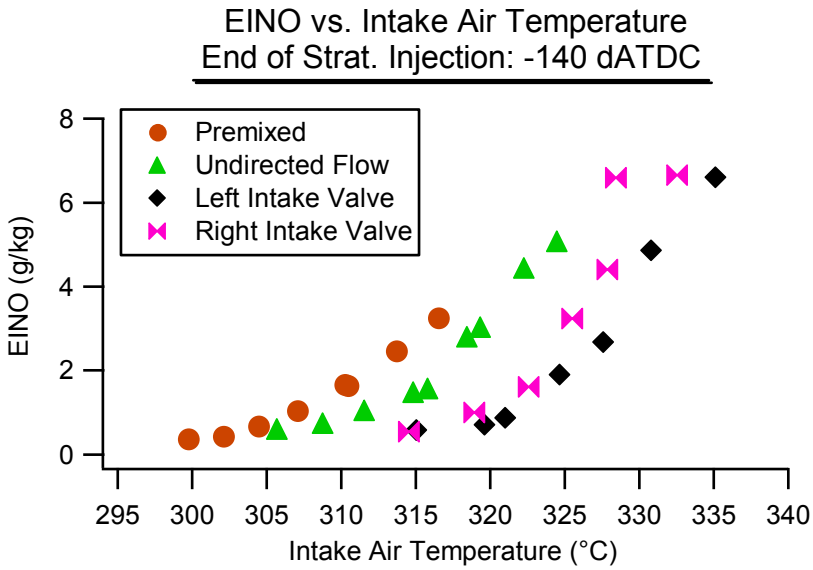

Figure A-22 Tip comparison: EINO for stratified EOI = -140 dATDC